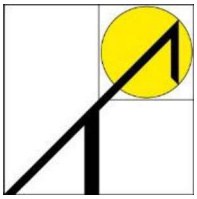
UCLouvain

Faculté d'architecture, d'ingénierie architecturale, d'urbanisme



# Airtightness of building components:

## Assessment of the direct component testing for *in-situ* measurement of building component airtightness.

**PhD examination board:**

Geoffrey Van Moeseke, thesis director
Christophe Delmotte, external examiner
Véronique Feldheim, external examiner
Valérie Leprince, external examiner
Gabrielle Masy, internal examiner
Felipe Ossio, external examiner
Denis Zastavni, chair

PhD thesis written by

**Martin Prignon**

For the completion of the degree of

**Docteur en art de bâtir et urbanisme**

Louvain-la-Neuve
Academic Year [2020–2021]

Place du Levant, 1 bte L5.05.02, 1348 Louvain-la-Neuve, Belgique
www.uclouvain.be/fr/facultes/loci/archi-cli

# Abstract

Air infiltration strongly impacts heating and cooling demands in buildings. However, limiting its impact to energy consumption would be prejudicial considering the many ways by which infiltration impacts indoor spaces. Air infiltration may impact the building durability by inducing excessive moisture migration and by reducing the hygrothermal performances of the insulation; the comfort of the occupants by transporting smells or causing draughts; and the health of the occupants by introducing particles from the outside. In addition, air infiltration may facilitate the spread of smoke and fire throughout rooms. Consequently, airtightness, which is the fundamental building property impacting air infiltration, is of considerable importance for the building sector.

The last decade has seen important developments, generating a tremendous increase in building airtightness testing and in the number of countries implementing qualification schemes for testers. However, the fan pressurisation test, the method used to measure building airtightness, assumes a uniform leakage distribution along the building envelope. Spending all available resources in the building-performance approach reveals a paradox in the current practice: airtightness is measured at a building scale while air infiltration occurs at a crack scale. In other words, measurement of building component airtightness assumes the leakage uniformly distributed along the building envelope while the consequences of air infiltration depend on the location of different leaks. This results in a poor understanding of pressure and airflow distributions along the envelope, which is crucial to grasp the challenges facing air infiltration and airtightness.

In this context, it is hypothesised that improving the methods for quantification of building component airtightness is a massive step towards a better assessment of air infiltration and its consequences. The most promising method in this context is the direct component testing that measures airtightness of

building components *in-situ*. Other methods are not expected to be as relevant because of the large impact of supervision and workmanship on airtightness and of the lack of crack data.

In this thesis, we thoroughly described the direct component testing and conducted multiple experiments to assess its effectiveness. These experiments consist of: evaluating the capability of the method to report the airflow exponent alongside the air leakage rate; quantifying the biases in airflow due to the background leakage and in pressure differences due to the pressure losses in the duct; quantifying the direct component testing uncertainty; and identifying the issues when using this method to measure building component airtightness *in-situ* and to determine building airtightness.

These experiments demonstrate that the direct component testing can measure *in-situ* the leakage characteristics of an opening with high reliability (between 3% and 10% of their value). Experiments also show that the reliability of the method depends on the design of the pressure chamber and may be affected by the human errors. Moreover, this thesis provides evidence that the direct component testing is appropriate to respond to the demand of the field for the update or the development of appropriate databases. The aim of these databases is to improve air infiltration models and prediction of building airtightness.

In conclusion, this thesis is a step forward in a better description of complex airflow and pressure distributions along the building envelope; and of the numerous consequences of air infiltration on buildings and on the comfort and the health of their occupants. Research efforts in the field should focus on generalising these results to other types of building components and on broadening the range of measurable air leakage rate and airflow exponent. Finally, future studies should also investigate the changes that improved databases of building component airtightness could introduce in the current practice. More specifically, how it affects the use and the reliability of air infiltration models and prediction of building airtightness.

# Acknowledgement

I want to take this opportunity to thank many people for their help and support that were essential in completing this thesis.

First of all, I am grateful to my supervisors from the university and the industry. To prof. Geoffrey Van Moeseke for the relevant questions that arose from our discussions and for his invaluable ability to understand and react appropriately when I was under a lot of stress. To Arnaud Dawans for his help in keeping the work grounded in the current practice and for his unconditional support and availability. I can't stress enough the decisive role they have played in the completion and the quality of this work.

Then, I need to thank all the members of the thesis' jury for their feedbacks that greatly contributed to this research. Christophe Delmotte and Dr. Valerie Leprince for the warm welcome to AIVC conferences, to the working group on wind uncertainty and to TAAC meetings ; Prof. Veronique Feldheim for the fresh look on the thesis ; Dr. Gabrielle Masy for her help in solving equations and in apprehending the numerical methods ; Prof. Felipe Ossio for his support and guidance through the doctoral steps along these four years ; and Prof. Denis Zastavni for the organisation and the coordination of the private defence, even under the unusual conditions caused by COVID.

I am very appreciative of all the constructive feedbacks on the database of components provided by the members of the *comité catalogue*: Claude Crabbé, Benjamin Biot, Jakob Eykens, Ludwik Kastory, Xavier Loncour and Clarisse Mees.

I also want to thank my "worldwide colleagues" with whom I spent time at conferences: Vitor Cardoso, Irene Poza Casado, Fredrik Domhagen, Jiří Novák and Benedikt Kölsch. They are the future of airtightness research.

I am thankful to many people inside the UCLouvain institution for supporting different aspects of my work. Notably Kathleen Servaty and Xavier Lampe for

the intermediate reports, Brigitte de Terwangne for the publication steps, Paul Muraille and David Phillips for the administrative and accounting tasks and Sergio Altomonte for the proofreading of scientific papers.

My acknowledgements also go to my former and current colleagues at *Entreprises Jacques Delens* and *Architecture et Climat*. Especially Benoît Arnold, Denis Degrave, Guillaume Foucart, Césaire Héma, Salomée Hinque, Clotilde Pierson and Dorothée Stiernon. All of them considerably brightened my working experience and became more friends than colleagues.

I also want to thank all the CORSCI's representatives for this incredible experience and all the members of the gender working group. I want to address a special greeting to Aurore, for our period as co-coordinators of that group.

I am profoundly grateful to Daniel De Vroey and his knowledge of the fan pressurisation test. Although his experience and his pedagogical skills helped me to enter in the world of airtightness, it is mostly the jokes, the poems and the teasing that I will remember.

These acknowledgments would be meaningless if I failed to mention my friends and my family.

Thank to Darwin, Iris, Léo, Matthias, Misha and all my other friends I do not mention here for the funny and entertaining moments that allowed me to get away from all this work when I needed to. I would like to address specific thanks to Edouard Goovaerts and Nicolas Beumier for their tremendous help in proofreading parts of this thesis and to François Bataille for the daily coworking during the COVID-crisis.

A big thanks to my parents, Claude and Mido, my sister, Laurie, and my brothers, Nico, Cédric, Dominique and Alain. You reassured me at every step of this project, just as you did at every step of my life. Big thanks also to Arnaud, Kirou, Laura, Linda, Manuela, Mathias and Mélanie, my "enlarged family".

My deepest thanks go to Zoé. Thank you for the time you spent helping me to prepare my presentations. Thank you for the patience you have shown and the help you have provided me when I was completely overwhelmed by this work. Thank you for your love, your joy, your daily attentions and your invaluable support.

# Table of Content

Table of Content ..... v
List of Figures ..... viii
List of Tables ..... x
Chapter 1. Introduction ..... 1
1.1. Context ..... 1
1.1.1. The Importance of the Building Sector ..... 1
1.1.2. Airtightness: A Key Performance for Buildings ..... 2
1.2. Research Gap: the Airtightness Paradox ..... 3
1.3. Research Question ..... 4
1.4. Thesis Outline and Reference Papers ..... 6
1.5. Conclusion ..... 9
Chapter 2. State-of-the-art on Airtightness and Air Infiltration in Buildings 11
2.1. Air Infiltration in Buildings ..... 11
2.1.1. The Mathematical Relation Between Air Leakage Rate and Pressure Difference ..... 12
2.1.2. Air Infiltration in the Indoor Environment Models ..... 13
2.2. Airtightness in Buildings ..... 15
2.2.1. Expressing Airtightness ..... 15
2.2.2. Measurement of Building Airtightness ..... 16
2.2.3. Variables Influencing Airtightness ..... 17
2.2.4. Predicting Building Airtightness ..... 19
2.2.5. Energy Policies and Building Airtightness ..... 21
2.3. Measuring Airtightness of Building Components ..... 22
2.3.1. Laboratory Testing ..... 22
2.3.2. *In-situ* Testing ..... 23
2.4. Meta-Analysis of Studies Measuring Building Component Airtightness ..... 25
2.4.1. Classification of Building Components ..... 27
2.4.2. Combined Outcome, Standard Error and Inconsistency Index ..... 29
2.4.3. Exploring the Heterogeneity and the Variables Influencing Window Airtightness ..... 31

2.4.4. Reporting Measurements of Building Component Airtightness..34
2.5. Summary of Chapter's Outcomes....36
Chapter 3. Protocol and Equipment for the Direct Component Testing....37
3.1. Measurement and Data Processing....37
3.1.1. Determining Airflow and Pressure Difference....39
3.1.2. Conducting a Linear Regression....40
3.1.3. Reporting Results....45
3.2. Equipment and Experimental Setup....45
3.3. Summary of Chapter's Outcomes....48
Chapter 4. Validation and Quantification of Biases for the Direct Component Testing....49
4.1. Validating the Direct Component Test on Known Openings....49
4.1.1. Methodology....49
4.1.2. Results....50
4.2. Bias in Airflow: the Background Leakage....51
4.2.1. The Experiment....52
4.3. Bias in Pressure: Pressure Losses in the Duct....53
4.3.1. Recirculation Flow....53
4.3.2. Pressure Losses in the Duct....54
4.4. Summary of Chapter's Outcomes....60
Chapter 5. Quantification of Uncertainties in the Direct Component Testing....63
5.1. Uncertainty in the Direct Component Testing....64
5.2. Methodology....65
5.2.1. Experimental Observations....65
5.2.2. Theoretical Calculations....66
5.2.3. Reported Results and Statistical Analysis....67
5.3. Reliability of the Direct Component Testing....70
5.3.1. Testing Conditions and Sources of Error....70
5.3.2. Results....70
5.4. Comparison Between the Direct and the Indirect Component Testing....75
5.4.1. Uncertainty in the Fan Pressurisation Test....76
5.4.2. Comparing Reliability of Direct and Indirect Component Tests.83

5.5. Summary of Chapter's Outcomes ..... 91
Chapter 6. Applications of the Direct Component Testing ..... 93
6.1. *In-situ* Measurement of the Building Components ..... 93
6.1.1. Issues with the Direct Component Testing ..... 94
6.1.2. Windows ..... 95
6.1.3. Small Discontinuities in Walls ..... 98
6.2. Comparison with the Single Zone Airtightness ..... 102
6.2.1. Results ..... 103
6.3. Summary of Chapter's Outcomes ..... 105
Chapter 7. Conclusion ..... 107
7.1. General Conclusion ..... 108
7.1.1. The Relevant Applications in Research and Practice ..... 108
7.1.2. Effectiveness of the Direct Component Testing ..... 109
7.1.3. Applications for the Direct Component Testing ..... 111
7.1.4. Answering the research question ..... 116
7.2. Implications ..... 117
7.2.1. Regarding Practice ..... 117
7.2.2. Regarding Research ..... 118
7.2.3. Regarding Policies ..... 120
7.3. Limitations ..... 121
7.4. Future Research ..... 122
References ..... 125
Appendix A. ..... 135
Appendix B. ..... 147
Appendix C. ..... 179
Appendix D. ..... 195
Appendix E. ..... 207
Appendix F ..... 221

# List of Figures

Figure 1: Classification of variables investigated by at least two studies. The numbers in brackets are the number of studies finding a significant (left) or not significant (right) impact on airtightness. The bold variables are those found mostly or unanimously significant. ..... 18
Figure 2: illustration of the first level classification of building components regarding the type of flow. ..... 27
Figure 3: 4-level classification of building components based on studies reporting at least two measurements of air leakage rates through building components. ..... 28
Figure 4: Forest plot obtained from the meta-analysis conducted on windows studies ..... 33
Figure 5: principle behind the direct component testing. ..... 38
Figure 6: experimental setup and equipment for a typical measurement using direct component testing. ..... 46
Figure 7: experimental setup for direct component test using plastic-sheet system with horizontal bars. ..... 47
Figure 8: experimental setup for direct component test using solid woodbox system. ..... 47
Figure 9: illustration of the increasing airspeed and the recirculation flows in the duct because of the sudden retraction and expansion of the cross-section. ..... 53
Figure 10: PVC tube at the entrance of the duct and the gauge placed at 13 cm of the calibrated disk ..... 58
Figure 11: PVC tube and the pressure gauge placed at the end of the duct. ..... 58
Figure 12: experimental setup to quantify pressure losses in the straight case. ..... 58
Figure 13: experimental setup to quantify pressure losses in the "two 90° angles" case. ..... 58
Figure 14: the pressure losses in the duct as a function of the measured airflow with (dashed lines) and without (full lines) singularities obtained by the experiment (black lines) and by the theoretical calculations using the method 1 (red lines) and the method 2 (yellow lines). ..... 59
Figure 15: the uncertainty of the envelope pressure in Pa (left) and in % (right) as a function of the pressure difference measured for four values of $\sigma\Delta p0$ ..... 78

Figure 16: the calculated and the observed uncertainties on the airflow rate (in %) as a function of the pressure difference for the OLS, the IWLS and the WLOC .....80
Figure 17: the calculated (error bars) and the observed (green zones) 95% confidence intervals of the airflow rate at 5 (left) and 50 (right) Pa for each of the 30 measurements for the three regression techniques. .....81
Figure 18: the mean air leakage rate at 50 Pa (black dot) and the observed uncertainty (blue lines) in both modes, obtained with the OLS, using the direct (left) and the indirect (right) component testing. .....90
Figure 19: the 95% confidence interval of air leakage rate at 50 Pa measured for each window, compared with the literature 95% confidence interval. .....97
Figure 20: the 95% confidence interval of airflow exponent in pressurisation (upper graph) and depressurisation (lower graph) measured for windows, compared with the literature interval. .....98
Figure 21: 95% confidence interval of air leakage rates at 50 Pa measured for discontinuities per unit (upper graph) and per discontinuity (lower graph), compared with the literature interval. .....100
Figure 22: 95% confidence interval of airflow exponent in pressurisation (upper graph) and depressurisation (lower graph) measured for discontinuities, compared with the literature interval. .....101
Figure 23: drawings of the apartment and the delimited zone (in red) to test. .....102
Figure 24: comparison between the total air leakage rate (the fan pressurisation test) and the sum of individual components (the direct component tests), in pressurisation, depressurisation and average. .....104

# List of Tables

Table 1: the number of studies combined, the combined mean and standard deviation, and the index of inconsistency in the air leakage rate at 50 Pa and the airflow exponent of different building components. Units for the air leakage rate at 50 Pa depend on the component: [a] = $m^3/(h.m^2)$, [b] = $m^3/(h.m)$ and [c] = $m^3/h$. ..... 30
Table 2: mean and standard deviation of defects in boards reported by (Hall and Hauser, 2003) and (Langmans et al., 2010a). ..... 31
Table 3: mean and standard deviation for defects in vapour membrane reported by (Hall and Hauser, 2003) and (Gullbrekken et al., 2017). ..... 31
Table 4: List of publication used for the meta-analysis on windows, including the authors, the year, the sample size (N), the type of measurement (laboratory or *in-situ*), the material (W = Wood, A = Aluminium or Um = Unspecified material) and the type (DW = Double window, SW = Single window, SL = Sliding window or Ut = Unspecified type) of windows measured. ..... 32
Table 5: sample size, mean, standard error (in $m^3/(h.m)$) and inconsistency for airflow at 50 Pa for three subgroups meta-analyses based on the measurement method, the type of window and the window material. ..... 34
Table 6: Accuracy and range of airflow measured with the equipment used in this thesis. Airflow is expressed in $m^3/h$ and its uncertainty in $m^3/h$ or in % of the airflow measured. ..... 47
Table 7: comparison between the airflow through four calibrated disks according to their calibration and to measurements with the direct component test. $A$ in $cm^2$, $C$ in $m^3/(h.Pa^n)$ and $q50$ in $m^3/h$. ..... 50
Table 8: Symbols, names and values for variables used in the calculation of pressure losses in compressible ducts using Eq. 25 to Eq. 34. ..... 57
Table 9: the statistical indicators for NHST and the effect-size analysis, depending on the type of comparison and the type of variables. ..... 68
Table 10: results of the repeatability study conducted on the window case. $q50$ in $m^3/(h.m)$. ..... 71
Table 11: results of the repeatability study conducted on the electrical outlet case. $q50$ in $m^3/h$. ..... 72
Table 12: $\Delta u$ obtained when comparing the observed standard deviation and the calculated uncertainty for both repeatability studies and both regression techniques. ..... 73

Table 13: statistical comparison between the OLS and the WLOC techniques for the plastic-sheet system. ..... 74
Table 14: statistical comparison between the OLS and the WLOC techniques for the woodbox system. ..... 75
Table 15: the number of tests, the mean air leakage rate at 50 Pa (in $m^3/h$) and the observed standard deviation (in %) of multiple repeatability studies previously published. ..... 78
Table 16: the mean values, the observed standard deviations and the calculated uncertainty for the leakage characteristics ($n$ and $CL$) in both modes using the three regression techniques. ..... 79
Table 17: results of the repeatability study conducted on the electrical outlet case with the direct component testing. $q50$ in $m^3/h$. ..... 84
Table 18: results of the statistical comparison between the OLS and the WLOC for the electrical outlet measured with the direct component testing. ..... 85
Table 19: results of the repeatability studies conducted with the fan pressurisation method pre- and post-sealing of the component. $q50$ in $m^3/h$. ..... 86
Table 20: results of the comparison between the OLS and the WLOC for the pre-sealing study. ..... 87
Table 21: results of the comparison between the OLS and the WLOC for the post-sealing study. ..... 87
Table 22: result of the repeatability study when looking at the component air leakage rate measured with the indirect component testing. ..... 88
Table 23: results of the repeatability studies conducted on the electrical outlet with the OLS and the WLOC, using the direct and the indirect component testing. $q50$ in $m^3/h$. ..... 89
Table 24: results of the 13 measurements conducted on windows including the type, the material and the dimensions of windows. The airflow exponent is given in pressurisation and depressurisation and the air leakage rate at 50 Pa per m of opening length is given in pressurisation, depressurisation and total. ..... 96
Table 25: results of 21 measurements conducted on discontinuities (e.g. the electrical outlets or the switches). This table includes the type of wall and the number of units tested, in addition to the airflow exponent (in pressurisation and depressurisation) and the air leakage rate at 50 Pa per unit (in pressurisation, depressurisation and total). ..... 99

Table 26: leakage characteristics and the air leakage rate at 50 Pa of the entire volume and of each component. $q50$ in $m^3/h$. .....103

# Chapter 1.Introduction

## 1.1. Context

### 1.1.1. The Importance of the Building Sector

People spend most of their time indoors, consuming energy to maintain their comfort. This explains the importance of the building sector in the energy consumption and in the $CO_2$ emissions.(IEA, 2019a), the last report of the Internal Energy Agency, demonstrated that building construction sector accounts for 36% of final energy use and 39% of energy and process-related $CO_2$ emissions. A few years ago, worldwide political leaders recognised the need for ambitious measures regarding energy consumption in buildings. In Europe, this awareness led to (European Parliament and Council, 2010) and (European Parliament and Council, 2012), two major directives on energy performance of buildings. More recently (European Parliament and Council, 2018) amended these directives, that set ambitious targets on the modernisation of the building sector. (IEA, 2019a) also reported that the global building stock emissions continue to rise. Indeed, the measures taken these last years are not efficient enough to counterbalance the increase in energy consumption induced by the expansion of floor space and population. Nevertheless, these measures have limited the growth of building energy use between 2010 and 2018 to 21%, instead of the 45% predicted assuming no measure would have been taken.

The role of buildings should not be limited to their impact on final energy use and $CO_2$ emissions. Their impact on the occupants' health and comfort should also be emphasised. (Hensen, 2018) explained that different aspects have been prioritised for the development of buildings over the years, and that people have shown a regain of interest in comfort and health since the beginning of the 21$^{st}$ century. (Pierson, 2019) pointed out that, nowadays, the development

of indoor spaces must answer three challenges: energy consumption, comfort and health. In this context, airtightness of buildings, which is the building characteristic responsible for air infiltration, is of major interest because of its impact on all these three aspects.

### 1.1.2. Airtightness: A Key Performance for Buildings

The 2010 and 2012 European directives triggered an increase of interest for building airtightness because of its impact on energy consumption. (Guillén-Lambea et al., 2019) found a strong correlation between airtightness performance and heating demands in buildings, especially for cities located in colder climates. (Jokisalo et al., 2009) demonstrated that in typical Finnish two-story detached houses, air infiltration accounts for 15% to 30% of the energy use for space heating. These figures increase up to 50% for very leaky houses. In another research, (Feijó-Muñoz et al., 2019b) showed that in Spanish residential buildings, air infiltration could increase the heating demands by 16.44 kWh/m² per year and the cooling demands by 3.06 kWh/m² per year. Although these figures vary with the type of construction, the climate zone or the performance of the insulation, they illustrate the importance of airtightness regarding energy consumption in buildings.

There is a close relation between the research and the practice, and therefore the policies, in the field of airtightness. Consequently, building standards and regulations have had a strong impact on this field. According to (Leprince et al., 2017b), energy policies following up European directives considerably increased the frequency of airtightness testing and the number of countries implementing qualification schemes for testers. These also encouraged the development of databases for building airtightness and of tools for architects and contractors. Consequently, the number of studies estimating airtightness performance of building stocks drastically increases over the last few years around the world. The most recent ones are (Moujalled et al., 2018) in France and (Feijó-Muñoz et al., 2019a) in Spain.

However, to limit the impact of air infiltration to an increase of energy demand would be prejudicial to the field of built environment because of the large variety of consequences air infiltration has on indoor spaces. (Lstiburek et al., 2002) analysed five cases where air infiltration causes troubles to the building and its occupant. In that work, they found three important troubles induce by

air infiltration: it impacts building durability by inducing excessive moisture migration and reducing the hygrothermal performances of the insulation; it affects comfort of the occupants by transporting odours or their health because of particles coming from the outside; and it facilitates the spread of smoke and fire throughout rooms. The magnitude of these different impacts depends on four aspects: the emitter (i.e. the source of trouble), the receptor (i.e. people or elements experiencing trouble), the pathway (i.e. the way the air infiltrates or exfiltrates the building) and the driving force (i.e. the cause and the magnitude of the pressure difference responsible for air displacement). (Lstiburek et al., 2002) stressed the need for a better assessment of these consequences and for a better description of the complex airflow and pressure distributions. Indeed, these may imply substantial changes at all stages of the building: design, commissioning, operations, maintenance, diagnostics and rehabilitation.

## 1.2. Research Gap: the Airtightness Paradox

The context described here above demonstrates the importance of airtightness in practice and policies, mainly because of its impact on building energy use. However, this performance-based approach caused by the increasing interest in building airtightness testing is a double-edged sword.

On the one hand, it promotes the development of guides and frameworks to help realise airtight buildings and hitting airtightness requirements imposed by building specifications.

On the other hand, spending every resource in this performance-based approach has enlighten two issues related to the measurement method: an uncertainty in building infiltration and a poor understanding of pressure and airflow distribution along the envelope.

- The fan pressurisation test measures building airtightness and determines building response to a pressure difference between the inside and the outside. To have a response independent from weather conditions, the test is conducted at higher pressure differences (typically 10–100 Pa) than those experienced occurring in a natural state (typically 0–20 Pa). Consequently, when looking at the consequences of airtightness, one must extrapolate from the performance measured to the pressure differences occurring in natural conditions. Recently, (Rogers, 2019a) found a deviation from -19%

to +78% between the extrapolated and the real air infiltration at 1 Pa depending on the distribution of unintentional openings along the envelope.
- The fan pressurisation reports the response of the entire building, assuming a uniform leakage distribution along the envelope. This fails to inform the tester of the experienced pressure distribution and the pathways while these are two of the four aspects the consequences of airtightness are depending on.

This illustrates the airtightness paradox: air infiltration is measured at a building scale assuming a uniform leakage distribution while it is occurring at a building component scale. This paradox induces high uncertainty in the extrapolation and narrows the consequences of airtightness down to energy consumption. This highlights the need for a deeper investigation of the building response to pressure differences at a component scale rather than a building scale to solve the paradox.

A wider use of methods quantifying building component airtightness and a deeper investigation of the results obtained would be a proper way to improve our knowledge about leakage distribution. Although these methods are already necessary in the present context, the demand is expected to increase in following years because of the regain of interest in building occupants' comfort and health. Moreover, these methods are particularly relevant in the context of renovation since it can assess the impact of solutions implemented along with the global performance of the building. The recent amendment to European directives that encourages countries to take strong measures for refurbishing their building stock should also generate an increasing demand for these methods.

## 1.3. Research Question

The general ambition of this research is to improve our knowledge about air infiltration in buildings and its consequences. This requires a better description of the complex airflow and pressure distributions along the building envelope. Having a better description of these issues would help to develop a consequence-based approach alongside the ongoing performance-based approach.

For this purpose, it is necessary to develop and promote reliable methods quantifying building component airtightness. However, only a few documentation and investigations about the efficiency and limitations of existing methods are available.

In this context, this research intends to contribute to the following general research question:

**How methods quantifying building component airtightness can be improved to match the present demand?**

This broad research question encompasses three questions: How effective are the methods quantifying building component airtightness? What are the needs of the current research, practice and policies in the field? How to improve the methods to match these needs?

First, assessing the effectiveness of a quantification method includes the evaluation of its practicability and its reliability. On the one hand, the practicability embraces three aspects: the range of building components that can be quantified; the price and the execution time; and the type of information provided. On the other hand, the reliability embraces two aspects: the error related to the quantification that includes measurement and assumption errors; and the error related to the difference between the conditions experienced when the method is applied and the condition experienced by the component in use.

Second, identifying the needs of the research, the practice and the policies involves the identification of relevant applications. For example, in the context of building component airtightness, those can be the update and the creation of databases, the improvement of air infiltration models or the prediction of building airtightness. The required effectiveness, including all aspects mentioned here above, depends on the selected application.

Third, improving the method is achieved by modifying the protocol, the equipment, the packaging or anything else that changes the method to match the needs of the desired application.

Methods quantifying building component airtightness aim to describe the relationship between pressure difference on both sides of an opening and the quantity of air flowing in the building through that opening. Different methods correspond to different contexts and include different characteristics, and each method can be applied with different levels of complexity.

Existing quantification methods fall in two categories: numerical models and measurements. Current knowledge limit numerical models of airflow paths to three typical cracks encountered in buildings, studied in (Hopkins and Hansford, 1974): straight through, L-shaped and multi-cornered cracks. These are expected to describe insufficiently the large variety of unintentional openings that should be modelled to describe airflow distribution in buildings properly. Regarding the measurement methods, these are further divided in laboratory and *in-situ* measurements. Laboratory measurements are conducted in controlled environments, reducing the error of the measurement itself but increasing the extrapolation error (i.e. the error related to the extrapolation from the measured performance to the performance of the component in use). This is expected to be a major drawback of this type of method because of the significant impact supervision and workmanship have on airtightness. These different quantification methods are more deeply reviewed and analysed in sections 2.1.2 and 2.3.

These two hypotheses suggest that *in-situ* measurement methods are more appropriate than others to satisfy the present demand. Among these methods, direct component technique is very promising. However, there is still a considerable lack of documentation and investigations regarding the protocol and the reliability of direct component testing.

Consequently, the thesis narrows its focus down to the following specific question:

**How effective is the direct component testing for *in-situ* measurement of building component airtightness?**

Although the core of the thesis is limited to that question, the broad research question is also investigated. The possible applications of quantification methods and their need in terms of effectiveness are investigated in parts of Chapter 2 and Chapter 6, and the conclusion (Chapter 7) explicitly addressed it.

## 1.4. Thesis Outline and Reference Papers

This chapter (*introduction*) gives a short overview of the background and present context in the field of airtightness, and identifies the research gap in the

quantification of building component airtightness. These observations result in defining two research questions (i.e. broad and narrowed) that this work aims to contribute to. Then, it establishes the structure of the thesis to help the reader navigate through its structure. In addition to this chapter, this work is articulated in six parts:

Chapter 2 *(State-of-the-art on Airtightness and Air Infiltration in Buildings*) provides the reader with fundamentals of air infiltration. In addition, it reviews the recent work conducted in the field to situate the research question in the present context. It highlights the importance of encouraging measurement of building component airtightness *in-situ* and the potential for direct component testing regarding the issues facing stakeholders.

Chapter 3 (*Protocol and Equipment for the Direct Component Testing*) describes the protocol, the data processing and the equipment for direct component testing. This includes the range of airflow and pressure difference measurements and the different methods for conducting a linear regression.

Chapter 4 (*Validation and Quantification of Biases for the Direct Component Testing*) reports and discusses the results of three experiments: one to assess the capability of the method to provide the desired results and two to quantify possible bias related to the protocol and the experimental setup.

Chapter 5 (*Quantification of Uncertainties in the Direct Component Testing*) studies the reliability of the direct component testing. This illustrates methodologies for theoretical calculation of uncertainty, experimental observation of uncertainty and statistical analysis of repeatability studies. Then, these methodologies are applied to five studies in order to: determine the uncertainty of the direct component testing; compare it with indirect component testing, another *in-situ* measurement method; and improve the uncertainty of both methods.

Chapter 6 (*Applications of the Direct Component Testing*) reports the results and the challenges related to two applications of the direct component testing. These are the measurement of different building components in newly constructed buildings and the use of direct component testing to determine building airtightness.

Lastly, Chapter 7 (*Conclusion*) concludes this thesis by recalling the main findings obtained from Chapter 2 to Chapter 6, and by highlighting their impact against the relevant literature. It points out and discusses the contribution this thesis

makes to both research questions. Finally, it illustrates the limitations of the study and the further work needed in the field of air infiltration.

Parts of chapters 2 to 6 are summaries of studies already published. The reader can find additional information in original papers, which are mentioned in the introduction of each chapter and are given in the appendices. These are, in order of appearance in the thesis:

- Appendix A: Prignon, M. and Van Moeseke, G. (2017). Factors influencing airtightness and airtightness predictive models: A literature review. Energy and Buildings, **146**: 87–97. https://doi.org/10.1016/j.enbuild.2017.04.062.
- Appendix B: Prignon, M., Ossio, F., Altomonte, S., Dawans, A. and Van Moeseke, G. (2020). Airtightness performance of building components: meta-analysis of laboratory and in-situ measurements. Under review in Building and Environment.
- Appendix C: Prignon, M., Delmotte, C., Dawans, A., Altomonte, S. and Van Moeseke, G. (2020). On the impact of regression techniques to airtightness measurement uncertainties. Energy and Buildings, **215**. https://doi.org/10.1016/j.enbuild.2020.109919.
- Appendix D: Prignon, M., Dawans, A. and Van Moeseke, G. (2018). Uncertainties in airtightness measurements: regression methods and pressure sequences. *In 39th AIVC – 7th TightVent & 5th Venticool Conference: Smart ventilation for buildings.* Antibes Juan-Les-Pins, France.
- Appendix E: Prignon, M., Dawans, A., Altomonte, S. and Van Moeseke, G. (2019). A method to quantify uncertainties in airtightness measurements: Zero-flow and envelope pressure. Energy and Buildings, **188–189**: 12–24. https://doi.org/10.1016/j.enbuild.2019.02.006.
- Appendix F: Prignon, M., Dawans, A. and Van Moeseke, G. (2020). Quantification of uncertainty in zero-flow pressure approximation. International Journal of Ventilation. https://doi.org/10.1080/14733315.2020.1777020.

## 1.5. Conclusion

This introduction section is made of four parts. First, it presents the context of this field of research, highlighting the importance of air infiltration and airtightness of buildings in the present context. Second, it points out the research gap and the airtightness paradox caused by the performance-based approach. This emphasises the need for deeper investigation of building component airtightness to address these issues. Third, it suggests a broad research question based on the research gap and a narrowed research question based on two research hypotheses. Fourth, it enumerates and briefly describes the six chapters of this thesis to help the reader navigate through the thesis structure.

In conclusion, this thesis contributes to reducing the importance of the airtightness paradox by investigating the effectiveness of direct component testing and its capability to respond to the demand for present research and practice. This would be a considerable step forward in the description of airflow and pressure distributions in buildings; and in the assessment of the numerous consequences air infiltration has on the building and its occupants.

# Chapter 2. State-of-the-art on Airtightness and Air Infiltration in Buildings

In this chapter, we aim to give the reader fundamentals of air infiltration and to provide an overview of the previous and current work in the field. This aims to have a good understanding of the importance of the work done in this thesis and of how it may affect the current practice, research and policies. This chapter refers to the work published in:

- Appendix A: Prignon M. and G. Van Moeseke (2017). Factors influencing airtightness and airtightness predictive models: A literature review. Energy and Buildings, **146**: 87–97. https://doi.org/10.1016/j.enbuild.2017.04.062.
- Appendix B: Prignon M., F. Ossio, S. Altomonte, A. Dawans and G. Van Moeseke (2020). Airtightness performance of building components: meta-analysis of laboratory and in-situ measurements. Under review in Building and Environment.

## 2.1. Air Infiltration in Buildings

(Sherman and Chan, 2006) defined air infiltration as the mass of air passing through unintentional openings induced by a pressure difference. In buildings, (ASHRAE, 2017) enumerated three causes for air infiltration:

- The wind induces a distribution of pressure along the building envelope, and at each opening. This pressure depends on the wind speed, the wind direction, the air density, the surface orientation and the surroundings.

- The stack effect is the pressure difference experienced when the two columns of air (on both sides of the opening) have different weights (i.e. when air density is different).
- The mechanically supplied or exhausted airflows induce a pressure difference between different zones of the building.

Air infiltration is tough to quantify and to predict because it takes place in unintentional openings, mostly due to human errors. In addition, it depends on the distribution of cracks along the envelope, on climatic conditions and on building orientation.

### 2.1.1. The Mathematical Relation Between Air Leakage Rate and Pressure Difference

In their review, (Younes et al., 2011) explained that the quantity of air flowing through an opening depends on the pressure difference and on the characteristics of the opening. For large cracks, flow is usually turbulent and Eq. 1 commonly represents it:

$$q = 3600.C_d A\left(\frac{2}{\rho}\Delta p\right)^{1/2} \quad \text{Eq. 1}$$

With $q$ the airflow rate [m³/h], $C_d$ the discharge coefficient, $\rho$ the air density (kg/m³), $\Delta p$ the pressure difference [Pa] and $A$ the area of the opening [m²].

For small cracks, the flow is expected to be laminar and Eq. 2 characterise it:

$$q = 3600.\frac{\Delta p}{8\mu L}.\pi r^4 \quad \text{Eq. 2}$$

With $\mu$ the dynamic viscosity [Pa.h], $L$ the length of the flow path [m] and $r$ the radius of the opening [m].

In practice, the flow through an opening is hardy fully laminar or fully turbulent and a combined equation is used: the quadratic form where both types of flows are separated (Eq. 3) or the power law where these are combined (Eq. 4).

$$\Delta p = \alpha q + \beta q^2 \quad \text{Eq. 3}$$

$$q = C_L(\Delta p)^n \quad \text{Eq. 4}$$

With $\alpha$ and $\beta$ two dimensionless constants, $C_L$ the air leakage coefficient [$m^3/(h.Pa^n)$], and $n$ the airflow exponent. In Eq. 4, $n$ bears information about the flow regime: its value is between 0.5 (fully turbulent) and 1.0 (fully laminar).

The power law is usually preferred since (Walker et al., 1998) demonstrated by a theoretical analysis, laboratory measurements and *in-situ* measurements that it is more reliable than the quadratic form.

### 2.1.2. Air Infiltration in the Indoor Environment Models

*Air infiltration in CFD and Multizone models*

(ASHRAE, 2017) presented two common methods for modelling the indoor environment in buildings: the Computational Fluid Dynamics (CFD) and the multizone network airflow modelling. These methods allow studying different aspects of the buildings, including the pressure distribution and the Indoor Air Quality (IAQ).

CFD is usually used for a microscopic view of the building and its components. It includes a rigorous application of Navier-Stokes equations and provides highly detailed results regarding the airflow, the temperatures or the contaminant concentration. However, the time necessary to develop models and solve equations limits its use. In CFD models, air infiltration is considered by adding inlets or outlets to the model for each potential opening or set of openings. Boundary conditions at these inlets/outlets are either a mass flow rate or a pressure. The second case is more relevant in the context of air infiltration since it is a better representation of reality: a pressure difference caused by wind and stack effect induces air infiltration in buildings.

In contrast, the multizone models provide a macroscopic view of the building. It is based on solving a network of mass balance equations between the different zones. This takes much less time than solving fundamental fluid mechanics equations. However, these models provide less detailed results than CFD, which lead to higher uncertainty in the approximation of scenarios. In the multizone models, the user adds "airflow paths" that are the elements through which air can move between two adjacent zones. These elements refer to small openings (e.g. cracks in the building envelope), large openings (e.g. doorways) or ventilation systems (e.g. exhaust fan).

*Crack Description*

The accuracy of air infiltration in these models depends on the precision level of cracks and of their distribution along the envelope. In the perfect case, the user locates and measures the value of each crack responsible for air leakage. This information is never exhaustively known, and it is up to the user to decide the level of approximation he or she desires.

One could consider cracks uniformly distributed along the building envelope (based on the result of a fan pressurisation test) or a different value for each façade (based on the result of a guard-zone test). (Emmerich, 2001) explained that leakage distribution, which is often unknown and difficult to estimate, is an important issue when validating multizone models. The same difficulty regarding the available crack data is expected in CFD since the operator must define the location of each inlet and outlet representing openings.

Besides the leakage distribution, one must describe the crack itself. In CONTAM for example, a widely used software for multizone models, (Dols and Polidoro, 2015) described different possible inputs for airflow paths, which include the effective leakage area at 4 Pa ($\mathbf{ELA_4}$), the air leakage rate at 50 Pa ($q_{50}$) or the airflow exponent and the air leakage coefficient ($n$ and $C_L$) for the power law. Section 2.2.1. describes these different ways to express airtightness. Since the airflow exponent bears some information on the flow regime, using $n$ and $C_L$ as inputs should provide a higher accuracy than using $\mathbf{ELA_4}$ or $q_{50}$. The same issue is encountered with CFD. Indeed, (Younes and Abi Shdid, 2013) highlighted the importance of crack data to be a realistic representation of the construction methods and the materials used in the building. However, in the methodology they suggested, they limit each opening to a straight crack, an angled crack or a gap between two elements. Although these cracks are the typical domestic cracks investigated by (Hopkins and Hansford, 1974), they reduce the relation between the air leakage rate and the pressure difference to a simple crack length.

However, the airflow exponent and the air leakage coefficient are not always available in literature since the databases and the studies measuring the air leakage of building components usually report $\mathbf{ELA_4}$ or $q_{50}$ instead of $n$ and $C_L$. In addition, not all the measurement methods provide these two parameters. Currently, two databases of building component airtightness are used: (ASHRAE, 2001) and (Orme et al., 1994). These databases have been fed

with data coming from studies performed until the early '90s. However, the large impact of the recent energy policies has made these databases less relevant to the current practice. Today, an update of the existing databases, including $n$ and $C_L$ rather than only $\mathrm{ELA}_4$ or $q_{50}$ is needed to improve air infiltration in indoor environment models of buildings.

## 2.2. Airtightness in Buildings

Unlike air infiltration that is the mass of air displaced because of a pressure difference, airtightness is the building characteristic responsible for air infiltration. (Guyot and Carrié, 2010) defined it as the resistance to air infiltration and exfiltration through unintentional openings in the building envelope. While air infiltration is mainly caused by a weather-induced pressure difference, airtightness is expected to be independent from them.

### 2.2.1. Expressing Airtightness

Airtightness is quantified with many different metrics, all labelled "air leakage". A high air leakage rate corresponds to a high air infiltration and a low airtightness performance. Usually, airtightness is expressed with $q_{50}$, the air leakage rate through an opening when it is submitted to a pressure difference of 50 Pa. According to (Sherman and Chan, 2006) this pressure difference is often preferred because it is low enough to be achieved with *in-situ* measurements and high enough to be reasonably independent of the weather conditions. However, sometimes a pressure difference of 4 Pa is used instead of 50 because it is closer to the ones that typically drive natural infiltration, which (Sherman and Dickinson, 1985) estimated between 0 and 10 Pa.

The effective leakage area at 4 and 10 Pa ($\mathrm{ELA}_4$ and $\mathrm{ELA}_{10}$) are also regularly used because of their intuitive meaning: it is the area of a large opening that would produce the same amount of airflow than the measured zone (Eq. 5):

$$\mathrm{ELA}_{\Delta \mathrm{p}} = \frac{q\sqrt{\frac{\rho}{2\Delta p}}}{C_d} \qquad \text{Eq. 5}$$

With $\mathrm{ELA}_{\Delta \mathrm{p}}$ the effective leakage area [m²], $q$ the airflow rate [m³/h], $C_d$ the discharge coefficient, $\rho$ the air density (kg/m³) and $\Delta p$ the pressure difference [Pa].

When comparing multiple buildings or openings, the normalised versions of $q_{50}$, $\mathrm{ELA}_4$ and $\mathrm{ELA}_{10}$ are sometimes used. For example, $\mathrm{NLA}_4$ is the normalised leakage area at 4 Pa, that is the $\mathrm{ELA}_4$ divided by the area of the measured leakage.

The airflow exponent is sometimes given, alongside $q_{\Delta p}$ or $\mathrm{ELA}_{\Delta p}$. This practice should be promoted since $n$ bears some information about the flow regime. In addition, it is used to convert from one metric to another with Eq. 4 and Eq. 5 when comparing studies reporting results in different metrics. In a vast empirical study, (Orme et al., 1994) found that the majority of airflow exponents for building components are within $\pm\, 0.1$ of their mean value, $0.6$. In a study conducted at a building scale, (Sherman and Dickerhoff, 1998) found that the mean airflow exponent for 2224 houses tested in the US was $0.65$ with a standard deviation of $0.08$.

In (Prignon and Van Moeseke, 2017) – Appendix A, we suggested that a standardised metric should: (i) have a simple meaning; (ii) allow the comparison of buildings with different sizes; (iii) be related to the regulations; and (iv) give information to the user of the main leakage paths in the building. In the same work, we stated that, in our opinion, none of the existing metric fulfil these requirements and that the possibility of adding complementary metrics when reporting the result of a fan pressurisation test should be investigated.

However, without further investigation, we choose to report the air leakage rate at 50 Pa ($q_{50}$) alongside the airflow exponent ($n$). The air leakage rate at 50 Pa is the most used in Europe, and the airflow exponent can be used to convert $q_{50}$ to the other mainly used metric (ELA).

### 2.2.2. Measurement of Building Airtightness

(Šadauskienė et al., 2016) showed that energy performance calculations are only reliable after verifying the building airtightness, pointing out the crucial role of airtightness measurements. Consequently, and as highlighted by (Leprince et al.,

2017b), airtightness measurement of new buildings is becoming a common practice in more and more countries.

The most popular test to measure building airtightness is the fan pressurisation method, also called the blower door test. It consists of the pressurisation and the depressurisation of the building while recording couples of airflows and pressure differences. A linear regression is then conducted with these measurements to determine the flow characteristics (i.e. $n$ and $C_L$). Once these are obtained, the result of the test can be expressed in the desired metric. This method assumes that the building is described as one "average" opening and, therefore, the relation between the airflow and the pressure difference is expressed by the power law (Eq. 4).

The norm related to the fan pressurisation measurement is (ISO 9972:2015, 2015). This norm also describes the calculations required to correct the bias induced by the wind and the temperature difference experienced during the measurement. The uncertainty related to the fan pressurisation test is strongly documented and is still a burning topic in the field.

The Pulse technique is a promising alternative to the fan pressurisation measurements in cases where large amount of airflow should be avoided in the building. It consists of releasing a pulse of compressed air in the building over a short period in order to create an instant pressure rise. A steady pressure drop follows this instant rise in order to induce a "quasi-steady" flow. For more information about these alternative measurement methods, the reader should refer to (Zheng et al., 2020) and (Zheng et al., 2019).

### 2.2.3. Variables Influencing Airtightness

Knowing the variables influencing airtightness is crucial to develop relevant models and to have a better overview of the issues related to this specific building performance. In (Prignon and Van Moeseke, 2017) – Appendix A, we identified, categorised and ranked the variables influencing airtightness performance of buildings. This work reviewed 14 studies conducted between 1984 and 2016 that investigated, or provided required data to investigate, how the different variables impacted airtightness of buildings.

Fifteen variables are identified in the review and classified in four categories: geometry; technology and materials; guidance and supervision; and others.

Figure 1 shows these variables, including the number of studies founding them significant (left numbers) and not significant (right number). The bold variables are those found mostly, or unanimously, significant. Eleven other variables are not included in the classification because they are investigated in only one study:

- Number of penetrations, insulation type, foundation type, insulation position, duct location, ceiling type and feedback and guidance are found significant.
- Roof type, heating systems, window material and floor structure are found not significant.

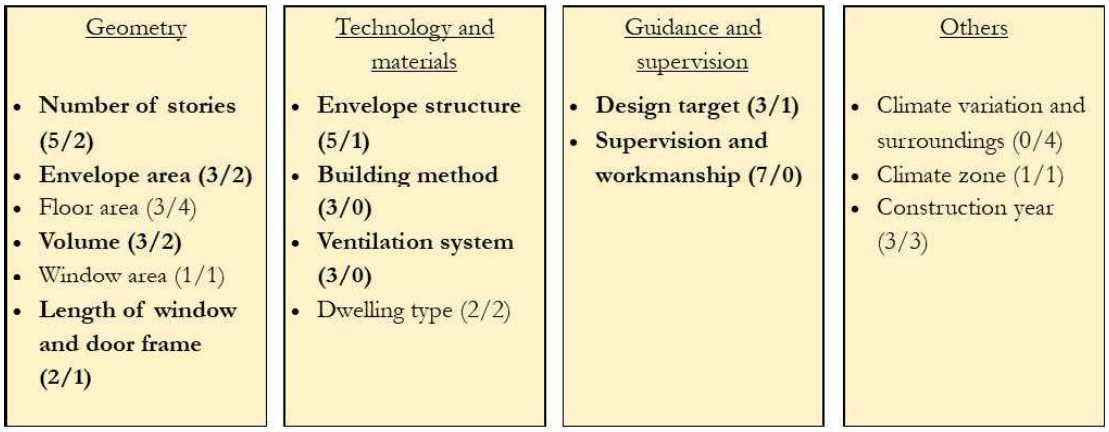



Figure 1: Classification of variables investigated by at least two studies. The numbers in brackets are the number of studies finding a significant (left) or not significant (right) impact on airtightness. The bold variables are those found mostly or unanimously significant.

Drawing a conclusion based on the observed trends in different studies is irrelevant for many variables because of the inconsistencies between studies. These inconsistencies could possibly explain the heterogeneity observed in the significance of some variables. These studies have the three following noticeable inconsistencies between them:

- The possible values for each variable. For example, in (Vinha et al., 2015) the number of stories is a Boolean (single-story or multi-stories) while in (Fernández-Agüera et al., 2016) it is an integer.
- The definition of variables. For example, the building method refers to the envelope materials in (Šadauskienė et al., 2016) and to the use of prefabricated elements in (Kalamees, 2007).

- The method for the statistical analysis and the way results are reported. For example, (Sinnott and Dyer, 2012) reported the raw data without a statistical analysis of these while (Bramiana et al., 2016) reported the p-values of ANOVA tests. In addition, all the studies limit their analysis to the statistical significance while reporting the effect sizes would give information about the magnitude of the impact these different variables have on building airtightness.

The differences in sample characteristics could also explain the heterogeneity of results: the country of the measurement, the equipment used, the testing procedure or the behaviour of the occupant. (Prignon and Van Moeseke, 2017) provides a deeper analysis of each variable and each category.

Although conclusions should be drawn carefully, two important outcomes should be mentioned and highlighted. First, although many variables related to "technology and materials" are found significant, (Vinha et al., 2015) demonstrated that good airtightness can be reached in every situation, regardless of the technological choices, the materials or the geometry. Second, the impact of "supervision and workmanship" variable is found unanimously significant and 7 out of 14 studies investigated it. This was expected since air infiltration is caused by unwanted openings in the building and since these are often created during the construction process. This observation highlights the importance of *in-situ* measurements since modelling the defects in computational software or simulating them in laboratory conditions may be difficult.

### 2.2.4. Predicting Building Airtightness

Modelling and predicting building airtightness sparks the interest of different stakeholders in the building sector, and this interest is expected to growth with the recent amendment of European Directives (European Parliament and Council, 2018). Models of building airtightness can have many different uses and forms. In (Prignon and Van Moeseke, 2017) – Appendix A, we identified four types of models used in this context:

Theoretical models develop the fundamental equations of fluid mechanics to determine the air leakage rate through the building envelope. They can have many different levels of complexity depending on how the equations are simplified and on the assumptions made. For example, one can describe the

flow through each crack individually with the complete Navier-Stokes equations or consider the building as one single "average" crack.

Empirical models define the air leakage rate through the building envelope as a weighted sum of different variables. The weight of each variable is usually obtained by conducting a multilinear regression analysis of the previous measurements. (Field et al., 2012) defined the multilinear regression as a statistical tool used to determine the relation between the variable of interest (e.g. airtightness performance) and numerous other variables. The accuracy of such model depends on the number of buildings used to develop the model and on how close the building modelled is from the buildings previously tested.

Building characteristic models define a basic leakage for the building. Then, increments and multiplication factors are applied to this basic leakage, depending on the building characteristics. The value of these increments and multiplication factors are determined by scientific judgement, which can be the result of experiments, the available literature or a personal experience.

Single component models are the most detailed version of the building characteristic model: starting with an air leakage rate of zero and using each building component as an increment. In fact, the total air leakage rate is the sum of the air leakage rate through each opening.

Despite the strong interest in prediction of building airtightness, nowadays none of these models is used in practice. (Relander et al., 2012) found that no researcher argues that models could replace airtightness measurements. The importance of supervision and workmanship, which are tough to implement in predictive models, explain this finding. In addition, two additional important drawbacks are barriers to their use. On the one hand, empirical models and building characteristic models based on measurements are suitable for buildings close to those used to develop the model. This suggests that they are appropriate for the short term since construction techniques are expected to change over time. On the other hand, the lack of updated crack data induces a lack of reliability in theoretical and single component models. In (Prignon and Van Moeseke, 2017) – Appendix A, we suggested that single component models are the most promising, provided the update and the enlargement (with reliable *in-situ* measurements) of available databases of building component airtightness.

### 2.2.5. Energy Policies and Building Airtightness

(Leprince et al., 2017a) reported the results of questionnaires sent to TAAC (TightVent Airtightness Association Committee) members that aim to investigate building airtightness requirements in 10 European countries: Belgium, Czech Republic, Estonia, France, Germany, Latvia, Ireland, Poland, Sweden and the UK. At that time, 7 out of 10 (all except Czech Republic, Sweden and Latvia) took airtightness into account in their energy performance regulation and 8 out of 10 (all except Sweden and Latvia) took it into account in their energy performance calculation programs. In a recent paper, (Poza-Casado et al., 2020) showed that in Europe and North America 25 countries have a regulation including mandatory values for airtightness in residential buildings but only 5 of them make the on-site testing mandatory. In addition, 4 countries have default values that may be improved with a fan pressurisation test and 1 has recommended value only. Lastly, 16 countries have no regulation regarding airtightness performance.

(Poza-Casado et al., 2020) showed that 27 out of 30 countries used a reference pressure of 50 Pa in the regulations. (Carrié and Wouters, 2012) stated that a pressure difference of 50 Pa is high enough to make wind and stack effects negligible compared to the pressure generated during the test. However, some countries (e.g., France or Netherlands) refers to a lower pressure difference (4 or 10 Pa) to have a better estimate of the infiltration flow at low-pressure difference that may be used in certain energy calculation methods. Regarding the normalisation of the airflow (Poza-Casado et al., 2020) showed that 16 out of 30 countries refer to an air change rate (i.e. air leakage rate divided by the volume), 2 out of 30 refer to a specific air leakage rate (i.e. air leakage rate divided by the envelope area) and 12 out of 30 refer to an air permeability rate (i.e. air leakage rate divided by the net floor area).

Spain is, to our knowledge, the only country to impose a maximum air leakage rate for building components. In (CTE HE1, 2019), Spain requires a maximum air leakage rate at 100 Pa for windows, depending on the climate zone. In addition to windows, the questionnaires sent to TAAC reported in (Leprince et al., 2017a) showed that 2 out of 10 countries (Belgium – Flemish region and France) considered ductwork airtightness as an input in the energy performance regulation but no minimum requirements. This is because of the consequences of poor ductwork airtightness. As for other building components, a poor ductwork airtightness induces an increase in the heating and cooling demands.

(Berthault et al., 2014) showed that the fan must compensate leakage through the duct system to supply enough airflow in different rooms, which has an impact on the fan energy use and the noise it generates. However, despite their importance, these are the only cases where the airtightness performance of components is considered in the energy performance regulation or the energy performance calculation programs.

## 2.3. Measuring Airtightness of Building Components

The previous section highlights the lack of crack data to integrate air infiltration accurately into the indoor environment models and to use the single component models to predict building airtightness. In this section, we review and discuss the existing methods to measure airtightness of building components. These are divided in two categories: the laboratory and the *in-situ* measurement methods.

### 2.3.1. Laboratory Testing

The laboratory testing is the most used method for measuring building component airtightness. (EN 12114:2000, 2000) and (ASTM 283, 2004) are respectively the European and the US standards for laboratory measurements of building component airtightness.

The laboratory measurement consists of the construction of a perfectly airtight pressure chamber surrounding the specimen tested, then pressurising and depressurising it with a fan. A flowmeter and a manometer are used to record the airflow – pressure difference couples that are then used to determine the air leakage characteristics (i.e. $C_L$ and $n$) of the specimen. The steps of this protocol are like the fan pressurisation test in (ISO 9972:2015, 2015). Multiple authors, including (Cosmulescu, 1997) and (Feldman et al., 1998), suggested an improved system made of two chambers to control the environment on both sides of the tested specimen. The strong advantage of using two pressure chambers is the possibility to simulate various combinations of indoor and outdoor environments.

The laboratory test can be very useful to observe directly how the component behaves, which can hardly be done *in-situ* since the defects in the measured components are often hidden behind other components. The visualisation of

the component helps to understand the airflow pattern and, consequently, to improve the airtightness performance. However, the specimens tested in laboratory conditions are expected to be more airtight than once installed since the workmanship error is lower thanks to the controlled and clean environment. This is an important issue related to the laboratory testing since the supervision and the workmanship are strongly impacting the airtightness of the building. These types of error can be simulated in the laboratory, but large differences with the errors experienced in practice are expected. Thus, the laboratory measurements can be less relevant for many building components because the main defects are caused during the construction process.

In addition, the laboratory testing measures the components that are not yet installed. This can be an important constraint for the durability studies. Indeed, when such studies are conducted in laboratory conditions, the impact of daily use on the component performance must be simulated, increasing the uncertainty of the result. An example of laboratory study conducted to investigate the impact of durability on airtightness performance is presented in (Litvak et al., 2019).

### 2.3.2. *In-situ* Testing

The *in-situ* testing aims to measure building components once installed on the site. This type of testing is very relevant when dealing with the airtightness since the biggest defects in building components occur during the component installation or during its use (deterioration). Therefore, being able to quantify the airtightness performance of building components in real configuration is a major concern in the field of building airtightness.

Despite their importance, the *in-situ* testing methods have low popularity in the current practice. Two drawbacks of this type of testing may probably explain this low popularity. First, for new constructions and retrofit, *in-situ* measurements must fit in the execution planning. Second, the environmental conditions, mostly the wind speed and its direction, have a huge impact on the results for some of these methods.

The *in-situ* tests of building components are hardly asked in the building specifications or the requirements for a new construction project. Nevertheless, it is sometimes used when looking for the causes that could explain that a performance is not reached. In the cases of retrofitting, these measurements

provide an insight about the improvement obtained with the solution implemented.

*In-situ* measurements of building components can be divided in four categories:

The guard-zone technique, also called the balanced fan pressurisation or the multizone air leakage measurement, is a zonal measurement. It consists of pressurising one zone while balancing the pressure in adjacent zones. In that way, the fan pressurisation test measures only leakage to the non-balanced zones. Although this method does not measure a specific building component, it measures the air leakage rate through one surface, which can be useful for the simplified multizone models. It is considered as an intermediate between the component and the building measurements. The uncertainty of the guard-zone technique is relatively well documented and is estimated in the literature between 10 and 15%. Recently, (Rohr et al., 2018) used this method to quantify the interior-to-exterior air leakage rate ratio and (Guyot et al., 2016) and (Shin and Jo, 2013) quantified the air leakage rate through interior partitions.

Acoustical methods consist of estimating the air leakage rate through the building components by measuring the sound transmission losses. (Hurel, 2016) pointed out that the low popularity of acoustical methods is due to the difficulty in generalising it to all building components: each building component has its own semi-empirical correlation between the sound transmission and the air leakage. Only a few studies investigate this method, and none of them discuss its uncertainty. The recent work on this method conducted by (Varshney et al., 2013) and (Kölsch et al., 2019) focused on the validation in laboratory conditions. However, (Varshney et al., 2013) and (Iordache and Catalina, 2012) tested the method *in-situ*, exclusively on windows. Besides these tests, (Hassan, 2013) developed a general model to evaluate the leakage area and air leakage rate of other building components, but his work was not validated on site.

The indirect component testing, also called the progressive or the reductive sealing, is the most used in practice. It consists of performing two successive fan pressurisation tests on a delimited zone: one in normal conditions and the second with the component of interest sealed. The difference between pre- and post-sealing measurements gives the air leakage rate attributed to the component. This method is often used in practice because it is easy to implement and can quickly measure multiple components. However, two

important issues are highlighted in the literature. First, (Almeida et al., 2017) found a hysteresis effect in the sealing order when they used it to measure multiple components. Second, (Colliver et al., 1992) and (Almeida et al., 2017) explained that the method has a large uncertainty. The uncertainty of the indirect method is estimated between 7.6% and 32%. This aspect is further investigated in section 5.4. Recently, (Pinto et al., 2011) used it to estimate the airtightness of multiple building components (self-regulated inlets, windows, roller-shutter boxes and doors) and (Almeida et al., 2017) estimated window airtightness with this method.

The direct component testing is the same setup and protocol as for the laboratory measurements with one chamber. It consists of the pressurisation and the depressurisation of a chamber that isolates the building component. As the fan pressurisation test for building measurements, this method measures the airflow required to maintain a constant pressure difference between inside and outside the pressure chamber. The direct component technique is expected to measure the airtightness of building components with a better accuracy than the indirect component testing since it is not based on the result of a fan pressurisation tests conducted on whole building. However, this method is more difficult to implement in practice and a particular attention must be paid to the airtightness and the resistance of the pressure chamber. (Colliver et al., 1992) stated that balancing the pressure in the room containing the chamber may improve the method. In fact, this would reduce the uncertainty and to avoid measuring an accidental leakage in the construction of the chamber. However, this increases the time and the complexity of the measurement; and involves additional constraints. Although promising, this method has never been described properly or validated, and its uncertainty has never been quantified thoroughly. There is no recent reference work on the use of this method.

## 2.4. Meta-Analysis of Studies Measuring Building Component Airtightness

In (Prignon et al., 2020c) – Appendix B, we conducted a meta-analysis to combine evidences and the results of studies reporting measurement of building component airtightness, whatever the method used. According to (Egger et al., 2002) and (Field and Gillett, 2010), a meta-analysis is a set of tools used to

consolidate rigorously the evidence of different studies from the literature, by weighting each evidence based on their reliability. (Tatsioni and Ioannidis, 2008) explained that the meta-analysis can also be used to explore the heterogeneity among studies (i.e. the reasons for the variations observed between studies). This second aspect is important since it can help to investigate and understand the factors influencing the variation in the results, which is crucial for their interpretation. (Borenstein et al., 2011) explained that the meta-analysis is not limited to effect sizes and can be used to combine *single group summaries* (e.g. the mean, the median, or the standard deviation). This is important in the context of building component airtightness since the studies commonly report the average leakage data rather than the effect size of evidence.

A meta-analysis includes three main steps:

- The study selection is based on a rigorous review of the literature that contributes to an unambiguous research question. (Field and Gillett, 2010) explained that a badly conducted research can bias the combined effect. Therefore, the meta-analysis does not have to include all studies targeting the research question. However, it is important when conducting a meta-analysis to describe thoroughly the protocol for the study selection, including the inclusion and the exclusion criteria for each study. Once all studies are selected, the outcome of interest must be extracted from each study. This can be an effect size or a simple group summary, but it must be consistent with the research question of the systematic review.
- The combination of studies consists of weighting each study according to its reliability. Then, the combined outcome and its standard error are computed.
- Exploring the heterogeneity consists of determining if the variations observed between studies are above the variations expected by chance. For this step, the index of inconsistency ($I^2$) is calculated. It is the proportion of total variation that is due to the heterogeneity between studies. Values of 25%, 50% and 75% correspond respectively to low, moderate, and high inconsistency.

For a more detailed description of each step, of the equations and of the application of the meta-analysis in this specific context, the reader should refer to (Prignon et al., 2020c) – appendix B. Three main outcomes obtained with the meta-analysis are summarised hereafter: the classification of building components, the combined results and the exploration of heterogeneity.

### 2.4.1. Classification of Building Components

The first result obtained from this review is a list of building components for which airtightness measurements are reported and which are expected to impact building airtightness. This list is used to build a 4-level classification of building components. Figure 2 illustrates the three types of flows identified in the first level of the classification: partitions and surfaces, junction between surfaces and discontinuities.

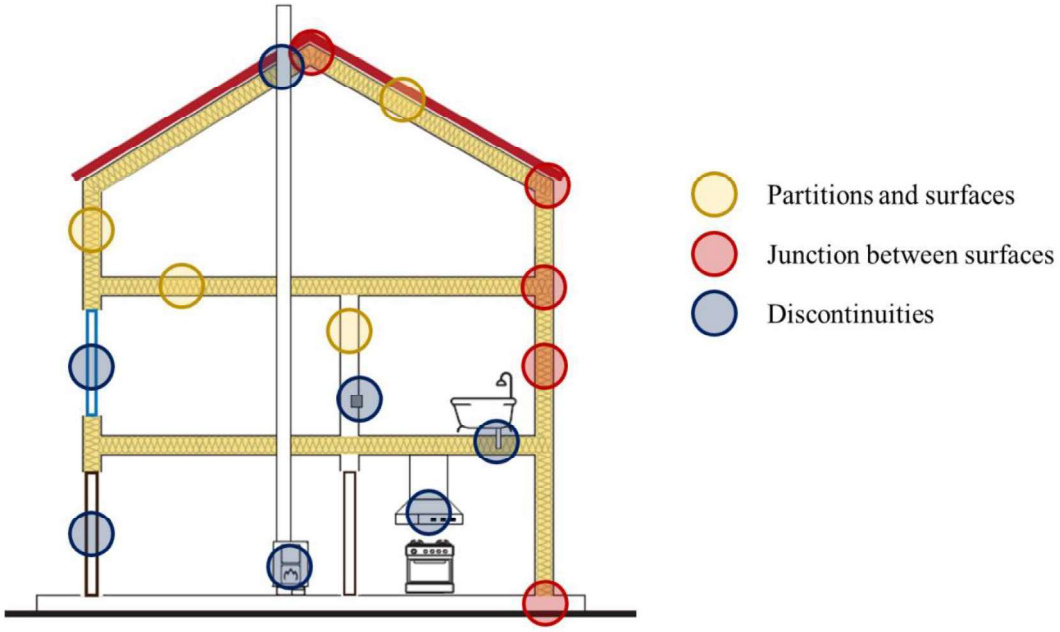



Figure 2: illustration of the first level classification of building components regarding the type of flow.

Each type of flow is further divided in three additional levels: the category of components (level 2), the components (level 3) and the type & treatment (level 4). Figure 3 shows the complete 4-level classification. The underlined components are those for which at least two studies met the inclusion criteria in order to conduct the meta-analysis.

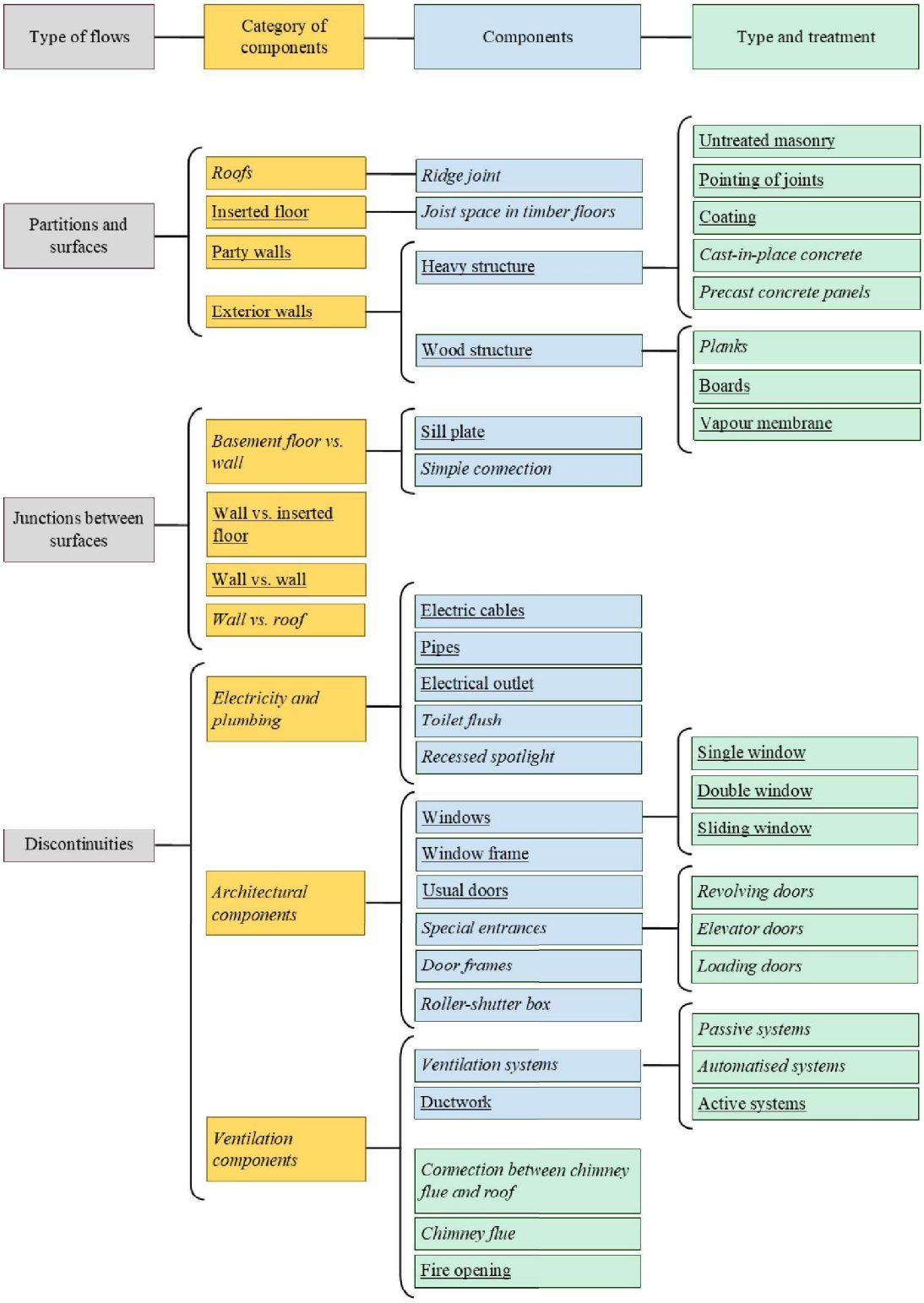



Figure 3: 4-level classification of building components based on studies reporting at least two measurements of air leakage rates through building components.

Since the classification is based on the building component measured in the studies reported, it is expected to enlarge and improve over the years, by including the future studies that report the measurements of building component airtightness.

### 2.4.2. Combined Outcome, Standard Error and Inconsistency Index

This section provides the results of the meta-analysis for each component investigated in the literature. These include the air leakage rate at 50 Pa and the airflow exponent, the number of studies combined, the combined mean and standard error, and the index of inconsistency. Table 1 presents this outcome of the meta-analysis. It also includes the mean and the standard deviation for components when only one study meets the inclusion criteria. The index of inconsistency is not computed since the meta-analysis is not conducted. (Prignon et al., 2020c) – Appendix B provided a detailed analysis of each component and a complete list of the references (included and excluded).

Table 1: Results of the meta-analysis. Units for the air leakage rate at 50 Pa depend on the component: [a] = $m^3/(h.m^2)$, [b] = $m^3/(h.m)$ and [c] = $m^3/h$.

| | $q_{50}$ | | | | $n$ | | | |
|---|---|---|---|---|---|---|---|---|
| | **N** | $q_{50}$ | **SE** | $I^2$ | **N** | $n$ | **SE** | $I^2$ |
| **Leakage through partition and surfaces** | | | | | | | | |
| Roof [a] | 1 | 95.8 | 55.4 | - | 1 | 0.63 | 0.18 | - |
| Inserted floor [a] | 3 | 1.4 | 1.5 | 36.7 | 1 | 0.59 | 0.10 | - |
| Party walls [a] | 2 | 2.9 | 0.6 | 0.0 | - | - | - | - |
| Exterior walls [a] | 11 | 1.6 | 0.5 | 88.6 | 5 | 0.76 | 0.06 | 29.6 |
| Untreated masonry [a] | 5 | 11.3 | 5.8 | 93.3 | 5 | 0.78 | 0.04 | 82.2 |
| Masonry with pointing of joints [a] | 2 | 1.0 | 0.7 | 0.0 | 1 | 0.81 | 0.10 | - |
| Masonry with coating [a] | 6 | 0.1 | 0.1 | 15.7 | 4 | 0.94 | 0.07 | 70.2 |
| Cast-in-place concrete [a] | 1 | 2.4 | 2.4 | - | 1 | 0.61 | 0.14 | - |
| Precast concrete panels [a] | 1 | 1.4 | 0.5 | - | 1 | 0.68 | 0.18 | - |
| Boards [a] | 6 | 0.0 | 0.0 | 31.6 | 3 | 0.98 | 0.01 | 15.1 |
| Planks [a] | 1 | 16.9 | 15.4 | - | 1 | 0.76 | 0.08 | - |
| Vapour membrane [a] | 2 | 0.1 | 0.1 | 0.0 | 2 | 0.76 | 0.08 | 0.0 |
| **Leakage through junctions between surfaces** | | | | | | | | |
| Basement floor vs. wall, sill plate [b] | 4 | 0.2 | 0.0 | 0.0 | 2 | 0.69 | 0.17 | 95.2 |
| Basement floor vs. wall, simple connection [b] | 1 | 17.9 | 25.0 | - | 1 | 0.71 | 0.20 | - |
| Wall vs. inserted floor [b] | 2 | 1.2 | 0.8 | 0.0 | 1 | 0.78 | 0.03 | - |
| Wall vs. wall [b] | 2 | 0.5 | 0.1 | 0.0 | 1 | 0.71 | 0.09 | - |
| **Leakage through electrical and plumbing components** | | | | | | | | |
| Electric cable penetration [c] | 2 | 0.1 | 0.1 | 96.4 | - | - | - | - |
| Pipe penetration [c] | 3 | 1.6 | 1.1 | 0.0 | 1 | 0.66 | 0.08 | - |
| Electrical outlet [c] | 4 | 2.7 | 0.9 | 0.0 | 1 | 0.69 | 0.13 | - |
| Toilet flush [c] | 1 | 21.0 | 5.9 | - | - | - | - | - |
| Recessed spotlight [c] | 1 | 10.6 | 13.3 | - | - | - | - | - |
| **Leakage through ventilation components** | | | | | | | | |
| Humidity-sensitive grille [c] | 1 | 61.4 | 39.2 | - | 1 | 0.58 | 0.11 | - |
| Self-regulated grille [c] | 1 | 37.0 | 0.4 | - | - | - | - | - |
| Extractors with damper close [c] | 1 | 11.5 | 5.8 | - | - | - | - | - |
| Extractors with damper open [c] | 3 | 52.3 | 14.0 | 0.0 | - | - | - | - |
| Fan – false ceiling connection [c] | 1 | 9.6 | 11.4 | - | - | - | - | - |
| Ductwork [a] | 2 | 0.8 | 0.9 | 0.0 | 1 | 0.59 | 0.04 | 0.0 |
| Chimney flue – roof connection [c] | 1 | 37.2 | 108.5 | - | 1 | 0.81 | 0.16 | - |
| Chimney flue [c] | 1 | 14.1 | 16.8 | - | 1 | 0.72 | 0.06 | - |
| Fire opening [c] | 3 | 141.9 | 57.8 | 95.6 | - | - | - | - |
| **Leakage through architectural components** | | | | | | | | |
| Windows [b] | 12 | 2.0 | 0.6 | 36.3 | 3 | 0.69 | 0.07 | 52.0 |
| Window frame [b] | 4 | 0.3 | 0.2 | 81.0 | - | - | - | - |
| Roller-shutter box [c] | 1 | 6.0 | 1.4 | - | - | - | - | - |
| Doors [c] | 8 | 137.6 | 46.7 | 87.3 | 3 | 0.62 | 0.16 | 0.0 |
| Elevator door [c] | 1 | 1049.6 | 156.7 | - | 1 | 0.59 | 0.12 | - |
| Revolving door [c] | 1 | 1908.0 | 1294.2 | - | 1 | 0.71 | 0.04 | - |

Although these are not directly measuring building components, two interesting results are worth mentioning. On the one hand, Table 2 summarises the work done by (Hall and Hauser, 2003) and (Langmans et al., 2010b) on the quantification of the air leakage rate induced by the typical faults in board walls. On the other hand, Table 3 summarises the work done by (Hall and Hauser, 2003) and (Gullbrekken et al., 2017) on how the installation or a defect in the vapour membrane or at the connection between two parts of the membrane affect its performance. These results illustrate the large impact human errors in the installation of the building components have on its airtightness performance.

Table 2: mean and standard deviation of defects in boards reported by (Hall and Hauser, 2003) and (Langmans et al., 2010a).

| Type of defect | $\overline{q_{50}}$ | $SE(\overline{q_{50}})$ |
|---|---|---|
| Tongue and groove joint ($m^3/(h.m)$) | 1.4 | 1.6 |
| Double-board corner joint ($m^3/(h.m)$) | 6.7 | 9.5 |
| Triple-board corner joint ($m^3/h$) | 3.7 | 3.1 |
| Hole in gypsum boards (between 5 and 55 mm in diameter) ($m^3/h$) | 12.4 | 7.3 |
| Space between boards (between 0.5 and 2.5 mm) ($m^3/(h.m)$) | 4.1 | 4.3 |

Table 3: mean and standard deviation for defects in vapour membrane reported by (Hall and Hauser, 2003) and (Gullbrekken et al., 2017).

| Type of defect | $\overline{q_{50}}$ | $SE(\overline{q_{50}})$ |
|---|---|---|
| Screws ($m^3/(h.screw)$) | 0.1 | 0.1 |
| Staples ($m^3/(h.staple)$) | 0.2 | 0.2 |
| Loose clamped joint ($m^3/(h.m)$) | 0.1 | 0.2 |
| Missing tape at vapour connection ($m^3/h$) | 0.7 | 0.3 |
| Cut in the foil ($m^3/(h.m)$) | 2.2 | 0.9 |
| Hole in the foil ($m^3/h$) | 4.5 | 3.8 |

### 2.4.3. Exploring the Heterogeneity and the Variables Influencing Window Airtightness

Window is the most reported component and most studies report larger samples than for the other components. The large impact of windows on airtightness, and the ease to measure the window airtightness on site compared to the other building components, explain this high interest. This higher

number of studies makes it possible to investigate deeper the heterogeneity among studies and the variables influencing window airtightness.

Table 4 provides details about the studies used in the meta-analysis on windows. For each study, the table provides the reference, which includes the authors and the year of publication, the sample size, the type of measurement performed (i.e. laboratory or in-situ), the material of windows (wood, aluminium or unspecified materials) and the type of windows (double window, single window, sliding window or unspecified type).

Table 4: List of publication used for the meta-analysis on windows, including the authors, the year, the sample size (N), the type of measurement (laboratory or *in-situ*), the material (W = Wood, A = Aluminium or Um = Unspecified material) and the type (DW = Double window, SW = Single window, SL = Sliding window or Ut = Unspecified type) of windows measured.

| # | Ref | N | Type of measurement | W | A | Um | DW | SW | SL | Ut |
|---|---|---|---|---|---|---|---|---|---|---|
| 1 | (Tamura, 1975) | 17 | *In-situ* | x | | | x | x | x | |
| 2 | (Lowinski, 1979) | 6 | Laboratory | x | | | x | x | | |
| 3 | (Almeida et al., 2017) | 23 | *In-situ* | x | x | | x | x | x | |
| 4 | (Weidt et al., 1979) | 192 | *In-situ* | x | x | | x | x | x | |
| 5 | (Larson et al., 1930) | 14 | Laboratory | x | | | x | | x | |
| 6 | (Van Den Bossche and Janssens, 2016) | 437 | Laboratory | | | x | x | x | x | |
| 7 | (Carruthers and Newman, 1977) | 131 | Laboratory | x | | | | x | | |
| 8 | (Pinto et al., 2011) | 3 | *In-situ* | | | x | | | x | |
| 9 | (Ward and Sharples, 1982) | 10 | *In-situ* | | | x | | | x | |
| 10 | (Hall and Hauser, 2003) | 10 | Laboratory | x | | | | x | | |
| 11 | (Persily and Grot, 1984) | 18 | *In-situ* | | | x | | | | x |
| 12 | (CMHC, 1991) | 6 | Laboratory | | | x | | | | x |

Figure 4 illustrates the results of the meta-analysis conducted on these 12 studies. Black lines represent, the 95% confidence interval ($\overline{q_{50}} \pm 2 * \mathrm{SE}(\overline{q_{50}})$) around the mean value ($\overline{q_{50}}$, black dots). The last line (in blue) is the total 95% confidence interval obtained when combining all studies, and the red dashed line is the mean value for the combined result. A confidence interval is a range of plausible values for the true quantity, based on the measured value, its

uncertainty and a coverage factor. It is $[y - k.u(y); y + k.u(y)]$, where $k$ is the coverage factor and $u(y)$ is the uncertainty of the variable $y$. When $y$ is normally distributed, $k = 1$, $k = 2$ and $k = 3$ define the confidence intervals having a 67%, 95% and 99% probability of containing the true quantity.

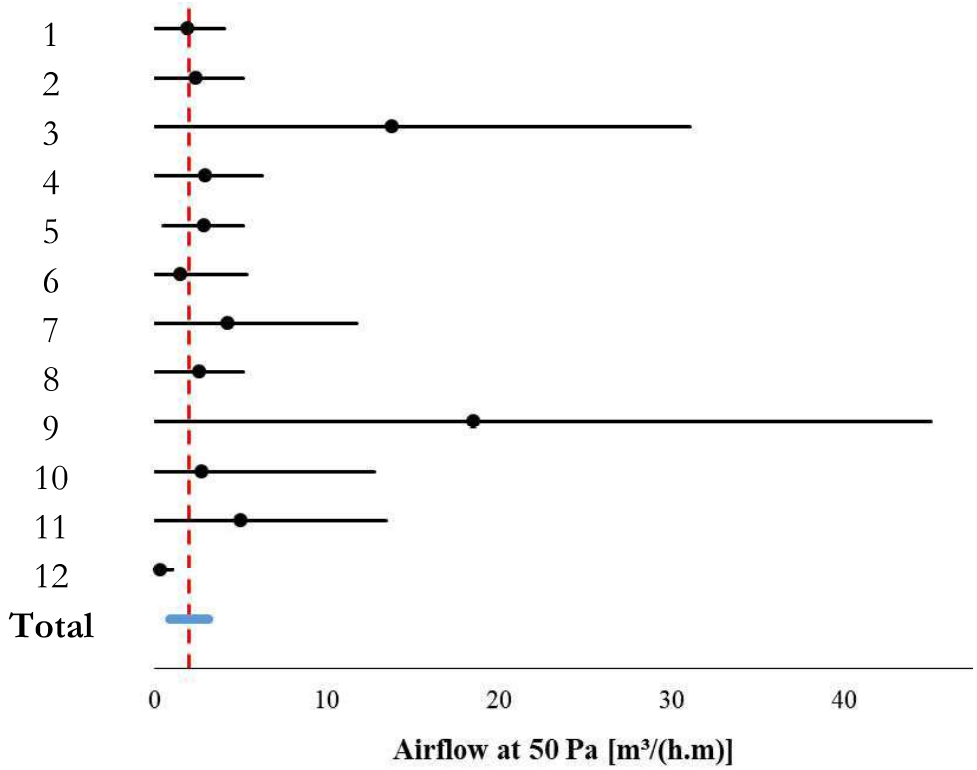



Figure 4: Forest plot obtained from the meta-analysis conducted on windows studies

This figure shows that the combined mean value (2.0 m³/(h.m)) falls outside the 95% confidence interval of one study (CMHC, 1991). The difference observed is because (CMHC, 1991) tested only inoperable windows, while the other studies look at the different types of operable windows. The meta-analysis conducted on the 11 other cases strengthens that this study was responsible for the inconsistency: $\overline{q_{50}} = 2.5$ m³/(h.m), $\mathrm{SE}(\overline{q_{50}}) = 0.5$ m³/(h.m) and $I^2 = 0.0$ %. Therefore, the following investigations involve a pool of 11 studies.

The subgroup meta-analysis provides an insight on how the variables influence the measurement of window airtightness. Table 5 shows the result of three subgroups meta-analysis conducted for different variables: the measurement methods, the type of windows and the materials. Remember that the subgroup

meta-analyses are conducted on fewer studies compared to the entire group used for the meta-analysis and, then, have a higher uncertainty as regards the calculation of $I^2$ and $\mathrm{SE}(\overline{q_{50}})$.

Table 5: sample size, mean, standard error (in m³/(h.m)) and inconsistency for airflow at 50 Pa for three subgroups meta-analyses based on the measurement method, the type of window and the window material.

| Subgroup analysis | | $q_{50}$ | | | |
|---|---|---|---|---|---|
| | | N | $\overline{q_{50}}$ | $\mathrm{SE}(\overline{q_{50}})$ | $I^2$ (%) |
| Measurement method | In-situ | 6 | 2.5 | 0.7 | 0.0 |
| | Laboratory | 5 | 2.5 | 0.8 | 0.0 |
| Type of windows | Single windows | 7 | 1.8 | 0.5 | 50.7 |
| | Double windows | 6 | 2.0 | 0.5 | 0.0 |
| | Sliding windows | 7 | 3.2 | 0.7 | 18.9 |
| | Unspecified | 1 | 5.0 | 4.2 | - |
| Window materials | Wood windows | 7 | 2.4 | 0.6 | 0.0 |
| | Aluminium | 2 | 4.1 | 1.5 | 0.0 |
| | Unspecified | 4 | 2.5 | 1.0 | 0.0 |

These subgroups meta-analyses show differences in the types of windows and in the window materials (different means and standard deviation), but not in the measurement methods (*in-situ* vs. laboratory). Other variables could have been relevant in this context (e.g. the year of implementation for windows measured *in-situ*), but the lack of information provided in the studies prevent the conduction of other subgroup meta-analyses.

### 2.4.4. Reporting Measurements of Building Component Airtightness

The meta-analysis reveals some important limitations related to the available literature: the low number of studies available; the lack of studies focusing on the treatment of components; and the missing information on the tested components. Consequently, the outcomes obtained should be considered in light of these limitations:

- More studies would reduce the uncertainty of $I^2$ and $\mathrm{SE}(\overline{q_{50}})$ for the meta-analysis and the subgroup meta-analyses, and would increase the potential

of the subgroup meta-analysis when exploring the heterogeneity by making it less likely to have subgroups created from only one study.
- Investigating the different treatments might induce different airtightness performances. Therefore, looking at each treatment individually would result in a smaller range of measured airflow and a lower standard deviation.
- Providing more information about the components tested would increase the possibilities for the subgroup meta-analysis.

These limitations not only influence the outcomes of the meta-analysis but also affect the results of any study reporting measurements of building components. This is a potential reason for the relatively sparse literature available on the airtightness performance of building components, despite its large potential. However, increasing the number of studies would not be helpful unless their experimental design and the methods to report results are appropriate for the meta-analysis. To improve the statistical power, the reliability, and the potential applicability of the meta-analysis approach, future studies should meet four requirements:

- Each study should measure at least two cases for each component and provide a standard deviation in addition to the mean value. Moreover, a larger number of measurements would result in a more accurate calculation of the standard deviation and, therefore, a more accurate weighting in the study combination.
- The characteristics of the measured sample should be described thoroughly based on previous research (e.g. the materials of the component, the year of testing, the year of implementation, etc.). The sample description should refer to the classification suggested in this paper as a new component, a new treatment or an additional evidence to a case already investigated.
- The airtightness performance of building components must be reported with the airflow exponent, and the information required for different normalisations encountered in the literature.
- The studies comparing different treatments of windows should report the effect size of the observed difference between the treatments to make them comparable with previous studies, even if these have inherent differences (e.g. differences in the outcomes reported or in the measurement methods).

## 2.5. Summary of Chapter's Outcomes

In this chapter, we provide the fundamental knowledge and information required to have a good overview of the airtightness-related issues. This is important to grasp the importance of the work done and presented in following chapters. Then, we provide an overview of the research conducted these last years in the field of airtightness of buildings and building components. Last, we propose an update of databases of building component airtightness using a strong protocol for the combination of studies (the meta-analysis).

While the previous chapter stressed the importance of working on building component airtightness for the comfort and the health of occupants and for the better calculation of energy consumption, this chapter highlights:

- The importance of developing crack data to improve the indoor environment models and the prediction of airtightness. It also points out that a lack of studies reporting the measurements of building component airtightness hinders the availability of reliable data about building component airtightness.
- The importance of developing *in-situ* testing of building components because of the considerable influence supervision and workmanship have on building airtightness. In addition, it reveals the lack of properly described, accurate and validated method for *in-situ* measurement of building components.

# Chapter 3. Protocol and Equipment for the Direct Component Testing

In this chapter, we describe the direct component testing. This description includes the measurement protocol, the data processing and the equipment used. Although most of the work done for this thesis is described in this chapter, some assumptions are based on two publications:

- Appendix C: Prignon M., C. Delmotte, A. Dawans, S. Altomonte and G. Van Moeseke (2020). On the impact of regression techniques to airtightness measurement uncertainties. Energy and Buildings, **215**. https://doi.org/10.1016/j.enbuild.2020.109919.
- Appendix D: Prignon M., A. Dawans and G. Van Moeseke (2018). Uncertainties in airtightness measurements: regression methods and pressure sequences. *In 39th AIVC – 7th TightVent & 5th Venticool Conference: Smart ventilation for buildings.* Antibes Juan-Les-Pins, France.

## 3.1. Measurement and Data Processing

The direct component test consists of the introduction of a constant flow in an airtight chamber that isolates the measured component. This airtight chamber is called the "pressure chamber". The constant flow generates a pressure difference between both sides of the component ($\Delta p = p_1 - p_2$), inducing an airflow through the component. At a steady-state pressure difference, the airflow going in ($q_{in}$) is assumed equal to the airflow going out ($q_{out}$). If the pressure chamber is highly airtight (i.e. its air leakage rate is negligible compared to the measured air leakage rate), all the airflow going out is attributed to the

measured component. Figure 5 illustrates the principle of the direct component testing.

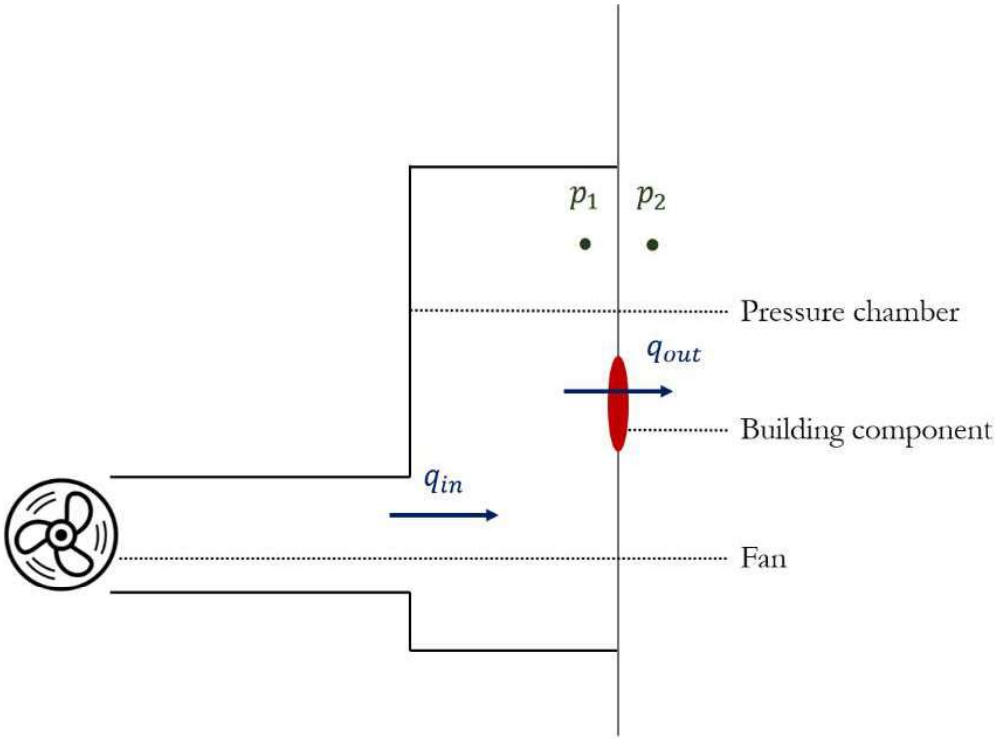



Figure 5: principle behind the direct component testing.

The objective of the direct component testing is to determine the relation between the airflow and the pressure difference for one specific building component. As explained in section 2.1.1, the power law (Eq. 4) is the generic form of this relation. Thus, the direct component testing aims to determine the airflow exponent ($n$) and the air leakage coefficient ($C_L$) in pressurisation and depressurisation.

The protocol for the direct component testing is similar to the fan pressurisation method for determining the air permeability of buildings, applied to smaller volumes. (ISO 9972:2015, 2015) describes this protocol. It has three main steps described in this section: to determine multiple ($\Delta p_i$ ; $q_i$) couples; to conduct the linear regression; and to report the results.

### 3.1.1. Determining Airflow and Pressure Difference

The first step of this test is to determine the airflow passing through an opening ($q_i$) generated by a pressure difference between both sides of the opening ($\Delta p_i$). This step requires multiple assumptions to convert the measured airflow ($q_m$) and the pressure differences ($\Delta p_m$) to the variables of interest ($q_i$ and $\Delta p_i$).

The pressure difference should be measured on both sides of the tested component. However, the "outside gauge" is hardly placed on the other side of the component because of accessibility issues. Consequently, the tester usually assumes that the pressure difference between inside and outside the chamber equals the pressure difference at both ends of the component. Particular attention should be paid to the location of the "outside gauge", which should be away from the flow disturbance induced by the fan. Regarding the "inside gauge", it may be placed in the duct connecting the fan to the pressure chamber or in the pressure chamber. This choice may induce biases in the pressure ($\delta p_L$) and/or the airflow ($\delta q_b$) measurements. These are discussed and quantified in sections 4.2 and 4.3.

The measured pressure difference ($\Delta p_m$) is a combination of the wind and the stack effects ($\Delta p_0$) and of the airflow artificially induced by the fan ($\Delta p_i$). Since the tester is interested in $\Delta p_i$, he or she must compute $\Delta p_0$ to correct $\Delta p_m$. $\Delta p_0$ is called the zero-flow pressure: it is the pressure difference measured when no flow is induced. Since $\Delta p_0$ can only be measured when the fan is not working, it is measured pre- ($\Delta p_{0,1}$) and post-test ($\Delta p_{0,2}$). It is assumed constant during the test and its value is the mean of $\Delta p_{0,1}$ and $\Delta p_{0,2}$.

Consequently, the pressure difference between both sides of the building component generated by the fan ($\Delta p_i$) is (Eq. 6) :

$$\Delta p_i = (\Delta p_m - \delta p_L) - \frac{\Delta p_{0,1} + \Delta p_{0,2}}{2} \quad \text{Eq. 6}$$

The direct component testing assumes that the airflow measured ($q_m$) equals the airflow leaking out through the component. However, based on the mass equilibrium in the chamber, this is true only if both fluxes have the same air density. Since the temperature impact air density, the ratio between the internal ($T_i$) and the external ($T_e$) temperatures are used to correct $q_m$ and to make this assumption valid. In addition, this method assumes that all the airflow goes out

through the component. However, in practice the pressure chamber is never perfectly airtight and the background leakage bias ($\delta q_b$) should be considered in the calculations (section 4.2).

Last, the fan is usually calibrated for a reference temperature that is different from the testing conditions. Thus, it must be corrected according to the relation provided by the manufacturer's technical sheets ($\alpha_c$) when the internal ($T_i$) and the external ($T_e$) temperatures experienced during the test are different from the reference temperature (usually 20°C).

Consequently, the airflow through the building component induced by the pressure difference between both sides equals (Eq. 7):

$$q_i = q_m \, \alpha_c(T_i, T_e) \left(\frac{T_i}{T_e}\right) - \delta q_b \qquad \text{Eq. 7}$$

This is, to our knowledge, an exhaustive list of the corrections investigated in the literature and, without more information, one should use Eq. 6 and Eq. 7 to correct the measured airflow and the pressure difference. However, some other corrections could be considered in future research. Examples are the impact of gust wind on the airflow measurements; the location of the outside pressure tap; and the position of the thermometer for temperature measurements. Although the temperature is hardly investigated in the case of fan pressurisation or direct component testing, the stratification effect is expected to impact the measured airflow and their uncertainty.

Regarding the choice of pressure difference sequence for the measurements, the same constraints were considered her than those suggested by the (ISO 9972:2015, 2015) standard for the fan pressurisation test of buildings. Those are: *increments of no more than approximately 10 Pa* ; *at least five approximately equally space data points between the lowest and the highest pressure difference* ; *the lowest pressure difference shall be approximately 10 Pa or five times the value of the zero-flow pressure difference, whichever is the greater* ; *the highest pressure difference shall be at least 50 Pa.* Those constraints should be applied in both pressurisation and depressurisation mode.

### 3.1.2. Conducting a Linear Regression

Once multiple different ($q_i - \Delta p_i$) couples are determined, one must take their logarithm to conduct a linear regression, based on the linearised power law (Eq.

8). The objective is to find the parameters $n$ (the airflow exponent) and $\ln(C_{env})$ (the logarithm of the airflow coefficient) that fits "the best" the observed datapoints.

$$\ln(q_i) = n\ln(\Delta p_i) + \ln(C_{env}) \quad \text{Eq. 8}$$

This problem can be solved with many different approaches mentioned in (Gillard, 2010). This thesis focuses on two specific approaches largely used in the literature: the Maximum Likelihood Estimation (MLE) and the Least Square Estimation (LSE). On one hand, MLE is a statistical approach that consists in finding the values for $n$ and $\ln(C_{env})$ that maximise the probability of the model to produce the observed dataset. On the other hand, the LSE approach consists in finding the parameters that minimise the distances between the datapoints and the linear model.

*Errors in one variable only*

Let's consider a case where each point has an error in the $y$ variable, that follows a gaussian distribution of mean 0 and variance $\sigma_{y_i}^2$ and that the error in the $x$ variable is negligible (i.e., $\sigma_{x_i}^2 = 0$). This corresponds to a case where $x$ is accurately measured.

The MLE approach requires to define the probability of the dataset to occur. Since the error in $y$ follows a gaussian distribution, the probability of the data is the product of the probability function of each point (Eq. 9). This is called the likelihood function.

$$P = \prod_{i=1}^{N} \frac{1}{\sqrt{2\pi\sigma_{y_i}^2}} e^{-\frac{1}{2}\left(\frac{y_i - y(x_i)}{\sigma_{y_i}}\right)^2} \quad \text{Eq. 9}$$

With $y(x_i)$ the value of the linear model at this specific $x_i$ (i.e., $ax_i + b$). Then, the logarithm of the negative of $P$ is taken. This is called the Negative Log-Likelihood function ($L$, Eq. 10). Maximising $P$ is equivalent to minimising $L$.

$$L = \sum_{i=1}^{N} \log\left(\sqrt{2\pi\sigma_{y_i}}\right) + \sum_{i=1}^{N} \frac{\left(y_i - y(x_i)\right)^2}{2\sigma_{y_i}^2} \quad \text{Eq. 10}$$

Since only $y(x_i)$ depends on the model parameters, only the second term of Eq. 10 must be optimised (Eq. 11).

$$L' = \sum_{i=1}^{N} \frac{\left(y_i - y(x_i)\right)^2}{\sigma_{y_i}^2} = \sum_{i=1}^{N} \frac{(y_i - (ax_i + b))^2}{\sigma_{y_i}^2} \quad \text{Eq. 11}$$

Then, solving this optimisation problem (i.e., Eq. 12 and Eq. 13) provides the "best" values for parameters $a$ and $b$.

$$\frac{\partial}{\partial a} \sum_{i=1}^{N} \frac{(y_i - (ax_i + b))^2}{\sigma_{y_i}^2} = 0 \quad \text{Eq. 12}$$

$$\frac{\partial}{\partial b} \sum_{i=1}^{N} \frac{(y_i - (ax_i + b))^2}{\sigma_{y_i}^2} = 0 \quad \text{Eq. 13}$$

In this specific case (negligible uncertainty in x variable), the LSE approach simply consists in minimising the sum of the squares of the vertical distances between the model and the dataset (Eq. 14). This is called the Ordinary Least Square (OLS) technique.

$$S = \sum_{i=1}^{N} \left(y_i - y(x_i)\right)^2 \quad \text{Eq. 14}$$

However, the OLS technique assumes that each datapoint has the same uncertainty while it is hardly the case in practice. To overcome this assumption, each point is weighted with the inverse of its own variance (Eq. 15). This is called the Weighted Least Square (WLS) technique.

$$S = \sum_{i=1}^{N} \omega(y_i) \left(y_i - y(x_i)\right)^2 \quad \text{Eq. 15}$$

One can see that under these hypotheses and if the weights are defined as the inverse of the variance (i.e., $\omega(y_i) = 1/\sigma_{y_i}^2$), MLE and LSE approaches result in the same optimisation problem.

In the context of the fan pressurisation measurement in buildings, multiple authors, including (Okuyama and Onishi, 2012) and (Delmotte, 2017), questioned the assumption of negligible uncertainty on $x$ variable.

*Errors in both variables*

When both variables are subjected to errors normally and independently distributed with zero means and variances $\sigma_{x_i}^2$ and $\sigma_{y_i}^2$, the problem must be handled differently.

For the MLE approach, (Krane and Schecter, 1982) suggested that one can still evaluate a probability for a univariate gaussian, but the denominator of Eq. 11 (i.e., the variance of the normal distribution) must be modified to include the fact that $\sigma_{x_i}$ affect the variance of the dataset. This results in Eq. 16:

$$L = \sum_{i=1}^{N} \left( \frac{y_i - a x_i - b}{\sigma_{y_i}^2 + a^2 \sigma_{x_i}^2} \right)^2 \qquad \text{Eq. 16}$$

Solving $\partial \chi^2 / \partial b = 0$ is straightforward and leads to Eq. 17 with $1/W_i = \sigma_{y_i}^2 + a^2 \sigma_{x_i}^2$.

$$b = \frac{\sum_{i=1}^{N} W_i y_i - a \sum_{i=1}^{N} W_i x_i}{\sum_{i=1}^{N} W_i} \qquad \text{Eq. 17}$$

On the other hand, $\partial \chi^2 / \partial a = 0$ leads to Eq. 18.

$$\sum_{i=1}^{N} W_i^2 \sigma_{x_i}^2 a (y_i - a x_i - b)^2 + \sum_{i=1}^{N} W_i (y_i - a x_i - b)(-x_i) = 0 \qquad \text{Eq. 18}$$

Once Eq. 17 is substitute into Eq. 18, it becomes an implicit cubic function of $a$ which has no analytical solution. Therefore, finding the roots of that function is not straightforward and requires methods for non-linear equations. For example, (Neri et al., 1989) used the bisection method (explained in chapter 9 of (Press et al., 1992)) to solve this problem.

Another way to handle this problem with the MLE approach is to consider the probability distribution of a bivariate normal rather than a univariate normal. In that case, the probability of the dataset is given by Eq. 19 with $r_i$ the correlation coefficient between $(x_i - x(y_i))$ and $(y_i - y(x_i))$.

$$P = \prod_{i=1}^{N} \left\{ \exp \left[ -\frac{1}{2} \frac{\left( \frac{y_i - y(x_i)}{\sigma_{y_i}} \right)^2 + \left( \frac{x_i - x(y_i)}{\sigma_{x_i}} \right)^2 - \frac{2 r_i \left( x_i - x(y_i) \right)\left( y_i - y(x_i) \right)}{\sigma_{x_i} \sigma_{y_i}}}{1 - r_i^2} \right] \right\} \qquad \text{Eq. 19}$$

This approach is complex and faces overidentification problems in multiple cases that are not discussed in this paper. The interested reader should refer to (Kendall and Stuart, 1961) and (Madansky, 1959) for additional information. However, it is worth mentioning that (Titterington and Halliday, 1979) developed these equations for the straight line case and showed good consistency with the LSE approach.

For the LSE approach, two alternatives are possible when error in $x$ is non-negligible: the Iterative Weighted Least Square (IWLS) and the Weighted Line of Organic Correlation (WLOC). Those name are chosen to be consistent with literature on building airtightness (see (Delmotte, 2017) or (Prignon et al., 2020b)). However, the literature refers to those methods under many different names that are listed in (Ludbrook, 2010).

IWLS consists in minimising the square of the orthogonal distance rather than the vertical distance between the point and the line. In that case, the sum to minimise (i.e., $S$) is defined by Eq. 20 with $\omega(x_i)$ defined as the inverse of the variance $\sigma_{x_i}^2$.

$$S = \sum_{i=1}^{N} \left( \omega(y_i)\left(y_i - (ax_i + b)\right)^2 + \omega(x_i)\left(x_i - \frac{(y_i - b)}{a}\right)^2 \right) \quad \text{Eq. 20}$$

(York, 1966) showed that the optimisation problem results in a cubic function with no analytical solution. He suggested an iterative process valid under the assumption of constant ratio of variances (i.e., $\sigma_{x_i}^2 / \sigma_{y_i}^2 = k$). In this thesis, the IWLS method refers to that iterative process. (York and Evensen, 2004) proved that the LSE approach using IWLS and the MLE approach are mathematically equivalent.

Another way to handle cases where both variables are subjected to errors is by minimising the product of vertical and horizontal distances (in absolute value) between the line and the datapoints. In that case $S$ is given by Eq. 21. This can be solved without iterative procedure and is referred in this work as the Weighted Line of Organic Correlation (WLOC).

$$S = \sum_{i=1}^{N} \left( \omega(y_i)\left|y_i - (ax_i + b)\right| . \omega(x_i)\left|x_i - \frac{(y_i - b)}{a}\right| \right) \quad \text{Eq. 21}$$

Regarding the assumptions, IWLS and WLOC are identical: the errors in both $x$ and $y$ variables are random errors and follow gaussian distributions. The

difference is the assumption of constant ratio of variance when using the specific equations of (York, 1966) with IWLS approach.

Since previous work in building airtightness focused on LSE approaches and that those were found mathematically equivalent to MLE under the hypothesis of bivariate normal distribution for errors, this thesis investigates the difference between OLS, IWLS and WLOC only (see Chapter 5). In (Prignon et al., 2020b) – appendix E we developed and presented in details the equations for the LSE using OLS, IWLS and WLOC methods.

### 3.1.3. Reporting Results

The regression parameters obtained with these methods are the airflow exponent ($n$) and the logarithm of the airflow coefficient ($\ln(C_{env})$). This second regression parameter is defined for the temperature experienced during the test while the airtightness is expected to be independent from the weather conditions. Therefore, it should be expressed at a reference temperature. Eq. 22 converts the logarithm of the airflow coefficient to the air leakage coefficient ($C_L$):

$$C_L = e^{\ln(C_{env})} \left(\frac{T_0}{T_i}\right)^{1-n} \quad \text{Eq. 22}$$

The possible metrics to report the results of the direct component testing are the same as for the building airtightness and are discussed in section 2.2.1. In our opinion, the results should be reported in pressurisation and depressurisation separately to identify the possible valve effect, which is the difference between both modes. When there is no distinction between pressurisation and depressurisation, one should assume that the result reported is the mean between both modes.

As explained in section 2.2.1, the choice made in this thesis is to report $q_{50}$ calculated with the power law (Eq. 4) and $n$.

## 3.2. Equipment and Experimental Setup

The direct component testing requires an equipment that pressurises and depressurises the pressure chamber and that measures the airflow and the pressure differences. The range of airflow measured with this method is lower

than for the building fan pressurisation test. The meta-analysis of section 2.4 shows that most components have an air leakage rate between 0 and 150 $m^3/h$.

Figure 6 shows a typical experimental setup for the direct component testing with the equipment used in this thesis. A compressible plastic duct ensures the connection between the fan (*MiniFan* from *BlowerDoor GmbH*) and the pressure chamber (a plastic membrane in the figure). The duct includes calibrated disks (*Micro Leakage Meter* from *BlowerDoor GmbH*) to determine precisely the airflow the fan blows in. A manometer (*DG-1000* from *BlowerDoor GmbH*) measures two pressure differences: inside and outside the chamber, and on both sides of the calibrated disks. The calibration data of the disks provided by the manufacturer gives the necessary information to convert the pressure difference measured at the disks in airflow.

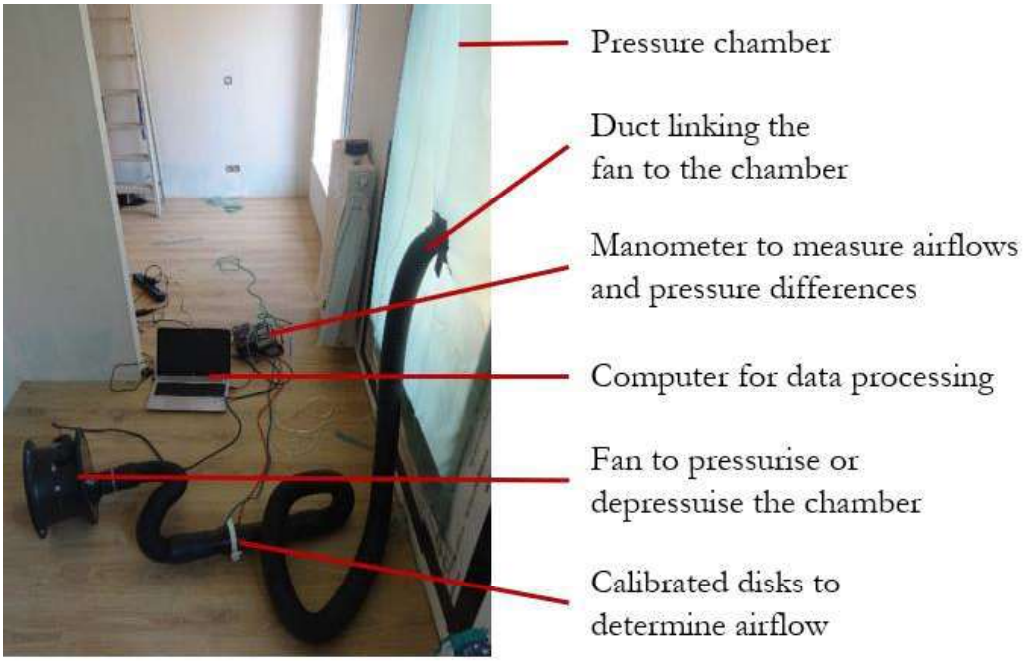



Figure 6: experimental setup and equipment for a typical measurement using direct component testing.

The range and the accuracy of the airflow and the pressure difference measurements depend on the equipment used. Table 6 reports the range of airflow measurement and the accuracy related to four calibrated disks used in this thesis. This equipment measures a pressure difference between 0 and 2500 Pa but should be limited to 100 Pa when conducting the tests *in-situ* to avoid

damaging the building. The accuracy of the pressure difference measured with the manometer is the maximum between $\pm 0.5\%$ of the reading and $\pm$ 0.2 Pa, and the resolution of the measurement is 0.1 Pa. The temperatures are measured with accuracy of $\pm$ 0.5 K.

Table 6: Accuracy and range of airflow measured with the equipment used in this thesis. Airflow is expressed in $m^3/h$ and its uncertainty in $m^3/h$ or in % of the airflow measured.

| Calibrated disk used | Range of measurable airflow [$m^3/h$] | Equipment accuracy [$m^3/h$] or [%] |
|---|---|---|
| Disk 1 or 2 | 2.15 – 78.5 | $\max(\pm 5\%; \pm 0.37)$ |
| Disk 3 | 0.65 – 3.23 | $\max(\pm 5\%; \pm 0.09)$ |
| Disk 4 | 0.17 – 0.83 | $\pm$ 0.04 |

The design of the pressure chamber depends on the element measured and can therefore differ from one measurement to another. On Figure 6 a simple airtight plastic membrane isolates the component. Figure 7 and Figure 8 show two other designs of tighter pressure chambers: a plastic-sheet system with horizontal bars preventing the inflation of the plastic membrane and a solid woodbox system.

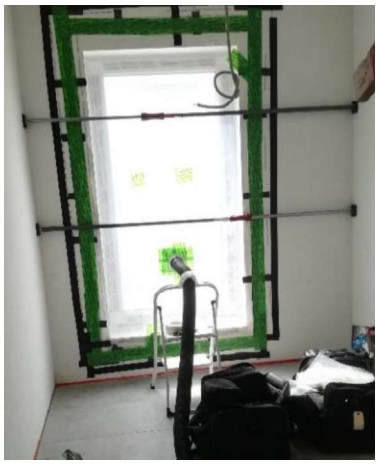


Figure 7: experimental setup for direct component test using plastic-sheet system with horizontal bars.



Figure 8: experimental setup for direct component test using solid woodbox system.

## 3.3. Summary of Chapter's Outcomes

In this chapter, we describe and explain the protocol and the equipment for the direct component testing. This includes the measurement principle; the data processing (i.e., transformation of the measured values and conduction of a linear regression); and the range of measurable components.

This chapter highlights the similarities between the direct component testing and the fan pressurisation measurement, and the attention that should be paid to the linear regression technique regarding their underlying hypotheses.

# Chapter 4. Validation and Quantification of Biases for the Direct Component Testing

In this chapter, we assess the capability of the direct component testing to provide the airflow exponent alongside the air leakage rate. To that extent, we report and analyse the results of a series of measurements conducted on four calibrated openings. Then, we investigate and quantify the different biases related to the protocol and the experimental setup. The work done in this chapter is not based other publications.

## 4.1. Validating the Direct Component Test on Known Openings

This section presents an experiment conducted to assess the capability of the direct component testing to estimate the leakage characteristics (i.e. airflow exponent $n$ and air leakage coefficient $C_L$). This is done by measuring four calibrated circular openings and comparing the results with their calibration.

### 4.1.1. Methodology

The solid woodbox system is used to measure four circular openings with diameters of 1.5, 2.1, 3.0 and 4.2 cm. The Bernoulli equation, simplified for this specific case, defines the relation between the air leakage rate and the pressure difference (Eq. 23):

$$q = C_d\, A \sqrt{(2\Delta p)/\rho} \qquad \text{Eq. 23}$$

Where $q$ is the air leakage rate (in m³/h), $C_d$ is the discharge coefficient, $A$ is the area of the opening (in m²), $\Delta p$ is the pressure difference between inside and outside the chamber (in Pa) and $\rho$ is the air density (in kg/m³). In a personal communication, (Rogers, 2019b), the disk's manufacturer, stated that the discharge coefficient is 0.61 for all these openings. The air density is 1.204 kg/m³ at the conditions of the experiment (20°C).

For each calibrated opening, the system is measured first with the opening sealed in order to determine the residual flow through the woodbox. The residual flow is below the measurable range of airflow (i.e. below 0.17 m³/h at 100 Pa) for these four specific setups.

### 4.1.2. Results

Table 7 shows the results of the validation experiment. First part of the table provides the opening area ($A$ in cm²) and the related air leakage rate at 50 Pa ($q_{50}$ in m³/h) for each opening. This is calculated with Eq. 23. The second part of the table shows the result of the measurement of the airflow exponent ($n$), the air leakage coefficient ($C_L$ in m³/(h.Pa$^n$)) and the air leakage rate at 50 Pa in each mode (i.e. pressurisation and depressurisation) and on average.

Table 7: comparison between the airflow through four calibrated disks according to their calibration and to measurements with the direct component test. $A$ in cm², $C$ in m³/(h.Pa$^n$) and $q_{50}$ in m³/h.

| | Calibrated Openings | | Direct Component Test | | | | | | |
|---|---|---|---|---|---|---|---|---|---|
| | $A$ | $q_{50}$ | $C_{L,+}$ | $n_+$ | $q_{50,+}$ | $C_{L,-}$ | $n_-$ | $q_{50,-}$ | $q_{50}$ |
| Opening 1 | 1.76 | 3.54 | 0.55 | 0.48 | 3.73 | 0.55 | 0.49 | 3.78 | 3.76 |
| Opening 2 | 3.46 | 6.93 | 1.05 | 0.49 | 7.24 | 1.02 | 0.50 | 7.10 | 7.17 |
| Opening 3 | 7.07 | 14.15 | 2.21 | 0.48 | 14.48 | 2.10 | 0.49 | 14.23 | 14.36 |
| Opening 4 | 13.85 | 27.73 | 3.99 | 0.49 | 27.62 | 4.14 | 0.49 | 28.39 | 28.01 |

The differences between the expected and the measured $q_{50}$ vary between 0.21 and 0.28 m³/h, depending on the opening. These differences are systematic: the

measurement leads to a larger air leakage rate than expected. The small background leakage (below 0.17 $m^3/h$ at 100 Pa) and the precision errors explain these. The differences observed between the pressurisation and the depressurisation modes are small (between 0.05 and 0.77 $m^3/h$) and not systematic. It is possibly due to the precision errors only.

The results also show that the airflow exponent computed with the direct component test is close to the expected value (0.5). The small differences (between 0.00 and 0.02) are probably due to the uncertainty in the measurements. These differences are systematic, which is surprising since the background leakage is expected to induce a systematic increase of the airflow exponent because the flow regime is not fully turbulent. Two reasons can possibly explain this systematic shift: a type II error in the observations made (i.e. observing an effect while there is not) or a difference in pressure sequences between these measurements and the laboratory calibration. Indeed, in the laboratory, the pressure sequences usually go up to 1000 Pa while these are limited to 100 Pa in this case. In (Prignon et al., 2018) – Appendix D, we demonstrated that for the fan pressurisation test, a change in pressure sequence may induce a bias in the air leakage rate at 50 Pa. The same is expected for the direct component testing and could explain this small systematic difference.

This experimental validation shows a good agreement between the laboratory calibration and the measurements using the direct component testing. However, this experiment involves two limitations related to the selected openings that would deserve a deeper investigation. First, the airflow exponent is limited to 0.5 while in practice the flow regime through building components are hardly fully turbulent. Second, the air leakage rate at 50 Pa is limited between 3.54 and 27.73 $m^3/h$ while the range of measurable airflow with this equipment is 0.17 – 78.5 $m^3/h$ according to the manufacturer.

## 4.2. Bias in Airflow: the Background Leakage

A bias error is a fixed variation of the measured value around its true quantity, that is unknown. These errors are difficult to identify and estimate because of their systematic pattern: no difference is observed between two repeated tests since both have the same bias. The protocol for the direct component testing may induce two biases: the background leakage ($\delta q_b$) and the pressure losses in the duct ($\delta p_L$).

The direct component testing assumes that all the measured airflow is attributed to the component tested, which means that the pressure chamber is perfectly airtight. The airflow leaking through the pressure chamber is called the background leakage and must be reduced as much as possible. Since it is never equal to zero, its quantification is essential to correct the airflow measurement and remove this bias from the reported result.

### 4.2.1. The Experiment

The woodbox system is used to measure a perfectly airtight plastic sheet made of tapes specifically designed for airtightness applications. In a study conducted on the airtightness performance of different sealing methods for windows, (Relander et al., 2008) found that the tapes used for airtightness applications result in a negligible air leakage rate. Consequently, this experiment assumes that all the measured airflow is the background leakage.

The background leakage is measurable (i.e. $> 0.17$ m³/h) only for the pressure differences $\geq 80$ Pa. The values for $n$ and $C_L$ obtained from interpolating the high-pressure measurements are 0.21 and 0.08 in pressurisation ($q_{50,+} = 0.18$ m³/h) and 0.49 and 0.02 in depressurisation ($q_{50,-} = 0.15$). The mean air leakage rate at 50 Pa is $0.17$ m³/h.

(Sherman and Palmiter, 1995) and (Prignon et al., 2018) – Appendix D, showed that using only the high-pressure measurements may induce a bias in the determination of the airflow exponent. This explains the value found for the airflow exponent that is outside the range of meaningful values [0.5;1.0]. This is expected to induce a bias in the air leakage rate below 80 Pa also.

Eq. 24 gives the equations to compute $\delta q_b$ as a function of $\Delta p$ for the woodbox system in pressurisation and depressurisation.

$$\begin{cases} \delta q_b = 0.08\ (\Delta p)^{0.21} & \text{if } \Delta p > 0 \\ \delta q_b = 0.02\ (\Delta p)^{0.49} & \text{if } \Delta p < 0 \end{cases} \quad \text{Eq. 24}$$

These values overestimate the real bias at low-pressure difference since a higher value of the leakage exponent would change the slope of the linearised relation between the air leakage rate and the pressure difference (Eq. 8). However, assuming a meaningful exponent (i.e. 0.5) instead of these values (0.21 and 0.49) is not appropriate because of the high correlation between $C_L$ and $n$.

## 4.3. Bias in Pressure: Pressure Losses in the Duct

The protocol for the direct component testing suggests two locations for the "inside gauge" when measuring the pressure difference: in the duct, close to the calibrated disk, or in the chamber, close to the component tested. The advantage of a pressure gauge close to the calibrated disk is the possibility to create an additional element to the equipment, reducing the background leakage due to an opening made during the test. The location of the "inside gauge" when placed in the duct involves two challenges that are described below: the recirculation flow and the pressure losses in the duct.

### 4.3.1. Recirculation Flow

The sudden retraction and expansion of the section of the duct because of the calibrated disks induce two disturbances in the flow speed: an increase in the centre and a recirculation flow on both corners after the retraction. Figure 9 illustrates the recirculation flows and the increase of airspeed.

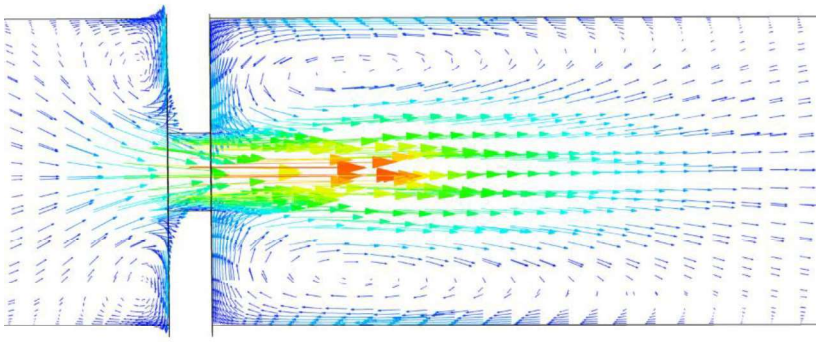


Figure 9: illustration of the increasing airspeed and the recirculation flows in the duct because of the sudden retraction and expansion of the cross-section.

This disturbance in the air speed involves a disturbance in the pressure distribution and can induce an uncertainty in the pressure measurement. Therefore, the "inside gauge" must be sufficiently distant from the calibrated disk to provide a reliable measurement. For this specific equipment, a

simulation using the FineOpen software defines a recirculation length varying between 8 and 13 cm, depending on the diameter of the calibrated disk.

### 4.3.2. Pressure Losses in the Duct

Placing the pressure gauge close to the calibrated disk induces a bias in the pressure measurements because of the pressure losses in the portion of the duct between the "inside gauge" and the component tested. This section presents the theoretical calculation and the experimental measurement of these pressure losses.

*Theoretical Calculations*

There are two types of pressure losses in ducts: the friction of molecules between them and against duct walls causing friction losses ($\delta p_f$); and the sudden perturbation in the flow speed or its direction causing the singular losses ($\delta p_s$). The total pressure loss ($\delta p_L$) is simply the sum of the friction losses along the duct and of each singularity experienced by the flow (Eq. 25):

$$\delta p_L = \delta p_f + \sum_{i=1}^{n} \delta p_{s,i} \qquad \text{Eq. 25}$$

The Darcy's law (Eq. 26) defines the friction losses:

$$\delta p_f = \frac{fL}{D} \frac{\rho V^2}{2} \qquad \text{Eq. 26}$$

Where $f$ is the friction coefficient [-], $L$ is the duct length [m], $D$ is the duct diameter [m], $\rho$ is the air density [kg/m$^3$] and $V$ the air velocity [m/s].

The friction coefficient depends on the flow regime (i.e. laminar, transitional or turbulent flow). In a laminar flow, the friction coefficient is only function of the Reynolds number (Eq. 27).

$$f = \frac{64}{\mathrm{Re}} \qquad \text{Eq. 27}$$

In a turbulent regime, the friction coefficient depends on the rugosity of the duct, on the absolute roughness and on the Reynolds number. Colebrook equation provides a good approximation of this relation but has no analytical solution and must be solved by iterative calculations (Eq. 28).

$$\frac{1}{\sqrt{f}} = -2\log\left(\frac{\varepsilon}{3{,}7\,D} + \frac{2{,}51}{\mathrm{Re}\sqrt{f}}\right) \quad \text{Eq. 28}$$

The relations between friction coefficient, absolute roughness and Reynolds number in the transitional regime are still not fully understood and are, therefore, not developed in this paper. For these calculations, the value of the friction coefficient in transitional flow is obtained by a linear interpolation between laminar and turbulent flows.

The flow regime depends on the Reynolds number, calculated with Eq. 29, where $\nu$ is the dynamic viscosity of air [m³/s]. The limit value of the Reynolds number for each regime depends on the relative roughness of the duct and can be deduced from Moody charts (ASHRAE, 2017). In this case, limit values between regimes are $\mathrm{Re} = 2300$ (between laminar and transitional) and $\mathrm{Re} = 3500$ (between transitional and turbulent).

$$\mathrm{Re} = \frac{VD}{\nu} \quad \text{Eq. 29}$$

(Abushakara et al., 2004) showed that when dealing with compressible ducts, which is the case here, a pressure drop correction factor ($f_{cor}$) is added to the pressure losses by friction in the fully stretched position ($\Delta p_{f,FS}$) in order to take into account the losses due to the compressible part of the structure (Eq. 30).

$$\Delta p_f = f_{cor}\,\Delta p_{f,FS} \quad \text{Eq. 30}$$

There are two methods based on the empirical observations to determine this pressure drop correction factor: one using constant coefficients (method 1 – Eq. 31) and one using the pitch-to-diameter ratio (method 2 – Eq. 32). This is the ration between the pitch (i.e., the distance between two consecutive spirals of the duct in the fully stretched position) and the diameter in this position. These two methods are developed in (Abushakara et al., 2004) for a series of compressible ducts of standardised diameter (150 mm, 200 mm and 250 mm).

$$f_{cor,1} = 1 + a\,r_c \quad \text{Eq. 31}$$

$$f_{cor,2} = 1 + 106\left(\frac{\lambda_{FS}}{D_{FS}}\right) r_c \quad \text{Eq. 32}$$

In Eq. 31, $r_c$ is the compression ratio and $a$ is an empirical value depending on the duct diameter. $r_c$ is deduced from Eq. 39 where $L_{FS}$ and $L$ are the length in fully stretch and normal conditions respectively.

$$r_c = \frac{L_{FS} - L}{L_{FS}} \quad \text{Eq. 33}$$

(ASHRAE, 2017) provided values of $a$ for ducts of diameter 150, 200 and 250 mm. For diameters outside this range, they suggested taking a value of 21 for $a$. In Eq. 32, $\lambda_{FS}$ is the pitch between two metallic circles, $D_{FS}$ is the diameter in fully-stretch position and $r_c$ is defined as previously (Eq. 33).

The singular pressure losses depend on the type of singularity encountered. It is calculated with Eq. 34 where $\zeta_i$ is the local loss coefficient for the singularity.

$$\delta p_{s,i} = \zeta_i \frac{\rho V^2}{2} \quad \text{Eq. 34}$$

Specific tables give $\zeta_i$ values for different types of singularities. (De Bie et al., 2014) explain that values encountered in literature strongly vary between publications.

Table 8 summarises the symbol and the name of the variables used in the calculation of pressure losses in compressible ducts, and the values used for the calculations performed in this thesis.

Table 8: Symbols, names and values for variables used in the calculation of pressure losses in compressible ducts using Eq. 25 to Eq. 34.

| Variables | | Value | Units |
|---|---|---|---|
| $\rho$ | Air density (RH 50% with 20 °C) | 1,199 | kg/m³ |
| $\nu$ | Air dynamic viscosity (RH 50% with 20 °C) | $1{,}5\,.\,10^{-5}$ | m²/s |
| $\varepsilon$ | Absolute roughness of the duct[a] | $4.6\,.\,10^{-}$ | m |
| Re | Reynolds number | – | - |
| $f$ | Friction coefficient | – | - |
| $L$ | Duct length in normal conditions | 2,9 | m |
| $L_{FS}$ | Duct length in fully-stretch conditions | 3,3 | m |
| $r_c$ | Compression ratio | 0,121 | - |
| $a$ | Correction coefficient | 21 | - |
| $f_{cor}$ | Pressure drop correction factor | 3,55 | - |
| $D_{FS}$ | Duct diameter in fully-Stretch conditions | 0,075 | m |
| $\lambda_{FS}$ | pitch between two metallic circles in fully-stretch conditions | 0,01 | m |
| $f_{cor,N}$ | Normalised pressure drop correction factor | 2,71 | - |
| $\zeta$ | Local loss coefficient [b] | 0,19 | - |

[a] Value for the absolute roughness is for drawn tubing (ASHRAE, 2017; Rogers, 2019b)

[b] Value taken from (ASHRAE, 2017)

*Experiment*

In parallel with the theoretical developments, the pressure losses in ducts are determined experimentally. The experiment consists of two tubes of rigid PVC placed at both ends of the duct: one close to the calibrated disk, respecting the 13 cm distance to avoid the recirculation flows (Figure 10) and one at the connection with the pressure chamber (Figure 11). Both tubes are drilled in order to place the pressure gauges (the green and the white gauges in the figures).



Figure 10: PVC tube at the entrance of the duct and the gauge placed at 13 cm of the calibrated disk



Figure 11: PVC tube and the pressure gauge placed at the end of the duct.

Two configurations are tested and compared to the theoretical measurements: one without singularities (Figure 12) and one with two 90° angles (Figure 13). The pressure between both sides of the duct and the airflow through the calibrated disks are measured.



Figure 12: experimental setup to quantify pressure losses in the straight case.

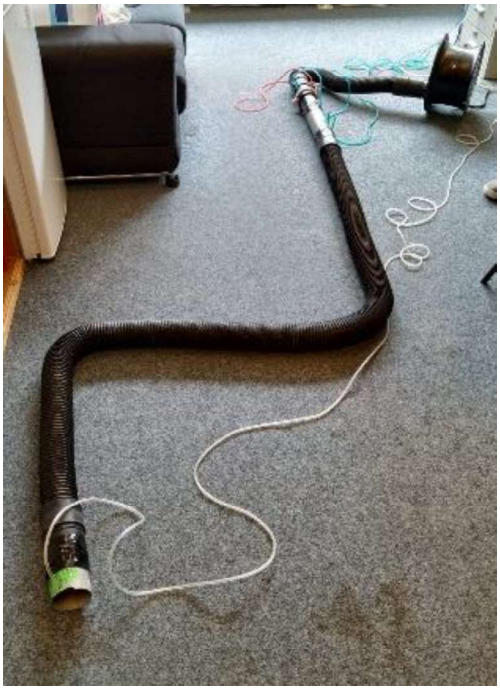


Figure 13: experimental setup to quantify pressure losses in the "two 90° angles" case.

*Results*

Figure 14 draws the pressure losses in the duct as a function of the airflow through the calibrated disks obtained with the experiment (black lines) and with the theoretical calculations using the method 1 (red lines) and the method 2 (yellow lines). The full lines refer to the straight case, and the dash lines refer to the "two 90° angles" case.

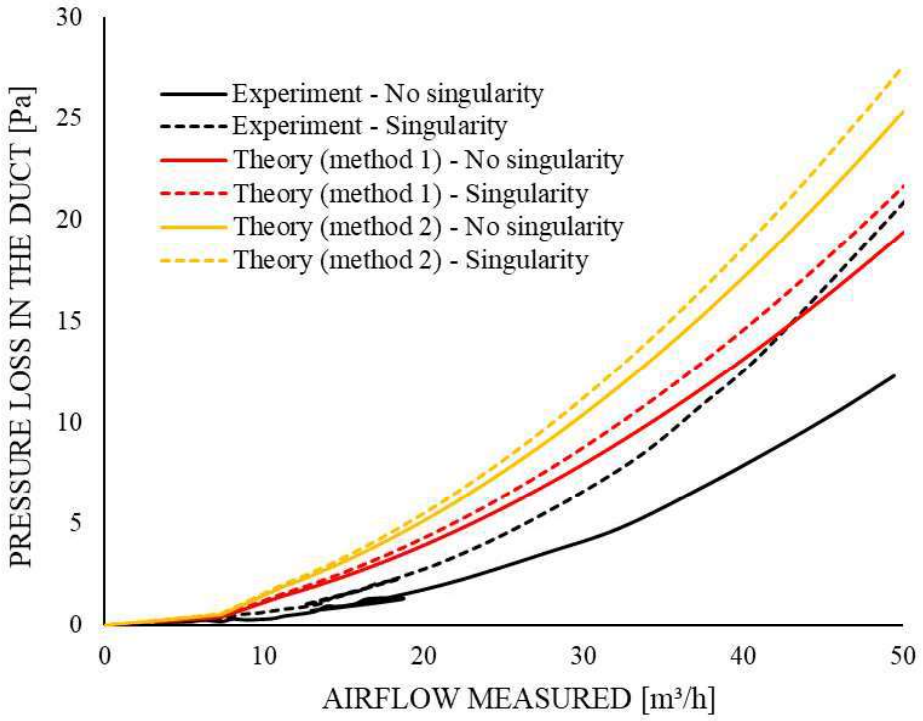



Figure 14: the pressure losses in the duct as a function of the measured airflow with (dashed lines) and without (full lines) singularities obtained by the experiment (black lines) and by the theoretical calculations using the method 1 (red lines) and the method 2 (yellow lines).

Experiment results on Figure 14 show a superposition of two different curves between 12 and 19 $m^3/h$. This is because the range of measurable airflows of disk 1 and 2 overlap in this zone. Therefore, this part of the curve is obtained once using disk 1, and once using disk 2.

The results show that the theoretical calculations overestimate the friction losses and underestimate the singularity losses. The overestimation is observed when comparing the full or the dash lines in the three cases while the underestimation is observed when comparing the difference between the full

and the dash lines for these cases. The overestimation is probably because the diameter of the duct used in this experiment is different from the ducts used in (Abushakara et al., 2004) to develop the models for compressible ducts. The underestimation is possibly due to the large variety of values found in the tables and in the difficulty to reproduce exactly the 90° angles during the experiment. In addition, the method 1 is closer to the measured losses than the method 2. This observation is surprising since there are more degrees of freedom in method 2 (pitch-to-diameter ratio) than in method 1 (constant). Moreover, this observation is expected to be specific to this diameter and this specific compression and could not lead to conclusions drawn about the choice between method 1 and method 2. Therefore, other diameters should be tested to compare these two methods.

Eq. 35 and Eq. 36 are two 2-degree polynomial equations describing with a high correlation ($R^2 > 0.99$) the relations between the airflow and the pressure losses in the duct observed (i.e. black lines in Figure 14). These equations refer to the case with and without a singularity respectively.

$$\delta p_{L,1} = 0.0090\, q_m^2 - 0.0389\, q_m \qquad \text{Eq. 35}$$

$$\delta p_{L,2} = 0.0054\, q_m^2 - 0.0193\, q_m \qquad \text{Eq. 36}$$

According to the generalised Bernoulli theorem, the airflow is constant in the duct for incompressible fluids and with a constant temperature. Consequently, this pressure loss impacts the measurement of the pressure difference only; and should be considered as a correction factor when the pressure gauge is placed at a location for which this loss is relevant (i.e. close to the calibrated disks).

$\delta p_L$ seems important for airflows $> 10$ m³/h and the increase of $\delta q_b$ due to the insertion of a pressure gauge in the pressure chamber is small if proper attention is paid to the setup of the chamber. Consequently, one should usually place the pressure gauge close to the measured component rather than the calibrated disk in order to reduce biases during the measurement process.

## 4.4. Summary of Chapter's Outcomes

In this chapter, we conduct one experiment to assess its capability to determine the airflow exponent and the air leakage rate at 50 Pa for small openings; one

experiment to quantify the airflow bias (the background leakage); and one experiment to quantify the pressure bias (the pressure losses in the duct).

These experiments show very promising results regarding the capacity of the method to determine $n$ and $C_L$; and regarding the limited magnitude of the biases. This reinforces the idea that this method is appropriate for practice. Nevertheless, we should acknowledge some limitations of these experiments:

- Some expected sources of bias are mentioned but not considered in this chapter: the impact of gust wind on the airflow measurement or the impact of the outside pressure gauge on the pressure measurements.
- The validation work is conducted on a limited range of air leakage rate [3.5;27.7] and of airflow exponent (0.5).
- The background leakage is quantified for the woodbox system only. This bias is expected to be influenced by the pressure chamber design.

These limitations pave the way for future studies and investigations that could reinforce the validation work and improve the description of the direct component testing. These are discussed in sections 7.3 and 7.4.

# Chapter 5. Quantification of Uncertainties in the Direct Component Testing

In this chapter, we investigate the uncertainty of the direct component testing in three steps. First, we describe the methodology for uncertainty determination and discuss its application in the context of building component airtightness. Second, we quantify the uncertainty of the direct component testing with the analysis of two repeatability studies. Third, we compare the direct and the indirect component testing with the analysis of three other repeatability studies. The work presented in this chapter refers to four publications:

- Appendix C: Prignon M., C. Delmotte, A. Dawans, S. Altomonte and G. Van Moeseke (2020). On the impact of regression techniques to airtightness measurement uncertainties. Energy and Buildings, **215**. https://doi.org/10.1016/j.enbuild.2020.109919.
- Appendix D: Prignon M., A. Dawans and G. Van Moeseke (2018). Uncertainties in airtightness measurements: regression methods and pressure sequences. *In 39th AIVC – 7th TightVent & 5th Venticool Conference: Smart ventilation for buildings.* Antibes Juan-Les-Pins, France.
- Appendix E: Prignon M., A. Dawans, S. Altomonte and G. Van Moeseke (2019). A method to quantify uncertainties in airtightness measurements: Zero-flow and envelope pressure. Energy and Buildings, **188–189**: 12–24. https://doi.org/10.1016/j.enbuild.2019.02.006.
- Appendix F: Prignon M., A. Dawans and G. Van Moeseke (2020). Quantification of uncertainty in zero-flow pressure approximation. International Journal of Ventilation. https://doi.org/10.1080/14733315.2020.1777020.

## 5.1. Uncertainty in the Direct Component Testing

(Coleman and Steele, 2009) used the concept *uncertainty* to describe the degree of goodness, or the likely amount of error, of a measurement. In their work, they refer to two types of errors: the random errors varying between two measurements and the systematic errors remaining constant. In this work, and more generally in the field of airtightness, the term "uncertainty" usually refers to the random errors exclusively since the reported results already includes a correction for all known biases. (Sherman and Palmiter, 1995) defined two broad sources of errors in the fan pressurisation measurements: the errors associated with the measurements and the errors associated with the model specifications. Because of the closeness between the fan pressurisation test and the direct component testing protocols, the same types of errors are considered for both.

The model specification errors, or modelisation errors, depend on the validity of the assumptions made in the different steps of the measurement. The numerous steps described in section 3.1 to convert the pressure differences and the airflow to the air leakage rate and the airflow exponent involves many different assumptions. Biases investigated in sections 4.2 and 4.3 are examples of modelisation errors since they come from two assumptions: the air leakage rate through the pressure chamber is negligible; and the pressure difference measured is the pressure difference applied between both sides of the building component. The model specification errors can also be random errors. For example, the assumption that $\Delta p_0$ experienced before and after the test equals $\Delta p_0$ during the test induces a random error. This specific error is investigated in section 5.4.1.

There are two ways to quantify the uncertainty of a measurement method: experimentally (the observed uncertainty) and theoretically (the calculated uncertainty). The methodologies for both ways and for the statistical analysis of the results are described in the following section.

## 5.2. Methodology

### 5.2.1. Experimental Observations

The experimental observation of the random errors consists of the successive measurement of the same measurand (i.e. the quantity subject to measurement). (JCGM, 2008), the guide to the expression of uncertainty in the measurement, defined two conditions for these repeated measurements: the repeatability (the successive measurements are carried out under the same conditions) and the reproducibility (the successive measurements are carried out under changing conditions) studies. These two conditions involve different sources of error and are the lower and the upper boundaries of the observed uncertainty.

In the field of airtightness, the repeatability or near-repeatability studies usually refer to the successive measurements conducted by the same operator, on the same measurand, using the same equipment and for a short period to avoid the seasonal variations. In this field, (Delmotte and Laverge, 2011) and (Novak, 2011) are the only researchers, to our knowledge, to report the results of reproducibility studies. They limit their investigation to a change of operator in the context of the fan pressurisation measurement.

For the repeatability and the reproducibility studies, (JCGM, 2008) stated that the observed uncertainty is the standard deviation of the available data. This is statistic estimates the population true standard deviation (i.e. the "true uncertainty" of the method). If the $N$ repeated measurements are assumed normally distributed, this statistic follows a $\chi^2$- distribution with $k = N - 1$ degree of freedom. The variance of a $\chi^2$-distribution is $2k$, hence the error on the observed uncertainty is the following (Eq. 37):

$$e\big(\sigma(X)\big) = (2[N-1])^{-0.5} \qquad \text{Eq. 37}$$

Where $e(\sigma(X))$ is the relative error on the standard deviation, $X$ is the measured variable and $N$ is the number of successive measurements conducted in the repeatability study.

The experimental standard deviation increases with the duration of the repeatability study because of the larger variety of weather conditions experienced. Consequently, choosing the right number of measurements for a repeatability study is a trade-off between reducing the error on the standard

deviation (i.e. $e(\sigma(X))$) and limiting the impact of the weather-induced uncertainty if those are undesired.

### 5.2.2. Theoretical Calculations

The theoretical calculation of the uncertainty consists of identifying and quantifying each possible source of error, then propagating them between each step of the protocol. This is because an error on the explanatory variables results in an error on the response variable that depends on the relation between both variables. (Rajan, 2018) stated that the simplest and most efficient method for uncertainty propagation is called the second moment method, also called the perturbation method. According to (Sudret, 2007), this method consists in calculating the second moment of a probabilistic function (i.e. its standard deviation), using a Taylor series expansion as an approximation of the function. The detailed mathematical development related to this method are out of the scope of this thesis and an interested reader should refer to (Kriegesmann, 2012) for those calculations.

In this context, and assuming a normally distributed continuous function that has continuous first and second order derivatives, the propagation law is simplified to Eq. 38:

$$u(y) = \sqrt{\sum_{i=1}^{N}\left(\frac{\partial f}{\partial x_i}u(x_i)\right)^2 + 2 * \sum_{i=1}^{N-1}\sum_{j=i+1}^{N}\left(\frac{\partial f}{\partial x_i}\right)\left(\frac{\partial f}{\partial x_j}\right)u(x_i)u(x_j)r(x_i,x_j)} \qquad \text{Eq. 38}$$

(Delmotte, 2013) developed all these equations for each step of the fan pressurisation measurement in the pressurisation and the depressurisation modes. Because of the numerous similarities in the measurement protocols, the direct component testing involves the same steps and, therefore, the same equations as the fan pressurisation measurement. (Delmotte, 2017) suggested the addition of an uncertainty component related to the zero-flow pressure approximation. We further investigated this component in (Prignon et al., 2019) – Appendix E and (Prignon et al., 2020a) – Appendix F. One important step in this protocol that deserves more attention when looking at the uncertainty is the regression technique. In fact, the uncertainty of regression parameters (i.e. the airflow exponent and the logarithm of the airflow coefficient) depends on the regression technique used. In (Prignon et al., 2020b) – appendix C, we

developed the equations for each of the three regression techniques investigated in the context of the fan pressurisation measurement (i.e. the OLS, the IWLS and the WLOC techniques).

Consequently, because of the similarities with the fan pressurisation test, the reader should refer to: (Delmotte, 2013) for the detailed equations of the different steps in the protocol; (Delmotte, 2017), (Prignon et al., 2019) – Appendix E and (Prignon et al., 2020a) – Appendix F for the detailed equations related to the zero-flow pressure approximation; and (Prignon et al., 2020b) – Appendix C for the detailed equations related to the three regression techniques.

If one identifies, quantifies and propagates all the sources of error properly at each step, the calculated uncertainty equals the real uncertainty. In practice, the observed uncertainty provides a better approximation of the real uncertainty since the theoretical calculations misses many sources of error experienced during the test. Nevertheless, the theoretical uncertainty is still highly relevant in practice since it requires only one test compared to the observed uncertainty that requires a complete repeatability study. Therefore, both aspects are investigated in this thesis.

### 5.2.3. Reported Results and Statistical Analysis

In a repeatability study, each test reports the airflow exponent ($n$), the air leakage coefficient ($C_L$) and the air leakage rate at 50 Pa ($q_{50}$) in pressurisation and depressurisation. It also reports, for each test, the mean air leakage rate at 50 Pa and the calculated uncertainty of each variable. In addition, the study determines, for each variable: one observed uncertainty, that is the standard deviation of all the tests; and one calculated uncertainty, that is the mean of all the calculated uncertainties.

The choice of a statistical indicator to compare the different results depends on the type of comparison. The indicators described hereunder are appropriate for datasets normally distributed. For other distributions, one should refer to the non-parametric statistical tests. A Shapiro-Wilk test applied on each variable of each study demonstrates that all the distributions are normal in this thesis.

Table 9 presents the appropriate indicators for the null hypothesis significance testing (statistical significance) and the effect size (practical significance),

depending on the type of comparison and the type of variable. (Pernet, 2015) defined the null hypothesis significance testing (NHST) as the statistical method to investigate the likelihood of a phenomenon to occur. However, it provides no information about the magnitude of the observed evidence. To that extent, (Ellis, 2010) explained that the effect size is a standardised measure of the difference between models: it provides a quantitative measure of a phenomenon's magnitude. The following paragraphs explain and discuss these statistical indicators.

Table 9: the statistical indicators for NHST and the effect-size analysis, depending on the type of comparison and the type of variables.

| | Mean value | | Standard deviation | |
|---|---|---|---|---|
| | NHST | Effect size | NHST | Effect size |
| Comparing two regression techniques | Paired t-test | Cohen's $d$<br>Hedge's $g$ | Pitman's $T$ | $\Delta\sigma$ |
| Comparing two measurement methods | Independent t-test | Cohen's $d$<br>Hedge's $g$ | F-test | $\Delta\sigma$ |
| Assessing the importance of valve effect | - | Cohen's $d$<br>Hedge's $g$ | - | - |
| Comparing observed and calculated uncertainty | - | $\Delta u$ | - | - |

When comparing two treatments within the same dataset, the data are dependent. A paired t-test is appropriate to compare the mean value and, according to (Ellis, 2010), the corresponding effect size is the Cohen's $d$ when variances are not statistically different and the Hedge's $g$ when they are. In these cases, (Pitman, 1939) suggested the use of Pitman's $T$ to compare the standard deviations. However, there is no appropriate effect size when comparing two standard deviations in this case. The choice made in this thesis is to report $\Delta(\sigma)$, which is the difference between both standard deviations ($\sigma(x_1)$ and $\sigma(x_2)$) divided by the mean of the first treatment ($\mu(x_1)$) (Eq. 39):

$$\Delta(\sigma) = \frac{\sigma(x_1) - \sigma(x_2)}{\mu(x_1)} \qquad \text{Eq. 39}$$

This equation is only valid if the mean difference between both datasets is negligible (i.e. $\mu(x_1) \approx \mu(x_2)$). The denominator can be $\sigma(x_1)$, $\sigma(x_2)$ or a

pooled standard deviation instead of $\mu(x_1)$ in cases where it is relevant to the objective of the study (e.g. when comparing a new technique to a reference technique). One should carefully interpret this indicator since it is not standardised as the other effect sizes.

When comparing two datasets, the data are independent. An independent t-test compares the mean value and the corresponding effect size is Cohen's $d$ when variances are not statistically different and Hedge's $g$ when they are. An F-test compares the standard deviations and $\Delta(\sigma)$ is reported in place of a standardised effect size.

There is no statistical analysis appropriate to compare the observed ($u_o(x_1)$) and the calculated ($u_c(x_1)$) uncertainties since one is a standard deviation and the other is a mean. In such cases, the choice made in this thesis is to report $\Delta(u)$, which is the difference between both uncertainties, divided by the observed uncertainty (Eq. 40):

$$\Delta(u) = \frac{u_o(x_1) - u_c(x_1)}{u_o(x_1)} \qquad \text{Eq. 40}$$

The choice of dividing by $u_0(x_1)$ is made to define a value independent from the magnitude of the uncertainty in order to use existing benchmarks for its interpretation. However, one could report the difference between observed and calculated uncertainty in order to have an indicator that is in the same unit as the observed variable ($x_1$) and that can be compared to its value.

When looking at the valve effect (the difference between the pressurisation and the depressurisation), only the effect size is interesting. This is because the objective is to have a quantitative measurement of the valve effect rather than to compute the likelihood of the valve effect to occur. This effect size is Cohen's $d$ or Hedge's $g$, depending on the difference in variance of both modes.

(Volker, 2006) recommended interpreting the effect sizes with the benchmarks suggested by (Cohen, 1992) in the absence of previous knowledge. In these benchmarks, effect sizes are small, medium and large for values $> 0.20, > 0.50$ and $> 0.80$ respectively. In this thesis, the Cohen's benchmarks are also used when interpreting $\Delta(\sigma)$ and $\Delta(u)$. The applicability of these benchmarks is discussed in section 5.5.

## 5.3. Reliability of the Direct Component Testing

This section presents the results of two repeatability studies conducted in November 2018 and July 2019. Those aimed at quantifying the uncertainty of the direct component test using different designs of pressure chambers.

### 5.3.1. Testing Conditions and Sources of Error

The first repeatability study measures a single hung timber-frame window, including the window-to-wall connection, in a newly constructed building using the plastic-sheet system with horizontal bars described in section 3.2. The window area is 2.42 $m^2$ and its opening length is 5.40 m. It is conducted on a four-day period between the 27$^{th}$ and the 30$^{th}$ of November 2018. The second study uses the woodbox system to estimate the uncertainty when measuring an electrical penetration in a plastered wall made of blocks in a newly constructed building. The study is conducted on a three-day period between the 11$^{th}$ and the 13$^{th}$ of July 2019.

Each repeatability study involves 10 tests, resulting in an error of 23.6% on the observed standard deviation. Both cases consider only the errors related to the equipment in the theoretical calculation of uncertainty.

In (Prignon et al., 2020b) – appendix C, we found that the IWLS and the WLOC regression techniques showed similar results, and we suggested that the WLOC technique should be preferred over the IWLS technique because of the absence of an iterative process. Thus, these repeatability studies investigate the OLS and the WLOC techniques only.

### 5.3.2. Results

The results of the repeatability studies involve three aspects: the overall results; the comparison between the calculated and the observed uncertainties; and the comparison between the different regression techniques (i.e. the OLS and the WLOC).

*Overall Results*

Table 10 and Table 11 show the results of the repeatability study conducted on the window opening using the plastic-sheet system with horizontal bars and on the electrical outlet using the woodbox system. These tables report the mean value, the observed and the calculated uncertainty in pressurisation, depressurisation and average, using the OLS and the WLOC techniques, for the airflow exponent and the air leakage rate at 50 Pa.

Table 10: results of the repeatability study conducted on the window case. $q_{50}$ in m³/(h.m).

| | | press | | depress | | total |
|---|---|---|---|---|---|---|
| | | $n_+$ | $q_{50+}$ | $n_-$ | $q_{50-}$ | $q_{50}$ |
| OLS | Mean | 0.85 | 0.55 | 0.81 | 0.57 | 0.56 |
| | Observed uncertainty | 0.03 | 0.07 | 0.08 | 0.06 | 0.05 |
| | Calculated uncertainty | 0.03 | 0.01 | 0.03 | 0.01 | 0.01 |
| WLOC | Mean | 0.84 | 0.55 | 0.82 | 0.57 | 0.56 |
| | Observed uncertainty | 0.03 | 0.06 | 0.08 | 0.06 | 0.05 |
| | Calculated uncertainty | 0.03 | 0.01 | 0.03 | 0.01 | 0.01 |

The overall leakage rate at 50 Pa of the window is 0.56 m³/(h.m), which is below the 95% confidence interval obtained with the meta-analysis (section 2.4): [0.8;3.2]. The airflow exponents are 0.85 in pressurisation and 0.81 in depressurisation, which are close to the upper limit of the 95% confidence interval: [0.55;0.83]. The observed uncertainty for the air leakage rate at 50 Pa is 0.05 (10%) on average and is 0.03 (4%) in pressurisation and 0.08 (10%) in depressurisation for the airflow exponent. There is a medium valve effect for the airflow exponent (Cohen's $d = -0.57$ for the OLS and $= -0.43$ for the WLOC) and a small valve effect on the air leakage rate at 50 Pa (Cohen's $d = 0.32$ for the OLS and $= 0.34$ for the WLOC).

Table 11: results of the repeatability study conducted on the electrical outlet case. $q_{50}$ in m³/h.

| | | press | | depress | | total |
|---|---|---|---|---|---|---|
| | | $n_+$ | $q_{50+}$ | $n_-$ | $q_{50-}$ | $q_{50}$ |
| OLS | Mean | 0.69 | 0.85 | 0.69 | 0.83 | 0.84 |
| | Observed uncertainty | 0.02 | 0.04 | 0.01 | 0.05 | 0.04 |
| | Calculated uncertainty | 0.02 | 0.01 | 0.03 | 0.01 | 0.01 |
| WLOC | Mean | 0.68 | 0.86 | 0.68 | 0.84 | 0.85 |
| | Observed uncertainty | 0.02 | 0.04 | 0.01 | 0.04 | 0.04 |
| | Calculated uncertainty | 0.03 | 0.01 | 0.03 | 0.01 | 0.01 |

The overall leakage rate at 50 Pa of the electrical outlet is 0.84 m³/h, which is also below the 95% confidence interval obtained with the meta-analysis: [0.9;4.5]. The airflow exponents are 0.69 in both pressurisation and depressurisation. Comparing this value with the meta-analysis would be inconsistent since only (Tenwolde et al., 1993) determined the airflow exponent of this building component and found a huge 95% confidence interval: [0.5;0.95]. The observed uncertainty is 0.04 (around 5%) for the total air leakage rate at 50 Pa, and 0.02 (around 3%) in pressurisation and 0.01 (around 2%) in depressurisation for the airflow exponent. When comparing the results in pressurisation and in depressurisation, there is no valve effect for the airflow exponent (Cohen's $d = 0.10$ for the OLS and $= -0.13$ for the WLOC) and a small valve effect for the air leakage rate at 50 Pa (Cohen's $d = -0.47$ for the OLS and $= -0.48$ for the WLOC).

Comparing the repeatability studies shows that using the woodbox system involves a lower observed uncertainty (5% instead of 10%). This is because the airtightness of a smaller pressure chamber (the second case) is easier to ensure. In addition, the inflation of the plastic-sheet system, although limited by horizontal bars, can randomly cause small defects in the pressure chamber.

### *Comparison Between the Observed and the Calculated Uncertainties*

Table 12 shows the results ($\Delta u$) of the comparison between the observed and the calculated uncertainty for each variable and for both repeatability studies.

Table 12: $\Delta u$ obtained when comparing the observed standard deviation and the calculated uncertainty for both repeatability studies and both regression techniques.

| | $n_+$ | $n_-$ | $q_{50,+}$ | $q_{50,-}$ | $q_{50}$ |
|---|---|---|---|---|---|
| OLS – window | 0.09 | 0.62 | 0.85 | 0.81 | 0.87 |
| OLS – electrical outlet | -0.20 | -2.05 | 0.67 | 0.68 | 0.77 |
| WLOC – window | -0.25 | 0.56 | 0.85 | 0.80 | 0.86 |
| WLOC – electrical outlet | -0.66 | -2.62 | 0.70 | 0.71 | 0.79 |

There are three interesting observations in these results:

- $\Delta u$ values are lower for the electrical outlet than for the window when looking at the air leakage rate and are higher when looking at the airflow exponent. This suggests that a larger $\Delta u$ for the airflow exponent does not necessarily induce a larger $\Delta u$ for the air leakage rate, because of the strong correlation between both regression parameters.
- $\Delta u$ is always positive when looking at the air leakage rate at 50 Pa. This means that the calculated uncertainty underestimates the observed uncertainty for all cases. This is not true for the airflow exponent.
- $\Delta u$ reported in Table 12 seems consistent with the values reported in Table 10 and Table 11. This suggests that the Cohen's benchmarks are appropriate to interpret $\Delta u$ (i.e. the comparison between the observed and the calculated uncertainty).

There are large differences between the observed and the calculated uncertainties in both cases and both regression techniques. This suggests that the accuracy and the resolution of the equipment is not sufficient to explain the observed uncertainty. This result strengthens the previous one: there is a large human error in the measurement because of the pressure chamber design and its construction. This highlights the need for the systems (e.g. the smoke generator) to control the pressure chamber's airtightness.

### *Comparison Between the OLS and the WLOC*

Table 13 and Table 14 present the results of the statistical comparison between the OLS and the WLOC method. The $p$ columns refer to the statistical significance (NHST) and the ES columns refer to the effect size, based on the statistical indicators detailed in section 5.2.3. On the one hand, $p$-values $> 0.05$,

$\leq 0.05$ and $\leq 0.001$ refer to non-significant, significant and highly significant. On the other hand, the Cohen's benchmarks stipulate that effect sizes $< 0.2$, $\geq 0.2$, $\geq 0.5$ and $\geq 0.8$ correspond to the effects of negligible, small, medium and large magnitude respectively.

Table 13: statistical comparison between the OLS and the WLOC techniques for the plastic-sheet system.

| | $n_+$ | | $n_-$ | | $q_{50,+}$ | | $q_{50,-}$ | | $q_{50}$ | |
|---|---|---|---|---|---|---|---|---|---|---|
| | $p$ | ES | $p$ | ES | $p$ | ES | $p$ | ES | $p$ | ES |
| Mean | * | NI | * | NI | * | NI | NS | NI | NS | NI |
| Observed uncertainty | NS | NI | NS | NI | NS | NI | NS | NI | NS | NI |
| Calculated uncertainty | ** | ++ | ** | + | NS | NI | NS | NI | NS | NI |

**$p$:** NS = Non-significant ($p > 0.05$), * = significant ($p \leq 0.05$), ** = highly significant ($p \leq 0.001$).

**ES:** NI = Negligible impact (ES $< 0.2$), + = small impact (ES $\geq 0.2$), ++ = medium impact (ES $\geq 0.5$), +++ = large impact (ES $\geq 0.8$).

The first repeatability study finds that the impact of changing the regression technique on the observed uncertainty is not statistically significant and with a negligible effect, whatever the variable. Regarding the mean value, such a change is statistically significant or not significant depending on the variable, and the effect is always negligible. Regarding the calculated uncertainty, a change of regression technique is not significant and has a negligible effect on the air leakage rate at 50 Pa but is highly significant and with a medium effect in pressurisation and a small effect in depressurisation for the airflow exponent.

Table 14: statistical comparison between the OLS and the WLOC techniques for the woodbox system.

| | $n_+$ | | $n_-$ | | $q_{50,+}$ | | $q_{50,-}$ | | $q_{50}$ | |
|---|---|---|---|---|---|---|---|---|---|---|
| | $p$ | ES | $p$ | ES | $p$ | ES | $p$ | ES | $p$ | ES |
| Mean | * | + | ** | +++ | ** | NI | ** | NI | ** | NI |
| Observed uncertainty | NS | NI | NS | NI | NS | NI | NS | NI | NS | NI |
| Calculated uncertainty | ** | +++ | ** | +++ | ** | +++ | ** | ++ | ** | +++ |

**$p$:** NS = Non-significant ($p > 0.05$), * = significant ($p \leq 0.05$), ** = highly significant ($p \leq 0.001$).
**ES:** NI = Negligible impact (ES $< 0.2$), + = small impact (ES $\geq 0.2$), ++ = medium impact (ES $\geq 0.5$), +++ = large impact (ES $\geq 0.8$).

The second repeatability study shows similar results regarding the observed uncertainty. Regarding the mean values, a change of regression technique is statistically significant for the airflow exponent in pressurisation and highly significant for the other variables. The effect size is small for the airflow exponent in pressurisation; large for the airflow exponent in depressurisation; and negligible for the air leakage rate at 50 Pa, whatever the mode. Regarding the calculated uncertainty, a change in the regression technique is statistically highly significant for all the variables and has a large impact for all the variables except the air leakage rate at 50 Pa in depressurisation (medium impact).

The results regarding the difference between the OLS and the WLOC techniques for the calculated uncertainty is surprising compared to the other values. Indeed, the statistical analyses show a large effect while the values reported in Table 10 and Table 11 show no differences. The inconsistency between the statistical analysis and the observed values suggests that the Cohen's benchmarks are not appropriate for comparing the impact of the different regression technique on the calculated uncertainty in this context.

## 5.4. Comparison Between the Direct and the Indirect Component Testing

The indirect component testing consists of two successive fan pressurisation measurements. The component of interest is sealed between both tests. The uncertainty of the air leakage rate at 50 Pa for the component ($u(q_{50,c})$) depends on the uncertainty of the pre- and the post-sealing fan pressurisation

tests ($u(q_{50,1})$ and $u(q_{50,2})$). According to the propagation law, Eq. 41 defines this uncertainty when assuming that both measurements are uncorrelated:

$$u(q_{50,c}) = \sqrt{u(q_{50,1})^2 + u(q_{50,2})^2} \quad \text{Eq. 41}$$

In this section, we first analyse a repeatability study conducted in October 2017 on the fan pressurisation test. Then, we analyse the results of two repeatability studies conducted in parallel with the same component: one using the indirect and one using the direct component testing.

### 5.4.1. Uncertainty in the Fan Pressurisation Test

This subsection summarises (Prignon et al., 2020b) – appendix C, a study that aimed to assess the impact of three regression techniques (the OLS, the IWLS and the WLOC) on the results of a fan pressurisation test. For additional information about the methodology, the reader should refer to the original paper.

This study investigates the results of a series of 30 successive measurements, resulting in an error of 13.1% on the observed standard deviation, of a newly constructed apartment of 228 m³ and with a floor area of 90 m² located in Brussels (Belgium). These tests are conducted within a period of 15 days in October 2017. There is no airtightness requirement for the apartment itself, but the entire building (i.e. all the apartments pressurised simultaneously) had to reach a maximum air change rate of $\mathbf{0.6}$ h$^{-1}$ at 50 Pa.

*Sources of Error Considered in the Theoretical Calculation*

This study introduces the additional source of error suggested by (Delmotte, 2017) that considers that the zero-flow pressure approximation is not always reliable. In fact, he questioned the assumption that $\Delta p_0$ experienced during the test equals the mean $\Delta p_0$ Measurements pre- and post-test. He proposed an additional component uncorrelated with the other components. Thus, the envelope uncertainty is (Eq. 42):

$$u(\Delta p) = \sqrt{u^2(\Delta p_m) + \frac{u^2(\Delta p_{0,1})}{4} + \frac{u^2(\Delta p_{0,2})}{4} + u^2(\Delta p_{0,a})} \quad \text{Eq. 42}$$

Where $u(\Delta p)$ is the uncertainty in envelope pressure, $u(\Delta p_m)$ is the uncertainty of pressure difference measurement, $u(\Delta p_{0,1})$ and $u(\Delta p_{0,2})$ are the uncertainties in zero-flow pressure measurements pre- and post-fan pressurisation test and $u(\Delta p_{0,a})$ is the additional component related to the zero-flow pressure approximation.

In (Prignon et al., 2019) – appendix E, we proposed and illustrated a method based on multi-level modelling for the quantification of $u(\Delta p_{0,a})$. We conducted and analysed 31 zero-flow pressure measurements. Then, for each test, we compare different zero-flow pressure approximations with the zero-flow pressure measurements that would have been experienced during a real fan pressurisation test.

Results show that $u(\Delta p_{0,a})$ varies between 0.42 and 1.52 Pa, depending on the wind speed and on the duration of the pre- and the post-test zero-flow pressure measurements. It also shows that changing the distribution for the zero-flow pressure assumed during the test or the time step between each measurement are not statistically significant and has a negligible effect on the value of $u(\Delta p_{0,a})$. In the continuity of that work, we applied the same methodology on 40 different buildings in (Prignon et al., 2020a) – appendix F, and concluded that the zero-flow pressure approximation uncertainty is a function of $\sigma(\Delta p_0)$, the standard deviation of the pre- and the post-test zero-flow pressure measurements (Eq. 43):

$$u(\Delta p_{0,a}) = \frac{0.11+0.98*\sigma(\Delta p_0)}{1.35} \quad \text{Eq. 43}$$

Figure 15 illustrates the uncertainty in the envelope pressure in Pa (left) and in % of the air leakage rate (right) as a function of the envelope pressure for four values of $\sigma(\Delta p_0)$, calculated with Eq. 42 and Eq. 43. This result highlights the large impact of the zero-flow pressure approximation uncertainty on the envelope pressure calculations.

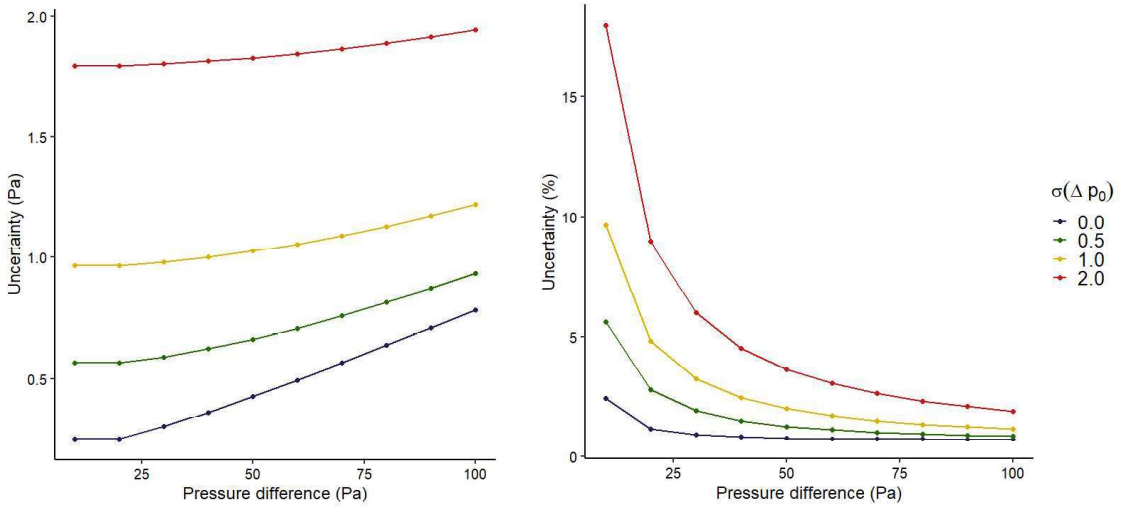



Figure 15: the uncertainty of the envelope pressure in Pa (left) and in % (right) as a function of the pressure difference measured for four values of $\sigma(\Delta p_0)$.

*Results*

Table 15 shows the observed standard deviation obtained in this repeatability study compared to the studies previously published in the literature. Except (Bracke et al., 2016) – House 2 and (Persily, 1982) which showed very low (132 m³/h) and very high (3860 m³/h) air leakage rate at 50 Pa, the different studies have observed a standard deviation between 1.3% and 1.8%.

Table 15: the number of tests, the mean air leakage rate at 50 Pa (in m³/h) and the observed standard deviation (in %) of multiple repeatability studies previously published.

| | Number of tests | Mean air leakage rate at 50 Pa (m³/h) | Observed standard deviation (%) |
|---|---|---|---|
| (Persily, 1982) | 17 | 3860 | 1.1 % |
| (Kim and Shaw, 1986) | 7 | 1104 | 1.6 % |
| (Delmotte and Laverge, 2011) | 10 | 732 | 1.4 % |
| (Novak, 2015) | 92 | 1005 | 1.8 % |
| (Bracke et al., 2016) – House 1 | 58 | 234 | 1.4 % |
| (Bracke et al., 2016) – House 2 | 53 | 132 | 2.3 % |
| This study | 30 | 252 | 1.3 % |

Table 16 shows the mean values, the observed and the calculated uncertainties for the leakage characteristics ($n$ and $C_L$) in both modes using the three

regression techniques. It shows that, for different regression techniques, the mean values are closed and the observed and the calculated uncertainties have small and large differences.

Table 16: the mean values, the observed standard deviations and the calculated uncertainty for the leakage characteristics ($n$ and $C_L$) in both modes using the three regression techniques.

| | Mean value | | | Observed uncertainty | | | Calculated uncertainty | | |
|---|---|---|---|---|---|---|---|---|---|
| | OLS | IWLS | WLOC | OLS | IWLS | WLOC | OLS | IWLS | WLOC |
| $n_+$ | 0.71 | 0.70 | 0.70 | 0.03 | 0.02 | 0.02 | 0.01 | 0.02 | 0.02 |
| $n_-$ | 0.69 | 0.68 | 0.68 | 0.04 | 0.01 | 0.02 | 0.01 | 0.02 | 0.02 |
| $C_{L,+}$ | 17.60 | 18.03 | 18.05 | 2.58 | 1.82 | 1.98 | 0.44 | 1.13 | 1.26 |
| $C_{L,-}$ | 15.48 | 15.49 | 15.53 | 2.40 | 0.82 | 1.13 | 0.37 | 1.11 | 1.29 |

Because of the large correlation between $n$ and $C_L$, it is impossible to draw a solid conclusion about the impact of the different regression techniques on the air leakage rate. Figure 16 draws, for the three regression techniques, the calculated and the observed uncertainties on the air leakage rate (in %) as a function of the pressure difference.

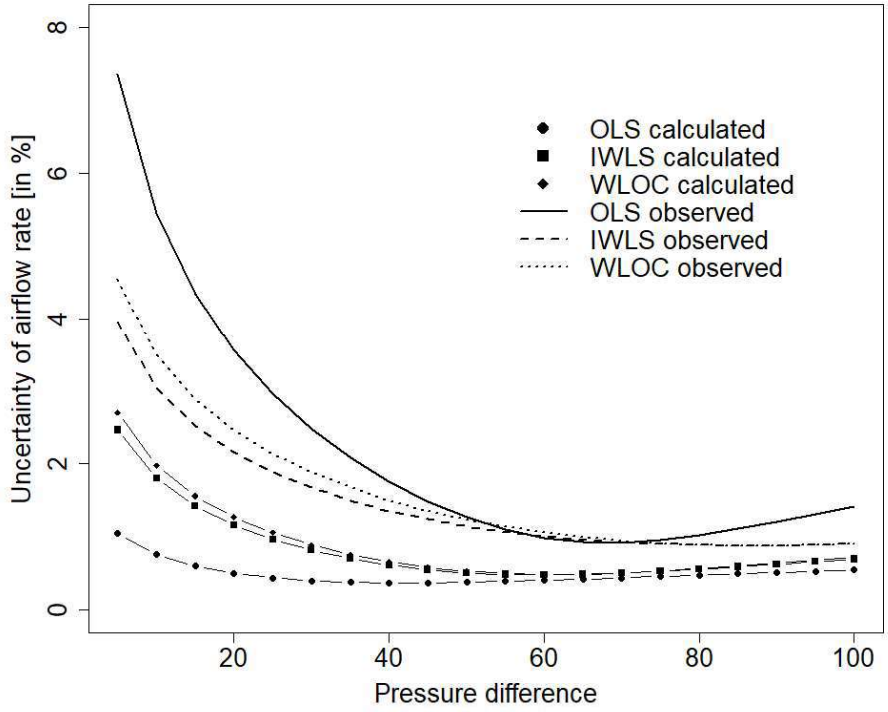



Figure 16: the calculated and the observed uncertainties on the airflow rate (in %) as a function of the pressure difference for the OLS, the IWLS and the WLOC

It shows that the observed uncertainty (lines) is larger for the OLS than for the IWLS and the WLOC, especially in low- and high-pressure differences. On the contrary, the calculated uncertainty is larger at low- and high-pressure differences for the IWLS and the WLOC than for the OLS. Consequently, the difference between the calculated and the observed uncertainty is lower for the IWLS and the WLOC than for the OLS. This result supports the need for alternative regression techniques as pointed out by (Okuyama and Onishi, 2012) and (Delmotte, 2013). Changing the regression technique would reduce the uncertainty and have a better fit between the observed and the calculated uncertainties.

Although the calculated uncertainty fits better the observed uncertainty with the WLOC and the IWLS than with the OLS, it still underestimates it, suggesting that a part of the uncertainty is still unknown. Examples of sources of errors that could improve the fitting between the calculated and the observed uncertainties are the human errors during the setup and the location of the pressure gauge as (Delmotte, 2019) and (Novak, 2019) suggested. Another possible explanation for this difference is that the data points do not fulfil the

assumption of constant ratio of x- and y- uncertainties of WLOC and IWLS methods (see section 3.1.2).

Figure 17 illustrates the difference between the three regression techniques regarding the air leakage rate at 5 Pa (left) and at 50 Pa (right) for each of the 30 measurements. This figure plots the calculated (error bars) and the observed (green zones) 95% confidence intervals.

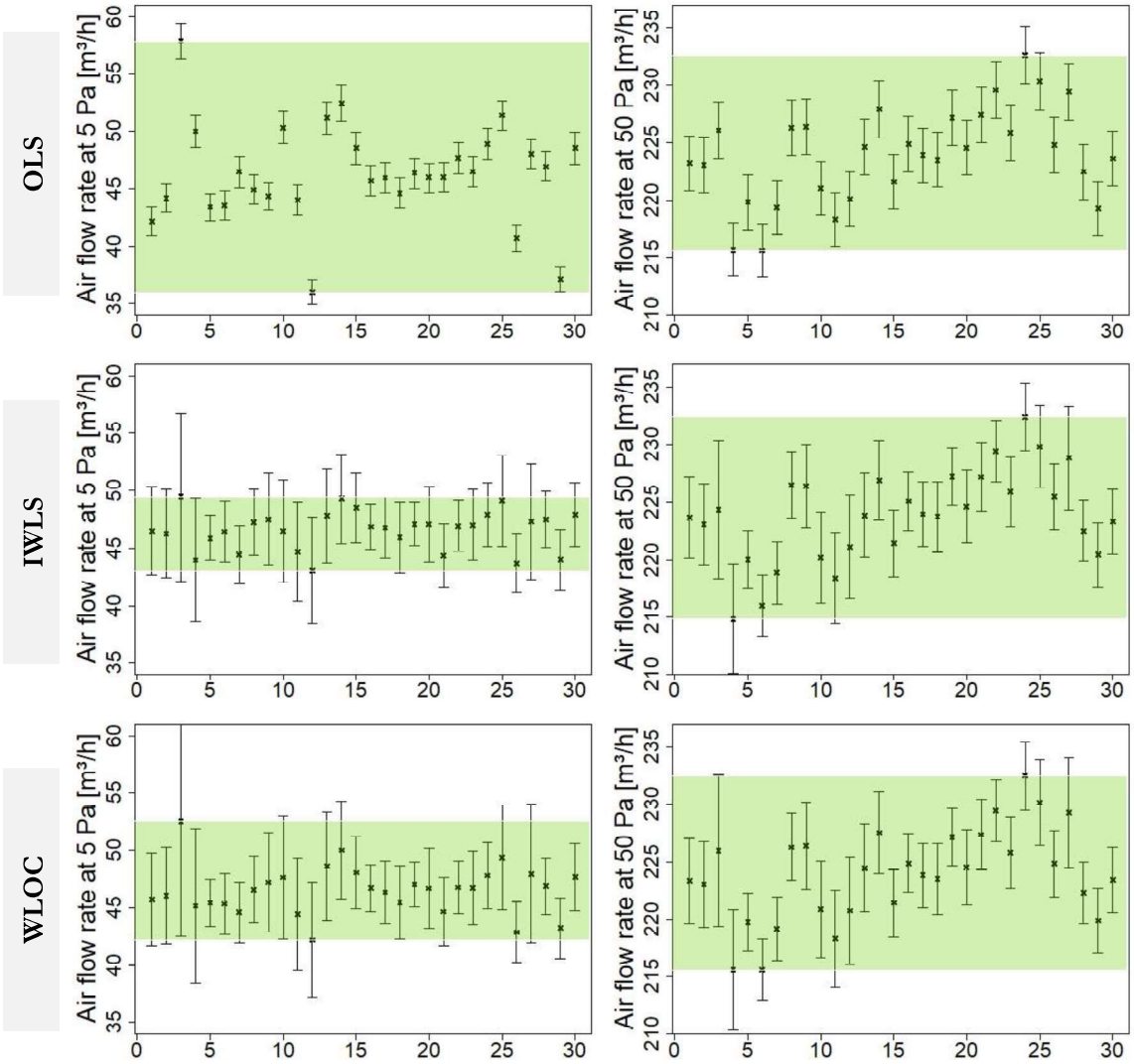



Figure 17: the calculated (error bars) and the observed (green zones) 95% confidence intervals of the airflow rate at 5 (left) and 50 (right) Pa for each of the 30 measurements for the three regression techniques.

An interesting result is that, at 5 Pa, each of the 95% confidence interval calculated with the WLOC and the IWLS includes most of the 29 other

measurements, which is not the case for the OLS. At 50 Pa, the WLOC and the IWLS show slightly better results than the OLS, but not as clearly as 5 Pa.

*Uncertainty of the Indirect Component Testing*

With the indirect component testing, the air leakage rate at 50 Pa through the component is the difference between the two fan pressurisation tests. If both are uncorrelated, the uncertainty is (Eq. 44):

$$u(q_{50,c}) = \sqrt{u(q_{50,1})^2 + u(q_{50,2})^2} \quad \text{Eq. 44}$$

Where $u(q_{50,c})$, $u(q_{50,1})$ and $u(q_{50,2})$ are the uncertainties of the air leakage rate at 50 Pa for the building component, the first and the second fan pressurisation tests.

If one considers that the uncertainty of the fan pressurisation test is a constant percentage of the air leakage rate (i.e. $u(q_{50,1}) = \alpha . q_{50,1}$ and $u(q_{50,2}) = \alpha . q_{50,2}$) and that $q_{50,2} = q_{50,1} - q_{50,c}$ where $q_{50,c}$ is the air leakage rate through the component of interest, Eq. 44 becomes Eq. 45:

$$u(q_{50,c}) = \sqrt{(\alpha\, q_{50,1})^2 + (\alpha\, q_{50,1} - \alpha\, q_{50,c})^2} \quad \text{Eq. 45}$$

Then, by defining $\beta = q_{50,c}/q_{50,1}$, Eq. 45 becomes Eq. 46:

$$u(q_{50,c}) = \sqrt{2\alpha^2 + \alpha^2\beta^2 - 2\alpha^2\beta} * q_{50,1} \quad \text{Eq. 46}$$

This last equation suggests that the uncertainty of the air leakage rate through the component is a function of $\alpha$, $q_{50,1}$ and $\beta$. An interesting observation in Eq. 46 is that when $q_{50,1}$ diminishes (e.g. by limiting the tested zone) $\beta$ increases, slowing the decrease of $u(q_{50,c})$. For the apartment tested in this section (i.e. $\alpha = 0.013$ and $q_{50,c} = 252$ m³/h), a component with an air leakage rate at 50 Pa of $25.2$ m³/h ($\beta = 0.1$) would be measured with an uncertainty of $13.7$ m³/h (54.4 % of its air leakage rate).

This calculation assumes a constant value for $\alpha$, which is questionable since the uncertainty of the fan pressurisation test depends on the zone measured (see Table 15). In addition, the selected value for $\alpha$ ($0.013$) is based on the result of the repeatability studies conducted on a 15-day period. In practice, both fan

pressurisation tests are conducted on the same day and, consequently, they experience lower variations than those observed in this repeatability study. Eq. 46 and related assumptions are discussed in a real case in the next section.

### 5.4.2. Comparing Reliability of Direct and Indirect Component Tests

In this section, we compare two repeatability studies conducted in parallel on the same component and during the same period, but with two methods. Both studies consist of 20 successive measurements, resulting in an error of 16.2% on the observed standard deviation. The measured component is an electrical outlet in a plastered wall of an existing building built in the '60s. The experiment took place between the 17$^{th}$ and the 30$^{th}$ of June 2020.

The first repeatability study uses the direct component testing with the woodbox system and the second repeatability study uses the indirect component testing with a limited zone (privative laundry room). For both reliability studies, the calculated uncertainty includes the errors related to the equipment and to the zero-flow pressure approximation. Without previous knowledge, the error related to zero-flow pressure approximation for the direct component testing is the same as for the fan pressurisation test (Eq. 43).

*Reliability of the Direct Component Testing*

Table 17 shows the results of the repeatability study conducted with the direct component testing. It reports the mean values, the observed and the calculated uncertainties for the airflow exponent and the air leakage rate at 50 Pa in pressurisation, depressurisation and average, using the OLS and the WLOC methods.

Table 17: results of the repeatability study conducted on the electrical outlet case with the direct component testing. $q_{50}$ in m³/h.

| | | press | | depress | | Total |
|---|---|---|---|---|---|---|
| | | $n_+$ | $q_{50+}$ | $n_-$ | $q_{50-}$ | $q_{50}$ |
| OLS | Mean | 0.60 | 3.37 | 0.60 | 3.35 | 3.36 |
| | Observed uncertainty | 0.02 | 0.10 | 0.02 | 0.11 | 0.10 |
| | Calculated uncertainty | 0.01 | 0.02 | 0.01 | 0.01 | 0.01 |
| WLOC | Mean | 0.59 | 3.37 | 0.60 | 3.35 | 3.36 |
| | Observed uncertainty | 0.02 | 0.10 | 0.01 | 0.11 | 0.10 |
| | Calculated uncertainty | 0.11 | 0.18 | 0.10 | 0.18 | 0.12 |

The overall leakage of the electrical outlet at 50 Pa is 3.36 m³/h, which is inside the 95% confidence interval obtained with the meta-analysis: [0.9;4.5]. The airflow exponents are 0.60 in pressurisation and depressurisation. The observed uncertainty is 0.10 (around 3 %) for the mean air leakage rate at 50 Pa and 0.02 (around 3 %) in pressurisation and depressurisation for the airflow exponent. These observed uncertainties are below the previous repeatability studies (section 5.3).

When comparing the pressurisation and the depressurisation results, there is a medium valve effect for the airflow exponent (Cohen's $d = -0.54$ for the OLS and $d = -0.62$ for the WLOC) and a negligible valve effect for the air leakage rate at 50 Pa (Cohen's $d = 0.18$ for the OLS and the WLOC).

When comparing the observed and the calculated uncertainties with the OLS, there are large differences for $q_{50+}$ ($\Delta u = 0.85$), $q_{50-}$ ($\Delta u = 0.88$) and $q_{50}$ ($\Delta u = 0.90$). When using the WLOC, these differences are medium for $q_{50+}$ ($\Delta u = 0.72$) and $q_{50-}$ ($\Delta u = 0.60$), and small for $q_{50}$ ($\Delta u = 0.25$). For the airflow exponent, the difference between the modes has a medium effect in pressurisation ($\Delta u = 0.71$) and depressurisation ($\Delta u = 0.62$) for the OLS, and a large effect in pressurisation ($\Delta u = 5.39$) and depressurisation ($\Delta u = 7.38$) for the WLOC. According to the results presented in Table 17, the uncertainty calculated with the WLOC overestimates the observed uncertainty while the uncertainty calculated with the OLS underestimates it.

Table 18 presents the results of the statistical comparison between the OLS and the WLOC for this repeatability study. $p$ columns refers to the statistical significance and the ES columns refer to the effect size, based on the statistical indicators detailed in section 5.2.3.

Table 18: results of the statistical comparison between the OLS and the WLOC for the electrical outlet measured with the direct component testing.

| | $n_+$ | | $n_-$ | | $q_{50,+}$ | | $q_{50,-}$ | | $q_{50}$ | |
|---|---|---|---|---|---|---|---|---|---|---|
| | $p$ | ES | $p$ | ES | $p$ | ES | $p$ | ES | $p$ | ES |
| Mean | ** | ++ | ** | ++ | NS | NI | NS | NI | NS | NI |
| Observed uncertainty | NS | NI | NS | NI | NS | NI | NS | NI | NS | NI |
| Calculated uncertainty | ** | +++ | ** | +++ | ** | +++ | ** | +++ | ** | +++ |

**$p$:** NS = Non-significant ($p > 0.05$), * = significant ($p \leq 0.05$), ** = highly significant ($p \leq 0.001$).

**ES:** NI = Impact of non-substantive magnitude ($ES < 0.2$), + = small impact ($ES \geq 0.2$), ++ = medium impact ($ES \geq 0.5$), +++ = large impact ($ES \geq 0.8$).

These observations highlight three main outcomes.

- For each mode, the difference of means for the air leakage rate at 50 Pa is not significant and the effect is negligible. Regarding the air leakage exponent, changing the regression technique is statistically highly significant and has a medium effect in pressurisation and depressurisation.
- A change of regression technique has no statistical difference and no practical impact when looking at the observed uncertainty.
- When looking at the calculated uncertainty, changing the regression technique is statistically highly significant and has a large effect, whatever the variable and the mode. However, unlike in the previous repeatability studies (section 5.3), the values reported in Table 17 also reveal this difference. The effect size (Hedge's $g$) in this case is between -18.7 and -34.3, depending on the variable while in the other repeatability studies it is between -0.02 and -0.73 for the window and between 0.37 and -2.74 for the electrical outlet. This comparison strengthens the idea that the Cohen's benchmarks may be inappropriate for this comparison.

Two other interesting results arise from the comparison of this reliability study with the previous ones. First, even with an increase of the duration of the testing period, the standard deviation of the measurements is lower. This suggests that increasing the number of tests in order to reduce the error on the observed standard deviation should be a priority over reducing the period of testing to reduce the variation in climatic conditions. Second, the impact of changing the regression technique on the calculated uncertainty is bigger when the zero-flow

pressure approximation is considered in the calculations. This highlights the need for a larger investigation of this uncertainty component in the case of the direct component testing.

*Reliability of the Indirect Component Testing*

There are two steps in analysing the repeatability study of the indirect component testing: analysing each fan pressurisation test individually and analysing the air leakage rate of the measured component.

Table 19 presents the results of pre- and post-sealing repeatability studies.

Table 19: results of the repeatability studies conducted with the fan pressurisation method pre- and post-sealing of the component. $q_{50}$ in m³/h.

| | | Pre-sealing study | | | | | Post-sealing study | | | | |
|---|---|---|---|---|---|---|---|---|---|---|---|
| | | press | | depress | | Tot | press | | depress | | Tot |
| | | $n_+$ | $q_{50+}$ | $n_-$ | $q_{50-}$ | $q_{50}$ | $n_+$ | $q_{50+}$ | $n_-$ | $q_{50-}$ | $q_{50}$ |
| OLS | Mean | 0.57 | 98.6 | 0.67 | 66.1 | 82.4 | 0.56 | 96.0 | 0.68 | 62.9 | 79.4 |
| | Observed uncertainty | 0.03 | 2.06 | 0.02 | 2.59 | 1.98 | 0.01 | 1.29 | 0.03 | 2.03 | 1.35 |
| | Calculated uncertainty | 0.01 | 0.36 | 0.01 | 0.35 | 0.25 | 0.00 | 0.31 | 0.01 | 0.30 | 0.22 |
| WLOC | Mean | 0.56 | 98.6 | 0.67 | 66.2 | 82.4 | 0.57 | 96.0 | 0.68 | 62.9 | 79.5 |
| | Observed uncertainty | 0.02 | 2.15 | 0.02 | 2.59 | 2.02 | 0.01 | 1.29 | 0.03 | 2.05 | 1.35 |
| | Calculated uncertainty | 0.02 | 0.97 | 0.02 | 0.64 | 0.58 | 0.02 | 0.94 | 0.02 | 0.62 | 0.56 |

For the first fan pressurisation test, the mean air leakage rate at 50 Pa is 82.4 m³/h with an observed standard deviation of 2.4 %. For the second repeatability study, the mean air leakage rate at 50 Pa is 79.4 m³/h with an observed standard deviation of 1.7 %. These high values for the standard deviation are consistent with the literature since (Bracke et al., 2016) found that the standard deviation expressed in % increases when measuring low air leakage rates.

These results also show that the WLOC and the OLS methods are equivalent when looking at the mean and the observed uncertainty and that the uncertainty calculated with the WLOC fits better the observed uncertainty than when the OLS is used.

The statistical analyses summarised in Table 20 and Table 21 comparing the OLS and the WLOC for the pre- and the post-sealing confirm these results.

The change of regression technique is highly significant and has a large impact on all the variables when looking at the calculated uncertainty, for both repeatability studies. When looking at the observed uncertainty, it is not significant and has a negligible impact except for the airflow exponent in pressurisation in the first study (small effect). Regarding the mean values, it is also not significant and with a negligible impact except for the airflow exponent (statistically significant and small effect) and the air leakage rate (statistically significant and negligible effect) in depressurisation for the first study and the air leakage rate (statistically significant with negligible effect) in total for the second repeatability study. All these results are in line with the results found in the literature and in the previous repeatability study.

Table 20: results of the comparison between the OLS and the WLOC for the pre-sealing study.

| | $n_+$ | | $n_-$ | | $q_{50,+}$ | | $q_{50,-}$ | | $q_{50}$ | |
|---|---|---|---|---|---|---|---|---|---|---|
| | $p$ | ES | $p$ | ES | $p$ | ES | $p$ | ES | $p$ | ES |
| Mean | NS | NI | * | + | NS | NI | * | NI | NS | NI |
| Observed uncertainty | NS | + | NS | NI | NS | NI | NS | NI | NS | NI |
| Calculated uncertainty | ** | +++ | ** | +++ | ** | +++ | ** | +++ | ** | +++ |

**$p$:** NS = Non-significant ($p > 0.05$), * = significant ($p \leq 0.05$), ** = highly significant ($p \leq 0.001$).

**ES:** NI = Impact of non-substantive magnitude ($ES < 0.2$), + = small impact ($ES \geq 0.2$), ++ = medium impact ($ES \geq 0.5$), +++ = large impact ($ES \geq 0.8$).

Table 21: results of the comparison between the OLS and the WLOC for the post-sealing study.

| | $n_+$ | | $n_-$ | | $q_{50,+}$ | | $q_{50,-}$ | | $q_{50}$ | |
|---|---|---|---|---|---|---|---|---|---|---|
| | $p$ | ES | $p$ | ES | $p$ | ES | $p$ | ES | $p$ | ES |
| Mean | NS | NI | NS | NI | NS | NI | NS | NI | * | NI |
| Observed uncertainty | NS | NI | NS | NI | NS | NI | NS | NI | NS | NI |
| Calculated uncertainty | ** | +++ | ** | +++ | ** | +++ | ** | +++ | ** | +++ |

**$p$**: NS = Non-significant ($p > 0.05$), * = significant ($p \leq 0.05$), ** = highly significant ($p \leq 0.001$).

ES: NI = Impact of non-substantive magnitude ($ES < 0.2$), + = small impact ($ES \geq 0.2$), ++ = medium impact ($ES \geq 0.5$), +++ = large impact ($ES \geq 0.8$).

The air leakage rate at 50 Pa through the component is the difference between the pre- and the post-sealing of the component. Table 22 presents the result of the repeatability study that investigates the component air leakage rate at 50 Pa.

Table 22: result of the repeatability study when looking at the component air leakage rate measured with the indirect component testing.

| | | $q_{50+}$ | $q_{50-}$ | $q_{50}$ |
|---|---|---|---|---|
| OLS | Mean | 2.66 | 3.23 | 2.94 |
| | Observed uncertainty | 1.99 | 2.64 | 1.78 |
| | Calculated uncertainty | 0.48 | 0.49 | 0.36 |
| WLOC | Mean | 2.64 | 3.24 | 2.94 |
| | Observed uncertainty | 2.08 | 2.66 | 1.83 |
| | Calculated uncertainty | 1.35 | 0.89 | 0.81 |

These results show a mean air leakage rate at 50 Pa of 2.94 $m^3/h$ with an observed standard deviation of 60.5 % for the OLS and 62.2 % for the WLOC. The uncertainty computed using Eq. 46 is 93.4 % with $\alpha = 2.4$ % and $\beta = 0.036$. The difference with the observed standard deviation is possibly due to four assumptions made to deduce Eq. 45:

- The standard deviation for the pre- and the post-sealing tests are assumed identical and constant, while the results show a difference between those (2.4 % and 1.7 % respectively).
- The standard deviation considered for the fan pressurisation test ($\alpha$) is based on multiple repeatability studies conducted on multiple days while in the case of the indirect component testing, these tests are conducted on the same day. Therefore, $\alpha$ overestimates the uncertainty of the fan pressurisation test used for the indirect component testing.
- $q_{50,1}$ and $q_{50,c}$ are assumed uncorrelated. However, based on the 20 measurements made in this study, a correlation coefficient (Pearson's $r$) of 0.75 is observed between $q_{50,c}$ and $q_{50,1}$ and of -0.22 between $q_{50,c}$ and $q_{50,2}$. These values are similar for OLS and WLOC. This is surprising since one would expect no correlation and no difference between pre- and post-sealing tests. Further investigations are necessary to exclude the possibility of a Type I error (a correlation is found in the dataset while there is not in the population), and to find the reason for this correlation.

- $q_{50,1}$ and $q_{50,2}$ are also considered uncorrelated while a correlation coefficient of $0.48$ using the OLS and $0.47$ using the WLOC are observed between both fan pressurisation tests in this dataset. This observation is not surprising since both tests are expected to be influenced by the same weather conditions and, therefore, to be biased in the same way.

A deeper investigation could help to draw a solid conclusion about the correlations between the zone tested and the component leakage, and between the pre- and the post-sealing tests. Before that, Eq. 46 should only be used to determine the order of magnitude of the expected uncertainty when using the indirect component testing.

### *Comparison Between the Direct and the Indirect Testing*

Table 23 groups the results from the Table 17 and the Table 22 to compare them. It shows the mean values, the calculated and the observed uncertainties for the air leakage rate at 50 Pa, for the direct and the indirect component testing, in pressurisation, depressurisation and total, and using the OLS and the WLOC regression techniques.

Table 23: results of the repeatability studies conducted on the electrical outlet with the OLS and the WLOC, using the direct and the indirect component testing. $q_{50}$ in m³/h.

| | | $q_{50+}$ | | $q_{50+}$ | | $q_{50}$ | |
|---|---|---|---|---|---|---|---|
| | | Indirect | Direct | Indirect | Direct | Indirect | Direct |
| OLS | Mean | 2.66 | 3.37 | 3.23 | 3.35 | 2.94 | 3.36 |
| | Observed uncertainty | 1.99 | 0.10 | 2.64 | 0.11 | 1.78 | 0.10 |
| | Calculated uncertainty | 0.48 | 0.02 | 0.49 | 0.01 | 0.36 | 0.01 |
| WLOC | Mean | 2.64 | 3.37 | 3.24 | 3.35 | 2.94 | 3.36 |
| | Observed uncertainty | 2.08 | 0.10 | 2.66 | 0.11 | 1.83 | 0.10 |
| | Calculated uncertainty | 1.35 | 0.18 | 0.89 | 0.18 | 0.81 | 0.12 |

In addition to the individual conclusions drawn in the previous sections, this table shows that some differences are observed in the mean values and in the observed uncertainties respectively. Figure 18 illustrates these observations for the OLS by plotting the mean air leakage rate at 50 Pa (black dot) and the 95% confidence interval for the observed uncertainty (blue lines). The WLOC lead to the same trends in the results.

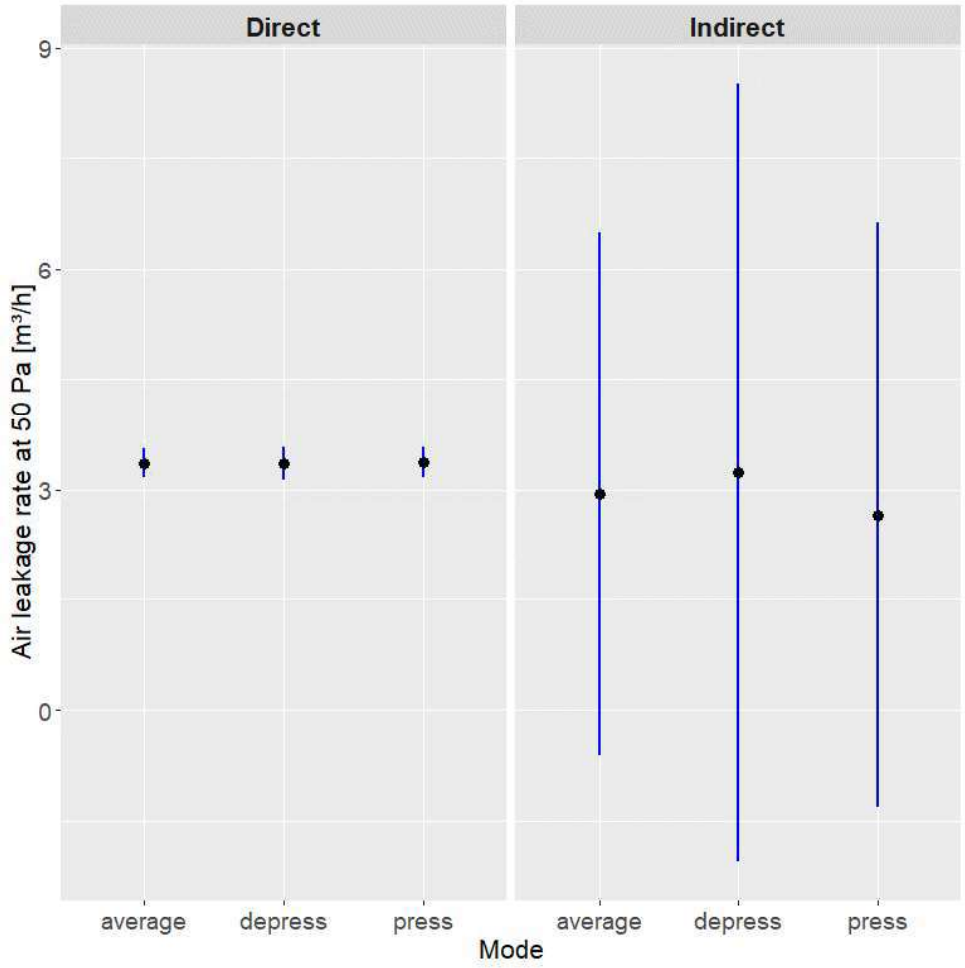



Figure 18: the mean air leakage rate at 50 Pa (black dot) and the observed uncertainty (blue lines) in both modes, obtained with the OLS, using the direct (left) and the indirect (right) component testing.

The small difference in the mean values and the large difference in the observed uncertainties shown in this figure are confirmed statistically. For all the modes, the difference between the mean values is not statistically significant and has a small effect ($t = 1.05$, $p = 0.31$ and $g = 0.32$) while the difference between the observed uncertainties is highly significant and with a medium effect ($F < 0.01$, $p < 0.001$ and $\Delta\sigma = 0.51$). The values are for the OLS regression technique, but the analysis of the WLOC technique leads to the same conclusion. Using Cohen's benchmarks to interpret $\Delta\sigma$ when comparing the different measurement methods is not appropriate since it indicates a medium effect while the Figure 18 and the Table 23 report huge differences in the values.

Regarding the differences between the observed and the calculated uncertainties, $\Delta u$ values are larger with the direct test using OLS ($0.89$ vs. $0.80$) and lower using WLOC ($-0.25$ vs. $0.56$).

## 5.5. Summary of Chapter's Outcomes

In this chapter, we illustrate methodologies for the theoretical calculation and the experimental observation of the uncertainty of the measurement methods. This includes the statistical indicators needed to compare the different datasets in this context. Then, we apply this method to five cases, resulting in five repeatability studies. The first two repeatability studies focus on the direct component testing and aim at quantifying the method uncertainty for two types of pressure chambers. The third focuses on the fan pressurisation test and provides the necessary information to predict the uncertainty of the indirect component testing. Fourth and fifth repeatability studies are conducted on the same component in parallel (i.e. in the same period) and aim at comparing the direct and the indirect component testing.

We found that the uncertainty in the direct component testing is between 3% and 10%, depending on the pressure chamber design and on the measured air leakage rate. This value is much lower than for the indirect component testing (around 60%). In addition, we found that for an experimental investigation of the uncertainties, increasing the number of tests should be preferred over reducing the testing period. In our opinion, a repeatability study should consider at least 14 tests to maintain the error on the observed uncertainty below 20%.

Two interesting results deserve more investigation:

- We found that the impact of changing the regression technique depends on the value of $u(\Delta p_{0,a})$, defined based on the values found in the fan pressurisation measurements. Further work should focus on the quantification of this component of the uncertainty specifically for the direct component testing.

We found that Cohen's benchmarks are inappropriate to compare the impact of different regression techniques on the calculated uncertainty and of different measurement methods on the observed uncertainty. Further work should focus on the definition of new benchmarks when interpreting these two indicators.

# Chapter 6. Applications of the Direct Component Testing

In this chapter, we present the results and the challenges related to two applications of the direct component testing. First is the measurement of multiple building components and the comparison of these results with the literature. Second is the determination of the airtightness performance of a single zone.

## 6.1. *In-situ* Measurement of the Building Components

This section presents the results of multiple measurements conducted with the direct component method, using the equipment described previously. Except for two cases later identified, all these measurements are conducted *in-situ* on buildings in the construction phase between 2018 and 2020. These results include the bias in background leakage quantified in section 4.2. In addition, their uncertainty is given by the repeatability studies of section 5.3: 10% for the plastic-sheet system and 5% for the woodbox system. However, the uncertainty obtained with the repeatability studies, expressed in % of the air leakage rate, may underestimate the real uncertainty at low air leakage rate. Therefore, the calculated uncertainty is used as a lower limit of the uncertainty. Consequently, the uncertainty considered is the greatest between the calculated uncertainty and the results obtained in repeatability studies.

This section is divided in three parts. First, it reports three issues encountered during these measurement campaigns. Second, it reports the results of 13 tests conducted on windows and compare them to the literature. Third, it reports the

results of 21 tests conducted on small discontinuities in walls (i.e. switches or electrical outlets) and compare them to the literature.

Most of those experiments were conducted on masonry apartments, which have represented a large share of new residential construction in Brussels over recent years. Consequently, those measurements do not include the large variety of cases that can be encountered in practice.

### 6.1.1. Issues with the Direct Component Testing

Two tests took place in March and September 2018 on windows with the plastic-sheet system. These tests reveal two important points of attention in the direct component testing:

- When nothing prevents large inflation and deflation of the plastic membrane, the system is likely to collapse at high-pressure difference, especially in pressurisation. In addition, even if the system does not collapse, small holes appear in the tape maintaining the pressure chamber and make the measurement unreliable. In such cases, an additional system must be used to prevent the inflation and the deflation of the pressure chamber (e.g. extendable propping bars as shown in section 3.2).
- When the leakage route (i.e. the way leakage goes through the building component) is not properly understood or identified, there is a risk of measuring an irrelevant leakage (e.g. a leakage going back inside the building). There are two ways to avoid this backward leakage: (1) using a smoke generator combined with the direct component testing to identify the leakage route or (2) pressurising the room simultaneously with the direct component test to measure only the leakage through the component. This second method also reduces the bias due to the background leakage, but it requires additional equipment and time for the experiment. This probably induces different uncertainties than those quantified in the previous chapters and requires a closed zone for the pressurisation test, which can be problematic depending on the progress of the construction process.

A third test measures a newly erected plastered wall within a multi-family dwelling in July 2019. The results show an air leakage rate of 0.01 $m^3/(h.m^2)$ with a calculated uncertainty of 0.03 $m^3/(h.m^2)$. This is below the range of measurable airflow, suggesting a higher uncertainty than the calculated one. This agrees with the literature that shows a 95% confidence interval of [0;0.3]

$m^3/(h.m^2)$. However, in this case the airflow exponent measured is 0.25 in pressurisation and 0.38 in depressurisation, which is outside the range of meaningful values. This is because only three points at high-pressure differences are used to perform the linear regression.

### 6.1.2. Windows

Table 24 shows the result of 13 windows tested and the general information about those: the type, the material, the total area and the opening length. For the third row, the equipment presented in section 3.2 is used in the laboratory rather than *in-situ*. Consequently, lower results than those that would be obtained *in-situ* are expected since it does not measure the defects in the construction process. However, the subgroup meta-analysis of the windows shows no differences between the laboratory and the in-situ measurements. In addition, the table provides the airflow exponent in pressurisation and depressurisation, and the air leakage rate at 50 Pa per meter of opening length in pressurisation, depressurisation and total. For two cases ($3^{rd}$ and $10^{th}$) the test was conducted in only one of both modes. The last two lines of the table are the mean and the standard deviation of the 13 measurements.

Table 24: results of the 13 measurements conducted on windows including the type, the material and the dimensions of windows. The airflow exponent is given in pressurisation and depressurisation and the air leakage rate at 50 Pa per m of opening length is given in pressurisation, depressurisation and total.

| # | Type | Material | A | L | $n_+$ | $q_{50,+}$ | $n_-$ | $q_{50,-}$ | $q_{50}$ |
|---|---|---|---|---|---|---|---|---|---|
| 1 | Single | Aluminium | 1.40 | 5.08 | 0.75 | 1.41 | 0.79 | 1.30 | 1.35 |
| 2 | Single | Wood | 2.42 | 5.40 | 0.85 | 0.57 | 0.81 | 0.57 | 0.57 |
| 3 | Sliding | Aluminium | 10.42 | 12.96 | 0.67 | 1.47 | | | 1.47 |
| 4 | Single | Aluminium | 2.90 | 6.86 | 0.62 | 1.48 | 0.56 | 1.30 | 1.39 |
| 5 | Double | Aluminium | 2.98 | 6.96 | 0.57 | 1.67 | 0.70 | 2.09 | 1.88 |
| 6 | Double | Aluminium | 4.00 | 8.00 | | | 0.61 | 1.31 | 1.31 |
| 7 | Single | Aluminium | 1.91 | 5.86 | 0.73 | 1.99 | 0.71 | 1.76 | 1.87 |
| 8 | Single | Aluminium | 1.91 | 5.86 | 0.49 | 2.91 | 0.63 | 3.13 | 3.02 |
| 9 | Single | Aluminium | 1.91 | 5.86 | 0.68 | 1.54 | 0.67 | 1.63 | 1.58 |
| 10 | Single | Aluminium | 1.16 | 2.45 | 0.61 | 2.31 | 0.61 | 2.30 | 2.63 |
| 11 | Single | Aluminium | 1.07 | 2.10 | 0.58 | 3.43 | 0.54 | 3.55 | 3.49 |
| 12 | Double | Aluminium | 2.88 | 6.8 | 0.79 | 0.77 | 0.63 | 0.73 | 0.75 |
| 13 | Double | Aluminium | 2.88 | 6.8 | 0.69 | 0.38 | 0.57 | 0.24 | 0.31 |
| | | | | | 0.65 | 1.70 | 0.65 | 1.67 | 1.66 |
| | | | | | 0.12 | 0.96 | 0.09 | 0.99 | 0.93 |

Figure 19 compares the 95 % confidence interval of each window measured (points and error bars) with the 95% confidence interval obtained with the meta-analysis. This second 95% confidence interval (coloured zone in the graph) is called the "literature interval" hereafter.

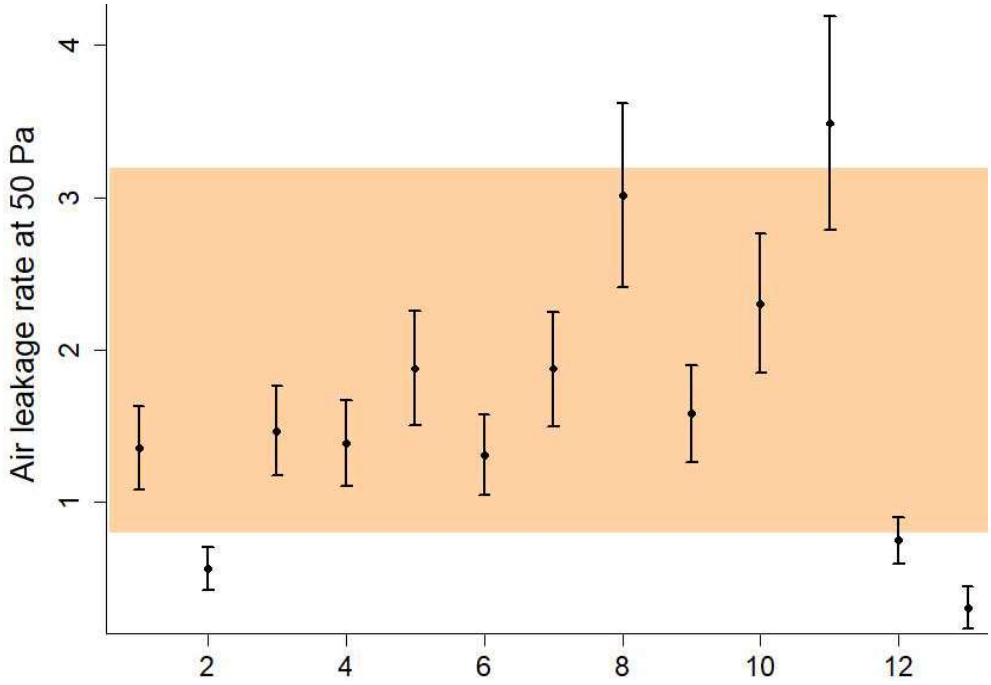



Figure 19: the 95% confidence interval of air leakage rate at 50 Pa measured for each window, compared with the literature 95% confidence interval.

This figure shows that all except two (2nd and 13th cases) 95% confidence intervals overlap the literature interval. These two cases are below the literature interval, suggesting that the literature interval overestimates the real observations made *in-situ*. In addition, the standard error found with the meta-analysis (0.60 $m^3/(h.m)$) is the same order of magnitude as the standard error found in this series of tests (0.93 $m^3/(h.m)$). The small observed difference is surprising since a smaller variety of windows is tested in this case than in the literature. Thus, a smaller variation would have been expected. However, these observations are based on 13 cases only, limiting their generalisation because of the large error on the observed standard deviation.

Figure 20 shows the same comparison applied to the airflow exponent in pressurisation (red zone – upper graph) and depressurisation (green zone – lower graph). For all cases, both confidence intervals overlap in pressurisation and depressurisation. In addition, the standard deviation observed in this dataset (0.12 in pressurisation and 0.09 in depressurisation) are close to those obtained in the meta-analysis (0.07 without distinction between depressurisation and pressurisation).

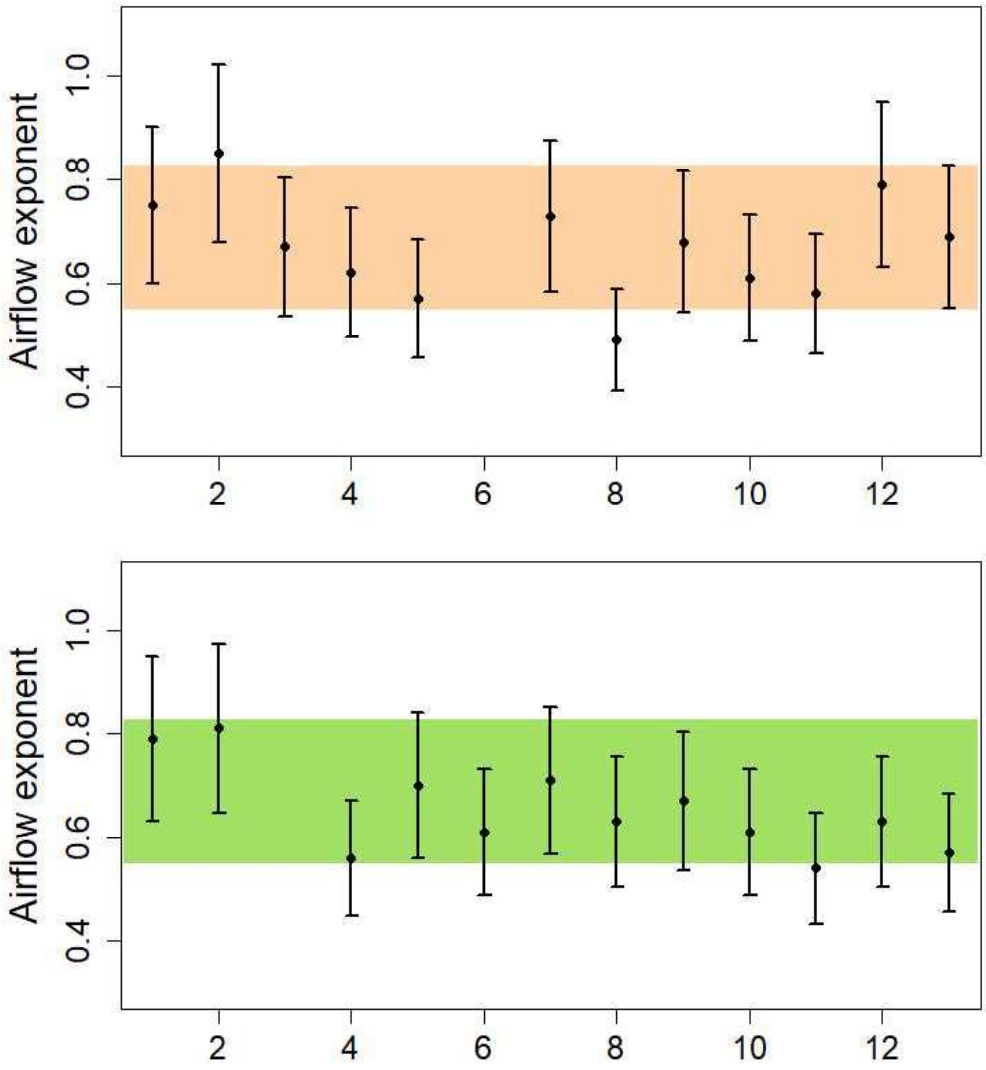



Figure 20: the 95% confidence interval of airflow exponent in pressurisation (upper graph) and depressurisation (lower graph) measured for windows, compared with the literature interval.

Although this study reports the type and the material of windows, more cases, and a larger variety of them, are necessary to conduct a solid subgroup analysis and to analyse the differences in window types and materials.

### 6.1.3. Small Discontinuities in Walls

Table 25 shows the results of 21 measurements conducted on two types of small discontinuities in walls: the electrical outlets and the switches. All discontinuities are in plastered walls in multi-family dwellings (heavy constructions). The table provides the number of components tested (one

discontinuity can include multiple outlets at once); the air leakage rate per unit (per outlet/switch); the airflow exponent; and the type of partition (interior – in a wall inside the apartment, or exterior – in the wall between apartments, directly to the outside or to a building space). Considering the air leakage rate per unit assumes that it is proportional to the total area of discontinuities rather than the number of discontinuities. Since no previous knowledge supports this assumption, the results analysed hereafter refer to both cases: per unit and per discontinuity.

Table 25: results of 21 measurements conducted on discontinuities (e.g. the electrical outlets or the switches). This table includes the type of wall and the number of units tested, in addition to the airflow exponent (in pressurisation and depressurisation) and the air leakage rate at 50 Pa per unit (in pressurisation, depressurisation and total).

| Test | # | Surface | $n_+$ | $q_{50,+}$ | $n_-$ | $q_{50,-}$ | $q_{50}$ |
|---|---|---|---|---|---|---|---|
| 1 | 2 | Interior | 0.69 | 0.25 | 0.69 | 0.28 | 0.27 |
| 2 | 2 | Exterior | 0.61 | 0.68 | 0.61 | 0.71 | 0.70 |
| 3 | 2 | Exterior | 0.66 | 1.13 | 0.64 | 1.12 | 1.13 |
| 4 | 2 | Exterior | 0.72 | 0.62 | 0.72 | 0.75 | 0.69 |
| 5 | 2 | Exterior | 0.71 | 0.60 | 0.71 | 0.61 | 0.61 |
| 6 | 1 | Exterior | 0.70 | 0.55 | 0.72 | 0.63 | 0.59 |
| 7 | 1 | Exterior | 0.60 | 4.80 | 0.59 | 4.67 | 4.74 |
| 8 | 2 | Exterior | 0.73 | 0.16 | 0.69 | 0.18 | 0.17 |
| 9 | 2 | Interior | 0.68 | 0.65 | 0.67 | 0.66 | 0.66 |
| 10 | 1 | Interior | 0.51 | 0.00 | 0.73 | 0.02 | 0.01 |
| 11 | 2 | Interior | 0.68 | 0.38 | 0.67 | 0.42 | 0.40 |
| 12 | 4 | Interior | 0.66 | 0.25 | 0.66 | 0.29 | 0.27 |
| 13 | 1 | Interior | 0.62 | 0.67 | 0.62 | 0.68 | 0.68 |
| 14 | 1 | Interior | 0.66 | 0.38 | 0.62 | 0.40 | 0.39 |
| 15 | 1 | Exterior | 0.62 | 1.80 | 0.62 | 1.87 | 1.84 |
| 16 | 1 | Interior | 0.80 | 0.65 | 0.8 | 0.70 | 0.68 |
| 17 | 1 | Interior | 0.69 | 0.78 | 0.69 | 0.82 | 0.80 |
| 18 | 1 | Interior | 0.65 | 1.15 | 0.65 | 1.24 | 1.20 |
| 19 | 1 | Interior | 0.65 | 0.36 | 0.65 | 0.39 | 0.38 |
| 20 | 1 | Exterior | 0.72 | 0.89 | 0.58 | 0.93 | 0.91 |
| 21 | 1 | Interior | 0.60 | 3.60 | 0.59 | 3.21 | 3.29 |
| | | | 0.66 | 0.96 | 0.66 | 0.98 | 0.97 |
| | | | 0.06 | 1.13 | 0.06 | 1.09 | 1.11 |

Figure 21 shows the comparison between the literature interval (in red) and the 95% confidence interval for each case considering the result per outlet (the upper graph) or per discontinuity (the lower graph). In the first case, 13 out of 21 units are outside the literature interval, and among these, 12 are below that interval. In the second case, 8 out of 21 discontinuities are outside the literature interval, with 7 below the limit. Regarding the standard deviation, the same order of magnitude is found in the literature (0.9 $m^3/h$) and in this study in both cases (1.1 $m^3/h$). These observations suggest that the value obtained in the literature overestimates the value found in this study. This is because these tests are conducted on newly constructed buildings while previous work investigated existing buildings. In addition, all these tests are on heavy structures while previous studies focused mainly on timber constructions.

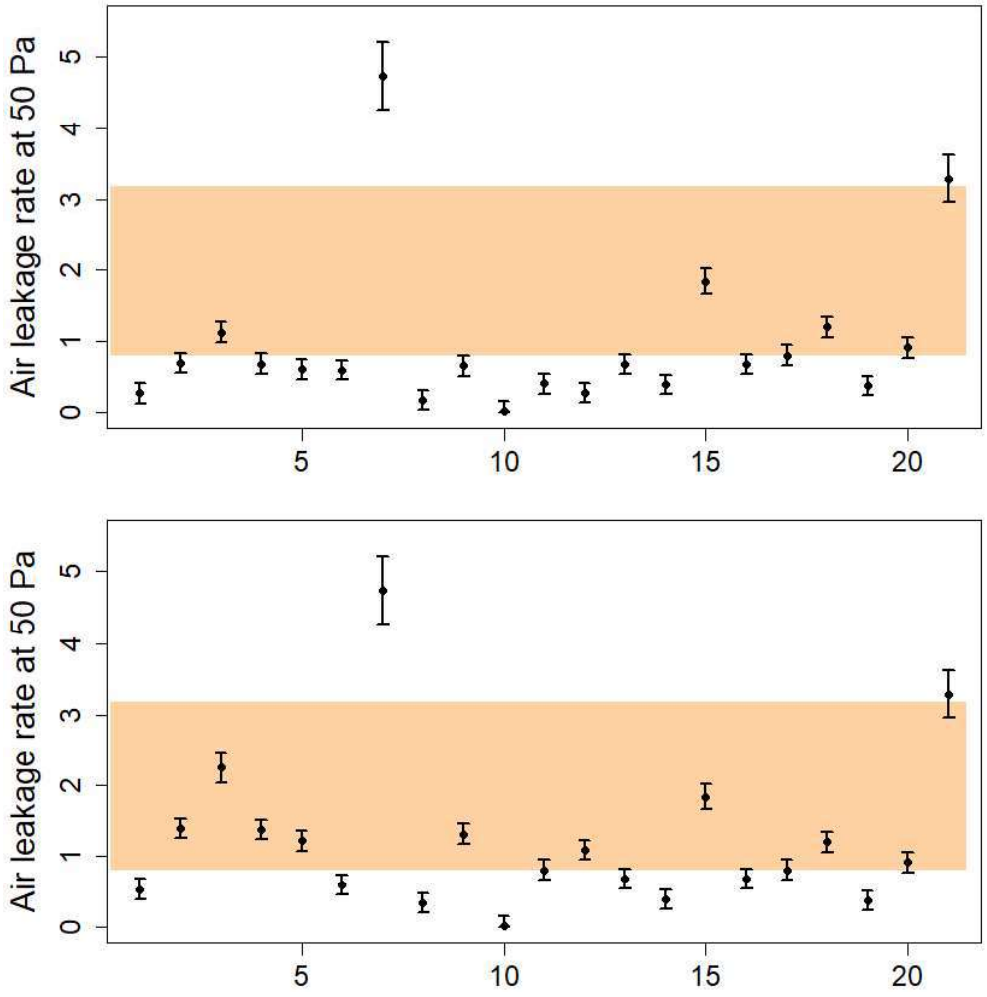



Figure 21: 95% confidence interval of air leakage rates at 50 Pa measured for discontinuities per unit (upper graph) and per discontinuity (lower graph), compared with the literature interval.

Figure 22 shows that for the airflow exponent all the cases overlap the literature interval for both modes (pressurisation and depressurisation). In addition, the standard error found in the literature is 0.13 while this study shows a standard deviation of 0.06 in pressurisation and depressurisation.

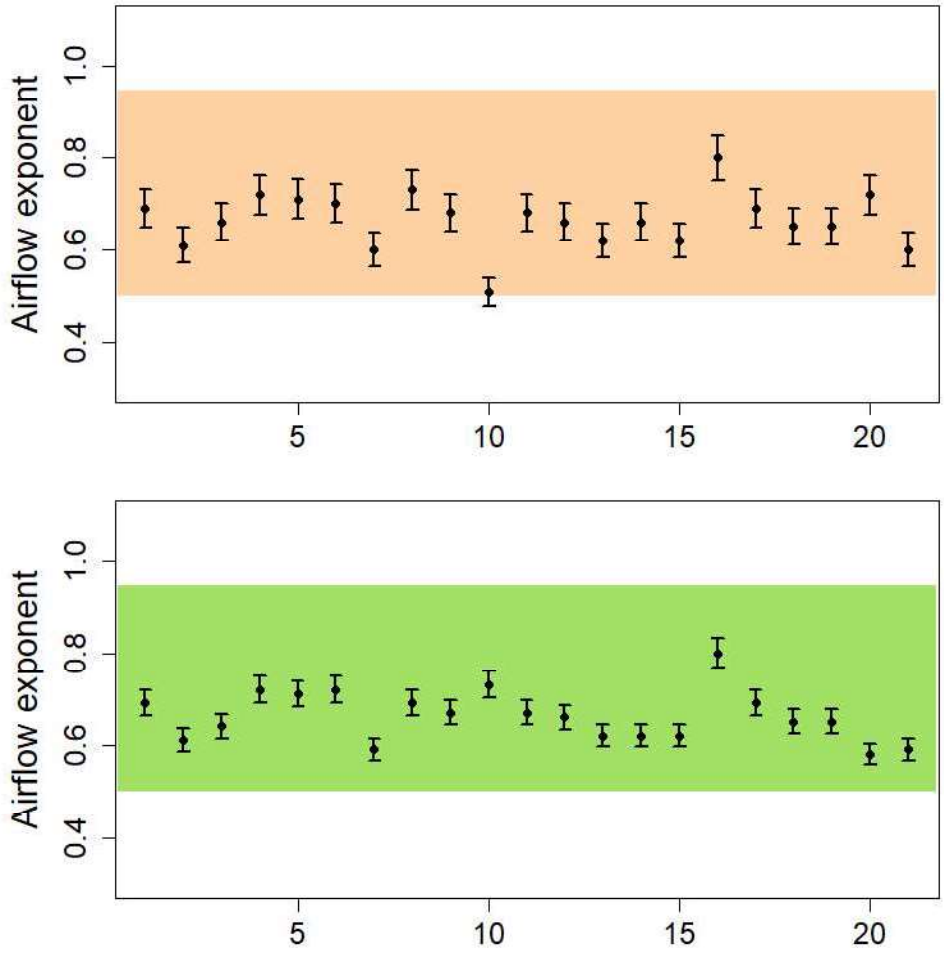



Figure 22: 95% confidence interval of airflow exponent in pressurisation (upper graph) and depressurisation (lower graph) measured for discontinuities, compared with the literature interval.

A subgroup analysis shows that the mean and the standard deviation are respectively 0.75 and 0.86 $m^3/h$ for the interior walls and 1.40 and 1.41 $m^3/h$ for the exterior walls. Similar conclusions are drawn when considering these results per discontinuity instead of per unit (0.93 and 0.83 $m^3/h$ for the interior walls and 1.79 and 1.30 $m^3/h$ for the exterior walls). These results are surprising.

Indeed, a better performance would have been expected for the exterior walls since more attention is generally paid because of their impact on the fan pressurisation test. However, all these results are obtained for the same type of building (multi-family dwellings), construction (heavy structures) and for the same contractor. This limits the conclusion since the type of construction is expected to strongly impact the airtightness performance of the building component.

## 6.2. Comparison with the Single Zone Airtightness

In this section, we investigate a second application of the direct component testing. This is when the airtightness performance of a single zone is determined by measuring all the building component airtightness (i.e. replacing the fan pressurisation test). In this objective, we measure the airtightness of a delimited zone using the fan pressurisation test and we compare the result obtained with the sum of single components measured with the direct component testing. These measurements took place in an apartment in Brussels (Belgium) in November 2019. Figure 23 shows the drawings of the apartment and, in red, the delimited zone to test.

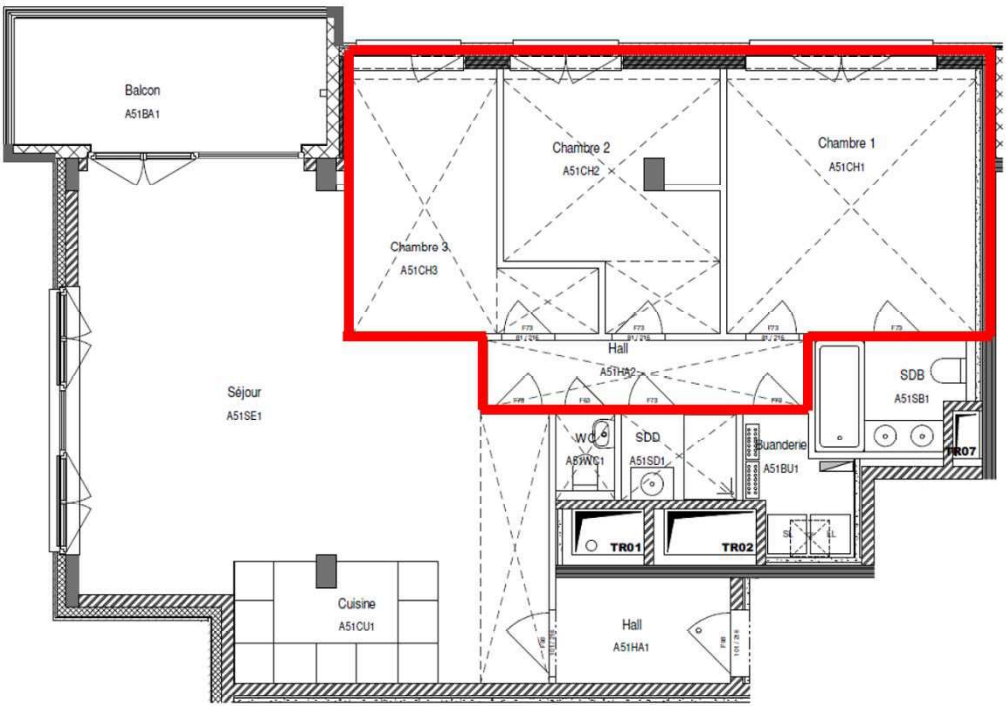



Figure 23: drawings of the apartment and the delimited zone (in red) to test.

Some components in the delimited zone (e.g. footwalls, doors and false-ceiling penetrations) are sealed in order to limit the zone to 17 components that impact significantly airtightness performance. These components are three windows and 14 small discontinuities in walls. These 17 components are measured with the direct component testing and their sum is compared to the result of a fan pressurisation test conducted on one zone.

### 6.2.1. Results

Table 25 and Figure 24 shows the leakage characteristics and the air leakage rate at 50 Pa of the entire volume and of each component. These are for pressurisation, depressurisation and average.

Table 26: leakage characteristics and the air leakage rate at 50 Pa of the entire volume and of each component. $q_{50}$ in m³/h.

| | $n_-$ | $C_-$ | $q_{50-}$ | $n_+$ | $C_+$ | $q_{50+}$ | $q_{50}$ |
|---|---|---|---|---|---|---|---|
| Entire volume | 0.60 | 11.61 | 119.83 | 0.69 | 6.68 | 98.25 | 109.4 |
| Window 1 | 0.79 | 0.24 | 5.25 | 0.63 | 0.43 | 4.97 | 5.11 |
| Window 2 | 0.69 | 0.17 | 2.57 | 0.57 | 0.18 | 1.64 | 2.11 |
| Window 3 | 0.58 | 5.05 | 48.71 | 0.50 | 8.17 | 58.25 | 53.48 |
| Discontinuities (14) | 0.67 | 0.05 | 0.71 | 0.68 | 0.05 | 0.71 | 0.71 |

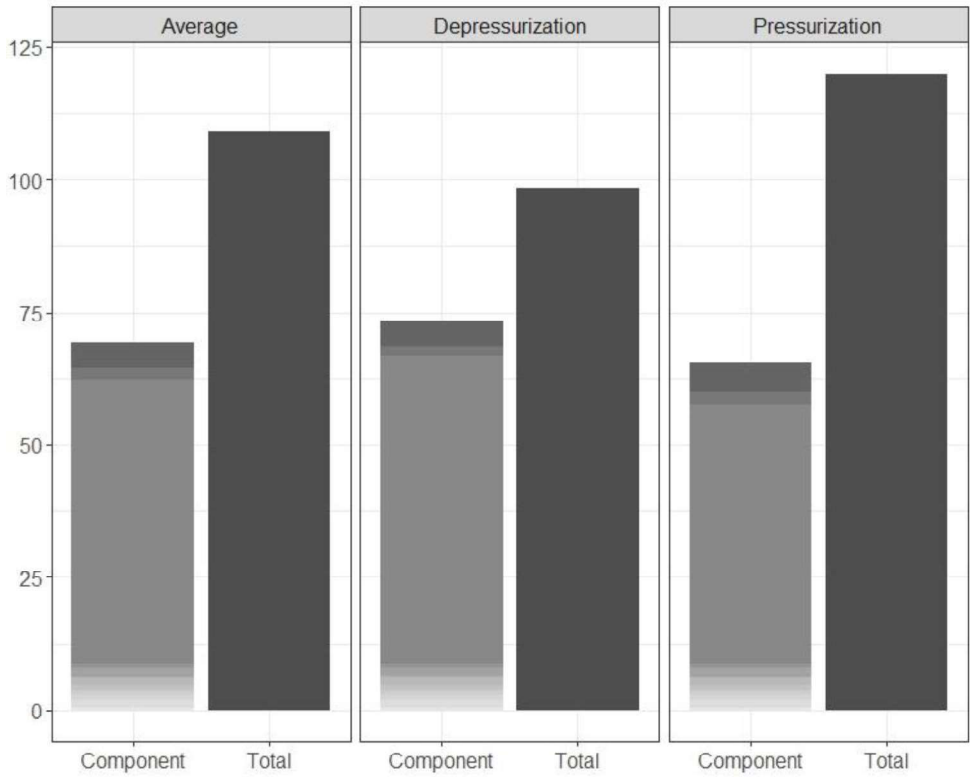



Figure 24: comparison between the total air leakage rate (the fan pressurisation test) and the sum of individual components (the direct component tests), in pressurisation, depressurisation and average.

This table and this figure illustrate two observations:

- The sum of the air leakage rates at 50 Pa of each component is lower than the total air leakage determined by the fan pressurisation test. Two reasons may explain this observation. First, it is likely that all the leaks are not identified and measured with the direct component testing. Second, small defects and leaks unintentionally created when placing the equipment for the fan pressurisation test are measured in the "total" case but not in the "component" case.
- The result in pressurisation is higher than in depressurisation for the single zone measurement, while it is the opposite when summing the contribution of each component. This is probably because the unmeasured leaks that explains the difference between the component and the total leakage, have an important valve effect.

Unfortunately, although a leakage detection using smoke generator was conducted, it was not possible to determine exactly which were the "missing

components" that could explain the difference between both methods. However, one could expect those components to have a large valve effect (e.g., joints or membranes) since a large difference is observed in the results.

## 6.3. Summary of Chapter's Outcomes

In this chapter, we illustrate the direct component testing through two applications. First, we report the results of 34 *in-situ* measurements of various building components and a comparison with the values found in the literature. Second, it compares the results of single zone measurement using the fan pressurisation test with the sum of the components measured individually with the direct component testing.

The first application points out three points of attention related to the direct component testing: (1) a huge inflation of the pressure chamber is likely to provide unreliable results, (2) a badly identified leakage route can induce the measurement of irrelevant leakage and (3) the values of the airflow exponents are unreliable when the linear regression is conducted with low-pressure or high-pressure data points only. It also demonstrates that the direct component testing could measure *in-situ* airtightness of building components and that these results have the same order of magnitude as the values found in literature.

The second application shows that the direct component testing is not ready yet to determine the single zone leakage. This is because it is difficult to identify all the components responsible for airtightness. A deeper investigation is needed before using the direct component testing in that context. A first relevant step for such an investigation would be to measure a well-documented zone in laboratory conditions.

# Chapter 7. Conclusion

This thesis's aim is to improve the methods quantifying building component airtightness in order to satisfy the demand from research and practice in the built environment. This encompasses three distinct tasks: to identify the relevant applications for the methods quantifying airtightness of building components and to determine their requirements in terms of practicability and reliability; assess the effectiveness of quantification methods in these same terms; and investigate the possible improvements required for each quantification methods to match the requirements. The core of this thesis focuses on assessing the reliability and the practicability of the direct component testing.

In this chapter, we conclude the thesis in five parts, structured as follows. In section 7.1, we recall the outcomes obtained in the thesis and we organise them in line with the aim. This includes two aspects: the relevant applications in research and practice (Chapter 2); and the effectiveness of the direct component testing (Chapter 3, Chapter 4, Chapter 5 and Chapter 6). In section 7.1.3, we identify the applications for which direct component testing could be appropriate. This section includes an analyse of the requirements for three applications and of the capability for the direct component testing to meet them. In section 7.2, we highlight the implications of this work on the practice, the research and the policies. There are two types of implications identified: the implications related to the popularisation of the direct component testing and the implications related to the specific outcomes of the different studies conducted. In section 7.3, we critically illustrate the limitations of the thesis, inherent to the experimental designs and the hypotheses. Following these limitations, we describe in section 7.4 the further steps needed in the field of building component airtightness. These include two types of work: work

needed to improve the direct component testing; and work needed to improve our description of air infiltration in buildings and the assessment of its consequences.

## 7.1. General Conclusion

This section recalls the outcomes obtained from the different investigations carried out in this thesis, structured in two parts to guide the reader through the different steps in answering the research questions. First, it presents relevant applications of quantification methods according to present knowledge in the field and the requirements in terms of practicability and reliability for these applications. Second, it characterises the effectiveness of the direct component testing in these terms.

### 7.1.1. The Relevant Applications in Research and Practice

Chapter 2 provides the reader with an overview of previous and current major works conducted in the field of building airtightness and air infiltration. Reviewing these works reveals two important contributions that a better quantification of building component airtightness could have on the body of knowledge: a better description of complex airflow and pressure distributions along the building envelope; and an improvement of predictive models of building airtightness. In addition, it also points out that investigating *in-situ* measurements of building component airtightness is an important step of these contributions.

Measurement methods can contribute to a better description of airflow and pressure distributions along the building envelope in two ways:

- Feed a database that provides information about pathways (i.e. $q_{50}$ and $n$). This aims to improve the capability of air infiltration models to describe airflow and pressure patterns in buildings.
- Determine the airtightness of buildings by summing up the results of *in-situ* measurements of building components that have a significant impact on airtightness. This aims to inform the tester of the leakage distribution along the building envelope. Two assumptions underline this application: all components that impact significantly the building airtightness can be

measured and the building airtightness can be described as a sum of the components' airtightness.

These methods can also contribute in one way to the improvement of predictive models of building airtightness:

- Feed a database providing the air leakage rate or the effective leakage area of the building components at a given pressure difference. This aims to improve single component models by increasing the availability, the accuracy and the suitability of leakage data. It would also improve empirical models by limiting the values of some coefficients in a range defined by the database. Indeed, the coefficients related to building components may be limited to the range of values provided in such databases. This is expected to give more meaning to these models and to make them more appropriate for larger variety of buildings. However, limiting the range of values available for coefficients is likely to reduce the reliability of empirical models.

### 7.1.2. Effectiveness of the Direct Component Testing

Section 1.3 suggests describing effectiveness of quantification methods in this context with five characteristics falling in two categories: the practicability and the reliability. On the one hand, the practicability embraces three aspects: the type of components that can be quantified; the price and the execution time of the method; and the type of information provided. On the other hand, the reliability embraces two aspects: the uncertainty related to the method, including measurement errors and errors related to the underlying assumptions; and the uncertainty related to the type of method, which is the uncertainty induced when the method measures the component in a different condition than *in-situ* conditions.

Chapter 3, Chapter 4 and Chapter 6 report experiments and investigations related to the practicability of the direct component testing. The following paragraphs describe the main outcome of these chapters:

Chapter 3 describes the protocol, the method and the equipment of the direct component testing. For the equipment used in this thesis, the range of measurable air leakage rate is between 0.17 and 78.5 $m^3/h$. According to the meta-analysis (section 2.4), this covers most building components except three that are above the measurable range (doors, chimneys and ventilation grilles)

and four that are below the measurable range (coated masonry, boards, vapour membranes and penetrations of electric cables). In addition, the type of measurable components is limited by the design of the pressure chamber and by the accessibility of the defect. For example, the different designs used in this research limit measurable components to defects in plane surfaces, excluding corner connections between surfaces.

Chapter 4 reports the tests conducted on four calibrated openings, demonstrating that the direct component testing provides accurate values for the air leakage rate at 50 Pa and the airflow exponent. This observation is strengthened by the first part of Chapter 6 that reports a good match between measurement and literature values for the air leakage rate and the airflow exponent of different building components.

Chapter 6 reports the results of two applications of the direct component testing. These applications reveal two additional constraints of the method that may reduce the range of measurable components and increase the price because of additional pieces of equipment. First, one must limit the inflation of the pressure chamber, for example with extendable propping bars, to avoid the measurement system to collapse. Second, one must clearly identify the air pathways, for example with a smoke generator, to avoid measuring an irrelevant leakage (i.e. an airflow going back to the building). When the irrelevant leakage is likely to occur or is detected, it is avoided by using an additional fan to balance the pressure between the pressure chamber and the building. However, the additional equipment induces more costs and supplementary constraints (e.g. the measured zone must be closed) that may impact the practicability of the method.

The price of the equipment and the accessories is equivalent to the equipment for the fan pressurisation test (around €2000). Since the equipment cost may be amortised over many tests, most part of the price for the method is related to the human labour and, therefore, to the execution time. The method is made of five steps: the setup of the pressure chamber; the measurement in pressurisation; the measurement in depressurisation; the disassembly of the equipment; and the generation of the test report. These five steps take about 1h30 in total, which is very similar to the fan pressurisation test. All steps except first have similar duration for the fan pressurisation test and for the direct component testing. For the direct component test, the first step depends on the type of pressure chamber and lasts between 10 and 30 minutes. For the fan

pressurisation test, this first step (building preparation) depends on the building size and may take more than 30 minutes.

Chapter 4 and Chapter 5 report the experiments and the investigations conducted to assess the reliability of the direct component testing. The following paragraph describes the main outcomes of these two chapters:

Chapter 4 reports two experiments conducted in order to quantify the bias in airflow measurements due to the background leakage and the bias in pressure difference measurements due to the pressure losses in the duct. Once quantified, these biases correct airflow and pressure difference measurements and do not impact significantly the reliability of the measurement method. Chapter 5 illustrates and applies a methodology for the theoretical calculation and the experimental observation of the direct component testing uncertainty. This also includes a methodology for the statistical analysis of the repeatability studies. This chapter demonstrates that the uncertainty of the direct component testing is between 3% and 10%, depending on the pressure chamber design and on the measured air leakage rate. This method is more reliable than the indirect component testing when both are compared on the same component (3% vs. 60%).

### 7.1.3. Applications for the Direct Component Testing

This section investigates in what way the main outcomes of this work contribute to the narrow and the broad research questions and on how the direct component testing may be improved to match the demand. This is done by defining the requirements in terms of practicability and reliability for each of the three applications identified in section 7.1.1; and by comparing them to the characteristics of the direct component testing recalled in section 7.1.2.

*Improve Air Infiltration Models*

This section describes the requirements in terms of practicability and reliability when the measurement method is used to feed a database used to improve air infiltration models.

There is no requirement about the type of components that the method can measure, but a reduced range of measurable components would limit its capability to feed the database. Consequently, it would limit the potential of

improvement this database has on air infiltration models. There is no requirement for the execution time and the price of the measurement method since those have no impact on the application itself (i.e. using the database). However, reducing the price and the execution time of the method promotes its use and, therefore, the development of consistent and large databases. Last, the measurement method used to feed these databases should always provide airflow exponent alongside the air leakage rate or effective leakage area. This is because the airflow exponent carries information about the flow regime that can increase the accuracy of air infiltration models. In addition, the method should report information about its reliability, in order to provide information about the quality of the data to the databases users.

The meta-analysis demonstrates that a proper combination of studies includes weighting studies based on their reliability. This means that the methods with high uncertainty result in a contribution of low significance in a well-designed database (i.e. a database based on a strong and appropriate protocol to combine the measurements from multiple sources). Therefore, to be relevant to this application, the measurement method must be at least equally reliable as other methods used to feed the database. Furthermore, the additional uncertainty related as the type of measurement depends on the method and on the component. *In-situ* measurement methods require no additional uncertainty since they measure the component in use. Laboratory measurements, on the contrary, measure the component in a controlled environment, reducing some potential sources of air leakage rate that would be caused by poor workmanship and supervision. The meta-analysis demonstrates that the windows have similar results when measured in the laboratory and *in-situ*, while a defect in a vapour barrier tremendously increases the air leakage rate at 50 Pa. This illustrates that the magnitude of this additional uncertainty should depend on how the component is impacted by the workmanship and the supervision.

For this specific application, the direct component testing appears appropriate in many cases since it reports the air leakage rate at 50 Pa alongside the airflow exponent measured *in-situ* with high reliability. It should be preferred over the other measurement methods when air leakage rate of the component of interest is in the range of measurable airflow and when a large difference is expected between a laboratory and an *in-situ* measurement. However, using only the direct component testing limits the database to the range of components that can be measured with the method. Consequently, the direct component test

should not be used as a replacement but as a complement for laboratory measurement methods; or for other future methods that quantify the air leakage rate and the airflow exponent of building components with enough reliability.

*Improve Predictive Models for Building Airtightness*

This section describes the requirements in terms of practicability and reliability when the measurement method is used to feed a database aiming to improve predictive models of building airtightness.

Regarding the measurable components, the price, the execution time and both aspects of the reliability, conclusions are the same as the previous application. There are no requirements but the more the method can feed the database, the more consistent is the database and the better are the predictive models based on it. In addition, the higher is the reliability of the method, the larger is its significance when combining results from different sources.

In fact, the only difference with the previous application regarding the requirements is in the information provided. The measurement method used to feed these databases only requires the air leakage rate or the effective leakage area at the pressure difference of interest. However, the airflow exponent is useful to convert the air leakage rate or the effective leakage area from one to another pressure difference. This results in more consistent databases (they combine values from more studies) and in more accurate predictive models of building airtightness.

As such as for the previous application, the direct component testing seems appropriate for many components when feeding a database used to improve predictive models for building airtightness. It should be preferred over the other measurement methods in the same cases as for the previous application. A database fed with the direct component testing only is limited in the range of components included, hence has a lower relevance. However, in this application less importance is paid to the airflow exponent. Thus, the direct component testing works as a complement for laboratory measurement methods, but also for the indirect component testing or the guard-zone technique that are not appropriate for the previous applications because of their inability to measure the airflow exponent.

*Determine Building Airtightness*

This section describes the requirements in terms of practicability and reliability when the measurement method is used to determine the airtightness of a building or a part of it. This is done by summing up the results of the *in-situ* measurements conducted on the building components responsible for the airtightness performance. For this application, the requirements are different.

Regarding the practicability, the measurement method must be able to measure all the components that significantly impact building airtightness. In addition, it must ensure that all the measured air leakage rate refers to airflow between inside and outside the zone of interest. The execution time should be low enough to measures all the building components in one day in order to avoid the large uncertainty caused by the variations in weather-induced pressure differences experienced on multiple-day measurements. The price for the measurement method should be of the same order of magnitude as for the fan pressurisation test. In a survey conducted by (IEA, 2019b), in the context of the 4th subtask of the EBC annex 71, the costs of a fan pressurisation test are estimated between 100 and 2000 euros, depending on the building size and its complexity. The information provided by the method should be the same as those reported in a fan pressurisation test in order to give comparable results: the air leakage rate or the effective leakage area at the pressure difference of interest and its uncertainty.

Regarding the reliability, the requirements depend on the desired uncertainty of the building airtightness. When the building airtightness is determined with *in-situ* measurements of the components' airtightness, uncertainty of the building airtightness is given by Eq. 47:

$$\beta * \left(\sum_{i=1}^{N} X_i\right) = \sqrt{\left(\sum_{i=1}^{N} \alpha_i^2 X_i^2\right)} \qquad \text{Eq. 47}$$

$\beta$ is the uncertainty of building airtightness (in %), $\alpha_i$ is the uncertainty of $X_i$ (in %), $X_i$ is the airtightness performance of the $i^{th}$ building component measured, and $N$ is the number of components having a significant impact on the building airtightness. This equation assumes that the building airtightness is a simple sum of the airtightness of the components and that those are uncorrelated.

Moreover, if we assume $\alpha = \alpha_i$ for $i = 1, 2, \ldots, N$; Eq. 47 becomes Eq. 48:

$$\beta = \frac{\alpha\sqrt{\sum(X_i)^2}}{\sum X_i}$$ Eq. 48

Eq. 48 shows that the uncertainty of the building airtightness ($\beta$ in % of the air leakage rate) depends on the uncertainty of the method measuring the component airtightness ($\alpha$ in % of the air leakage rate) and on the ratio between the sum and the root sum squared of the airtightness of the components. Since the uncertainty of the result depends on this ratio, which depends on the test case, it is impossible to determine a single value of $\alpha$ as a function of a desired value for $\beta$. However, the root sum squared is always lower than the simple sum; thus, their ratio is always lower than one and $\beta$ is always greater than $\alpha$. According to (Carrié and Leprince, 2016), the uncertainty of the fan pressurisation measurement can go up to 12% on windy days when expressing airtightness in air leakage rate at 50 Pa. Without previous knowledge of the desired uncertainty for the building airtightness determined with *in-situ* measurements of the components, this value of 12% is arbitrarily chosen as an upper limit for $\alpha$. This means that when all the components induce negligible air leakage rates except the leakiest one (i.e., when $N = 1$), the uncertainty of building airtightness determined by this method is below 12%.

This application is only feasible with *in-situ* measurements since it is expected to replace the fan pressurisation test. Therefore, considering an additional uncertainty depending on the type of measurement is not relevant in this case.

For this application, the direct component testing is not appropriate. Although the method shows an acceptable uncertainty (below 10%), it has a limited range of measurable components and can, therefore, not fulfil the practicability requirements of this application. In addition, although the method takes less time than a fan pressurisation test, repeating it for all the components significantly impacting building airtightness can drastically increase the time needed for this application and its price. One should prefer the indirect component testing or the guard-zone technique over the direct component testing for this application. Although these methods show a lower reliability, they are more appropriate to provide the tester an overview of the leakage distribution along the building envelope.

### 7.1.4. Answering the research question

As a conclusion of this section, we can use these results to answer the two research questions identified in section 1.3:

- How effective is the direct component testing for in-situ measurement of building component airtightness?

The direct component testing can measure air leakage rate between 0.17 and 78.5 $m^3/h$ of defects in walls. Its uncertainty varies between 3% and 10%, depending on the pressure chamber design. The price of the test, including the equipment and the human labour, is equivalent to the fan pressurisation test. An attention should be paid to limit the inflation of the pressure chamber and to identify the air pathways clearly. Those issues may involve additional equipment and, consequently, increasing the price of the test.

- How methods quantifying building component airtightness can be improved to match the present demand?

Two specific applications for methods quantifying building component airtightness are identified. The first is to feed a database that provides information about pathways in order to improve the capability of air infiltration models to describe airflow and pressure patterns in buildings. Such a database can also be used to improve airtightness predictive models. The second is to determine airtightness of buildings by summing up the results of *in-situ* measurements of building components in order to inform the tester of the leakage distribution along the building envelope.

For the first application, the direct component testing is practicable and reliable enough. However, the range of applicable components should be increased to improve the consistency of these databases. For the second application, the range of applicable component should be increased, and the execution time of the method should be considerably reduced since all components have to be measured.

## 7.2. Implications

This work has two types of implications: the implications related to one or another aspect of the work done, which can be a specific outcome or a methodology; and the implications related to the popularisation of the direct component testing. Indeed, the lack of well-documented protocols and of uncertainty assessment are two aspects limiting the popularisation of this method. Consequently, this thesis is a step in the popularisation of the direct component testing used to measure *in-situ* the airtightness of building components.

### 7.2.1. Regarding Practice

We demonstrate the need for major improvements in the practicability and the reliability of the direct component testing before using it to determine the building airtightness. However, the popularisation of the direct component testing is still expected to contribute strongly to the practice in the construction field. Three specific implications this method has in practice are described in the following paragraphs: improve the cost-to-impact ratio of the measures taken to achieve good airtightness by using intermediate testing; identify the potential weak points of a specific building design by using predictive models; and improve the current use of the direct component testing.

(Aurlien, 2013) highlighted the fact that locating and repairing leaks at early-construction stage is very cost-effective. In addition, skilled craftsmen very appreciate to be valued on their capacity to reach technical goals and not only on the aesthetic finish of their work. In his paper, Aurlien mentioned three different types of intermediate testing: testing representative small parts of the envelope, testing zones and testing of wind-tight-layer. In his paper, he strengthened. The direct component testing allows a fourth type of intermediate testing: testing component. The method can be executed earlier in the construction process since it does not require the building envelope to be completely closed. In addition, it provides a quantification rather than a detection of the airtightness weak points, providing an important information about the potential of improvement that the contractor has on each weak point. Consequently, the direct component testing strengthens the common practice of intermediate testing by providing new possible timing and scales to perform them.

The improvement of airtightness predictive models would provide a better grasp of the airtightness weak points in the building to contractors and architects, depending on the type of construction, the materials and the building design. They could use them to control the impact that a measure has on building airtightness, hence the costs and the time necessary to reach the desired airtightness.

This method is already sparsely used in practice to assess if the leakiness of a component is due to its installation on the site or to its manufacturing. This can be of a great help for the contractor to point out the flaws in the construction process. As mentioned previously, this can also be a strong support for the workers to value the technical quality (i.e., its capability to achieve desired airtightness performance) of his or her work. In these contexts, the direct component testing is preferred over the indirect method since one is interested in an actual air leakage rate rather than an order of magnitude. The popularisation of this method that this work could generate is expected to reduce its execution time and its price gradually. This would make these applications more affordable and more reliable for contractors and architects in their daily practice.

A specific part of the work that is expected to have an implication in practice is the meta-analysis. The classification (section 2.4.1) provides a comprehensive list of building components studied in previous research due to their impact on building airtightness. This classification can be of great support in the building practice to understand how to deal with some specific components. In addition, the meta-analysis (section 2.4.2) results in an updated database (i.e. it provides new reference values for the airtightness of multiple building components) that can also support the building practice the same way that intermediate tests or predictive models would. It provides a better grasp of the airtightness weak points in buildings to contractors and architects.

### 7.2.2. Regarding Research

The biggest implication the direct component testing has on research is due to its capability to measure *in-situ* the airflow exponent alongside the air leakage rate or the effective leakage area. This is hugely important since it is the only *in-situ* measurement method that provides information about the flow regime through the component. This is expected to improve the potential of databases

fed with the measurements conducted with this method. This refers to both applications identified previously: improving models of air infiltration and of airtightness prediction. More generally, the implication these two applications have on the research is a better description of the complex airflow and pressure distributions along the building envelope, and of the infiltration and exfiltration flow regimes.

In addition, developing the databases of building component airtightness that includes the airflow exponent would be a large step forward in the quantification of the valve effect (i.e. the difference of the measured airtightness in pressurisation and depressurisation) and in the identification of the building components responsible for this valve effect. In this context, measuring the airflow exponent is important since a change of behaviour between pressurisation and depressurisation may also involve a change in the flow regime.

Further implications of this work on research in the built environment, and more precisely in air infiltration and airtightness, lies in three specific parts of the work done:

First, the 4-level classification suggested in the meta-analysis. This is of major interest in research since it allows comparing the performance of different components consistently. That piece of work also investigates the applicability of the meta-analysis, a strong protocol to combine results from different studies, in the context of the built environment. In addition, it identifies four requirements for future studies to improve the statistical power, the reliability, and the potential applicability of the meta-analysis. In fact, this provides some important methodological guidelines for future studies reporting measurement of building component airtightness and for future studies updating or developing the databases that combine results from different sources.

Second, the methodology for the theoretical calculation and the experimental observation of the uncertainty presented in section 5.2. This section also presents multiple appropriate tools for the statistical analysis of future repeatability studies, depending on the type of data analysed and on the purpose of the analysis. Moreover, it investigates the appropriateness of Cohen's benchmark to interpret the results of these statistical analyses. This is useful in the research context for future analyses of repeatability studies. This aspect may

be transferred to the other domains of the built environment, providing that it is not previously investigated for that specific domain.

Third is the investigation of the pressure losses in compressible ducts (section 4.3.2). In this thesis, the pressure losses calculated using the models developed by (Abushakara et al., 2004) are compared with an experiment. This experiment demonstrates that those models are not appropriate for compressible ducts of non-standardised sizes. Therefore, a deeper investigation is needed in order to extent these models to all the compressible ducts.

### 7.2.3. Regarding Policies

This work could impact policies in three ways: estimate the airtightness performance of building stock; generate a new European standard for *in-situ* assessment of the building component airtightness; and improve (ISO 9972:2015, 2015) standard. First and second contributions refer to the direct component testing while the third refers to one specific aspect of this work. These contributions are described hereafter.

The improvement of airtightness predictive models, and more specifically of the empirical models, induced by the popularisation of the direct component testing could be of great interest for new policies. In fact, the empirical models could provide an overview of the airtightness performance of a building stock based on the fan pressurisation tests conducted so far. This takes advantage of the increasing number of fan pressurisation tests induced by (European Parliament and Council, 2010) and (European Parliament and Council, 2012) to help countries to select an effective and appropriate retrofitting strategy to implement (European Parliament and Council, 2018).

This work describes a strong protocol to determine with high reliability the airtightness of building component once installed on the site. This could be used to generate a standard, similar to (ISO 9972:2015, 2015), for the *in-situ* measurement of the air permeability of building components. This thesis only validates the protocol for the measurements of defects in plane sections of walls (e.g. windows, switches or electrical outlets). However, that standard could be used by countries to impose requirements on the *in-situ* performances of the building components in addition to the laboratory performances or to the *in-situ* performances of buildings.

The work summarised in section 5.4.1 is a large contribution to the uncertainty calculation of the fan pressurisation test. It highlights the irrelevant assumptions of the Ordinary Least Square (OLS) regression technique in this context and the large uncertainties its use induces. Moreover, it points out the lack of reliability of the uncertainty calculated using the OLS and suggests the use of alternative regression techniques (WLOC: Weighted Line of Organic Correlation or IWLS: Iterative Weighted Least Square). This thesis demonstrates that providing the formula of the WLOC or the IWLS techniques rather than – or in addition to – the OLS in annex C of (ISO 9972:2015, 2015) would be an improvement for this European standard.

## 7.3. Limitations

Four methodological limitations, inherent to the experimental designs, hinders the generalisation of the work done in this thesis and should be acknowledged.

- In the absence of previous knowledge of the direct component testing, multiple assumptions in the protocol and in the different investigations are based on fan pressurisation test because of the similarity in protocols. Examples of such assumptions are the value of uncertainty of zero-flow pressure approximation or the fact that the WLOC and the IWLS techniques provide similar results. Although some of these assumptions could be reasonable, others are questionable in the case of the direct component testing.
- The experiment conducted to assess the capability of the direct component testing to measure the airflow exponent is limited to the calibrated openings with an airflow exponent of 0.5. However, the capability of the method to provide reliable values of the airflow exponent is not expected to depend on the value of this exponent but on the data points used to conduct the linear regression.
- The repeatability studies are conducted on components with an air leakage rate at 50 Pa between 0.84 and 3.80 $m^3/h$. The uncertainties in the air leakage rate and the airflow exponent are expected to be different for the components with an air leakage rate closer to the upper (78.5 $m^3/h$) or lower (0.17 $m^3/h$) boundaries of the range of measurable airflow.
- All the experiments conducted on real building components (e.g. the repeatability studies or the applications), measure discontinuities in plane

sections of walls. Although this covers a large part of the components having a significant impact on airtightness (e.g. windows, doors or electrical outlet), other types of components would induce other designs of pressure chambers.

## 7.4. Future Research

This thesis is an important step in the quantification of *in-situ* airtightness performances of building components. Nonetheless, there is still considerable room for improving our understanding of air infiltration in buildings and its consequences. The future research in this field should focus on the improvement of the direct component testing and on its use in various applications.

There are five important pieces of work related to the limitations of this work that could be investigated to continue improving the direct component testing method:

- The possibility of increasing the range of measurable airflow, especially the upper boundary of this range. This is because most doors, which are important components regarding the airtightness and are always present in buildings, are above this limit according to meta-analysis.
- The assessment of the assumptions validity when these are based on the work on the fan pressurisation test. Although there are many similarities between protocols for the direct component testing and the fan pressurisation tests, future studies should investigate them separately.
- The capability for the direct component testing to report a reliable airflow exponent in the range [0.5;1.0] and a reliable air leakage rate in the range [0.17;78.5]. This includes the value of the measurement, but also a proper definition of the uncertainty of the measurement as a function of the measured air leakage rate.
- The characterisation of the direct component testing for other pressure chamber designs than those investigated in this research (the woodbox system and the plastic-sheet system with horizontal bars presented in section 3.2). This is important since the design of the pressure chamber is expected to have a large impact on the characteristics of the method.
- The impact of other sources of error on the uncertainty of the direct component testing. This is done by analysing reproducibility studies –

instead of repeatability studies – including a change in the operator or a change in the equipment between each test.

Although it is not an improvement of the method itself, similar designs of pressure chambers could be used to measure the infiltration rate through building components rather than the air leakage rate at higher pressure differences. (Ghazi and Marshall, 2014) studied the use of tracer gas methods to measure air infiltration rate of building components in laboratory conditions. To our knowledge, these types of measurements have never been investigated *in-situ*.

Regarding the use of the direct component testing to improve our knowledge about air infiltration in buildings, future work should focus on using a better description of building component airtightness to improve air infiltration models; and on the improvement of empirical models to predict building airtightness. On the one hand, improved air infiltration models could be used to grasp the airflow distribution in buildings and the consequences of air infiltration. In addition, a sensitivity analysis of these models would help to determine the importance of the leakage distribution along the envelope and, therefore, an idea of how accurate its description should be. On the other hand, improved empirical predictive models could provide a description of a building stock anywhere. This would help to determine the needs and the priorities for retrofitting strategies regarding airtightness. In addition, such work should also investigate how limiting the possible range of values for the coefficients of these models impact their accuracy.

The increasing interest in the fan pressurisation test induced by European directives generates an airtightness paradox, hindering our assessment of air infiltration consequences and our capability to assess them. This thesis contributes to reducing the importance of this paradox by investigating the effectiveness of the direct component testing and its capability to respond to the demand for both research and practice. This is a step forward in the description of the complex airflow and pressure distributions along the building envelope; and in the assessment of the many consequences air infiltration has on the building and its occupants.

# References


Abushakara, B., Walker, I., and Sherman, M. 2004. 'Compression effects on pressure loss in flexible HVAC ducts', HVAC&R Research, **10**: 275-89.

Almeida, R. M. S. F., Ramos, N. M. M., and Pereira, P. F. 2017. 'A contribution for the quantification of the influence of windows on the airtightness of Southern European buildings', Energy and Buildings, **139**: 174-85.

ASHRAE. 2001. Handbook of Fundamentals (American Society Heating, Refrigerating and Air-conditioning Engineers: Atlanta).

ASHRAE. 2017. Handbook of Fundamentals (American Society Heating, Refrigerating and Air-conditioning Engineers: Atlanta).

ASTM 283 (US). 2004. Standard Test Method for Determining Rate of Air Leakage Through Exterior Windows, Curtain Walls and Doors Under Specified Pressure Differences Across the Specimen.

Aurlien, T. 2013. 'Performing intermediate checks and early-stage testing of airtightness', REHVA Journal, **01/2013**.

Berthault, S., Boithias, F., and Leprince, V. 2014. 'Ductwork airtightness: reliability of measurements and impact on ventilation flowrate and fan energy consumption.' In 35th AIVC conference: Ventilation and airtightness in transforming the building stock to high performance. Poznan, Poland.

Borenstein, M., Hedges, L. V., Higgins, J. P., and Rothstein, H. R. 2011. Introduction to meta-analysis (John Wiley & Sons).

Bracke, W., Laverge, J., Van Den Bossche, N., and Janssens, A. 2016. 'Durability and Measurement Uncertainty of Airtightness in Extremely Airtight Dwellings', International Journal of Ventilation, **14**: 383-94.

Bramiana, C. N., Entrop, A. G., and Halman, J. I. M. 2016. 'Relationships between Building Characteristics and Airtightness of Dutch Dwellings', Energy Procedia, **96**: 580-91.

Carrié, F. and Wouters, P. 2012. 'Building airtightness: a critical review of testing, reporting and quality schemes in 10 countries.' In, edited by TightVent Europe.
Carrié, F. R. and Leprince, V. 2016. 'Uncertainties in building pressurisation tests due to steady wind', Energy and Buildings, **116**: 656-65.
Carruthers, J. and Newman, C. 1977. 'The repeatability and reproduceability of test results on windows and wall span elements and the expected results.' In Paul Rousseau Symposium on the testing of wall elements and windows. Vilvorde, Belgium.
CMHC. 1991. 'Research Project Testing of Air Barrier Construction Details.' In. Ottawa, Canada: Canada Mortgage and Housing Corporation.
Cohen, J. 1992. 'A power primer', Psychological Bulletin, **112**: 155-59.
Coleman, H. W. and Steele, W. G. 2009. Experimentation, Validation, and Uncertainty Analysis for Engineers, Third Edition.
Colliver, D., Murphy, W., and Sun, W. 1992. 'Evaluation of the techniques for the measurement of air leakage of building components.' In ASHRAE Research Project (Final Report).
Cosmulescu, C. 1997. 'Experimental procedure to evaluate air leakage through different building materials', Concordia University.
CTE HE1 (Spain). 2019. Código técnico de la Edificación (CTE). Documento básico HE 1: Limitación de la demanda energética.
De Bie, M., Debruyne, R., Ledoyen, G., Nouwynck, J., and Delmotte, C. 2014. 'Calcul des pertes de pression et dimensionnement des réseaux aérauliques.' In, edited by Jan Venstermans. CSTC - WTCB - BBRI.
Delmotte, C. 2013. 'Airtightness of buildings - Calculation of combined standard uncertainty.' In 34th AIVC Conference " Energy conservation technologies for mitigation and adaptation in the built environment: the role of ventilation strategies and smart materials". Greece.
Delmotte, C. 2017. 'Airtightness of Buildings – Considerations regarding the Zero-Flow Pressure and the Weighted Line of Organic Correlation.' In 38th AIVC Conference "Ventilating healthy low-energy buildings". Nottingham, UK.
Delmotte, C. 2019. 'Airtightness of buildings – Considerations regarding place and nature of pressure taps.' In 40th AIVC - 8th TightVent - 6th venticool Conference. Ghent, Belgium.
Delmotte, C. and Laverge, J. 2011. 'Interlaboratory tests for the determination of repeatability and reproducibility of buildings airtightness measurements.' In 32nd AIVC conference and 1st TightVent Conference: Towards Optimal Airtightness Performance. Brussels, Belgium.

Dols, W. S. and Polidoro, B. J. 2015. 'CONTAM user guide and program documentation version 3.2.' In.: National Institute of Standards and Technology.

Egger, M., Ebrahim, S., and Davey Smith, G. 2002. 'Where Now for Meta-Analysis?', International Journal of Epidemiology, **31**.

Ellis, P. D. 2010. The Essential Guide to Effect Sizes: Statistical Power, Meta-Analysis, and the Interpretation of Research Results (Cambridge University Press: Cambridge).

Emmerich, S. 2001. 'Validation of multizone IAQ modelling of residential-scale buildings: a review.' In ASHRAE Summer Meeting. US.

EN 12114:2000 (Europe). 2000. Thermal Performance of Buildings–Air Permeability of Building Components and Building Elements-Laboratory Test Method.

European Parliament and Council. 2010. 'European Parliament and Council directive 2010/31/EU on the energy performance of buildings.' In 2010/31/EU, 13-35. Official journal.

European Parliament and Council. 2012. 'European Parliament and Council directive 2012/27/EU on energy efficiency.' In 2012/27/EU, 1-56. Official journal.

European Parliament and Council. 2018. 'European Parliament and Council directive 2018/844 amending Directive 2010/31/EU on the energy performance of buildings and Directive 2012/27/EU on energy efficiency.' In 2018/844, 75-91. Official journal.

Feijó-Muñoz, J., González-Lezcano, R. A., Poza-Casado, I., Padilla-Marcos, M. Á., and Meiss, A. 2019a. 'Airtightness of residential buildings in the Continental area of Spain', Building and Environment, **148**: 299-308.

Feijó-Muñoz, J., Pardal, C., Echarri, V., Fernández-Agüera, J., Assiego de Larriva, R., Montesdeoca Calderín, M., Poza-Casado, I., Padilla-Marcos, M. Á., and Meiss, A. 2019b. 'Energy impact of the air infiltration in residential buildings in the Mediterranean area of Spain and the Canary islands', Energy and Buildings, **188-189**: 226-38.

Feldman, D., Stathopoulos, T., Cosmulescu, C., and Wu, H. 1998. 'A simple apparatus for the evaluation of air infiltration through building envelope components', Journal of Wind Engineering and Industrial Aerodynamics, **77-78**: 479-89.

Fernández-Agüera, J., Domínguez-Amarillo, S., Sendra, J. J., and Suárez, R. 2016. 'An approach to modelling envelope airtightness in multi-family social housing in Mediterranean Europe based on the situation in Spain', Energy and Buildings, **128**: 236-53.

Field, A., Miles, J., and Field, Z. 2012. Discovering statistics using R (Sage Publications Inc.: London).
Field, A. P. and Gillett, R. 2010. 'How to do a meta-analysis', British Journal of Mathematical and Statistical Psychology, **63**: 665-94.
Ghazi, C. J. and Marshall, J. S. 2014. 'A CO2 tracer-gas method for local air leakage detection and characterization', Flow Measurement and Instrumentation, **38**: 72-81.
Gillard, J. 2010. 'An overview of linear structural models in errors in variables regression', Revstat - Statistical Journal, **8**: 57-80.
Guillén-Lambea, S., Rodríguez-Soria, B., and Marín, J. M. 2019. 'Air infiltrations and energy demand for residential low energy buildings in warm climates', Renewable and Sustainable Energy Reviews, **116**: 109469.
Gullbrekken, L., Rüther, P., and Kvande, T. 2017. 'Air leakage defects in vapour barrier of compact roofs.' In 38th AIVC Conference - "Ventilating healthy low-energy buildings". Nottingham, UK.
Guyot, G. and Carrié, F. 2010. 'Stimulation of good building and ductwork airtightness through EPBD ' In ASIEPI Project.
Guyot, G., Ferlay, J., Gonze, E., Woloszyn, M., Planet, P., and Bello, T. 2016. 'Multizone air leakage measurements and interactions with ventilation flows in low-energy homes', Building and Environment, **107**: 52-63.
Hall, M. and Hauser, G. 2003. 'In situ Quantifizierung von Leckagen bei Gebäuden in Holzbauart.' In AIF–Forschungsvorhaben Nr. 12611 N. Kassel, Germany: Universität Kassel - Fachgebiet Bauphysik.
Hassan, O. A. B. 2013. 'An alternative method for evaluating the air tightness of building components', Building and Environment, **67**: 82-86.
Hensen, L. C. 2018. 'On the history of indoor environment and it's relation to health and wellbeing', REHVA Journal, **55**: 14-20.
Hopkins, L. and Hansford, B. 1974. 'Air flow through cracks', Building Services Engineer, **42**: 123-31.
Hurel, N. 2016. 'Impact of air infiltration on buildings' performance: focus on the experimental study within timber-frame walls', Université Grenoble Alpes.
IEA. 2019a. '2019 Global Status Report for Buildings and Construction: Towards a zero-emissions, efficient and resilient buildings and construction sector.' In.: International Energy Agency.
IEA. 2019b. 'Annex 71: Building energy performance assessment based on in-situ measurements. Subtask 4: Towards Quality Assassment.' In, edited by IEA EBC Annex 71.

Iordache, V. and Catalina, T. 2012. 'Acoustic approach for building air permeability estimation', Building and Environment, **57**: 18-27.

ISO 9972:2015 (Europe). 2015. Thermal performance of buildings - Determination of air permeability of buildings - Fan pressurization method.

JCGM. 2008. 'Evaluation of measurement data — Guide to the expression of uncertainty in measurement.' In, edited by Joint Committee for Guides in Metrology, 134.

Jokisalo, J., Kurnitski, J., Korpi, M., Kalamees, T., and Vinha, J. 2009. 'Building leakage, infiltration, and energy performance analyses for Finnish detached houses', Building and Environment, **44**: 377-87.

Kalamees, T. 2007. 'Air tightness and air leakages of new lightweight single-family detached houses in Estonia', Building and Environment, **42**: 2369-77.

Kendall, M. G. and Stuart, A. 1961. The Advange Theory of Statistics: Vol. 2 - Inference and Relashionship (London).

Kim, A. and Shaw, C. 1986. 'Seasonal Variation in Airtightness of Two Detached Houses', Measured Air Leakage of Buildings: 17-32.

Kölsch, B., Schiricke, B., Schmiedt, J. E., and Hoffschmidt, B. 2019. 'Estimation of Air Leakage Sizes in Building Envelope using High-Frequency Acoustic Impulse Response Technique.' In 40th AIVC - 8th TightVent - 6th venticool Conference "From energy crisis to sustainable indoor climate - 40 years of AIVC". Ghent, Belgium.

Krane, K. S. and Schecter, L. 1982. 'Regression line analysis', American Journal of Physics, **50**: 82-84.

Kriegesmann, B. 2012. 'Probabilistic Design of Thin-Walled Fiber Composite Structures', Gottfried Wilhelm Leibniz Universität.

Langmans, J., Klein, R., De Paepe, M., and Roels, S. 2010a. 'Potential of wind barriers to assure airtightness of wood-frame low energy constructions', Energy and Buildings, **42**: 2376-85.

Langmans, J., Klein, R., and Roels, S. 2010b. 'Air permeability requirements for air barrier materials in passive houses – Comparison of the air permeability of eight commercial brands of OSB.' In 5th International Symposium on Building and Ductwork Air-tightness. Copenhagen/Lyngby, Denmark.

Larson, G., Nelson, D., and Kubasta, R. 1930. 'Air infiltration through double-hung wood windows', ASHVE Trans. ; (United States), **37**: 571-605.

Leprince, V., Carrié, F. R., and Kapsalaki, M. 2017a. 'Building and ductwork airtightness requirements in Europe – Comparison of 10 European

countries.' In 38th AIVC Conference "Ventilating healthy low-energy buildings". Nottingham, UK.
Leprince, V., Kapsalaki, M., and Carrié, F. R. 2017b. 'Impact of Energy Policies on Building and Ductwork Airtightness.' In.: AIVC.
Litvak, A., Allègre, F., Moujalled, B., and Leprince, V. 2019. 'Assessment of the durability of airtightness products in laboratory controlled conditions: development and presentation of the experimental protocol.' In 40th AIVC-8th TightVent & 6th venticool Conference-From energy crisis to sustainable indoor climate.
Lowinski, J. 1979. 'Thermal performance of wood windows and doors', ASHRAE Trans. ; (United States), **85**: 548-66.
Lstiburek, J., Pressnail, K., and Timusk, J. 2002. 'Air Pressure and Building Envelopes', Journal of Thermal Envelope and Building Science, **26**: 53-91.
Ludbrook, J. 2010. 'Linear regression analysis for comparing two measurers or methods of measurement: but which regression?', Clin Exp Pharmacol Physiol, **37**: 692-9.
Madansky, A. 1959. 'The Fitting of Straight Lines When both Variables are Subject to Error', Journal of the American Statistical Association, **54**: 173-205.
Moujalled, B., Leprince, V., and Melois, A. 2018. 'French database of building airtightness, statistical analyses of about 215,000 measurements: impacts of buildings characteristics and seasonal variations.' In 39th AIVC conference "Smart ventilation for buildings". Antibes Juan-Les-Pins, France.
Neri, F., Saitta, G., and Chiofalo, S. 1989. 'An accurate and straightforward approach to line regression analysis of error-affected experimental data', Journal of Physics E Scientific Instruments, **22**: 215.
Novak, J. 2011. 'A round-robin test of Czech airtightness test providers.' In 6th International BUILDAIR-Symposium. Germany.
Novak, J. 2015. 'Repeatability and reproducibility of blower door tests – four years' experience of round-robin tests in the Czech Republic.' In 9th International Buildair Symposium. Germany.
Novak, J. 2019. 'Influence of the external pressure tap position on the airtightness test result.' In 40th AIVC - 8th TightVent - 6th venticool Conference. Ghent, Belgium.
Okuyama, H. and Onishi, Y. 2012. 'Reconsideration of parameter estimation and reliability evaluation methods for building airtightness measurement using fan pressurization', Building and Environment, **47**: 373-84.

Orme, M., Liddament, M., and Wilson, A. 1994. Numerical Data for Air Infiltration and Natural Ventilation Calculations.
Pernet, C. 2015. 'Null hypothesis significance testing: a short tutorial', F1000Research, **4**: 621-21.
Persily, A. 1982. 'Repeatability and accuracy of pressurization testing.' In ASHRAE/DOE Conference "Thermal performance of the exterior envelope of the building II". USA.
Persily, A. and Grot, R. 1984. 'Pressurization testing of federal buildings.' In Measured air leakage of buildings. A symposium on performance of building constructions. Philadelphia, USA.
Pierson, C. 2019. 'Discomfort Glare Perception from Daylight: Influence of Socio-Environmental Context', UCLouvain.
Pinto, M., Viegas, J., and de Freitas, V. P. 2011. 'Air permeability measurements of dwellings and building components in Portugal', Building and Environment, **46**: 2480-89.
Pitman, E. J. G. 1939. 'A Note on Normal Correlation', Biometrika, **31**: 9-12.
Poza-Casado, I., Cardoso, V. E. M., Almeida, R. M. S. F., Meiss, A., Ramos, N. M. M., and Padilla-Marcos, M. Á. 2020. 'Residential buildings airtightness frameworks: A review on the main databases and setups in Europe and North America', Building and Environment, **183**: 107221.
Press, W. H., Teukolsky, S. A., Flannery, B. P., and Vetterling, W. T. 1992. Numerical recipes in Fortran 77: volume 1, volume 1 of Fortran numerical recipes: the art of scientific computing (Cambridge university press).
Prignon, M., Dawans, A., Altomonte, S., and Van Moeseke, G. 2019. 'A method to quantify uncertainties in airtightness measurements: Zero-flow and envelope pressure', Energy and Buildings, **188-189**: 12-24.
Prignon, M., Dawans, A., and Van Moeseke, G. 2018. 'Uncertainties in airtightness measurements: regression methods and pressure sequences.' In 39th AIVC-7th TightVent & 5th venticool Conference Smart ventilation for buildings. Antibes Juan-Les-Pins, France.
Prignon, M., Dawans, A., and van Moeseke, G. 2020a. 'Quantification of uncertainty in zero-flow pressure approximation', International Journal of Ventilation: 1-10.
Prignon, M., Delmotte, C., Dawans, A., Altomonte, S., and van Moeseke, G. 2020b. 'On the impact of regression technique to airtightness measurements uncertainties', Energy and Buildings, **215**.
Prignon, M., Ossio, F., Altomonte, S., Dawans, A., and Van Moeseke, G. 2020c. 'Airtightness performance of building components: meta-

analysis of laboratory and in-situ measurements', Building and Environment (Under Review).
Prignon, M. and Van Moeseke, G. 2017. 'Factors influencing airtightness and airtightness predictive models: A literature review', Energy and Buildings, **146**: 87-97.
Rajan, A. 2018. 'Moment-Based Uncertainty Propagation Using Multivariate Polynomials. Advances in Probabilistic Engineering Design', Monash University.
Relander, T.-O., Holøs, S., and Thue, J. V. 2012. 'Airtightness estimation—A state of the art review and an en route upper limit evaluation principle to increase the chances that wood-frame houses with a vapour- and wind-barrier comply with the airtightness requirements', Energy and Buildings, **54**: 444-52.
Relander, T.-O., Vincent, J. T., and Gustavsen, A. 2008. 'Air tightness performance of different jointing methods for windows in wood-frame buildings.' In 8th Symposium on Building Physics in the Nordic Countries. Copenhagen, Denmark.
Rogers, S. 2019a. 'How Accurate is our Leakage Extrapolation? Modeling Building Leakage Using the Darcy-Weisbach Equation.' In 40th AIVC - 8th TightVent - 6th venticool Conference. Ghent, Belgium.
Rogers, S. 2019b. Personnal Communication.
Rohr, A., Kaschuba-Holtgrave, A., Rolfsmeier, S., and Solcher, O. 2018. 'Individual unit and guard-zone air tightness tests of apartment buildings.' In 39th AIVC Conference "Smart Ventilation for Buildings". Antibes Juan-Les-Pins, France.
Šadauskienė, J., Šeduikytė, L., Paukštys, V., Banionis, K., and Gailius, A. 2016. 'The role of air tightness in assessment of building energy performance: Case study of Lithuania', Energy for Sustainable Development, **32**: 31-39.
Sherman, M. and Dickerhoff, D. 1998. 'Airtightness of US dwellings.' In 1998 ASHRAE Annual Meeting. Toronto, Canada.
Sherman, M. and Dickinson, J. 1985. 'The prediction of air infiltration.' In CLIMA 2000 World Congress on Heating, Ventilating and Air-Conditioning, edited by P Fanger. Copenhagen.
Sherman, M. and Palmiter, L. 1995. 'Uncertainties in fan pressurization measurements.' in, Airflow performance of building envelopes, components, and systems (ASTM International: Philadelphia, USA).
Sherman, M. H. and Chan, W. 2006. 'Building Air Tightness: Research and Practice.' in Mat Santamouris and Peter Wouters (eds.), Building Ventilation: The State of the Art (London).

Shin, H. K. and Jo, J. H. 2013. 'Air leakage characteristics and leakage distribution of dwellings in high-rise residential buildings in Korea', Journal of Asian Architecture and Building Engineering, **12**: 87-92.

Sinnott, D. and Dyer, M. 2012. 'Air-tightness field data for dwellings in Ireland', Building and Environment, **51**: 269-75.

Sudret, B. 2007. 'Uncertainty propagation and sensitivity analysis in mechanical models. Contribution to structural reliability and stochastic spectral methods.' In.: Université Blaise Pascal.

Tamura, G. T. 1975. 'Measurement of air leakage characteristics of house enclosures', ASHRAE Trans.;(United States), **81**: 202-08.

Tatsioni, A. and Ioannidis, J. P. A. 2008. 'Meta-Analysis.' in Harald Kristian Heggenhougen (ed.), International Encyclopedia of Public Health (Academic Press: Oxford).

Tenwolde, A., Carll, C., and Malinauskas, V. 1993. 'Airflows and Moisture Conditions in Walls of Manufactured Homes.' In Airflow performance of building envelopes, components and systems, 137-55. Dallas, United States.

Titterington, D. M. and Halliday, A. N. 1979. 'On the fitting of parallel isochrons and the method of maximum likelihood', Chemical Geology, **26**: 183-95.

Van Den Bossche, N. and Janssens, A. 2016. 'Airtightness and watertightness of window frames: Comparison of performance and requirements', Building and Environment, **110**: 129-39.

Varshney, K., Rosa, J. E., Shapiro, I., and Scott, D. 2013. 'Air-Infiltration Measurements in Buildings Using Sound Transmission Loss Through Small Apertures', International Journal of Green Energy, **10**: 482-93.

Vinha, J., Manelius, E., Korpi, M., Salminen, K., Kurnitski, J., Kiviste, M., and Laukkarinen, A. 2015. 'Airtightness of residential buildings in Finland', Building and Environment, **93**: 128-40.

Volker, M. A. 2006. 'Reporting Effect Size Estimates in School Psychology Research', Psychology in the Schools, **43**: 653-72.

Walker, I. S., Wilson, D. J., and Sherman, M. H. 1998. 'A comparison of the power law to quadratic formulations for air infiltration calculations', Energy and Buildings, **27**: 293-99.

Ward, I. and Sharples, S. 1982. 'An investigation of the infiltration characteristics of windows and doors in a tall building using pressurisation techniques.' In. UK: Department of Building Science, Faculty of Architectural Studies University of Sheffield.

Weidt, J., Weidt, J., and Selkowitz, S. 1979. 'Field air leakage of newly installed residential windows.' In ASHRAE/DOE Conference. Florida, USA.

York, D. 1966. 'Least-square fitting of a straight line', Revue canadienne de physique, **44**: 1079-86.

York, D. and Evensen, N. M. 2004. 'Unified equations for the slope, intercept, and standard errors of the best straight line', American Journal of Physics, **72**.

Younes, C. and Abi Shdid, C. 2013. 'A methodology for 3-D multiphysics CFD simulation of air leakage in building envelopes', Energy and Buildings, **65**: 146-58.

Younes, C., Shdid, C. A., and Bitsuamlak, G. 2011. 'Air infiltration through building envelopes: A review', Journal of Building Physics, **35**: 267-302.

Zheng, X., Cooper, E., Gillott, M., and Wood, C. 2020. 'A practical review of alternatives to the steady pressurisation method for determining building airtightness', Renewable and Sustainable Energy Reviews, **132**: 110049.

Zheng, X., Cooper, E., Zu, Y. Z., Gillott, M., Tetlow, D., Riffat, S., and Wood, C. 2019. 'Experimental Studies of a Pulse Pressurisation Technique for Measuring Building Airtightness', Future Cities and to Environment, **5**: 1-17.

# Appendix A.

Prignon, M. and Van Moeseke, G. (2017). Factors influencing airtightness and airtightness predictive models: A literature review. Energy and Buildings, **146**: 87–97. https://doi.org/10.1016/j.enbuild.2017.04.062.

Energy and Buildings 146 (2017) 87–97

Contents lists available at ScienceDirect

Energy and Buildings

journal homepage: www.elsevier.com/locate/enbuild

Review

# Factors influencing airtightness and airtightness predictive models: A literature review

Martin Prignon*, Geoffrey Van Moeseke

*Université catholique de Louvain, Architecture et climat, 1 Place du Levant, 1348 Louvain-la-Neuve, Belgium*

ARTICLE INFO

*Article history:*
Received 4 October 2016
Received in revised form 18 April 2017
Accepted 21 April 2017
Available online 24 April 2017

*Keywords:*
Airtightness review
Airtightness models
Airtightness influencing factors
Blowerdoor test
Infiltration

ABSTRACT

In recent decades there has been a growing awareness regarding energy consumption in buildings. Unfortunately, at a time when all building actors should get involved in the challenge to reduce energy consumption, designers cannot rely on effective tools to help them in their decision making process concerning airtightness. This literature review allows the identification of two important issues: new airtightness predictive models are complex to develop and existing airtightness predictive models do not meet the needs of designers and contractors. This paper is divided into three main parts in addition to the introduction and the conclusion. The first part deals with the key concepts of infiltration and airtightness, the second part with influencing factors and the third part with airtightness predictive models. These different chapters highlight a need for standardization regarding the metrics used for data presentation, parameters definition and statistical quantification. The lack of standardization hinders the development of a new airtightness predictive tool for designers and contractors. Along with the problem of standardization, supervision and workmanship are parameters that are difficult to model. Their significant impact can explain why designers and contractors find some existing models unreliable. This paper concludes that none of the existing models can be used in their present form as design tools. Further work should focus on the standardization of data presentation and on the development of a new airtightness predictive model. The first step in the development of such a model is to draw an appropriate classification of "air paths."

© 2017 Elsevier B.V. All rights reserved.

**Contents**

1. Introduction ..... 88
2. Key concepts ..... 88
   2.1. Air infiltration phenomenon ..... 88
   2.2. Differences between infiltration and airtightness ..... 88
   2.3. Airtightness measurement methods ..... 88
   2.4. Flows through cracks ..... 89
   2.5. Nomenclature and metrics ..... 89
3. Factors influencing airtightness ..... 89
   3.1. References ..... 90
   3.2. Parameters ..... 90
      3.2.1. Geometry ..... 90
      3.2.2. Technology & materials ..... 91
      3.2.3. Guidance & supervision ..... 91
      3.2.4. External ..... 91
   3.4. Standardization ..... 92
4. Predictive models ..... 93

* Corresponding author.
*E-mail address:* martin.prignon@uclouvain.be (M. Prignon).

http://dx.doi.org/10.1016/j.enbuild.2017.04.062
0378-7788/© 2017 Elsevier B.V. All rights reserved.

4.1. Theoretical models ..... 93
4.2. Empirical models ..... 93
4.3. Building characteristic models ..... 94
4.4. Single component model ..... 94
4.5. Discussion ..... 94
5. Conclusion ..... 95
5.1. Further work ..... 95
References ..... 96

## 1. Introduction

A few years ago, worldwide political leaders recognized the need to set ambitious challenges in energy consumption. Europe [1,2], the United States [3] and Russia [4] developed energy strategies for the next decades. The building sector plays a large role in final energy consumption and thus requires particular attention. The European Commission adopted the 2010 Energy Performance of Buildings Directive [5] and the 2012 Energy Efficiency Directive [6]. Today, energy challenges concern the entire building sector, from field workers to researchers. Air infiltration can be responsible for up to 30% of the heating demand in winter [7–9] and it impacts insulation thermal performances, hygrothermal performances, occupant comfort, ventilation system efficiency and acoustic insulation [10–17]. Furthermore, industry members and organizations highlight the responsibility of air leakages in many types of building failures [18]. Despite its impact on energy consumption, air infiltration phenomenon remains poorly developed by researchers and equally mastered by designers and contractors.

Airtightness is the main envelope property impacting infiltration [19]. Most national regulations require minimum performances for new buildings. Up until now, the experience of designers and contractors, and practical guides were enough to ensure acceptable airtightness [20–22]. Airtightness requirements have been strengthened over the last few years. Today, their implementation is expensive and time-consuming due to the lack of knowledge and tools. Researchers need airtightness predictive models to model the infiltration phenomenon and designers and contractors need such models to control costs and time in implementing the regulations. Why, when designers and contractors need new tools, aren't predictive tools being developed that would be suitable for practical use?

This literature review reveals two issues: the lack of standardization hinders the development of new airtightness predictive models and existing airtightness predictive models do not meet the needs of designers and contractors. The lack of standardization is discussed in the first and second chapters while existing models are discussed in the third chapter. The first chapter deals with infiltration and airtightness key concepts, the second with airtightness influencing factors and the third with existing predictive models.

## 2. Key concepts

Authors develop in this chapter four key concepts: the air infiltration phenomenon, the difference between infiltration and airtightness, the measurement methods, the theory about flow through cracks and, finally, the nomenclature and metrics. This last section highlights an inconstancy between authors regarding the metrics.

### 2.1. Air infiltration phenomenon

Infiltration is the mass of air passing through cracks or other unintentional envelope openings. This airflow is driven by pressure difference across the envelope [23]. In buildings, such pressure difference occurs because of stack effect and wind pressure. The stack pressure difference is a gradient over the building height caused by a temperature difference. The wind pressure is caused by air flows around the building. It depends on location, geometry, air density, wind speed and wind direction [24]. Infiltration modeling is important since it is a key to understand and predict airtightness. Nevertheless, this literature review focuses on airtightness and not on infiltration.

### 2.2. Differences between infiltration and airtightness

Airtightness should not be confused with infiltration. On the one hand, infiltration is a physical phenomenon: under a pressure difference, air infiltrates the building through envelope cracks or unintentional openings. On the other hand, airtightness is the main envelope property impacting infiltration and is defined as the flow of air infiltrating the building at a pressure difference of 50 Pa. The infiltration phenomenon depends on wind speed, temperature and location while airtightness is intended to be independent of climate variations. Climate influence is reduced by taking a 50 Pa pressure difference [19].

Although airtightness and infiltration are different, they can be mathematically linked. The first empirical relation is known as "rule of thumb." It simply consists in the assumption that the infiltration in a building is 1/20th of its airtightness [25]. This relation does not take into account numerous parameters impacting the infiltration. In 1987 Sherman developed the well-known model: "LBL (Lawrence Berkeley Laboratory)" model. Sherman suggested correction factors to take into account the building height, the wind exposure and the type of cracks [26]. Another existing empirical model is the "AIM-2 (Alberta air Infiltration Model)" developed by Walker and Wilson in 1990. This model assumes that the total airflow is a function of the stack flow and the wind flow [27].

### 2.3. Airtightness measurement methods

For airtightness, measurement is crucial. Sadauskiene et al. show that energy performance calculations seem only reliable after verifying the building airtightness [28]. To our knowledge, correlated with Relander et al. [29], none of the references argue that estimations could replace measurements.

The most popular tests to measure airtightness is the fan pressurization method or blowerdoor test. It consists in the successive building pressurization and depressurization with a fan placed in an opening (door or window) [24]. Sensors record airflow required to maintain a given pressure difference. $Q - \Delta P$ couples are recorded and $n$ and $C$ (Eq. (2)) can be determined. Norm EN 13829 [30] suggests the use of the least square method to determine mean building value for $n$ and then to determine $C$. Okuyama and Onishi [31] questioned this methodology. In their paper, Okuyama and Onishi suggest a weighted least-squares method, a correction of the parameter estimation equation and the deduction of the uncertainty propagation equation. In our view, although these authors present an improved method, it should be trialed in more field studies before drawing solid conclusions. Such investigations would be

useful to reduce uncertainties which are an important issue for blowerdoor test measurements [32].

Other methods are much less used since another device is needed, on the top of the measurement device, to fix the pressure difference between in- and outside at 50 Pa. In recent years acoustic methods have emerged. These methods try to quantify airflow based on the ultrasound reduction recorded between a wave transmitter on one side of the envelope and the wave receiver on the other side. Further development of these techniques would be useful to create an effective component leakage measurement method. Unfortunately, even though these methods are effective to localize air leakage, they are not yet validated to quantify air leakage [33,34]. Other new measurement techniques have been developed to determine airtightness in specific cases. One of them is the sudden expansion from a compressed chamber used to measure airtightness in rooms [35,36]. The tracer gas method does not measure airtightness, but it must be still mentioned as the most common method to measure infiltration [37,38]. Tracer gases are also sometimes combined with the fan pressurization method to localize air leakages.

### 2.4. Flows through cracks

Air flows ($Q$) through cracks is due to a pressure difference ($\Delta P$) between both sides of the crack. The relation between $Q$ and $\Delta P$ depends on the type of crack. $Q$ is proportional to $\Delta P$ in cracks dominated by laminar flows and $Q$ is proportional to $\sqrt{\Delta P}$ in cracks dominated by turbulent flows [19,39]. In practice dominating flows in cracks are neither completely laminar nor completely turbulent. Thus, Etheridge suggested in 1977 a relation (quadratic) where both type of flows are separated (Eq. (1)) [40].

$$\Delta P = \alpha Q + \beta Q^2 \tag{1}$$

Nowadays, the power law (Eq. (2)) is almost the only relation encountered both in literature and practice. The exponent $n$ characterizes the type of flow dominating the crack. Exponent is 1 for laminar flows and 0.5 for turbulent ones.

$$Q = C(\Delta P)^n \tag{2}$$

Researchers widely discussed the use of one or other expression. In 1987, Baker et al. [41] developed the case of parallel plates. He suggested that the quadratic form represents the experimental data better than the power law. In 1992, Sherman [42] showed that both representation can be interchanged in the case of short pipes. In 1998, Walker et al. validated the use of power law in standards and measurement procedures. This validation was based on theoretical analysis, laboratory measurements and in situ testing [43]. They prove that power law represents better the relation between $Q$ and $\Delta P$ in many cases. Nowadays, authors almost always use the power law.

The issue of flow through cracks and openings is important. These last years research focus often on global building airtightness. Nevertheless, some papers focus on the air flow through components: duct leakage studied by LBNL [44,45] and leakage through wood-frame houses component by Relander et al. [46–48].

### 2.5. Nomenclature and metrics

An important metric used is the Effective Leakage Area (ELA). ELA is based on the orifice equation (Eq. (3)) where $C_d$ is the discharge coefficient, $A$ the orifice area and $\rho$ the air density.

$$Q = AC_d\sqrt{\frac{2\Delta P}{\rho}} \tag{3}$$

**Table 1**
Paper nomenclature, European norm, units and mathematical relations of air tightness variables.

| Paper notation | European norm [30] | Unit | Mathematical relation |
|---|---|---|---|
| $Q_{\Delta P}$ | / | $m^3/h$ | None |
| $ACH$ | / | $h^{-1}$ | $ACH = Q_{real}/V$ |
| $ACH_{50}$ | $n_{50}$ | $h^{-1}$ | $ACH_{50} = Q_{50}/V$ |
| $q_{50}$ | $q_{50}$ | $m^3/(h\,m^2)$ | $q_{50} = Q_{50}/A_E$ |
| $w_{50}$ | $w_{50}$ | $m^3/(h\,m^2)$ | $w_{50} = Q_{50}/A_F$ |

ELA is defined in ASHRAE as "the area of an orifice [...] that would produce the same amount of leakage as the building envelope at the reference pressure" (Eq. (4)) [24].

$$ELA = \frac{Q\sqrt{\frac{\rho}{2\Delta P}}}{C_d} \tag{4}$$

NLA is a derived quantities of ELA and is also used as metric. It is simply defined as ELA divided by the area across which pressure difference occurs.

Other metrics have been used, in norms and regulations. Terms used in European standard can sometimes be confusing and are then not used in this review paper. Table 1 shows a list of terms, units and mathematical relation linking different metrics.

$Q_{\Delta P}$ is used to define the airflow entering the building by infiltration at a given pressure difference. $Q_{real}$ is used for infiltration flow to avoid confusion in subscripts, but it is never used neither in literature nor in practice. $ACH$ is the Air Change Rate in actual conditions. It is the ratio between infiltration and building volume. $ACH_{50}$ is the air change rate at a 50 Pa pressure difference. $q_{50}$ is the building air permeability: ratio between infiltration flow and envelope area. $w_{50}$ is the building specific leakage: ratio between infiltration flow and floor area.

The metric used depends on the author, the country or the goal of the project. This huge lack of uniformity makes results difficult to compare and conclusions difficult to draw. Urquhart et al. already highlight the need of metric standardization [49]. A standardized metric should: (i) have a simple physical meaning; (ii) allow the comparison of buildings of different size; (iii) be related to regulations and; (iv) give an information to the user about main leakage paths in the building. In their paper, Urquhart et al. recommend the use of NLA as a standard metric. ELA has a simple meaning but do not fulfill other requirements. NLA has a simple meaning and allows the comparison of buildings of different size, but is not related to regulation. $ACH_{50}$ and $q_{50}$ are directly linked to regulations but have no simple meaning.

In our point of view, none of the current metric could be used as a standardized metric. We think that more than one metric should be used to describe the building airtightness. For example the main metric could be ELA since it gives a simple meaning. Three complementary metrics could then be added: the airflow at 50 Pa could be divided once by the enclosure area ($q_{50}$), once by the total length of linear air leakage paths and once by the number of punctual air leakage paths. An experienced designer would be able to extract information from the comparison of these three complementary metrics. Tables of typical values for different building sizes would help less experienced designers or contractors to choose an appropriate retrofit to achieve good airtightness.

## 3. Factors influencing airtightness

To understand or develop a predictive model, factors impacting airtightness must be known and understood. This part deals with impacting factors identified in literature and tries to understand how such factors impact airtightness. This section reveals and discusses other standardization problems.

**Table 2**
Summary of the different references performing air tightness measurements to identify influencing factors.

| Ref. | Year | Country | # of unit | Significance analysis |
|---|---|---|---|---|
| [51] | 2016 | Netherlands | 300 | Multiple regression analysis |
| [52] | 2016 | Czech Republic | 150 | Spearman's Rank correlation |
| [53] | 2016 | Spain | 45 | ANOVA test |
| [54] | 2014 | Belgium | 153 | *t*-test |
| [55] | 2015 | Finland | 226 | *t*-test |
| [56] | 2013 | US | 134,000 | Multiple regression analysis |
| [57] | 2012 | Italy | 20 | None[a] |
| [58] | 2012 | Ireland | 28 | None[a] |
| [59] | 2011 | Uk | 53 | None[a] |
| [60] | 2010 | France | 251 | Multiple regression analysis |
| [61] | 2010 | Uk | 287 | Multiple regression analysis |
| [62] | 2008 | Greece | 20 | Regression analysis |
| [7] | 2007 | Estonia | 32 | *t*-test |
| [63] | 1984 | Canada | 200 | None[a] |

[a] References without statistical analysis, but such analysis is made in this paper based on available test results.

### 3.1. References

For years, many authors have performed blowerdoor tests. These works can be compared to understand how factors impact airtightness. Table 2 summarizes main information about references analyzed. A (*) symbol means that the significance is not assessed in the paper but test results are available and this review paper made a statistical analysis. A huge recent database is not mentioned in the table because it has not yet been analyzed, but Bailly et al. recently gathered results of 65,000 blowerdoor tests [50].

A residential leakage database (ResDB) was created In US in mid 1990s. ResDB has been updated several times and now contains data from about 147,000 homes [64]. Various analysis of ResDB were performed in 1994 [65], 2002 [66], 2005 [67], 2006 [68], 2007 [69], 2012 [70] and 2013 [56]. Only the last analysis is presented in Table 3. This analysis covers the largest number of measurements and seems the most relevant in the context of this review paper.

### 3.2. Parameters

These references discuss many different parameters. Sometimes authors use different names for the same variable and sometimes the same name can have different definitions. In this review, parameters are divided into four categories: Geometry, Technology & Materials, Guidance & Supervision and External. Table 3 summarizes results. The parameter ranking is shown in the leftmost column. This ranking is an indicator of the impact significance. It is a value between 0 (not significant), 1 (significant) and 2 (highly significant). (*) is used for parameters not enough discussed in references and (?) for parameters not directly linked to the infiltration. This ranking must be carefully used and it should always be compared to the number of cross-references leading to these conclusions.

#### 3.2.1. Geometry

Most geometry parameters are available and are often presented in studies even if they are not always related to the infiltration phenomenon. In these parameters, one can observe an important inconsistency among papers. This is probably due to the indirect link between these parameters and infiltration. For example, volume is sometimes found correlated to airtightness. If the volume of a building increases, weak joints are multiplied. The increase of leakage is not directly linked to the volume increase but it a correlation could be found in some cases. Unlike areas or junctions, the volume is not an air path.

**Table 3**
Factors influencing building airtightness with references dealing with it and results from the crossing of references. This ranking is an indicator of the impact significance. 0 = not significant. 1 = significant. 2 = highly significant. * = not enough discussed. ? = parameters not directly linked to infiltration phenomenon.

| Parameters and ranking | | Significant | Not significant |
|---|---|---|---|
| | *Geometry* | | |
| ? | Number of stories | [7,63,57,62,60] | [55,53] |
| ? | Envelope area | [58,61,63] | [53,57] |
| ? | Floor area | [53,60,56] | [61,57,51,63] |
| ? | Volume | [53,58,62] | [57,63] |
| * | Window and frame area | [53] | [57] |
| * | Frame length | [53,62] | [57] |
| * | Number of penetrations | [61] | |
| | *Technology and materials* | | |
| 2 | Envelope structure | [51,55,59–61] | [54] |
| 2 | Building method | [55,51,7] | |
| 2 | Ventilation system | [7,55,54] | |
| 1 | Dwelling type | [59,61] | [51,58] |
| * | Insulation type | [55] | |
| * | Foundation type | [56] | |
| * | Insulation position | [60] | |
| * | Duct location | [56] | |
| * | Ceiling type | [55] | |
| 0 | Roof type | | [51] |
| 0 | Heating system | | [60] |
| 0 | Window material | | [57] |
| 0 | Floor structure | | [55] |
| | *Guidance and supervision* | | |
| 2 | Design target | [54,58,61] | [51] |
| 2 | Supervision and workmanship | [55,54,58,61,7,63,59] | |
| 2 | Feedback and guidance | [59] | |
| | *Other* | | |
| 0 | Climate variation and surroundings | | [52,61,57,62] |
| ? | Climate zone | [56] | [53] |
| ? | Construction year | [60,56,51] | [55,58,57] |

Usually the number of story is defined according to two categories (one story and multi-story houses), but authors define more categories. One-story houses are shown to be more airtight than multi-story houses in many papers. One of the papers showed no significant differences in averages, but authors found a statistically significant relation for the $ACH_{50}$ values in the case of concrete and masonry houses [55]. They did not find this significance for $q_{50}$ values. The difference between $q_{50}$ and $ACH_{50}$ is due to the evolution of the volume–area ratio. The increase of volume and area leads to the decrease of $ACH_{50}$ and $q_{50}$ values, but not in the same way. For example, in timber-framed houses the number of stories has a significant impact on $q_{50}$ values. The multiplication of weak ceiling-wall joints with the increasing number of stories explains this significant impact. This significance is not found in $ACH_{50}$. Indeed, the decrease of $ACH_{50}$, due to the rise of the total volume, counterbalances its increase linked to the multiplication of weak joints. In the case of $q_{50}$, it doesn't decrease enough with the increase in area to counterbalance the increasing number of weak joints. such situations reinforce the need for metric standardization.

Envelope area and floor area are interesting parameters linked to infiltration phenomenon. Air can infiltrate in the building through porous surfaces and should then be related to the different envelope surfaces. However, due to air barriers in walls, the leakages through surfaces are negligible compared to junction leakages at 50 Pa. This is why most of the researchers found the impact of this parameter not significant. Nevertheless, the increase of the envelope area can be correlated to the increase of leakage junction and can lead to an "indirect" correlation with airtightness in addition to the weak direct correlation.

Authors almost always know the volume and then give it in their results table. But unlike envelope and floor areas which are

both indirectly and directly linked to air infiltration, volume is only indirectly linked to it.

The area of window frames, the number of significant envelope penetrations (windows, doors) and the frame length are rarely discussed but must be further investigated. Indeed, wall-window junctions are often identified as weak points in building airtightness.

#### 3.2.2. Technology & materials

Parameters in this category are linked to the building "quality" instead of its geometry. These parameters are discussed in many references, but never with a clear definition.

The best example of this issue is the most studied parameter in this category: the envelope structure. In [55], Vinha et al. select seven types: timber-framed, logs, blocks of autoclaved aerated concrete, lightweight aggregate concrete, bricks, concrete blocks and concrete elements. The research shows major differences between "concrete & blocks" and "timber-framed & log houses." The second group is found more porous than the first one. Inside the "timber-framed & log" group, log is found more porous than timber-framed. The subgroups of "concrete & blocks" were too small to draw a conclusion. In [54], Laverge et al. found a statistically significant difference between massive and wood frame. The results presented in [59] show that wet/mechanically plastered masonry seems more airtight than dry-lined masonry and steel framed constructions. In [60] the structure is divided into light structures (wood or steel frame constructions) and heavy structures (concrete, bricks or masonry). Light structures appear to be less airtight than heavy structures, and the difference is found statistically significant. In [61] the structure of the envelope (called build method) considers four types: traditional masonry, reinforced concrete, timber frame and precast concrete panels. The differences between these types were found statistically significant, except between reinforced concrete frame and traditional masonry. These two are less airtight than timber frame which is less airtight than precast concrete panel. Lastly, in [51] the envelope structure is divided into concrete, steel, timber and masonry. As it can be seen with this parameter, the lack of standardization makes these references very difficult to compare.

Building method is also defined differently from one paper to another, but key points can be extracted from references: a significant difference can be found between prefabricated buildings (more airtight) and on-site constructed building. In [61], prefabricated constructions are discussed in envelope structure.

Three papers discuss the ventilation system and draw the same conclusion: mean $ACH_{50}$ values between ventilation systems with heat recovery have been found to be statistically different to other systems (natural ventilation and mechanical exhaust). In [54], Laverge et al. explain this difference by the test method standards: the stacks have to be closed with existing shutters (not often present) while ventilation ducts are sealed during the test. Before drawing any conclusion, this explanation should be more investigated.

When papers discuss dwelling types, flats are often significantly more airtight than houses. But apartments are often constructed with different envelope structures and building methods. [61] observe no significant differences between subcategories (end-terraced, mid-terraced, detached and semi-detached for houses and ground floor, mid-floor and top floor for apartments).

The roof type, the heating system, the floor structure and the window materials have been studied by only one reference and each one showed no significant impact on airtightness.

All other parameters presented in Table 3 (insulation type, insulation position, foundation type, duct location and ceiling structure) shows an impact on airtightness in only one reference. For these parameters, further investigation should be performed to confirm the first observation. For insulation type, the lowest air change rate is found for polyurethane insulation. Concerning insulation position, insulation from the interior seems to provide the higher level of airtightness. Five foundation types are observed in [56]: unconditioned basement, vented crawlspace, unvented crawlspace, conditioned basement and slab foundation. Ducts are divided in four locations: conditioned space, unconditioned basement, unconditioned attic and vented crawlspace. Concrete-framed ceilings are more airtight than timber-framed ones.

Results here are much more consistent than geometry variables. It highlights that the "quality" of the element has probably more impact than its geometry. Constructive modes are still gathered based on characteristics not directly linked to airtightness. Structures or elements should be gathered based on elements responsible for airtightness (e.g. presence/absence of an air barrier).

#### 3.2.3. Guidance & supervision

Parameters in this category are important: almost all references agree that they have a significant impact on airtightness. Unfortunately, these parameters are difficult to define and to take into account in a predictive model. The importance of this section can partially explain the different conclusions drawn by authors for other parameters.

Some authors observed the impact of the design target in different ways. This parameter is closely related to the next one: Supervision & workmanship. [54] compares two groups: the first is made of randomly selected cases while the second is made of dwellings intended to be airtight already during the design phase. The difference between both samples is highly statistically significant. The conclusion in [58] highlights the positive influence that airtightness testing can have on building energy performances. In [61], the correlation between the maximum $q_{50}$ value allowed and the final airtightness obtained is found to be significant. Only [51] observe that there is no correlation between design target and airtightness. The work of Meiss and Feijó-Muñoz [8] is not in the table due to the low number of measured units but it can still be interesting in this context. It studies the airtightness of buildings submitted to three different Spanish standards. Results show important differences in $ACH_{50}$ values between the different standards.

Many references study the supervision & workmanship impact, and most conclusions highlight the importance of this parameter in airtightness performances. For this parameter, authors often compare different contractors or compare houses constructed with and without professional supervision.

The impact of feedback & guidance is only discussed in [59]. Johnston et al. did their research in three phases. Two different sets of tests are performed, in the first and third phases. Buildings in the first phase are constructed before the "feedback & guidance" phase (phase 2) while buildings in the third phase are constructed after the second phase.

#### 3.2.4. External

This category deals with a number of parameters which are not directly related to the building itself but to the construction context: construction year or surroundings.

Climate variation & surroundings are expected to have no influence on airtightness since the test norms are made in order to be independent from these parameters. All references confirm this expectation. Nevertheless, [56] studied different climate zones and found statistically significant differences. This observation is probably due to the construction techniques varying from one to another climate zone.

The construction year is discussed in many papers and is the source of many debates. Some authors observed correlation between construction year and airtightness while others did not.

This difference is due to the changes in construction techniques and regulations. It can then vary a lot from one building sample to another. An interesting point – not directly studied as an influence factor – is the deterioration of envelope airtightness performance over time. Measurements from Bracke et al. [71] and Vanwelde and Dartevelle [72] show an increase of $ACH_{50}$ over time up to 28% between one and five years after the building was erected.

### 3.3 Conclusion

A first point highlighted by the analyze of references is the huge lack of consistency in the definition of parameters and the evaluation of parameter significance. For instance, the number of stories is chosen between one or more in some papers and between one, two, three and four in others. Sometimes the same name is given for two different parameters, for instance the building method is the envelope materials in [28] and the use of prefabricated elements in [7]. The correlation between parameters and airtightness is sometimes only observed based on averages and sometimes deals with a *p*-value from ANOVA or *t*-test. Some correlations found by authors cannot be compared to other data set because of the lack of consistency. A standardization could increase the contribution of research by the comparison with other research. The lack of standardization hinders the generalization of tendency observed in papers performing measurements on a small number of measurements.

Despite the lack of consistency, some trends can be observed between references. Some factors are pointed out as having an impact on airtightness: the number of stories, the building method, the envelope structure, the ventilation system, the design target and the supervision. The choice of simple design with prefabricated elements and good supervision can achieve good airtightness, while the same building with complex design and bad supervision can lead to bad performances. However, even if many influencing factors are observed, a very good airtightness can be reached in almost every situation and regardless of the technological choices, materials, geometry or external factors [55]. Disagreements between authors can be attributed to many parameters (e.g. the country, the sample of buildings tested, the measurement equipment). According to Wei Pan, interactions linking different influencing factors can also explain the difference between authors [61]. For example, the ventilation system can be linked to the design target or, as Ramos et al. [73] develop, to the human behavior which is a poorly understood issue.

The huge influence of supervision and workmanship is also an interesting point highlighted in this chapter. This parameter is difficult to integrate in a mathematical model and its importance can explain why designers and contractors found some existing models unreliable.

## 3.4. Standardization

As mentioned in Section 2.5, the lack of standardization regarding used metric was highlight by Urquhart et al. To our knowledge, nobody tackled the issue of lack of standardization neither in parameter definition nor in the significance evaluation.

Parameter definition and classification should be done carefully. A good classification must deal with the infiltration phenomenon: the air flows through areas (walls, roofs, windows, ...), through junctions between elements (wall-floor, wall-roof, window-wall, ...) and through small individual points (electricity, plumbing, ...). Fig. 1 schematically represents these three different kinds of air paths.

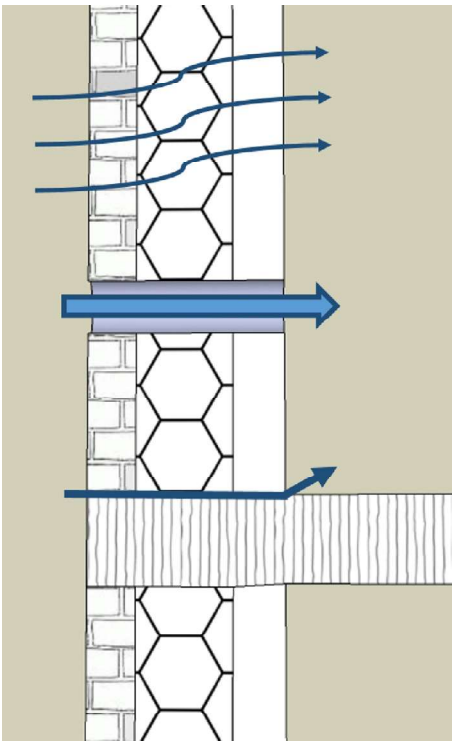


**Fig. 1.** Three examples of different type of air paths.

This paper suggests an example of the relation dealing with these three types of air paths (Eq. (5)), with newly defined "quality coefficients."

$$Q_{50} = \sum_{\alpha=1}^{areas} A_\alpha C_{qs,\alpha} + \sum_{\beta=1}^{junctions} L_\beta C_{ql,\beta} + \sum_{\gamma=1}^{penetrations} C_{qp,\gamma} \quad (5)$$

$Q_{50}$ is the total air flow passing through the envelope at a pressure difference of 50 Pa in $m^3/h$, $A$ is the area of an envelope part in $m^2$, $L$ is the length of junctions in m, $C_{qs}$ is the surface quality coefficient in $m^3/(h\,m^2)$, $C_{ql}$ is the linear quality coefficient in $m^3/(h\,m)$ and $C_{qp}$ is the point quality coefficient in $m^3/h$. This equation is divided in three terms: first for surface air losses, second for linear air losses and third for point air losses.

A number of cases encountered in practice would be classified as "hybrid cases" because of their nature. These have to be classified in one of the equation terms, depending on their dominant behavior. An example of hybrid case is shown in Fig. 2. One must choose if this example is a point loss (regarding the external membrane) or a surface loss (regarding the internal membrane). In our view, internal membrane should be taken as a reference since a good practice is to set the air barrier in the wall closer to the inside in order to avoid internal condensation in mild and cold climates. The example would be then considered as a surface loss.

Except for the third term of the equation, each has a "geometry" variable and a "quality" variable. Parameters identified in this section stand behind all these variables. Important parameters to include in the classification can be directly determined from this equation. Table 4 describes these parameters.

The table is divided in two parts, in the first are parameters already discussed in literature while in the second are new parameters. The ventilation system should probably be added to this list (as quality variable in point losses), but the issue of test standards discussed in Section 3.2.2 must first be investigated. The envelope structure is an important parameter, but in our point of view the definition used in different papers is not appropriate for infiltra-

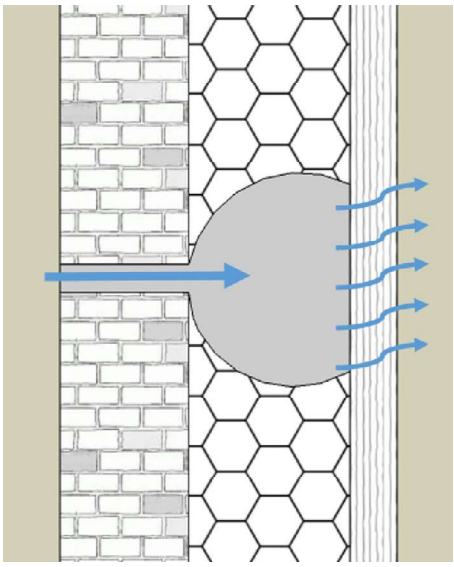


**Fig. 2.** Example of a hybrid air path.

**Table 4**
Classification of important parameters regarding infiltration phenomenon.

| Influencing factor | Variable type | Losses type |
|---|---|---|
| *Already discussed parameters* | | |
| - Envelope area ($m^2$) | Geometry | Surface losses |
| - Frame length (m) | Geometry | Linear losses |
| - # of stories (one or more) | Geometry | Linear losses |
| - # of penetration (number) | Geometry | Point losses |
| - Construction method (prefabricated or on site construction) | Quality | Linear losses |
| - Envelope structure (materials and air barrier) | Quality | Surface losses |
| - Supervision &workmanship (contractor description) | Quality | All losses |
| - Design target (required performances) | Quality | All losses |
| *New suggested parameters* | | |
| - Length of wall-roof junction (m) | Geometry | Linear losses |
| - Type of penetration (electric, plumbing, . . .) | Quality | Point losses |

tion. It is considered as an "already discussed parameter" in Table 4 but its definition has been modified.

To quantify the impact of parameter on airtightness, standardization should be done regarding a statistical indicator. *p*-values are often used in literature to determine a level of significance (0.05 is usually chosen as the limit between significant and not significant values). These values are easy to understand and well-known by researchers. The difficulty arises when authors must choose a statistical tool to compute *p*-values. Numerous statistical tools exist and the choice depends on the situation. One can determine *p*-values by comparison of means (*t*-test or one-way ANOVA test), by variable interaction study (two-way ANOVA) or by correlation study (r-Pearson). The choice of the most suited tool is an important task in the standardization of results but depends a lot on the variables studied. It is important that in each work, authors clearly mention and explain the statistical tools used to perform their analysis in each work.

Standardization is important to compare data and to have a better understanding of airtightness. With such a standardization, the idea of collecting worldwide data to draw a single conclusion would be tempting. However, structure type, construction technique, building technologies or other influencing factors vary from one country to another. Single conclusion could probably not be drawn from such a database, but different countries and techniques could be compared.

## 4. Predictive models

With the strengthening of airtightness requirements, good supervision and design are not always enough to achieve required airtightness. Predictive tools for contractors or designers are more necessary than ever. This section aims to describe existing predictive models, divided in four categories: theoretical models, empirical models, building characteristic models and single component models. Regarding these models, particular attention will be paid on their drawback, their intended use and how they deal with influencing factors.

### 4.1. Theoretical models

Theoretical models are based on equations expressing the flow through individual cracks and openings as described in Section 2.1 and 2.5 (Eqs. (2) and (3)). These equations can be used to model each crack individually or the entire building. Indeed, the building can be seen as an aggregation of numerous cracks. Mean values for *C* and *n* are usually obtained with blowerdoor tests. If the airtightness has to be predicted before construction, one can find these two parameters in literature. But without testing, these coefficients lead to huge simulation inaccuracy [39]. They can be found in a building with similar location, geometry, techniques or materials but such a model does not deal with supervision and workmanship quality.

If cracks are studied individually, governing equations must be used to model each crack or opening. This can be done by using CFD (Computational Fluid Dynamics). Besides the literature databases, numerical method (CFD, Computational Fluid Dynamics) can be used to predict air flows, heat and mass transfers after the problem discretization [74]. CFD can be very precise or not, depending on theoretical hypothesis. For example, a simple model would consider only one virtual huge crack (which would be the sum of each real crack) while a complex model would consider each crack individually. Younes and Shdid recently discussed the use of CFD in this field, highlighting the fact that they are not suited for practical use [75]. Main CFD drawback is its important computation time. Wang and Chen explain that for a building in steady-state conditions, calculations can take from several hours to several days [76]. While not impossible, the use of CFD in practice is often limited by the important computation time and calculation power necessary to obtain reliable models. Nevertheless CFD could be used to create a suitable tool instead of being used as a predictive tool. It can also be used to study the influence of specific parameters by theoretically freezing other influencing factors to avoid interactions.

### 4.2. Empirical models

Empirical models are based on huge sets of blowerdoor data. This paper presents two types of empirical models: the regression analysis and the artificial neural network. The regression analysis is a statistical tool used to evaluate the relation between variables. Such models establish mathematical relations between airtightness and numerous parameters [77]. Regression analyses on airtightness have been performed by Chan et al. in 2005 [67] and in 2013 [56], Montoya et al. in 2010 [60], Pan the same year [61] and more recently Fernàndez-Agüera et al. [53] in 2015 and Bramiana et al. [51] in 2016. Regression models are accurate in describing buildings close to the set used for the analysis. Consequently, these models are usually used to describe and analyze the building stock.

They can also be used as predictive tools but are only accurate for buildings close to the data used for the original analysis.

Artificial Neural Network is a model with human capabilities: learning and adaptation. It consists of a few simple processing units and many connections. These connections lead to modifications of units in order to adapt them if new data are obtained [78]. Krstic et al. [79] recently tested the neural network to predict the airtightness of a building set in Croatia. One year later, a second paper validated this methodology by its application on another set of buildings from the republic of Serbia [80]. This powerful estimation tool shows strong capabilities but still requires an important validation work.

Hybrid models can be mentioned in this section. These models are not yet used for airtightness prediction, but can be a path to explore. Hybrid models are based on both empirical relations and theoretical considerations. An example is the formula established by Dietz used to determine *ACH*. It deals with temperature difference and wind speed, driving forces of infiltration, and other parameters as the generalized house leakiness factor or the terrain sheltering [81]. Nowadays, hybrid models are only valid for a reduced set of data when uncertainty of parameters is important [82].

### 4.3. Building characteristic models

This type of model is the most suitable for designer use: based on building characteristics, airtightness can be determined by using simple mathematical formula or calculation sheets. Such formula has been presented first as the SBR method 1 [83]: Q10 (in [L/s]) is calculated by multiplying coefficients depending on the type of construction, the type of roof, the workmanship and the building envelope area. De Gids further develops this method in 2010 [84] to take into account the facade and the building form in addition to previous coefficients. Relander underlines that this method is not accurate for new sets of buildings [29]. With AIVC worksheets a designer can determine the $ACH_{50}$ of a building. Starting with a basic value depending on the building type, a bonus/penalty increase based on parameters (construction technologies or materials) lead to a final value for the building. Even if this method is really interesting and could be a powerful tool for designers, it is outdated (1998) because of the development in construction techniques and the strengthening of requirements [85]. Such worksheets are easy to use, but infiltration phenomenon is the airflow through components and is not linked to general building characteristics. These worksheets do not deals with the physical phenomenon of infiltration, which could be problematic for future necessary updates or future requirements strengthening.

### 4.4. Single component model

Single component models aim to describe the airtightness of building parts instead of the whole building (e.g. a window or a wall-roof junction). The contributions of all the different component leakages can be summed in order to obtain the whole building leakage. This sum was already suggested in Section 3.4 through the choice of parameters (Eq. (5)). These models are really promising since they give the designer direct information on the impact of construction and technical choices and to the contractor direct information about effective retrofit actions.

The first type of single component models is the databases found in literature. The AIVC database based on the work of Orme [85] (in 1998) and ASHRAE database based on the work of Dickerhoff and Harrje [24,86] (in 1982) were widely used in previous years. Table 5 shows an example of a typical table found in the work of Orme.

Unfortunately such databases are nowadays outdated in Europe: they were developed a long time before European energy regulations which have been a watershed in the evolution of building performances throughout Europe. Moreover the component choice is often made based on construction technology or on thermal bridges. Although linked, heat and air transfer are not the same phenomenon and a specific classification should be used.

**Table 5**
Example of windows flow coefficient ($C$) values taken from the work of Orme in 1998 [85].

| Component | Lower quartile | Median | Upper quartile | Sample size |
|---|---|---|---|---|
| *Windows weatherstripped* | | | | |
| Hinged | 0.086 | 0.13 | 0.41 | 29 |
| Sliding | 0.079 | 0.15 | 0.21 | 19 |
| *Windows non-weatherstripped* | | | | |
| Hinged | 0.38 | 0.74 | 01.1 | 42 |
| Sliding | 0.18 | 0.23 | 0.37 | 36 |

Another model is the sound reduction method developed by Hassan. The calculation of the component infiltration rate is based on the sound reduction index [87]. This model is based on acoustic measurements but can be considered as a predictive model because one can deduce the reduction index from the theory of sound insulation. It always depends on geometry and boundary conditions, but one can often use the theory of infinite plates to determine this reduction index [88]. Eq. (6) gives an example of reduction index formula for plane wave incidence [89]. Unfortunately the theory of sound insulation in the context of airtightness has not been developed in practice.

$$R = 10 \cdot \log\left[1 + \left(\frac{\pi f M \cos(\theta)}{\rho_0 c}\right)^2\right] dB \tag{6}$$

$R$ is the sound reduction index, $f$ is the wave frequency (Hz), $M$ is the specific mass (kg/m$^2$), $\theta$ is the angle of wave incidence (°), $\rho_0$ is the air density (kg/m$^3$) and $c$ is the sound velocity in air (m/s).

If cracks or openings can be identified and dimensioned in a given component, theoretical models presented in Section 4.1 (either fundamental equations or CFD models) can also be used to predict single component leakages.

### 4.5. Discussion

In previous sections, the lack of standardization at different levels and the impact of workmanship and supervision partially explain why reliable and suitable models are difficult to develop. This section shows that numerous airtightness models already exist. However the lack of predictive tools in the construction field nowadays is still important.

Different factors can explain this issue. Firstly, the need of accurate predictive tools has only came out recently with the strengthening of requirements. Second, explanation related to the model can be highlighted. All models are not intended to be used as predictive tools. Some are used to make statistical analysis of existing buildings as regression analysis. Nevertheless regression analysis can be used as predictive tools in conditions close to the one used to determine the empirical relation. Moreover, all of the predictive models have small drawbacks making them unsuitable for practical use as predictive tools. For governing equations, the need of literature leads to high inaccuracy. For CFD simulations, the calculation time, the powerful computation tools needed and the crack distribution, which is sometimes difficult to obtain, make these models difficult to use in practice. Empirical models, both regression analysis and neural network, do not deal with the infiltration phenomenon and require huge sets of data. Building characteristic models are really simple but completely outdated. An update of these models would probably be useful, but the lack

**Table 6**
Summary table – type of models, their influencing factors and practicability.

| Models | BG | TM | GS | Drawbacks | Intended use |
|---|---|---|---|---|---|
| *Theoretical models* | | | | | |
| Governing equations | Y | Y | Y | Inaccurate | Predictive |
| CFD simulations | Y | Y | Y | Time consuming | Predictive |
| *Empirical models* | | | | | |
| Regression analysis | Y | Y | Y | Reduced set of buildings | Statistics |
| Neural network | Y | Y | Y | Reduced set of buildings | Statistics |
| *Building characteristics* | | | | | |
| Formula | Y | Y | Y | Outdated | Predictive |
| Worksheets | Y | Y | N | Outdated | Predictive |
| *Component models* | | | | | |
| Databases | [a] | [a] | N | Outdated | Predictive |
| Sound reduction | [a] | [a] | N | Not enough developed | Predictive |

[a] Non-sense due to scale.

of physical considerations could become a limitation if requirements strengthen further. Regarding component models, the sound reduction model is still not fully developed and single component databases are outdated. Third, some models do not deal with all the influencing factors. For CFD, it depends on the hypothesis and geometry and for governing equations it depends on the coefficients and on the hypothesis. Empirical models deal with influencing factors chosen in the original analysis. Current versions of building characteristic models deal with the main influencing factors. An update should add "supervision and workmanship" as a model parameter. Influencing factors taken into account in single component models are different from other models because of the scale difference. As for building characteristic models, an update should include the "supervision and workmanship" factor as a model parameter.

The three points presented in the previous paragraph are summarized in Table 6 for each model. The capability to deal with main influencing factors (Building Geometry (BG), Technology & Materials (TM) and Guidance & Supervision (GS)), the main drawback and the intended use of each model are mentioned. Today none of these models seem suitable for designer practical use.

In our view, single component models are the most promising predictive tools. These models deal with infiltration and the main influencing factors since they are based on the air flowing through building components. An update of these models could lead to a suitable tool for designers, similar to the thermal bridges catalog [90]. This update is very challenging in two aspects: the measurement method and the integration of supervision and workmanship. First, blowerdoor tests measure only whole building performances. One way to measure the leakage of an individual component would be to compare successive blowerdoor tests: one made before and one after sealing the component. The difference between both values is then defined as the component leakage. Dickerhoff [86] or more recently Pereira et al. [91] use this methodology. In this method the uncertainty analysis is crucial and has to consider the measurement method, the regression to obtain $n$ and $C$, the average made between pressurization and depressurization results and the derived quantities ($ACH_{50}$, $q_{50}$, $w_{50}$, ...) [32]. Second, the impact of supervision and workmanship quality is most of the time unknown or undefinable. It can be considered as a parameter or as an uncertainty on the measurement. With such an uncertainty, results are not a leakage value anymore but a range or even a probability distribution when enough data is collected. Different quartiles would correspond to different construction quality as Orme et al. did in their work [85].

## 5. Conclusion

Enhanced requirements reveal a need for predictive tools for designers and contractors. This paper discusses the development of new predictive tools and the existing airtightness predictive models. To explain why predictive tools are still missing, the paper develops two questions: "why has no new appropriate model been developed today" and "why are existing predictive model not used"? The first question is assessed in both the first and second chapters, highlighting the lack of standardization and the difficulties encountered in modeling. The first chapter deals with airtightness and infiltration key concepts and highlights the problem of metric standardization. The second chapter deals with influencing factors and highlights two other standardization problems: factors classification and impact quantification. In addition to standardization problems, this second chapter points out the significant impact of supervision and workmanship, a parameter difficult to integrate in predictive models. The second question is addressed in the third chapter. This chapter describes numerous existing predictive models, their drawbacks, how they deal with identified influencing factors and whether they are intended to be used as predictive or descriptive tools.

Conclusions are unanimous: none of the existing predictive models can be used, in their present form, as a design tool and the development of a new predictive model is hindered by the lack of standardization and the necessity for the integration of "supervision and workmanship." However, such conclusions logically lead to possible future works to develop an effective model suitable for practical use.

### 5.1. Further work

The first and most important point is the lack of standardization. A significant piece of work has to be done, focusing on metric, parameter definition and impact quantification. In our point of view, none of the metrics used nowadays are appropriate and new metrics must be established and tested. These new metrics would be useful for designers and contractors and would give information about main building leakage types. The choice of new metrics is discussed in Section 2.5, but suggestions by themselves are not enough and future reflections should be nourished by test results. Regarding the definition of parameters, the list suggested in Section 3.4 is not exhaustive and should be developed in future researches too. Finally, a statistical tool to quantify significance should be assigned to each parameter in the list.

Besides standardization issues, a predictive tool should be developed to meet the needs of designers and contractors. The use of such a tool should be easy and it should take into account the physics underlying airtightness and infiltration. Interesting step in this direction would be the classification of "air leakage paths" based on the way air flows around them. This classification would provide a better understanding of the phenomenon and would logically lead to appropriate design tools based on components air leakages, similar to thermal bridge catalogs.

Some interesting points are presented in literature and could be further investigated. For example, research on parameters such as the length of frames and the number of significant penetration areas/points is rather limited while, intuitively, it seems intuitively highly correlated to airtightness. Some criticized results should also be more investigated as well as the difference between different ventilation systems.

## References


[1] E. Commission, Energy 2020 A Strategy for Competitive, Sustainable and Secure Energy, Communication from the Commission to the European Parliament, the Council, the European Economic and Social Committee and the Committee of the Region.
[2] E. Commission, Energy Roadmap 2050, Communication from the Commission to the European Parliament, the Council, the European Economic and Social Committee and the Committee of the Region.
[3] The White House Council on Environmental Quality, Implementing Instructions for Executive Order 13693 Planning for Federal Sustainability in the Next Decade, 2015.
[4] Institute of Energy Strategy, Approved by Decree No. 1715-r of the Government of the Russian Federation. Energy Strategy of Russia, 2010.
[5] E. Commission, Directive 2010/31/EU of the European Parliament and of the Council of 19 May 2010 on the Energy Performance of Buildings.
[6] E. Commission, Directive 2012/27/EU of the European Parliament and of the Council of 25 October 2012 on Energy Efficiency, Amending Directives 2009/125/EC and 2010/30/EU and Repealing Directives 2004/8/EC and 2006/32/EC Text with EEA Relevance.
[7] T. Kalamees, Air tightness and air leakages of new lightweight single-family detached houses in estonia, Build. Environ. 42 (6) (2007) 2369–2377, http://dx.doi.org/10.1016/j.buildenv.2006.06.001.
[8] A. Meiss, J.F. Muñoz, The energy impact of infiltration: a study on buildings located in north central Spain, Energy Effic. 8 (2015) 51–64, http://dx.doi.org/10.1007/s12053-014-9270-x.
[9] J. Jokisalo, J. Kurnitski, M. Korpi, T. Kalamees, J. Vinha, Building leakage, infiltration, and energy performance analyses for finnish detached houses, Build. Environ. 44 (2) (2009) 377–387, http://dx.doi.org/10.1016/j.buildenv.2008.03.014.
[10] S. Thébault, R. Bouchié, 6th International Building Physics Conference, IBPC 2015 estimating infiltration losses for in-situ measurements of the building envelope thermal performance, Energy Proc. 78 (2015) 1756–1761.
[11] W. Robert, K. Piotr, Seeming air tightness of construction partitions, Energy Proc. 78 (2015) 1519–1524, http://dx.doi.org/10.1016/j.egypro.2015.11.294.
[12] D. Watt, S. Sjöberg, P. Wahlgren, 6th International Building Physics Conference, IBPC 2015 hygrothermal performance of a light weight timber wall assembly with an exterior air barrier, Energy Proc. 78 (2015) 1419–1424, http://dx.doi.org/10.1016/j.egypro.2015.11.164.
[13] J. Langmans, R. Klein, S. Roels, Hygrothermal risks of using exterior air barrier systems for highly insulated light weight walls: a laboratory investigation, Build. Environ. 56 (2012) 192–202, http://dx.doi.org/10.1016/j.buildenv.2012.03.007.
[14] D. Sinnott, Dwelling airtightness: a socio-technical evaluation in an irish context, Build. Environ. 95 (2016) 264–271, http://dx.doi.org/10.1016/j.buildenv.2015.08.022.
[15] W.A.Y. Anis, The impact of airtightness on system design, ASHRAE J. 43 (12) (2001) 31–35.
[16] D. MacPhaul, C. Etter, HVAC System Design for Humid Climates, 2010 (website – last view on 14.04.17) https://www.wbdg.org/resources/hvac_humidclimates.php.
[17] H.K. Park, H. Kim, Acoustic insulation performance of improved airtight windows, Constr. Build. Mater. 93 (2015) 542–550, http://dx.doi.org/10.1016/j.conbuildmat.2015.05.058.
[18] H.C. Fennell, J. Haehnel, Setting airtightness standards, ASHRAE J. 47 (2005).
[19] M. Sherman, R. Chan, Building airtightness: Research and practice, Tech. rep., Lawrence Berkeley National Laboratory, 2004.
[20] CSTC, L'étanchéité á l'air des batiments, technical information note, 2015.
[21] M. Jaggs, C. Scivyer, A practical guide to building airtight dwellings, Tech. rep., NHBC Foundation, 2009.
[22] F. Carrié, R. Jobert, V. Leprince, Methods and techniques for airtight buildings, Tech. Rep. 14, AIVC, 2012.
[23] M.H. Sherman, Air infiltration in buildings (Ph.D. thesis), University of Californie – Lawrence Berkeley Laboratory, 1980.
[24] A.S. Committee, et al., Ashrae Handbook: Fundamentals 2013, 2013.
[25] M.W. Liddament, Air Infiltration Calculation Techniques: An Applications Guide, Air Infiltration and Ventilation Centre Berkshire, UK, 1986.
[26] M.H. Sherman, Estimation of infiltration from leakage and climate indicators, Energy Build. 10 (1) (1987) 81–86.
[27] I. Walker, D. Wilson, AIM 2: The Alberta Air Infiltration Model, University of Alberta, Department of Mechanical Engineering Report 71, 1990.
[28] J. Šadauskienė, L. Šeduikytė, V. Paukštys, K. Banionis, A. Gailius, The role of air tightness in assessment of building energy performance: case study of Lithuania, Energy Sustain. Dev. 32 (2016) 31–39, http://dx.doi.org/10.1016/j.esd.2016.02.006.
[29] T.-O. Relander, S. Holøs, J.V. Thue, Airtightness estimation – a state of the art review and an en route upper limit evaluation principle to increase the chances that wood-frame houses with a vapour- and wind-barrier comply with the airtightness requirements, Energy Build. 54 (2012) 444–452, http://dx.doi.org/10.1016/j.enbuild.2012.07.012.
[30] E. NBN, 13829, Thermal Performance of Buildings – Determination of Air Permeability of Buildings – Fan Pressurization Method, CEN, Brussels, Belgium, 2001.
[31] H. Okuyama, Y. Onishi, Reconsideration of parameter estimation and reliability evaluation methods for building airtightness measurement using fan pressurization, Build. Environ. 47 (2012) 373–384, http://dx.doi.org/10.1016/j.buildenv.2011.06.027, International Workshop on Ventilation, Comfort, and Health in Transport Vehicles.
[32] S. Caillou, P. Van den Bossche, C. Delmotte, D. Van Orshoven, L. Vandaele, Measurement of building airtightness in the EPB context: specific procedure and sources of uncertainties, in: Building Physics Symposium, Leuven, Belgium, 2008.
[33] N. Duray, B. Michaux, Elaboration d'un protocole expérimental en vue de déterminer l'étanchéité à l'air de bâtiments et de parois via les ultrasons, Rev. Sci. Ing. Ind. 29 (2015).
[34] G. Raman, K. Chelliah, M. Prakash, R.T. Muehleisen, Detection and quantification of building air infiltration using remote acoustic methods, 43rd International Congress on Noise Control Engineering November (2014) 16–19.
[35] M.J. Lee, N.I. Kim, H.S. Ryou, Air tightness measurement with transient methods using sudden expansion from a compressed chamber, Build. Environ. 46 (10) (2011) 1937–1945, http://dx.doi.org/10.1016/j.buildenv.2011.04.001.
[36] S. Bae, H. Moon, M.J. Lee, N.I. Kim, H.S. Ryou, Improvement in the applicability of the air tightness measurement using a sudden expansion of compressed air, Build. Environ. 61 (2013) 133–139, http://dx.doi.org/10.1016/j.buildenv.2012.12.017.
[37] G. Hong, B.S. Kim, Field measurements of infiltration rate in high rise residential buildings using the constant concentration method, Build. Environ. 97 (2016) 48–54, http://dx.doi.org/10.1016/j.buildenv.2015.11.027.
[38] C. Ghazi, J. Marshall, A $\{CO_2\}$ tracer-gas method for local air leakage detection and characterization, Flow Meas. Instrum. 38 (2014) 72–81, http://dx.doi.org/10.1016/j.flowmeasinst.2014.05.015.
[39] C. Younes, C.A. Shdid, G. Bitsuamlak, Air infiltration through building envelopes: a review, J. Build. Phys. 35 (3) (2011) 267–302.
[40] D. Etheridge, Crack flow equations and scale effect, Build. Environ. 12 (3) (1977) 181–189.
[41] P. Baker, S. Sharples, I. Ward, Air flow through cracks, Build. Environ. 22 (4) (1987) 293–304.
[42] M. Sherman, A power-law formulation of laminar flow in short pipes, J. Fluids Eng. 114 (4) (1992) 601–605.
[43] I.S. Walker, D.J. Wilson, M.H. Sherman, A comparison of the power law to quadratic formulations for air infiltration calculations, Energy Build. 27 (3) (1998) 293–299.
[44] C. Wray, M.H. Sherman, Duct Leakage Modeling in EnergyPlus and Analysis of Energy Savings from Implementing SAV with InCITeTM, Lawrence Berkeley National Laboratory, 2010.
[45] C.P. Wray, R.C. Diamond, M.H. Sherman, Rationale for Measuring Duct Leakage Flows in Large Commercial Buildings, Lawrence Berkeley National Laboratory, 2005.
[46] T.-O. Relander, B. Heiskel, J.S. Tyssedal, The influence of the joint between the basement wall and the wood-frame wall on the airtightness of wood-frame houses, Energy Build. 43 (6) (2011) 1304–1314.
[47] T.-O. Relander, T. Kvande, J.V. Thue, The influence of lightweight aggregate concrete element chimneys on the airtightness of wood-frame houses, Energy Build. 42 (5) (2010) 684–694.
[48] T.-O. Relander, G. Bauwens, S. Roels, J.V. Thue, S. Uvsløkk, The influence of structural floors on the airtightness of wood-frame houses, Energy Build. 43 (2) (2011) 639–652.
[49] R. Urquhart, R. Richman, G. Finch, The effect of an enclosure retrofit on air leakage rates for a multi-unit residential case-study building, Energy Build. 86 (2015) 35–44, http://dx.doi.org/10.1016/j.enbuild.2014.09.079.
[50] A. Bailly, G. Guyot, V. Leprince, 6 years of envelope airtightness measurements performed by French certified operators: analysis of about 65,000 tests, in: 12th REHVA World Congress, Aalborg, Denmark, 2016.
[51] C. Bramiana, A. Entrop, J. Halman, Relationships between building characteristics and airtightness of Dutch dwellings, Energy Proc. 96 (2016) 580–591, http://dx.doi.org/10.1016/j.egypro.2016.09.103.
[52] M. Kraus, P. Charvátová, Location as a determinative factor of building airtightness, Proc. Eng. 161 (2016) 1532–1537, http://dx.doi.org/10.1016/j.

proeng.2016.08.622, World Multidisciplinary Civil Engineering-Architecture-Urban Planning Symposium 2016 {WMCAUS} 2016.
[53] J. Fernández-Agüera, S. Domìnguez-Amarillo, J.J. Sendra, R. Suárez, An approach to modelling envelope airtightness in multi-family social housing in Mediterranean Europe based on the situation in Spain, Energy Build. 128 (2016) 236–253, http://dx.doi.org/10.1016/j.enbuild.2016.06.074.
[54] J. Laverge, M. Delghust, N.V.D. Bossche, A. Janssens, Airtightness assessment of single family houses in Belgium, Int. J. Vent. 12 (4) (2014) 379–390.
[55] J. Vinha, E. Manelius, M. Korpi, K. Salminen, J. Kurnitski, M. Kiviste, A. Laukkarinen, Airtightness of residential buildings in Finland, Build. Environ. 93 (Part 2) (2015) 128–140, http://dx.doi.org/10.1016/j.buildenv.2015.06.011.
[56] W.R. Chan, J. Joh, M.H. Sherman, Analysis of air leakage measurements of US houses, Energy Build. 66 (2013) 616–625.
[57] F. Alfano, M. Dell'Isola, G. Ficco, F. Tassini, Experimental analysis of air tightness in Mediterranean buildings using the fan pressurization method, Build. Environ. 53 (2012) 16–25, http://dx.doi.org/10.1016/j.buildenv.2011.12.017.
[58] D. Sinnott, M. Dyer, Air-tightness field data for dwellings in Ireland, Build. Environ. 51 (2012) 269–275, http://dx.doi.org/10.1016/j.buildenv.2011.11.016.
[59] D. Johnston, D. Miles-Shenton, M. Bell, J. Wingfield, Airtightness of buildings - towards higher performances, Tech. rep., Leeds Beckett University, Final Report, 2011.
[60] M.I. Montoya, E. Pastor, F.R. Carrié, G. Guyot, E. Planas, Air leakage in Catalan dwellings: developing an airtightness model and leakage airflow predictions, Build. Environ. 45 (6) (2010) 1458–1469, http://dx.doi.org/10.1016/j.buildenv.2009.12.009.
[61] W. Pan, Relationships between air-tightness and its influencing factors of post-2006 new-build dwellings in the {UK}, Build. Environ. 45 (11) (2010) 2387–2399, http://dx.doi.org/10.1016/j.buildenv.2010.04.011.
[62] A. Sfakianaki, K. Pavlou, M. Santamouris, I. Livada, M.-N. Assimakopoulos, P. Mantas, A. Christakopoulos, Air tightness measurements of residential houses in Athens, Greece, Build. Environ. 43 (4) (2008) 398–405, http://dx.doi.org/10.1016/j.buildenv.2007.01.006, Part Special: Building Performance Simulation.
[63] M. Sulatisky, Airtightness tests on 200 new houses across Canada: Summary of results. A research report, bETT Publication No 84.01, 1984.
[64] LBNL, Residential Diagnostics Database, http://resdb.lbl.gov/, website – last view on 14.04.17.
[65] M. Sherman, D. Dickerhoff, Air-tightness of US dwellings, Document-Air Infiltration Centre AIC Proc, Oscar Faber PLC (1994), 225–225.
[66] M.H. Sherman, N.E. Matson, Air Tightness of New Houses in the US: A Preliminary Report, Lawrence Berkeley National Laboratory, 2002.
[67] W.R. Chan, W.W. Nazaroff, P.N. Price, M.D. Sohn, A.J. Gadgil, Analyzing a database of residential air leakage in the United States, Atmos. Environ. 39 (19) (2005) 3445–3455.
[68] J. McWilliams, M. Jung, Development of a Mathematical Air-Leakage Model from Measured Data, Lawrence Berkeley National Laboratory, 2006.
[69] M.H. Sherman, J.A. McWilliams, Air Leakage of US Homes: Model Prediction, Lawrence Berkeley National Laboratory, 2007.
[70] W.R. Chan, J. Joh, M.H. Sherman, Air leakage of US homes: Regression analysis and improvements from retrofit, Tech. rep., Lawrence Berkeley National Laboratory, LBNL-5966E, 2012.
[71] W. Bracke, J. Laverge, N.V.D. Bossche, A. Janssens, Durability and measurement uncertainty of airtightness in extremely airtight dwellings, Tech. rep., Ghent University, 2016.
[72] O. Dartevelle, V. Vanwelde, Measure - mesures de performances réelles et de satisfaction des occupants dans les bâtiments résidentiels á hautes performances energétiques, intermediate report, 2016.
[73] N.M. Ramos, R.M. Almeida, A. Curado, P.F. Pereira, S. Manuel, J. Maia, Airtightness and ventilation in a mild climate country rehabilitated social housing buildings – what users want and what they get, Build. Environ. 92 (2015) 97–110, http://dx.doi.org/10.1016/j.buildenv.2015.04.016.
[74] A. Bakker, Introduction to CFD, Course of Computational Fluid Dynamics at Dartmouth College, 2006.
[75] C. Younes, C.A. Shdid, A methodology for 3-D multiphysics {CFD} simulation of air leakage in building envelopes, Energy Build. 65 (2013) 146–158, http://dx.doi.org/10.1016/j.enbuild.2013.05.050.
[76] L. Wang, Q. Chen, Validation of a coupled multizone-CFD program for building airflow and contaminant transport simulations, HVAC&R Res. 13 (2) (2007) 267–281.
[77] A. Skyles, An Introduction to Regression Analysis, Inaugural Coase Lecture at University of Chicago Law School, 1993.
[78] B. Kröse, P. van der Smagt, An Introduction to Neural Network, Lecture course at Université d'Avignon, 1996.
[79] H. Krstić, Ž. Koški, I.I. Otković, M. Španić, Application of neural networks in predicting airtightness of residential units, Energy Build. 84 (2014) 160–168, http://dx.doi.org/10.1016/j.enbuild.2014.08.007.
[80] H. Krstic, I.I. Otkovic, G. Todorovic, Validation of a model for predicting airtightness of residential units, Energy Proc. 78 (2015) 1525–1530, http://dx.doi.org/10.1016/j.egypro.2015.11.182.
[81] R.N. Dietz, R.W. Goodrich, E.A. Cote, R.F. Wieser, Detailed description and performance of a passive perfluorocarbon tracer system for building ventilation and air exchange measurements, in: Symposium on Measured Air Leakage Performances of Buildings, Brookhaven National Laboratory, 1985.
[82] M.S. Breen, B.D. Schultz, M.D. Sohn, T. Long, J. Langstaff, R. Williams, K. Isaacs, Q.Y. Meng, C. Stallings, L. Smith, A review of air exchange rate models for air pollution exposure assessments, J. Expo. Sci. Environ. Epidemiol. 24 (6) (2014) 555–563.
[83] S. BouwResearch, Luchtdicht bouwen-deel a: Ontwerpaanbevelingen, Stichting Bouwresearch, 2001.
[84] W.D. Gids, H. Cornelissen, P. Jong, Infiltratieverliezen u bouw, TNO Bouw en Ondergrond, Delft, 2010.
[85] M. Orme, M.W. Liddament, A. Wilson, Numerical data for air infiltration & natural ventilation calculations, Tech. Rep. 44, AIVC, 1998.
[86] D. Dickerhoff, D. Grimsrud, R. Lipschutz, Component leakage testing in residential buildings, in: Proceedings of the American Council for an Energy-Efficient Economy, 1982 Summer Study, Lawrence Berkeley National Laboratory, 1982.
[87] O.A. Hassan, An alternative method for evaluating the air tightness of building components, Build. Environ. 67 (2013) 82–86, http://dx.doi.org/10.1016/j.buildenv.2013.05.007.
[88] O.A. Hassan, Building Acoustics and Vibration, Theory and Practice, World Scientific, 2009.
[89] L.L. Beranek, I.L. Ver, Noise and Vibration Control Engineering: Principles and Applications, John Wiley & Sons, Inc., 1992, pp. 1.
[90] I. SàRL, Catalogue des ponts thermique, office fédéral de l'énergie, 2003.
[91] P.F. Pereira, R.M.S.F. Almeida, N.M.M. Ramos, Testing for building components contribution to airtightness assessment, 35th AIVC Conference: Ventilation and Airtightness in Transforming the Building Stock to High Performance (2014).

# Appendix B.

Prignon, M., Ossio, F., Altomonte, S., Dawans, A., and Van Moeseke, G. (2020). Airtightness performance of building components: meta-analysis of laboratory and in-situ measurements. Under review in Building and Environment.

# Airtightness performance of building components: meta-analysis of laboratory and in-situ measurements

**Abstract**

The scientific literature lacks comprehensive and updated information regarding the airtightness of building components, this hindering the development and improvement of models for a robust prediction of their performance. To fill this gap, this paper presents a meta-analysis conducted on literature studies reporting laboratory and in-situ measurements of airtightness for various building components. Meta-analysis is a powerful methodological tool to compare and combine data from previous research, even when they have inherent differences. The results of the meta-analysis allowed to attain three outcomes: a classification of building components related to their airtightness performance; the update and improvement of existing databases of building component airtightness; and, the identification of factors specifically influencing airtightness performances of windows. In addition, the critical appraisal of the findings led to the definition of the requirements for future studies reporting measurements of airtightness of building components. This study offers a step ahead from existing knowledge by improving existing databases and by proposing a methodological framework of analysis that can be extended to several other domains of the built environment.

**Keywords:** Building Components; Meta-analysis; Airtightness; Air infiltration; Measurements

## 1. Introduction

Building standards and regulations have made a significant impact in the field of airtightness because of the large influence that air infiltration has on energy demands [1]. Energy policies driven by these regulations considerably increase the number of airtightness tests that need to be performed on buildings and, as a consequence, the number of countries that have implemented qualification schemes for testers [2]. However, considerations related to airtightness should not be limited to energy consumption, since air infiltration also impacts smoke and fire propagation, indoor air quality, and the comfort and well-being of occupants [3]. These implications are largely influenced by the location and distribution of leakage around the building envelope, which is fundamentally associated to the measurement of airtightness at the level of individual components rather than for the whole building.

Various authors have highlighted substantial knowledge gaps in the airtightness performance of building components. Among others, Virtanen pointed out the difficulties, when modelling infiltration, to determine the actual leakage route inside built structures [4]. Liu and Nazaroff emphasised the lack of information regarding leakage characteristics of building components to reliably predict pollutant

penetration into buildings [5]. Younes and Shdid explained that the reliability of CFD analysis depends on the capability for the crack data to be a realistic representation that is applicable to the construction techniques and the materials used in practice [6]. Prignon and Van Moeseke stressed the large potential of single component models to predict building airtightness, provided that reliable and updated data are available for the airtightness performance of building components [7].

Currently, there are two databases that are commonly used to characterise building component airtightness: these are provided by ASHRAE [8] and AIVC [9]. These databases have been fed with data coming from studies performed until the early '90s. However, the large impact of new energy policies has made these databases less relevant in current construction practice due to their insufficient reliability for modelling infiltration and airtightness prediction. Consequently, there is an urgent need to update these databases, identifying the impact of individual components on building airtightness, re-computing their airtightness performance, and drawing conclusions based on previous and new studies.

Nevertheless, reviewing the appropriate literature should not be limited to listing relevant studies, and combined results should not be limited to calculation of simple mean averages. In fact, a thorough review of previous research data featuring direct measurements needs to be rigorous and based on solid and well-documented protocols. In addition to computing averages or variation among different components, it should also quantify and investigate the causes of such variation of component performance between studies (e.g., difference in the selected samples or in the experimental design).

Meta-analysis provides a set of tools that could answer the need for a rigorous protocol to compare and combine the results of previous research. A meta-analysis is a set of methods used to consolidate evidence (e.g., effect sizes) of different studies from the literature [10]. This type of analysis is often conducted in clinical research [11], but its application is still rather sparse in the domain of the built environment. This methodological approach could be used as a robust protocol to combine studies reporting measurements of building component airtightness or effects related to these measurements (e.g., the impact of different treatments of an identified leak). The same method could be transferred to the analysis of many other environmental parameters (e.g., indoor air quality, acoustic, lighting or thermal performance), factors influencing occupant comfort, or to compare the energy efficiency of different solutions and strategies in buildings.

In this study, we conduct a meta-analysis in order to compare and combine the results of various studies measuring airtightness of building components. The structure of the paper is as follows. In section 2, we illustrate the steps of a meta-analysis, including the criteria for study selection and the equations to obtain a combined mean, a combined standard deviation, and an inconsistency index (that is, the selected indicator for the variation between studies). In section 3, we provide two outcomes derived from the meta-analysis: a classification of building components related to their airtightness performance and the combined means, combined standard deviations, and index of inconsistency for specific building

components. In section 4, we appraise these outcomes and discuss their impacts to both building practice and research. This also includes a critical overview of the results of the meta-analysis, together with a discussion of their limitations with respect to the existing literature and the selected methodology. Guidelines are then drawn for future studies in order to improve the reliability of airtightness measurements, and the application of meta-analysis to other cognate domains of the built environment. Finally, in section 5, we summarise the outcomes of this study and illustrate the further research needed in the measurement of building component airtightness.

## 2. Methodology

A meta-analysis consists in the weighting of each evidence (e.g., the effect size) based on the reliability of the study: studies with high variability are expected to be less accurate and have less weight in the analysis [12]. Meta-analysis can also be used to combine *single group summaries* (e.g., mean, median, or standard deviation) rather than effect sizes [13]. This is important in this context, and more generally for research in the field of the built environment, since studies hardly report effect sizes. For airtightness of building components, studies reporting measurements commonly provide average leakage data for a given component rather than effect sizes. The role of a meta-analysis is to synthetize data, but also to look at the pattern of studies targeted by the research question [13]. For example, a powerful tool brought by the meta-analysis is the exploration of heterogeneity in the results (i.e., the reasons for variations between studies) [14]. This is important since it can help to investigate and understand the factors influencing the variation in results, which is crucial for their interpretation. For example, variations can be explained by a difference in the selected sample, in the countries where studies are conducted, or in the experimental design. A meta-analysis is made of three main steps: data acquisition; studies combination; and, exploration of heterogeneity. These are presented hereafter, with special focus given to their application in the field of building component airtightness.

### 2.1. Data acquisition

A meta-analysis aims at combining studies that respond to the same research question. It is, therefore, crucial to formulate an unambiguous research question based on which the relative literature can be reviewed. The protocol used to perform the literature review must be thoroughly described in order to be replicable (e.g., the research terms and platform used should be explicitly stated). Not all studies targeting the research question have to be necessarily included in the meta-analysis, since a badly conducted research can bias the combined effect [12]. However, for each study excluded from the meta-analysis, the reasons and criteria for the exclusion should be clearly stated.

Statistically, there is no restriction about the "required similarity" of studies to be combined in a meta-analysis [13]. However, the studies should be relevant for the defined research question and the results of the combination must be interpreted against the initial objectives. This is illustrated in this paper through section 3: initially, the result of a meta-analysis conducted on studies reporting the measurement of building component airtightness is presented, without looking at different possible treatments for the same component; then, the meta-analysis focuses on the case of windows, including different types of openings and various materials. Both meta-analyses are valid statistically, however interpretation of the results, and the contexts in which these would be relevant, are different.

Once all studies are selected, the outcome of interest must be extracted from each study. As previously explained, this can be effect size or simple group summary (e.g., mean, median, or standard deviation), but it must be consistent with the defined research question on which the systematic review is based. If the studies are addressing similar outcomes expressed in different ways, it is up to the researcher to decide if their combination is meaningful [13]. The selection of inclusion and exclusion criteria for a meta-analysis should be based on the field of research, the objective of the study, and previous research. Without prior knowledge to support decisions, this step can be difficult. Due to their large influence on the combined results, it is important to clearly state these criteria, to justify them, and to discuss their implications. The inclusion and exclusion criteria chosen for this study are presented in section 3.2.

## 2.2. Combined outcome

Once the outcome of each study is extracted, it must be weighted according to its reliability: high reliability studies have more importance in the combination than low-reliability studies. In meta-analysis, weighting can be based on fixed-effect and random-effect models. Fixed-effect models assume that the true outcome (which is unknown) is the same for all studies. If this assumption is implausible, a random-effect model should be used instead [15]. In the context of building component airtightness, studies are expected to be similar but not identical. The true outcome will vary among studies because of differences in experimental design or selected sample; hence random-effect models should be used.

In random-effect models, the number of studies combined can play a role in the precision of the results. When a small number of studies are combined, the estimate of the error and of result inconsistency (described later in this section) may have large uncertainty. However, there are no good alternatives and the results should be reported with a clear explanation of their limitations [13].

In random-effect models, there are two sources of error: within-study and between-study variations. Both must be considered in the weighting of studies and the observed variance must be decomposed in its two components [13]. A random-effect model is described with Equation 1where $T_i$, $\tau_i$ and $\varepsilon_i$ are

respectively the outcome, the within-study error, and the between-study error for the $i^{th}$ study, and $\mu$ is the true outcome, which is unknown.

*Equation 1*

$$T_i = \mu + \tau_i + \varepsilon_i$$

These two levels of error induce two steps for the weighting. The first step is the fixed-effect weighting ($w_i$) and is defined as the inverse of the total variance (combining within-study and between-study deviations). The second step, the random-effect weighting ($w_i^*$), is more complex to determine since it is the inverse of the sum of the within-study and between-study variance. It can be determined based on the following steps.

First, the total variance $Q$ is calculated based on Equation 2.

*Equation 2*

$$Q = \sum_{i=1}^{k} w_i T_i^2 - \frac{\left(\sum_{i=1}^{k} w_i T_i\right)^2}{\sum_{i=1}^{k} w_i}$$

Then, the between-study variance ($\tau^2$) is computed by Equation 3, where $df$ is the degree of freedom (number of studies $-1$) and $C$ a scaling factor (Equation 4) necessary because $Q$ is a weighted sum of squares [15].

*Equation 3*

$$\tau^2 = \begin{cases} \frac{(Q-df)}{C} & if\ Q > df \\ 0 & if\ Q \leq df \end{cases}$$

*Equation 4*

$$C = \sum_{i=1}^{k} w_i - \frac{\sum_{i=1}^{k} w_i^2}{\sum_{i=1}^{k} w_i}$$

Lastly, random weights are given by Equation 5

*Equation 5*

$$w_i^* = \frac{1}{\frac{1}{w_i} + \tau^2}$$

Once weights are computed for each study included in the meta-analysis, the combined outcome is simply the weighted mean (Equation 6) and its standard error is the square root of the variance, that is the inverse of the weights (Equation 7).

*Equation 6*

$$\overline{T} = \frac{\sum_{i=1}^{k} w_i^* T_i}{\sum_{i=1}^{k} w_i^*}$$

*Equation 7*

$$\mathrm{SE}(\bar{T}) = \sqrt{\frac{1}{\sum_{i=1}^{k} w_i^*}}$$

## 2.3. Exploring heterogeneity with subgroup meta-analysis

A statistical heterogeneity is observed when the variation between different studies is above the variation expected by chance. This can be explained by the characteristics of the tested samples, a variation in the treatments, in the execution of the experiment, or in the experimental design [14, 16]. In this context, the calculation of $I^2$, the index of inconsistency, is suggested. It is interpreted as the proportion of total variation that is due to the heterogeneity between studies (Equation 8) [14, 17].

*Equation 8*

$$I^2 = \begin{cases} \frac{Q-(k-1)}{Q} \text{ x } 100\% & \text{for } Q > (k-1) \\ 0 & \text{for } Q \leq (k-1) \end{cases}$$

The interpretation of $I^2$ depends on the field of study and should, therefore, be further investigated for airtightness of building components. Without prior knowledge, the interpretation of $I^2$ in this study has been based on the same values than those suggested for clinical research: 25%, 50% and 75% respectively for low, moderate, and high inconsistency [16]. Compared to clinical research, there are generally less standardised protocols in sample selection, experimental design, or statistical analysis of the results for data collected in fields related to building physics. As a consequence, a larger deviation between studies, and a larger $I^2$, is expected in this domain of research. Although this should be stressed when conducting and interpreting the results of a meta-analysis, deeper investigations should be conducted before defining new values for interpretation of $I^2$ in built environment studies.

One method to explore the heterogeneity derived from between-study variations consists in creating subgroups of studies (e.g., laboratory vs. field measurements) and comparing the heterogeneity of the subgroups with the heterogeneity of all studies [16].

# 3. Airtightness of building components

This section presents the results of the meta-analysis conducted to combine studies reporting measurements of airtightness of building components. The objective of this combination is to approach the “true” airtightness performance of components (i.e., the mean and the standard deviation of the whole population). As pointed out in the introduction, this can be very helpful for several applications such as infiltration modelling and airtightness prediction.

The relevant studies were identified based on the following keywords and their combinations: “airtightness”, “air infiltration”, “air leakage”, “air permeability”, “building components”, and “building elements”. These were used as search terms in the AIVC publication database [18], Sciencedirect and Google Scholar [19]. For each paper, the abstract and the result section were read to ensure that the study reported the measurements performed on building component airtightness, regardless of the specific methodology applied. In addition, specific research was conducted on papers mentioned in the AIVC [9] and ASHRAE [8] databases focusing on airtightness of building components. In total, 79 relevant studies reporting results of measurements performed between the mid-20’s and today were included in the review. These included journal papers, conference papers, and technical reports. These studies cover around 40 different building components and their treatments.

## 3.1. Classification of building components airtightness

The first result obtained from this analysis is a list of building components for which airtightness measurements were reported. This list was used to build a 4-level classification of building components related to the way air flows through and around them. This classification provides an overview of the building components that impact airtightness performance. Figure 1 illustrates these components and classifies them in three different types of flows (level 1 classification): partitions and surfaces, junctions between surfaces, and discontinuities.

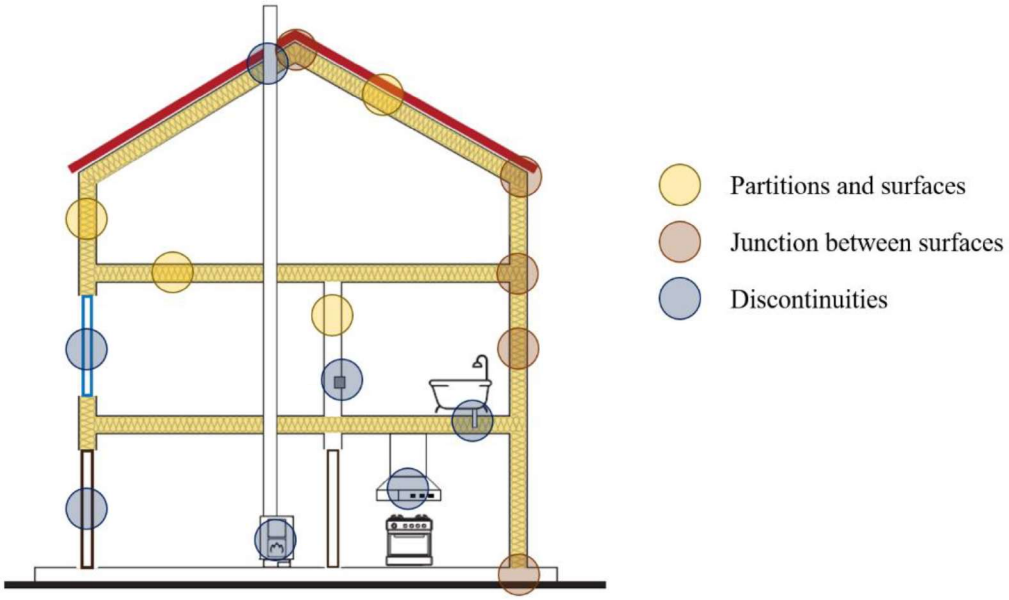



*Figure 1 – Illustration of the level 1 classification of building components regarding airtightness. Source: authors.*

Each type of flow is further divided in three additional levels: Category of components (level 2); Components (level 3); and, Type and treatment (level 4). Figure 2 shows the complete classification suggested on the basis of this study. The components underlined are those for which a sufficient number of studies could be included in the meta-analysis.

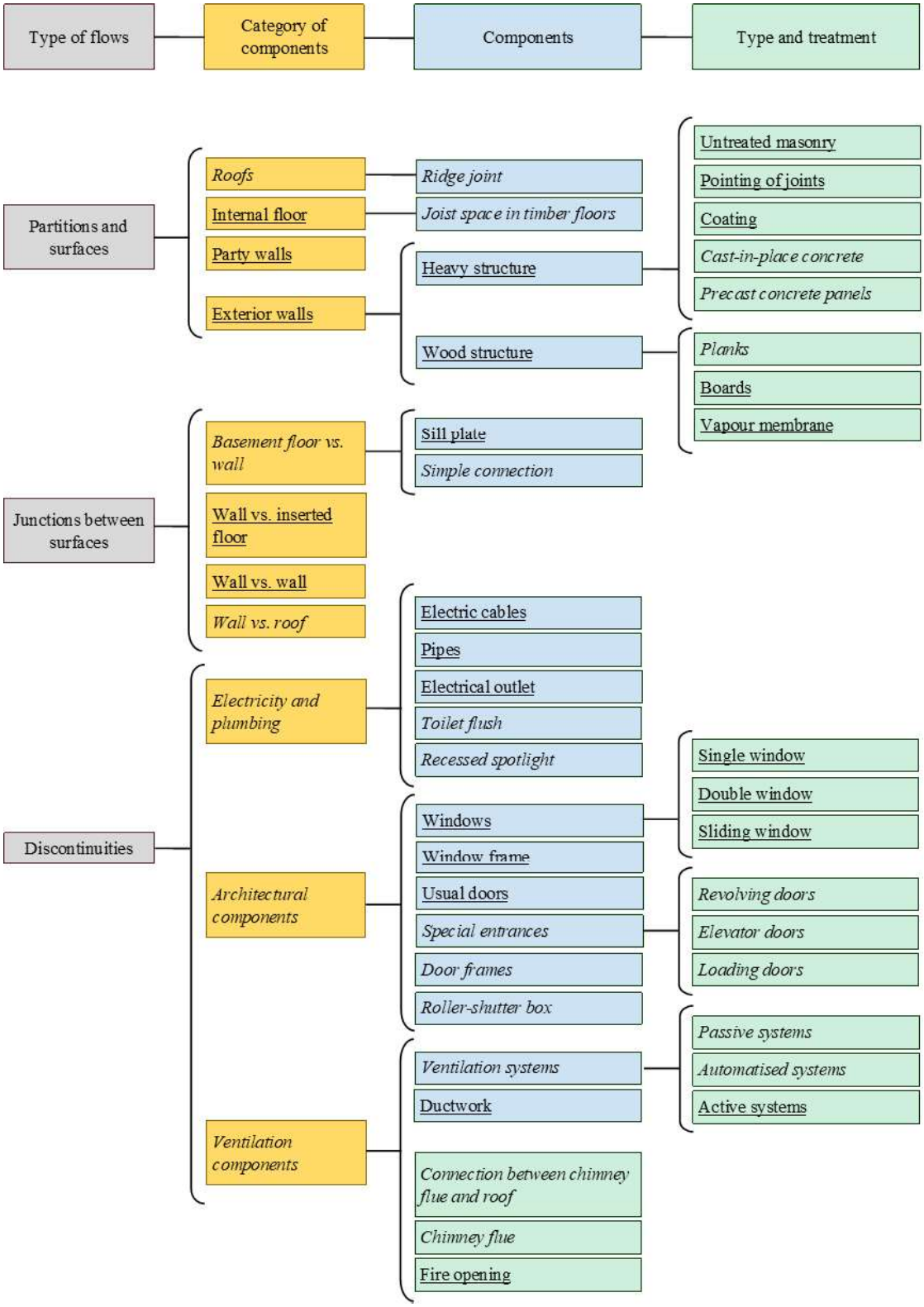



*Figure 2 – Four level classification of building components based on studies reporting airflow values. Source: authors.*

This classification is expected to expand and improve over the years as the data from new studies reporting measurements of airtightness of building components is included. This is further illustrated in the discussion section (section 4).

## 3.2. Airtightness performance of building components

Airtightness performance of building components can be expressed in many different units and metrics [20]. However, most can be translated into airflow at 50 Pa ($q_{50}$), which is largely used in regulations, practice, and research [2, 21]. This translation can be direct (i.e., change of units) or indirect (i.e., using the power-law relation), for which the leakage exponent ($n$) is needed.

In this analysis, when the metric used could not be directly translated to $q_{50}$, and $n$ was not reported in the study, a value of 0.65 was assumed [9, 22]. The meta-analysis aimed at determining combined mean, standard deviation, and index of inconsistency for both $q_{50}$ and $n$. When there was no information available to translate from one normalisation to another, the study was excluded from the meta-analysis. In addition, studies reporting only one measurement, or the mean of multiple measurements without providing information about standard deviation, were also excluded from the meta-analysis since they could not be weighted. Without previous knowledge on meta-analysis in the field of airtightness to support this decision, the choice was made to systematically include studies reporting measurements of airtightness performance if the following two criteria were met:

1) The study reports the outcome in normalised $q_{50}$, or in a different manner from which it can be calculated directly (i.e., change of unit), or using the power-law with or without an assumption about the leakage exponent.
2) It is possible to determine the standard deviation based on the results reported. This means that the measurements are conducted at least in two cases for each component and that, when all data are not available, standard deviation and mean can be computed from the information available.

Regarding the first condition, the normalisation of $q_{50}$ depends on the component. It is sometimes normalised per unit of length or surface. For components with different normalisation used in different studies (e.g., windows), the most frequently reported was selected for the meta-analysis. This was an arbitrary choice, because the reliability of the meta-analysis depends on the number of combined studies.

The meta-analysis was conducted for each building component that had at least two studies meeting the inclusion criteria. However, to provide a more exhaustive list of building components measured in previous research, the tables presenting the results also include the mean and standard deviation for

components that had only one study meeting the inclusion criteria. In these cases, $I^2$ cannot be computed since the meta-analysis could not be conducted.

Table 1 to Table 14 present the results of the meta-analysis conducted on different components according to the equations presented in section 2.2. These tables provide, for each variable (i.e., the airflow at 50 Pa, $q_{50}$, and the leakage exponent, $n$), the number of studies considered in the analysis (N), the combined mean ($\overline{q_{50}}$ and $\overline{n}$), the combined standard deviation (SE($\overline{q_{50}}$) and SE($\overline{n}$)), the inconsistency in the results $I^2$, and the reference studies used for the meta-analysis. The units used for $\overline{q_{50}}$ and SE($\overline{q_{50}}$) depend on the normalisation of the component.

### 3.2.1. Leakage through partitions and surfaces

Table 1 presents the results of the meta-analysis performed on roofs, internal floors, party walls and exterior walls. Three studies were excluded from the meta-analysis since they reported only one single measurement [23-26].

| Type of partition | $q_{50}$ | | | | $n$ | | | | References |
|---|---|---|---|---|---|---|---|---|---|
| | N | $\overline{q_{50}}$ | SE($\overline{q_{50}}$) | $I^2$ (%) | N | $\overline{n}$ | SE($\overline{n}$) | $I^2$ (%) | |
| Roof | 1 | 95.8 | 55.4 | - | 1 | 0.63 | 0.18 | - | [27] |
| Internal Floor | 3 | 1.4 | 1.5 | 36.7 | 1 | 0.59 | 0.10 | - | [28-30] |
| Party wall | 2 | 2.9 | 0.6 | 0.0 | - | - | - | - | [29, 31] |
| Exterior wall | 11 | 1.6 | 0.5 | 88.6 | 5 | 0.76 | 0.06 | 29.6 | [28, 29, 31-38] |

*Table 1 – mean, standard error and inconsistency for airflows at 50 Pa (in m³/(h.m²)) and leakage exponent calculated through the meta-analysis of studies measuring leakage by partition.*

The high mean air leakage through the roof (95.82 m³/(h.m²)) was expected since the study refers to tile roofs only, with nothing to prevent air leakage between tiles [27]. Similar performance is found on internal floors (1.4 m³/(h.m²)) and exterior walls (1.6 m³/(h.m²)) but with different standard deviation (1.5 m³/(h.m²) on internal floors and 0.5 m³/(h.m²) on exterior walls). Party walls are found to be leakier (2.9 m³/h) than exterior walls, probably due to less attention paid in construction practice. This is because party walls have a lower impact on energy consumption than exterior walls and will often have no impact on the results of fan pressurization measurements. The leakage exponent is found to be lower than the average building exponent (0.65) for roofs (0.63) and internal floors (0.59), but it is higher for exterior walls (0.76).

The large inconsistency between studies focusing on exterior walls (88.6%) was expected because many different types of leakage are measured on exterior walls and different studies probably investigated different airflows. In addition, results are expected to strongly vary between construction types (heavyweight vs. timber construction) and measurement methods (laboratory vs. in-situ measurements).

Joist spaces in timber floors and ridge joints are studied in [39] and [40], respectively. These components should be a subsection of the internal floors and roofs categories, but since both studies reported only one measurement, they were excluded from the meta-analysis.

Table 1Table 2 presents the results of the meta-analyses performed on external wall surfaces for heavyweight structures (untreated masonry, masonry with pointing of the joints, masonry with coating, cast-in-place concrete, and precast concrete panels) and timber-frame structures (boards, planks and vapour membrane). In total, six studies were excluded from the meta-analysis because only one measurement was performed [25, 34, 39, 41-43].

| Type of surface | $q_{50}$ | | | | $n$ | | | | References |
|---|---|---|---|---|---|---|---|---|---|
| | N | $\overline{q_{50}}$ | SE($\overline{q_{50}}$) | $I^2$ (%) | N | $\overline{n}$ | $SE(\overline{n})$ | $I^2$ (%) | |
| Untreated masonry | 5 | 11.3 | 5.8 | 93.3 | 5 | 0.78 | 0.04 | 82.2 | [44-48] |
| Pointing joints | 2 | 1.0 | 0.7 | 0.0 | 1 | 0.81 | 0.10 | - | [46, 49] |
| Coating | 6 | 0.1 | 0.1 | 15.7 | 4 | 0.94 | 0.07 | 70.2 | [36, 44, 46-49] |
| Cast-in-place concrete | 1 | 2.4 | 2.4 | - | 1 | 0.61 | 0.14 | - | [32] |
| Precast concrete panels | 1 | 1.4 | 0.5 | - | 1 | 0.68 | 0.18 | - | [25] |
| Boards | 6 | 0.0 | 0.0 | 31.6 | 3 | 0.98 | 0.01 | 15.1 | [49-53] |
| Planks | 1 | 16.9 | 15.4 | - | 1 | 0.76 | 0.08 | - | [53] |
| Vapour membrane | 2 | 0.1 | 0.1 | 0.0 | 2 | 0.76 | 0.08 | 0.0 | [53, 54] |

*Table 2 – mean, standard error and inconsistency for airflows at 50 Pa (in m³/(h.m²)) and leakage exponent calculated through the meta-analysis of studies measuring leakage through external wall surfaces.*

Untreated masonry reached high airflow values (11.3 m³/(h.m²)), which can be substantially reduced by pointing the joints (1.0 m³/(h.m²)) and by coating one or both sides of the wall (0.1 m³/(h.m²)). Cast-in-place concrete and precast concrete panels showed higher leakage than expected (2.4 m³/(h.m²) and 1.4 m³/(h.m²)), but these also showed large standard deviation (2.4 m³/(h.m²) and 0.5 m³/(h.m²)), which implies a large 95% confidence interval for the mean value. Leakage exponents for heavy constructions were found to be higher than the buildings mean value. This was expected, since air flows through surface are a mixture of air flowing through cracks and air flowing through the material itself, which is characterized by an airflow assumed as fully laminar (flow exponent of 1.0) [55]. This becomes especially evident when coating is added, since it covers the cracks in masonry joints.

A large heterogeneity was found in untreated masonry (93.3%), which can possibly be explained by the differences in the type of masonry (e.g., clay-brick or hollow concrete block), the wall thickness, and workmanship quality.

Timber structures can be divided into two different behaviours: boards and planks. On one hand, boards – which include fibreboard, particle board, plywood, OSB panels and asphalt impregnated fibreboards – have a mean airflow at 50 Pa below 0.1 m³/(h.m²) with a standard deviation of 0.1 m³/(h.m²). On the other hand, planks showed much higher leakage (16.4 m³/(h.m²)) and standard deviation (15.4 m³/(h.m²)). A large difference was also observed in mean leakage exponents (0.98 on boards and 0.76

on planks). These differences suggest that air mostly leaks through the material rather than through board cracks, but also through the space between plank elements. However, a study [53] showed that adding a gypsum board to plank walls made them as efficient as board walls.

With respect to board walls, junctions between boards and faults of the board itself can lead to large leakage. Table 3 shows the results of two studies that focused on these faults [52, 56]. These could not be combined because of the different fault types that were studied. Table 3 reports therefore the results of individual studies.

| Type of defect | $\overline{q_{50}}$ | SE($\overline{q_{50}}$) | References |
|---|---|---|---|
| Tongue and groove joint (m³/(h.m)) | 1.4 | 1.6 | [52] |
| Double-board corner joint (m³/(h.m)) | 6.7 | 9.5 | [52] |
| Triple-board corner joint (m³/h) | 3.7 | 3.1 | [56] |
| Hole in gypsum boards (between 5 and 55 mm of diameter) (m³/h) | 12.4 | 7.3 | [56] |
| Space between boards (between 0.5 and 2.5 mm) (m³/(h.m)) | 4.1 | 4.3 | [56] |

*Table 3 – Mean and standard deviation of defects in boards reported by Hall and Hauser [56] and Langmans et al. [52].*

In timber constructions, vapour membranes are often used to avoid condensation and hygrothermal issues with the insulation. These membranes are found to have good airtightness performance (Table 2 – 0.1 m³/(h.m²)) and can therefore compensate eventual faults on the boards. Two studies went further and looked into how the installation, or a defect in the vapour membrane (either in the membrane itself or at the connection between two parts of the membrane), can affect its performance at 50 Pa [56, 57]. As in Table 3, Table 4 reports the results from individual studies.

| Type of defect | $\overline{q_{50}}$ | SE($\overline{q_{50}}$) | References |
|---|---|---|---|
| Screws (m³/(h.screw)) | 0.1 | 0.1 | [57] |
| Staples (m³/(h.staple)) | 0.2 | 0.2 | [56] |
| Loose clamped joint (m³/(h.m)) | 0.1 | 0.2 | [57] |
| Missing tape at vapour connection (m³/h) | 0.7 | 0.3 | [56] |
| Cut in the foil (m³/(h.m)) | 2.2 | 0.9 | [56] |
| Hole in the foil (m³/h) | 4.5 | 3.8 | [56] |

*Table 4 – Mean and standard deviation for defects in vapour membrane reported by Hall and Hauser [56] and Gullbrekken [57].*

Although Table 3 and Table 4 do not present new values obtained from meta-analysis, reporting them here allows to compare these results with those featured in Table 2.

### 3.2.2. Leakage through junctions between surfaces

Table 1Table 5 presents the results of the meta-analysis performed on the following junctions: basement floor vs. wall, wall vs. internal floor, and wall vs. wall. Wall vs. roof junctions were not reported in this table since all studies reported only one measurement and were therefore excluded from the meta-

analysis [40, 52, 56, 58]. With respect to other junctions, seven studies were excluded because only one measurement was performed [23, 56, 59-63]. Study [62] measures typical construction joints including, without distinction, junctions between metal panels, wall to ceiling/floor, and wall to wall. This study was excluded from the analysis since it did not focus on one specific component. Airflow through window-wall or door-wall connections (i.e., window-frames and door-frames) are featured in the "discontinuity" category and are investigated in following section.

| Type of surface | $q_{50}$ | | | | $n$ | | | | References |
|---|---|---|---|---|---|---|---|---|---|
| | N | $\overline{q_{50}}$ | SE($\overline{q_{50}}$ | $I^2$ (%) | N | $\overline{n}$ | $SE(\overline{n})$ | $I^2$ (%) | |
| Basement floor vs wall, sill plate (BF/W) | 4 | 0.2 | 0.0 | 0.0 | 2 | 0.69 | 0.17 | 95.2 | [26, 40, 64, 65] |
| Basement floor vs. wall, simple connection (BF/W) | 1 | 17.9 | 25.0 | - | 1 | 0.71 | 0.20 | - | [66] |
| Wall vs. internal floor (W/IF) | 2 | 1.2 | 0.8 | 0.0 | 1 | 0.78 | 0.03 | - | [40, 67] |
| Wall vs. wall | 2 | 0.5 | 0.1 | 0.0 | 1 | 0.71 | 0.09 | - | [26, 40] |

*Table 5 – Mean, standard error and inconsistency for airflows at 50 Pa (in m³/(h.m)) and leakage exponent calculated through the meta-analysis of studies measuring leakage through junctions between surfaces.*

Junctions between surfaces can account for large airflows, especially basement floor vs. wall for simple connection detail (17.9 m³/(h.m)) and wall vs. internal floor (1.2 m³/(h.m)). However, when the detail of the basement floor vs. wall junction includes a sill plate, it subsequently reduces airflows (0.2 m³/(h.m)). Regarding the leakage exponents, these stand between 0.69 and 0.78, which is a higher value than the mean leakage exponent.

The large heterogeneity found in the leakage exponent in basement floor vs. wall junctions (95.2 %) can be explained by the fact that both studies investigating leakage exponents [26, 64] focused on different treatments of the sill plate detail, which potentially leads to different flow regimes and, therefore, to different flow exponents.

### 3.2.3. Leakage through discontinuities in the air barrier

This section focuses on the purpose-provided openings applied to the air barrier during the construction process. These can entail partial penetration in the wall (e.g., electrical outlets) or total penetration of the wall (e.g., pipes, doors or windows) and induce intentional (e.g., ventilation systems) or adventitious airflows. These discontinuities to the air barrier are subdivided in 3 types: electricity and plumbing; ventilation; and, architectural components.

#### 3.2.3.1. Electricity and plumbing

Table 6 presents the results of the meta-analyses performed on the following electricity and plumbing components: electric cables (below 20 mm of circumference), electrical outlets, and pipes (more than

130 mm of circumference). Two studies on pipes were excluded: one because it reported only one measurement [68], and one because it measured the pipe penetration and the bath enclosure at once [58]. A study on electrical outlets [60] was excluded because it provided the mean of 65 tests, without information about the standard deviation of the results. Studies [69] and [68] were excluded because results were reported in total leakage per house and not per electrical outlet. In addition, 6 results in study [70] were not considered since they measured airflow through part of a ventilated wall, including an electrical outlet, with an external vapour membrane. Therefore, the measured airflow was related to the leakage through the wall including the electrical outlet, rather than through the electrical outlet itself. Lastly, study [26] reported only one measurement of bathtub vs exterior wall connection ($q_{50} = 4.3$ m³/(h.m) and $n = 0.74$)and, therefore, had to be excluded from the meta-analysis.

| **Type of surface** | $q_{50}$ | | | | $n$ | | | | **References** |
|---|---|---|---|---|---|---|---|---|---|
| | N | $\overline{q_{50}}$ | $SE(\overline{q_{50}})$ | $I^2$ (%) | N | $\overline{n}$ | $SE(\overline{n})$ | $I^2$ (%) | |
| Electric cable | 2 | 0.1 | 0.1 | 96.4 | - | - | - | - | [43, 56] |
| Pipes | 3 | 1.6 | 1.1 | 0.0 | 1 | 0.66 | 0.08 | - | [26, 43, 56] |
| Electrical outlet | 4 | 2.7 | 0.9 | 0.0 | 1 | 0.69 | 0.13 | - | [26, 56, 70, 71] |
| Toilet flush | 1 | 21.0 | 5.9 | - | - | - | - | - | [56] |
| Recessed spotlight | 1 | 10.6 | 13.3 | - | - | - | - | - | [56] |

*Table 6 – Mean, standard error and inconsistency for airflows at 50 Pa (in m³/h) and leakage exponent calculated through the meta-analysis of studies measuring leakage through electricity and plumbing components.*

These results highlighted a good sealing performance of the electrical outlets and pipe penetrations since these can induce large airflows (1.6 m³/h and 2.8 m³/h respectively) and are often found in buildings. However, these results are expected to vary as a function of the wall type. In addition to the type of wall, the standard deviation observed on pipes (1.1 m³/h) can be explained by the variation in diameters, especially when it is not properly sealed [43], and by differences in sealing methods. Toilet flush and recessed spotlight showed large airflows, but their relevance depends on their location in the building and the possible presence of a second air barrier behind them. For example, recessed spotlights are often penetrations through the false ceiling, but the air leakage can, in this instance, be stopped by the ceiling or by the internal floor.

The large inconsistency (96.4 %) among studies reporting measurements performed on electric cables can be explained by their experimental design. . One study reported the measurement of the penetration through a board [43] and the other through a foil [56], which can tear around the penetration in case of large deformations.

#### 3.2.3.2. Ventilation

Ventilation components should not be considered in the same manner as other building components since they do not intend to be airtight when in use. In fact, they induce or extract air intentionally to provide proper ventilation. These components are still interesting since they highly impact the building's global airtightness. This section divides them in three types of components: ventilation systems; ductworks; and, chimneys.

*Ventilation systems*

Ventilation can be obtained through passive (e.g., ventilation grilles or ridge), automatised (e.g., self-regulated or humidity-sensitive grilles), or active (e.g., exhaust fans) systems.

For passive systems, the airflow induced depends on the size of the opening and the need for ventilation. All the values reported for this component came from single-measurement studies and were, therefore, not included in the results [56, 62, 72, 73]. However, it is of interest to mention that one study found that even though window ventilation grilles were closed, they still induced air leakage [72].

Table 7 reports the results of studies on automatized and active ventilation systems. Results from [72] about self-regulated grilles were excluded from the meta-analysis since only one measurement was reported. For active systems (i.e., extractors in Table 7), one study reported only one measurement and it was excluded from the meta-analysis [56].

| Type of ventilation system | $q_{50}$ | | | | $n$ | | | | References |
|---|---|---|---|---|---|---|---|---|---|
| | N | $\overline{q_{50}}$ | SE($\overline{q_{50}}$) | $I^2$ (%) | N | $\overline{n}$ | $SE(\overline{n})$ | $I^2$ (%) | |
| Humidity-sensitive grilles | 1 | 61.4 | 39.2 | - | 1 | 0.58 | 0.11 | - | [72] |
| Self-regulated grilles | 1 | 37.0 | 0.4 | - | - | - | - | - | [74] |
| Extractors with damper close | 1 | 11.5 | 5.8 | - | - | - | - | - | [69] |
| Extractors with damper open | 3 | 52.3 | 14.0 | 0.0 | - | - | - | - | [69, 75] |
| Junctions between the fan and the wall | 1 | 9.6 | 11.4 | - | - | - | - | - | [71] |

*Table 7 – Mean, standard error and inconsistency for airflows at 50 Pa (in m³/h) and leakage exponent calculated through the meta-analysis of studies measuring leakage through ventilation systems.*

Automatised systems are an alternative to passive systems with an opening varying as a function of the pressure difference (self-regulated) and relative humidity (humidity-sensitive). The leakage of automatised systems was found to be lower than those of open passive systems (61.4 for humidity-sensitive and 37.0 m³/h self-regulated). The large standard deviation in humidity-sensitive grilles can be explained by the variation of the opening with the relative humidity of the building: measurements were conducted with different relative humidity [72]. For self-regulated grilles, the leakage exponent was not constant during a fan pressurisation test since the flow regime, and therefore the leakage exponent, may vary with the pressure difference. This is also expected in humidity-sensitive grilles if the building's humidity varies during the test.

Even when switched off, active systems can induce large airflows (52.3 m³/h) when a pressure difference of 50 Pa is applied on both sides. However, these systems are often used with a damper to improve airtightness performance, resulting in a substantial decrease of leakage (11.5 m³/h). In addition to leakage through the extractor, its junction with the wall or the false ceiling is also found to be responsible for air infiltration (9.6 m³/h). However, large standard deviations were observed for that component (11.4 m³/h).

*Ductwork*

As for other building components, poor ductwork airtightness induces an increase of heating and cooling demands. In addition, the fan must compensate for any leakage through the duct system in order to supply enough airflow in different rooms, which has an impact on fan energy use and noise [76, 77]. This explains the recent increasing concerns about ductwork airtightness and why some countries consider including their performance in energy regulations [78]. Ductwork performance can be divided in four classes according to the European standard [79]. Table 8 provides an overview of the air leakage limit for each class, as well as its corresponding value in airflow at 50 Pa per hour to remain consistent with this analysis.

| **Ductwork class** | $f_{max}$ | $q_{50,max}$ |
|---|---|---|
| Class A | $0.027 * \Delta p^{0.65} * 10^{-3}$ | 1.24 |
| Class B | $0.009 * \Delta p^{0.65} * 10^{-3}$ | 0.41 |
| Class C | $0.003 * \Delta p^{0.65} * 10^{-3}$ | 0.14 |
| Class D | $0.001 * \Delta p^{0.65} * 10^{-3}$ | 0.05 |

*Table 8 – Air leakage limit in m³/(s.m²) and in airflow at 50 Pa (m³/(h.m²) for each class of ductwork according to the European standard. Table adapted from [79].*

In fact, the meta-analysis included only two studies that report ductwork measurements by m³/(h.m²) [80, 81]. A large study (more than 1200 measurements) was excluded since it expressed the results as a percentage of measured ductwork in each class [82], two studies were excluded since they expressed the results in total leakage (m³/h) rather than per ductwork square meter [69, 83], and one study was excluded since it reported only one measurement [60]. Since the same number of studies reported the results in m³/(h.m²) and in m³/h, and in m³/(h.m²), this criterion was selected for the reported result to remain consistent with the European standard [79]. The meta-analysis on both studies selected showed a mean airflow of 0.8 m³/(h.m²), a standard deviation of 0.9 m³/(h.m²), and an inconsistency in results of 0.0 %. Regarding the leakage exponent, the analysis resulted in a mean value of 0.59, a standard deviation of 0.04, and an inconsistency of 0.0%.

Both studies reported field measurements, but a large inconsistency would have been expected for a meta-analysis combining in-situ and laboratory measurements since the absence of joints in some elements of the ductwork is often observed *in-situ* [84]. In addition, ductwork often does not reach the

expected performance once installed on site since some joints might be missing [82]. This highlights the need for *in-situ* measurements of ductwork airtightness.

*Chimneys*

Study [85] showed that the airtightness performance of chimneys should be divided in three types of airflows: airflow 1 at the connection between the chimney flue and roof; airflow 2 through the chimney flue; and, airflow 3 at the opening itself. These are schematised in Figure 3.

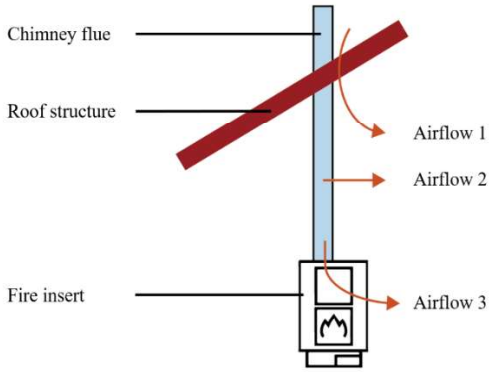



*Figure 3 – Types of airflows encountered in chimneys. Sources: authors.*

Table 9 presents the results of the analysis conducted on the three different types of airflows in chimneys. Three studies were excluded because they reported only one measurement [58, 60, 86].

| **Type of airflows** | $q_{50}$ | | | | $n$ | | | | **References** |
|---|---|---|---|---|---|---|---|---|---|
| | N | $\overline{q_{50}}$ | SE($\overline{q_{50}}$) | $I^2$ (%) | N | $\overline{n}$ | $SE(\overline{n})$ | $I^2$ (%) | |
| Connection with roof | 1 | 37.2 | 108.5 | - | 1 | 0.81 | 0.16 | - | [85] |
| Connection with roof + chimney flue | 1 | 35.3 | 42.5 | - | 1 | 0.78 | 0.13 | - | [87] |
| Chimney flue | 1 | 14.1 | 16.8 | - | 1 | 0.72 | 0.06 | - | [85] |
| Fire opening | 3 | 141.9 | 57.8 | 95.6 | - | - | - | - | [56, 69, 75] |

*Table 9 – Mean, standard error and inconsistency for airflows at 50 Pa (in m³/h) and leakage exponent calculated through the meta-analysis of studies measuring leakage through chimneys.*

Chimneys were found to be very leaky, whatever the airflow considered. All these airflows showed large standard deviation, especially airflow 1. This is due to the difference between the untreated detail (345.9 m³/h) and treated detail (mean of 8 reported results is 3.3 m³/h), which are both considered in the calculation of the standard deviation. In the case of airflow 3, one of the studies found surprisingly low standard deviation (1.4 m³/h [56]) compared to others (23.1 [75] and 45.7 m³/h [69]), which explains the large inconsistency between results (95.6 %). Since this standard deviation was calculated from only two measurements, it showed a large uncertainty [88] that in turn resulted in large uncertainty for $I^2$ and SE($\overline{q_{50}}$) when combining studies. Another reason that can possibly explain this large inconsistency

among studies is the difference in measurement methods (*in situ* vs. laboratory) and the differences in sample characteristics (e.g., presence of dampers and fire inserts).

Values of leakage exponents were found to be higher than average (0.81, 0.78 and 0.72 for airflows 1, 1+2 and 2). No study investigated the leakage exponent of airflow 3, which is expected to be close to 0.5 because of the large opening (the flow regime is more likely turbulent), especially with an open damper and no insert.

#### 3.2.3.3. Architectural components

Table 10 presents the results of the meta-analyses performed on windows, window frames, and doors. Six studies were excluded for windows [62], window-frame [58, 63, 68, 89], and doors [68]. Two studies were excluded for roller-shutters [68, 74] because they reported only one measurement. This resulted in only study meeting the inclusion criteria, therefore preventing the meta-analysis. In addition to this, four studies focusing on windows were excluded because results were expressed per square meter of window area [90, 91] or per window [58, 92] rather than per opening length.

| Type of architectural component | $q_{50}$ | | | | $n$ | | | | References |
|---|---|---|---|---|---|---|---|---|---|
| | N | $\overline{q_{50}}$ | SE($\overline{q_{50}}$) | $I^2$ (%) | N | $\overline{n}$ | $SE(\overline{n})$ | $I^2$ (%) | |
| Windows | 12 | 2.0 | 0.6 | 36.3 | 3 | 0.69 | 0.07 | 52.0 | [30, 56, 71, 74, 93-100] |
| Window frame | 4 | 0.3 | 0.2 | 81.0 | - | - | - | - | [39, 40, 101, 102] |
| Roller-shutter box | 1 | 6.0 | 1.4 | - | - | - | - | - | [56] |
| Doors | 8 | 137.6 | 46.7 | 87.3 | 3 | 0.62 | 0.16 | 0.0 | [30, 56, 58, 60, 74, 75, 92, 99] |
| Elevator door | 1 | 1049.6 | 156.7 | - | 1 | 0.59 | 0.12 | - | [32] |
| Revolving door | 1 | 1908.0 | 1294.2 | - | 1 | 0.71 | 0.04 | - | [103] |

*Table 10 – Mean, standard error and inconsistency for airflows at 50 Pa (in m³/(h.m) for windows and window frames and in m³/h for doors) and leakage exponents calculated through the meta-analysis of studies measuring leakage through architectural components.*

*Windows and window frames*

There are numerous windows in buildings, which make this component very important for achieving the building's airtightness requirements. The mean value (2.0 m³/(h.m)) appeared to be large compared to what would be acceptable for new constructions today. The leakage exponent was found to be close to the mean observed in buildings. This component is further investigated via subgroup meta-analysis in section 3.2.3.4.

Another type of leakage related to window elements is the connection of the window with walls, generally referred to as window frame. This leakage was found to be of lower importance than the air leakage through the windows themselves (0.3 m³/(h.m)). One possible reason of the large inconsistency between these results (81.0 %) could be represented by variations in junction treatments, type of window, material and wall type.

Roller-shutter boxes also showed large leakage (6.0 m³/h), but the variation among results was lower than expected (1.4 m³/h). Larger variation was anticipated since the performance can strongly change depending on the model. The study reported in Table 10 measured only 2 cases focusing on airtight models of roller-shutters, while other studies, which were excluded, reported results of different models (10.2 and 517.4 m³/h). Further investigation of roller-shutter boxes should be performed in order to characterise the airtightness performance of these components.

*Doors and door frames*

Usually, there are few doors around the measured volume of a building, but these are responsible for large leakage (137.6 m³/h). In this meta-analysis, no distinction was made between internal doors, external doors, sliding glass doors, and trap doors (e.g., doors providing access to an attic or crawl space), which are expected to have different airflows because of different sizes and treatments. This is a possible explanation of the large standard deviation of air leakage (46.7 m³/h) and the large inconsistency (87.3%) between results (induced by the sample characteristics). In addition, these studies combined different testing methods, including laboratory and *in-situ* measurements. For doors, the leakage exponent (0.62) was slightly below the mean in buildings.

There are three types of doors that were considered differently because of their function: revolving doors (1908.0 m³/h), elevator doors (1049.6 m³/h), and sectional doors (one study with one measurement obtaining a value of 9504.0 m³/h [73]). These doors were found to be much leakier and should be positioned in a location where they do not entail pollutant penetration, discomfort, or increased energy demands, or they should be carefully treated to substantially improve their performance. However, all these values were based on single study analyses.

No study investigated directly door frames, but these were considered in many "combined studies" as explained hereafter.

*Combined studies*

Many studies report architectural components mixed with other components; these have been categorised as "combined studies". Among these, four were excluded from the door + window frame [52, 61, 75, 89] and one from windows + doors [23] due to a single measurement. In the case of windows + doors, one study was excluded because the results were reported in total leakage for one house rather than per crack meter [30]. Table 11 presents the results of the meta-analysis and single relevant studies performed on windows + window frames, window frames + door frames, and windows + doors.

| **Type of architectural component** | $q_{50}$ | | | | $n$ | | | | **References** |
|---|---|---|---|---|---|---|---|---|---|
| | N | $\overline{q_{50}}$ | SE($\overline{q_{50}}$) | $I^2$ (%) | N | $\overline{n}$ | $SE(\overline{n})$ | $I^2$ (%) | |
| Windows + window frame | 2 | 4.3 | 2.6 | 0.0 | - | - | - | - | [56, 63] |
| Window + door frame | 1 | 0.0 | 0.0 | - | - | - | - | - | [104] |
| Windows + doors | 1 | 8.1 | 8.9 | - | - | - | - | - | [58] |

*Table 11 – mean, standard error and inconsistency for airflows at 50 Pa and leakage exponent calculated through the meta-analysis of "combined studies" of architectural components.*

Two studies performed in-situ tests using direct technique on the window and the window-wall junction at once (7.8 m³/h) [56, 63]. One study looked at typical window frames and door frames joints treated with PUR (Polyurethane rigid foam) in timber structures (0.0 m³/(h.m)) [104]. Lastly, one study reported results without making a distinction between windows and doors (8.1 m³/(h.m)) [58]. The results obtained were of the same order of magnitude than the results observed in the other un-combined studies presented in this section.

#### 3.2.3.4. Exploring heterogeneity of windows airtightness

Windows represent the most studied and reported architectural element, with larger samples than for other components. This is due to multiple reasons: the standards of laboratory measurement of windows [105, 106]; the large impact of windows on airtightness; and, the ease to measure window airtightness on site compared to other building components. The higher number of studies available makes it possible to investigate more in depth heterogeneity among studies and variables influencing window airtightness.

Table 12 provides details about the studies used in the meta-analysis on windows. For each study, the table provides the authors, the year of publication, the size of the sample (N), the type of measurement performed (i.e., laboratory or *in-situ*), the material (timber, aluminium, or unspecified materials) and the type of windows measured (double window, single window, sliding window, or unspecified type).

| Ref | Author(s) | Year | N | Type of measurement | T | A | Um | DW | SW | SL | Ut |
|---|---|---|---|---|---|---|---|---|---|---|---|
| [30] | Tamura | 1975 | 17 | In-situ | x | | | x | x | x | |
| [93] | Lowinski | 1979 | 6 | Laboratory | x | | | x | x | | |
| [94] | Almeida et al. | 2017 | 23 | In-situ | x | x | | x | x | x | |
| [95] | Weidt et al. | 1979 | 192 | In-situ | x | x | | x | x | x | |
| [96] | Larson et al. | 1930 | 14 | Laboratory | x | | | x | | x | |
| [97] | Van den Bossche and Janssens | 2016 | 437 | Laboratory | | | x | x | x | x | |
| [98] | Carruthers and Newman | 1977 | 131 | Laboratory | x | | | | x | | |
| [74] | Pinto et al. | 2011 | 3 | In-situ | | | x | | | x | |
| [99] | Ward and Sharples | 1982 | 10 | In-situ | | | x | | | x | |
| [56] | Hall and Hauser | 2003 | 10 | Laboratory | x | | | | x | | |
| [100] | Persily and Grot | 1984 | 18 | In-situ | | | x | | | | x |
| [71] | CMHC | 1991 | 6 | Laboratory | | | x | | | | x |

*Table 12 – List of publication used for the meta-analysis on windows, including the authors, the year, the sample size (N), the type of measurement, the material (T= Timber, A = Aluminium and Um = Unspecified material) and the type (DW = Double window, SW = Single window, SL = Sliding window and Ut = Unspecified type) of window measured.*

Figure 4 illustrates the results of the meta-analysis conducted on these 12 studies. Black lines represent the 95% confidence interval ($\overline{q_{50}} \pm 2 * \mathrm{SE}(\overline{q_{50}})$) around the mean value ($\overline{q_{50}}$, black dot). The last line

(in blue) represents the total 95% confidence interval, while the red dashed line indicates the mean value for the combined results.

This figure shows that the combined mean value (2.0 m³/(h.m)) falls outside the 95% confidence interval for one study [71]. The reason for the low mean leakage and standard deviation of [71] is probably due to the sample characteristics. In fact, study [71] tested only inoperable windows, while other studies looked at different types of operable windows. This hypothesis is strengthened by the inconsistency index ($I^2$) obtained from the meta-analysis conducted without this study ($\overline{q_{50}} = 2.5$m³/(h.m), SE($\overline{q_{50}}$) = 0.5m³/(h.m) and $I^2 = 0.0\%$). Therefore, the following investigations are conducted on the pool of 11 studies. In addition, two studies found much higher mean values [94, 99] but these are less weighted in the combination since their standard deviation was higher.

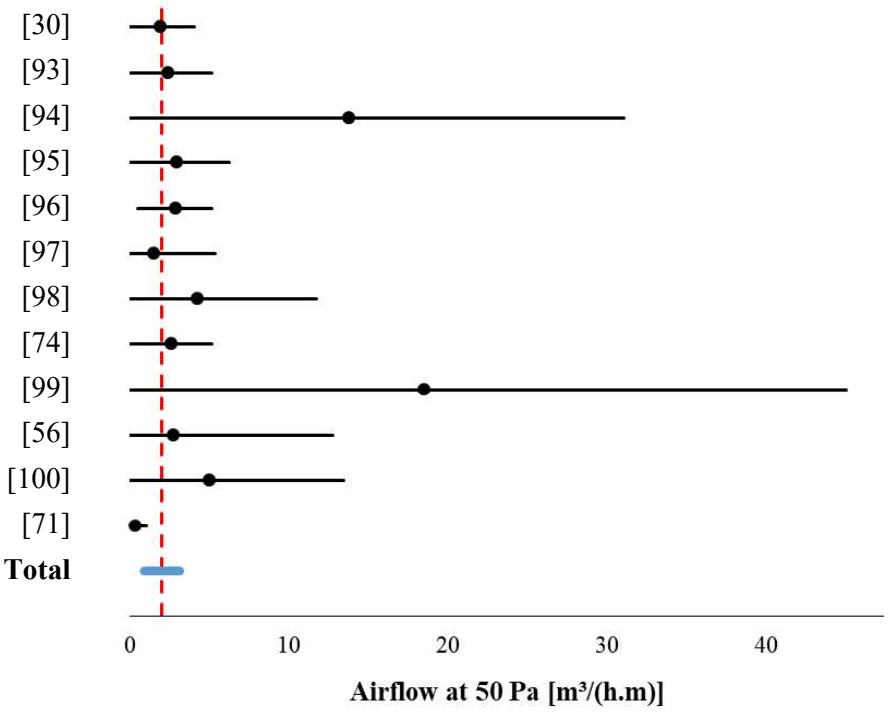



*Figure 4 – Forest plot obtained from the meta-analysis conducted on windows study presented in Table 10*

Subgroup meta-analysis can be used to explore reasons for heterogeneity, but it also provides an insight on how the variables influence the measurement of airtightness of windows. Table 13 shows the results of the subgroup meta-analysis conducted for three variables: measurement methods, type of windows, and materials. It is important to keep in mind that subgroup meta-analyses are conducted on fewer studies compared to whole group meta-analysis and, therefore, have higher uncertainty with respect to the calculation of $I^2$ and SE($\overline{q_{50}}$).

| Subgroup analysis | | $q_{50}$ | | | | References |
|---|---|---|---|---|---|---|
| | | N | $\overline{q_{50}}$ | SE($\overline{q_{50}}$) | $I^2$ (%) | |
| Measurement method | In-situ | 6 | 2.5 | 0.7 | 0.0 | [30, 62, 74, 95, 99, 100] |
| | Laboratory | 5 | 2.5 | 0.8 | 0.0 | [56, 93, 96-98] |
| Type of windows | Single windows | 7 | 1.8 | 0.5 | 50.7 | [30, 56, 93-95, 97, 98] |
| | Double windows | 6 | 2.0 | 0.5 | 0.0 | [30, 93-97] |
| | Sliding windows | 7 | 3.2 | 0.7 | 18.9 | [30, 74, 93-95, 97, 99] |
| | Unspecified | 1 | 5.0 | 4.2 | - | [100] |
| Window materials | Timber windows | 7 | 2.4 | 0.6 | 0.0 | [30, 56, 93-95, 98, 99] |
| | Aluminium | 2 | 4.1 | 1.5 | 0.0 | [94, 95] |
| | Unspecified | 4 | 2.5 | 1.0 | 0.0 | [71, 74, 97, 99, 100] |

*Table 13 – Sample size, mean, standard error (in m³/(h.m)) and inconsistency for airflow at 50 Pa for three subgroups meta-analyses based on the measurement method, the type of window, and the window material.*

These subgroup meta-analyses highlight that differences should be expected among various types of windows and window materials (different means and standard deviation), but not between measurement methods (*in-situ* vs. laboratory). These three variables are further investigated in the following sections. Other variables could have been relevant in this context (e.g., year of implementation for windows measured *in-situ*) but could not be included due to lack of information in the studies analysed.

For the first variable, all studies used either laboratory or *in-situ* measurements (i.e., none of them looked at the difference between both). The results obtained with the subgroup meta-analysis suggested that the differences detected considering this variable were not significant. This was confirmed with an independent t-test, which showed that there was no statistical ($p$-values) nor practical (effect size) evidence of differences between mean values calculated in studies performing *in-situ* and laboratory measurements ($t = 0.017$; $p = 0.988$; $g = 0.01$). The Hedge's g coefficient was preferred over other indicators (e.g., Cohen's d and Glass's) because the standard deviation of independent groups and their sizes were different [107].

Multiple studies compared different types of windows and a meta-analysis could be conducted to determine a combined difference in means among various window types. Since none of the studies reported effect sizes, these must be calculated based on the data provided. In this context, the raw mean difference is appropriate since the outcome is reported in a meaningful scale (airflows in m³/h). Raw mean difference can be used because studies reporting results in other type of outcomes (i.e., excluded from the meta-analysis conducted in 3.2.3.3) did not investigate the impact of window type on air leakage [90-92]. The main advantage of using this measure of effect size rather than standardized differences (e.g., Cohen's $d$ or Hedge's $g$) is that the result of the meta-analysis is intuitively meaningful [13].

The combination of relevant studies reported in Table 14 shows that double windows were leakier than single windows, and that both single and double windows were tighter than sliding windows. However,

for the three cases, a large inconsistency was found between studies, pointing out the need of additional research looking at these specific types of windows.

| | D | | | | References |
|---|---|---|---|---|---|
| | N | D | SE(D) | $I^2$ (%) | |
| Double - Single | 5 | 0.98 | 0.73 | 94.8 | [30, 93-95, 97] |
| Single - Sliding | 5 | -1.58 | 0.75 | 95.6 | [30, 94, 95, 97, 98] |
| Double - Sliding | 4 | -0.37 | 0.37 | 70.5 | [30, 94, 95, 97] |

*Table 14 – Mean, standard deviation and inconsistency for the raw difference of means of different types of windows*

Likewise, as for the type of windows, three studies looked at different window materials [94, 95, 97], and a similar methodology can be used to conduct the meta-analysis. However, one of the studies did not report sufficient details and results regarding differences between window materials to include them in the meta-analysis [97].

The meta-analysis conducted on two studies showed a higher mean airflows for timber windows ($D = 4.8$ m³/(h.m)) than aluminium windows but with a high standard deviation ($SE(D) = 9.1$ m³/(h.m)) and high inconsistency among studies ($I^2 = 71.3$ %). This makes this conclusion quite uncertain, in addition to the need for further research to explore the heterogeneity between these studies.

# 4. Discussion

A thorough review of studies measuring airtightness performances of building components, and the meta-analysis of reported measurements, resulted in three different outcomes: 1) a classification of building components related to their airtightness performance (section 3.1); 2) "new" means and standard deviations and inconsistency indices of building components' performance calculated on the basis of a weighted combination of studies (3.2) the identification of variables influencing airtightness performances of windows (section 3.2.3.4).

These three outcomes bring novelty to the literature in the field of building airtightness and, more generally, within the domain of the built environment.

The classification provides a comprehensive list of building components studied in previous research due to their impact on building airtightness. The proposed 4-level classification allows to understand the different type of flows (level 1), the different components category for each type of flow (level 2), the components falling into each category (level 3), and the possible treatments or type of each component (level 4). Having this 4-level structure can be of great support in building practice, to understand how to deal with which component, and in research, to consistently compare the performance of different components (e.g., it is often more relevant to compare a component with others of the same category).

Updating and improving existing databases of airtightness performance of building components is also of significant interest because of three important additions to current knowledge:

- Consideration of the studies conducted between the mid-90's and today, which is very important because of the changes in construction practice driven by recent energy policies;
- Relevance of a weighted combination of studies, which gives more importance to studies with higher accuracy and, therefore, with larger sample size and / or more rigorous experimental design;
- Evidence of the inconsistency between different studies, which is an additional information for the user regarding possible additional errors in the combined values.

Exploring heterogeneity among studies focusing on window airtightness also responds to questions related to the impact of window type and window material on airtightness performance. The analysis presented shows that only the type of window has a practically relevant impact on window airtightness, although large inconsistencies appear among studies when looking at raw mean differences.

In addition to these three outcomes related to the field of airtightness, this paper has explored the transfer of meta-analysis methods to the domain of the built environment (e.g., using mean or raw differences rather than effect sizes). This is of a great interest for research, since this approach can offer a robust protocol to combine evidence from different studies based on an estimation of their accuracy.

Nevertheless, some limitations should be acknowledged in the review of studies and in the meta-analysis. Among these: the low number of studies available; the lack of studies focusing on the treatment of components; some missing information on the tested components; and, the lack of statistical evidence when reporting some of the results. Consequently, the outcomes obtained should be considered in light of these limitations.

The low number of studies available impacts the three outcomes in different ways. First, in the classification, many third level blocks are missing since these are not studied in literature. Second, more studies would reduce the uncertainty of $I^2$ and $\mathrm{SE}(\overline{q_{50}})$ for meta-analysis and subgroup meta-analysis. Finally, a larger number of studies would increase the potential of subgroup meta-analysis when exploring heterogeneity by making it less likely to have subgroups created from only one study.

The lack of studies investigating treatments also impacts the three outcomes. First, it would lead to additional blocks at the fourth level of classification. Second, looking at different treatments individually could reduce the standard deviation observed in the results of meta-analysis, since different treatments might induce different airtightness performance. Therefore, looking at each treatment individually would result in a smaller range of measured airflows and lower standard deviation. Lastly, studying different treatments is only feasible if the number of studies looking at the treatments of one specific component is larger than the number of treatments investigated.

The lack of information reported in the tested component is a limitation for the subgroup meta-analysis since it reduces the possibilities of selecting subgroups to explore heterogeneity among studies. For example, the absence of information regarding the year of implementation of windows for *in-situ* measurements in some studies prevents conducting subgroup meta-analysis, which is expected to have an impact on airtightness performance.

These limitations not only influence the outcomes of the meta-analysis but can also affect the results of any study reporting measurements of building components. This is a potential reason for the relatively sparse literature available on the airtightness performance of building components, despite its large potential in improving infiltration models and airtightness prediction. However, increasing the number of studies would not be helpful unless their experimental design, and the methods to report results, is appropriate for the application of meta-analysis methodologies. To improve the statistical power, reliability, and the potential applicability of meta-analysis approaches based on the limitations here identified, future studies should meet four requirements:

- Each study should measure at least two different cases for each component and provide a standard deviation in addition to the mean value. Moreover, a larger number of measurements would result in a more accurate calculation of the standard deviation and, therefore, a more accurate weighting in the combination of studies.
- The characteristics of the measured sample should be thoroughly described based on previous research for future analysis (e.g., materials of the component, year of testing, year of implementation, etc.). The sample description should refer to the classification suggested in this paper as an improvement (new component), to increase precision (new treatments), or to reinforce evidence for an existing case (already identified in the classification).
- The airtightness performance of building components must be reported with the leakage exponent and the information required for the different normalisations encountered for the component (e.g., area-to-length ratio for windows). This would increase the number of studies to be considered in the meta-analysis.
- Studies comparing different treatments of windows should report the effect size of the observed difference between treatments to make them comparable with previous studies even if these have inherent differences (e.g., differences in outcomes or measurement methods).

## 5. Conclusion

This paper presented the results of a meta-analysis conducted on a critical synthesis of literature studies reporting measurements of building component airtightness.

Its main conclusions can be summarised in three different outcomes: a 4-level classification of building components based on their airtightness performance (i.e., type of flows, category of components, components and type/treatments); an update of existing airtightness databases; and, a thorough investigation of factors influencing airtightness performance of building components.

A critical appraisal of these findings, and of the limitations encountered, led to the definition of requirements that future studies should meet to improve the reliability of meta-analyses.

These outcomes offer a step ahead from existing knowledge by adding new evidence to existing industry references and providing a framework for future research. In this context, meta-analysis – a study procedure commonly used in clinical research – is a rigorous method that can allow to compare data from previous studies, even when they have inherent differences. Other than a strong need for additional studies reporting measurement of airtightness performance of building components, the application of meta-analysis protocols revealed that some aspects of the methodology should be further investigated in future studies (e.g., the index of inconsistency or the desired number of studies for each meta-analysis) to improve its potential use. Nevertheless, this can be of substantial interest to many practitioners and researchers due to its possible application to many other domains of the built environment.

# 6. References


1. Guillén-Lambea, S., B. Rodríguez-Soria, and J.M. Marín, *Air infiltrations and energy demand for residential low energy buildings in warm climates.* Renewable and Sustainable Energy Reviews, 2019. **116**: p. 109469.
2. Leprince, V., M. Kapsalaki, and F.R. Carrié, *Impact of Energy Policies on Building and Ductwork Airtightness*. 2017, AIVC.
3. Lstiburek, J., K. Pressnail, and J. Timusk, *Air Pressure and Building Envelopes.* Journal of Thermal Envelope and Building Science, 2002. **26**(1): p. 53-91.
4. Virtanen, M. *Thermal coupling of leakage airflows and heating load in buildings components and buildings*. in *Proceedings 12th AIVC Conference*. 1991. Ottawa, Ontario, Canada.
5. Liu, D.-L. and W.W. Nazaroff, *Modeling pollutant penetration across building envelopes.* Atmospheric Environment, 2001. **35**(26): p. 4451-4462.
6. Younes, C. and C. Abi Shdid, *A methodology for 3-D multiphysics CFD simulation of air leakage in building envelopes.* Energy and Buildings, 2013. **65**: p. 146-158.
7. Prignon, M. and G. Van Moeseke, *Factors influencing airtightness and airtightness predictive models: A literature review.* Energy and Buildings, 2017. **146**: p. 87-97.
8. ASHRAE, *Handbook of Fundamentals*. 2001, Atlanta: American Society Heating, Refrigerating and Air-conditioning Engineers.
9. Orme, M., M. Liddament, and A. Wilson, *Numerical Data for Air Infiltration and Natural Ventilation Calculations*. Technical Note AIVC - 44, ed. A.I.a.V. Center. 1994. 100.
10. Egger, M., S. Ebrahim, and G. Davey Smith, *Where Now for Meta-Analysis?* International Journal of Epidemiology, 2002. **31**.
11. Hoffman, J.I.E., *Chapter 36 - Meta-analysis*, in *Biostatistics for Medical and Biomedical Practitioners*, J.I.E. Hoffman, Editor. 2015, Academic Press. p. 645-653.
12. Field, A.P. and R. Gillett, *How to do a meta-analysis.* British Journal of Mathematical and Statistical Psychology, 2010. **63**(3): p. 665-694.
13. Borenstein, M., et al., *Introduction to meta-analysis*. 2011: John Wiley & Sons.
14. Tatsioni, A. and J.P.A. Ioannidis, *Meta-Analysis*, in *International Encyclopedia of Public Health*, H.K. Heggenhougen, Editor. 2008, Academic Press: Oxford. p. 442-450.
15. Borenstein, M., L. Hedges, and H. Rothstein, *Meta-analysis: Fixed effect vs. random effects.* Meta-analysis. com, 2007.
16. Higgins, J.P.T., et al., *Measuring inconsistency in meta-analyses.* BMJ, 2003. **327**(7414): p. 557.
17. Higgins, J.P. and S.G. Thompson, *Quantifying heterogeneity in a meta-analysis.* Statistics in medicine, 2002. **21**(11): p. 1539-1558.
18. AIVC. *Bibliographic database Airbase*. 2020; Available from: https://www.aivc.org/resources/airbase.
19. Elsevier. *Explore scientific, technical, and medical research on ScienceDirect*. 2020; Available from: https://www.sciencedirect.com/.
20. Sherman, M.H. and W. Chan, *Building Air Tightness: Research and Practice*, in *Building Ventilation: The State of the Art*, M. Santamouris and P. Wouters, Editors. 2006: London.
21. Jamieson, M., et al., *Energy Performance of Buildings Directive (EPBD) Compliance Study*. 2015: Publications Office of the European Union. 138.
22. ASHRAE, *Handbook of Fundamentals*. 2017, Atlanta: American Society Heating, Refrigerating and Air-conditioning Engineers.
23. Treado, S.J., D.M. Burch, and C.M. Hunt, *An investigation of air infiltration characteristics and mechanisms for a townhouse.* 1979, National Bureau of Standards: Tehcnical Note 992.
24. Shaw, C., R. Magee, and J. Rousseau, *Overall and component airtightness values of a five-story apartment building.* ASHRAE Trans. ; (United States), 1991. **97**(2): p. 347-353.
25. Tamura, G.T. *Predicting air leakage for building design*. in *6th CIB Congress on the impact of Research on the Built Environment*. 1974. Budapest.

26. CMHC, *Research Project Testing of Air Barrier Construction Details II*. 1993, Canada Mortgage and Housing Corporation: Ottawa, Canada.
27. Abrantes, V. and E. De Oliveira Fernandes, *Experimental determination of empirical flow coefficients for air infiltration through pitched roofs*, in *Passive and Low Energy Architecture*, S. Yannas, Editor. 1983, Pergamon. p. 427-433.
28. Tamura, G.T. and C.Y. Shaw, *Studies on exterior wall air tightness and air infiltration of tall buildings.* ASHRAE Trans.;(United States), 1976. **82**.
29. Shin, H.K. and J.H. Jo, *Air leakage characteristics and leakage distribution of dwellings in high-rise residential buildings in Korea.* Journal of Asian Architecture and Building Engineering, 2013. **12**(1): p. 87-92.
30. Tamura, G.T., *Measurement of air leakage characteristics of house enclosures.* ASHRAE Trans.;(United States), 1975. **81**: p. 202-208.
31. Guyot, G., et al., *Multizone air leakage measurements and interactions with ventilation flows in low-energy homes.* Building and Environment, 2016. **107**: p. 52-63.
32. Tamura, G.T. and C.Y. Shaw, *Air leakage data for the design of elevator and stair shaft pressurization systems.* ASHRAE Trans. ; (United States), 1976. **82**: p. 179-190.
33. Tamura, G.T. and A. Wilson, *Pressure differences caused by chimney effect in three high buildings and building pressures caused by chimney action and mechanical ventilation.* ASHRAE Trans. ; (United States), 1968. **73**(2): p. II. 1.1-II. 1.20.
34. Thorogood, R., *Resistance to air flow through external walls*. 1979, Building Research Establishment.
35. Tamura, G.T., *The calculation of house infiltration rates.* ASHRAE Trans. ; (United States), 1979. **85**: p. 58-71.
36. Cosmulescu, C., *Experimental procedure to evaluate air leakage through different building materials*. 1997, Concordia University: Montreal, Quebec, Canada.
37. Hurel, N., *Impact of air infiltration on buildings' performance: focus on the experimental study within timber-frame walls*. 2016, Université Grenoble Alpes.
38. Tuluca, A. and P. Keyes. *Leakage areas for opaque wood frame walls - a preliminary study*. in *Symposium on air infiltration, ventilation and moisture transfer*. 1988. Forth Worth, Texas, USA: Building Envelope Coordinating Council.
39. Lowe, R., et al., *Airtightness in masonry dwellings: Laboratory and field experience.* Building Services Engineering Research and Technology, 1994. **15**(3): p. 149-155.
40. Kalamees, T., Ü. Alev, and M. Pärnalaas, *Air leakage levels in timber frame building envelope joints.* Building and Environment, 2017. **116**: p. 121-129.
41. Funkhouser, P., *Air infiltration effects on the thermal transmittance of concrete building systems.* ASHRAE Trans. ; (United States), 1979. **85**: p. 918-928.
42. Dickson, D., *Air flow through and within masonry walls*, in *Report ECRC/M1420*. 1981, Electricity Council Research Center.
43. Bracke, W., N. Van Den Bossche, and A. Janssens. *Airtightness of building penetrations: air sealing solutions, durability effects and measurement uncertainty*. in *35th AIVC Conference - Ventilation and airtightness in transforming the building stock to high performance*. 2014. Poznan, Poland.
44. Houghten, F. and M. Ingles, *Infiltration through pastered and unplastered brick walls.* ASHVE Trans. ; (United States), 1927. **33**: p. 377-386.
45. Larson, G., C. Braatz, and D. Nelson, *Air infiltration through various types of brick wall construction.* ASHVE Trans. ; (United States), 1927. **33**: p. 125.
46. Lecompte, J. *Airtightness of masonry walls*. in *Proceedings 8th AIVC Conference*. 1987. Überlingen, Germany.
47. Sasaki, J., *Air leakage characteristics of some brick and concrete block walls*, in *Technical Note 525*. 1968, National Research Council of Canada, Division of Building Research.
48. Becker, R., *Air permeability and thermal performance of concrete block wall specimens.* Journal of Building Physics, 2010. **34**(2): p. 163-177.

49. Kronvall, J., *Air flow in building components*, in *Byggnadsfysik LTH*. 1980, Lunds Tekniska Högskola. p. 194.
50. CMHC, *Air permeance of building materials: summary report.* 1988, Canada Mortgage and Housing Corporation: Ottawa, Canada.
51. Langmans, J., R. Klein, and S. Roels. *Air permeability requirements for air barrier materials in passive houses – Comparison of the air permeability of eight commercial brands of OSB*. in *5th International Symposium on Building and Ductwork Air-tightness*. 2010. Copenhagen/Lyngby, Denmark.
52. Langmans, J., et al., *Potential of wind barriers to assure airtightness of wood-frame low energy constructions.* Energy and Buildings, 2010. **42**(12): p. 2376-2385.
53. Larson, G., D. Nelson, and B. C, *Air infiltration through various types of wood frame construction.* ASHVE Trans. ; (United States), 1930. **36**: p. 397-428.
54. Hildebrand, G., *Mise au point de procédés et de méthodes d'essai visant l'évaluation de membranes pare-air pour murs en maçonnerie*. 1990, Canada Mortgage and Housing Corporation: Ottawa, Canada.
55. Nield, D.A. and A. Bejan, *Convection in porous media*. Vol. 3. 2006: Springer, Cham.
56. Hall, M. and G. Hauser, *In situ Quantifizierung von Leckagen bei Gebäuden in Holzbauart*, in *AIF–Forschungsvorhaben Nr. 12611 N*. 2003, Universität Kassel - Fachgebiet Bauphysik: Kassel, Germany.
57. Gullbrekken, L., P. Rüther, and T. Kvande. *Air leakage defects in vapour barrier of compact roofs*. in *38th AIVC Conference - "Ventilating healthy low-energy buildings"*. 2017. Nottingham, UK.
58. Bassett, M.R., *Building Site Measurements for Predicting Air Infiltration Rates*, H.R. Trechsel and P.L. Lagus, Editors. 1986, ASTM International: West Conshohocken, PA. p. 365-383.
59. Figley, D. and R. Dumont, *Techniques for measuring the air leakage characteristics of below grade foundation components.* Air and Wasre Management Association, 1989.
60. Caffey, G., *Residential air infiltration.* ASHRAE Trans. ; (United States), 1979. **85**(1): p. 41-57.
61. Brinks, P., O. Kornadt, and R. Oly, *Air infiltration assessment for industrial buildings.* Energy and Buildings, 2015. **86**: p. 663-676.
62. Pereira, P.F., et al. *Testing for building components contribution to airtightness assessment*. in *35th AIVC Conference " Ventilation and airtightness in transforming the building stock to high performance"*. 2014. Poznan, Poland.
63. Shaw, C., *Methods for conducting small-scale pressurization tests, and air leakage data of multi-storey apartment buildings.* ASHRAE Trans. ; (United States), 1980. **86**.
64. Baker, P., S. Sharples, and I. Ward. *The validation and application of a portable pressurisation test facility for the measurement of the flow characteristics of background leakage areas*. in *3rd International Congress on Building Energy Management, III Ventilation, air movement and air quality: field measurement and energy auditing*. 1987. Lausanne, Switzerland.
65. Relander, T.-O., B. Heiskel, and J.S. Tyssedal, *The influence of the joint between the basement wall and the wood-frame wall on the airtightness of wood-frame houses.* Energy and Buildings, 2011. **43**(6): p. 1304-1314.
66. Alev, Ü., P. Antsov, and T. Kalamees, *Air Leakage of Concrete Floor and Foundation Junctions.* Energy Procedia, 2015. **78**: p. 2046-2051.
67. Relander, T.-O., et al., *The influence of structural floors on the airtightness of wood-frame houses.* Energy and Buildings, 2011. **43**(2): p. 639-652.
68. Tietsma, G. and B. Peavy, *The thermal performance of a two-bedroom mobile home*. 1978, National Bureau of Standards Building Science.
69. Dickerhoff, D., D. Grimsrud, and R. Lipschutz, *Component leakage testing in residential buildings*, in *Santa Cruz, United States*, S.S.i.E.E. Buildings, Editor. 1982, Lawrence Berkeley Laboratory.

70. Tenwolde, A., C. Carll, and V. Malinauskas. *Airflows and Moisture Conditions in Walls of Manufactured Homes*. in *Airflow performance of building envelopes, components and systems*. 1993. Dallas, United States.
71. CMHC, *Research Project Testing of Air Barrier Construction Details*. 1991, Canada Mortgage and Housing Corporation: Ottawa, Canada.
72. Alfano, F.R.d.A., et al., *An Experimental Investigation on the Air Permeability of Passive Ventilation Grilles.* Energy Procedia, 2015. **78**: p. 2869-2874.
73. Jones, P. and G. Powell. *Comparison of air infiltration rate and air leakage tests under reductive sealing for an industrial building*. in *10th AIVC Conference "Progress and trends in air infiltration and ventilation research"*. 1989. Espoo, Finland.
74. Pinto, M., J. Viegas, and V.P. de Freitas, *Air permeability measurements of dwellings and building components in Portugal.* Building and Environment, 2011. **46**(12): p. 2480-2489.
75. Senave, E. and H. Hens, *Case Study Zolder: results of the measuring campaign 1986-1987*, C.a.E. IEA Annex XIV, Editor. 1987, Katholieke Universiteit Leuven.
76. Berthault, S., F. Boithias, and V. Leprince. *Ductwork airtightness: reliability of measurements and impact on ventilation flowrate and fan energy consumption*. in *35th AIVC conference: Ventilation and airtightness in transforming the building stock to high performance*. 2014. Poznan, Poland.
77. Leprince, V. and F.R. Carrié, *Impact of ductwork airtightness on fan energy use: Calculation model and test case.* Energy and Buildings, 2018. **176**: p. 287-295.
78. Leprince, V., F.R. Carrié, and M. Kapsalaki. *Building and ductwork airtightness requirements in Europe – Comparison of 10 European countries*. in *38th AIVC Conference "Ventilating healthy low-energy buildings"*. 2017. Nottingham, UK.
79. *EN 12237 : Ventilation for buildings - Ductwork - Strength and leakage of circular sheet metal ducts*. 2003.
80. Carrié, F., J. Andersson, and P. Wouters, *Improving ductwork: a time for tighter air distribution systems*, G. TP, Editor. 1999, Air Infiltration and Ventilation Center: Coventry, UK. p. 126.
81. Carrié, F., E. Balas, and V. Patriarca, *Perméabilité des réseaux aérauliques*. 1996, ADEME: Sophia-Antipolis, France.
82. Bassam, M., V. Leprince, and A. Mélois. *Statistical analysis of about 1,300 ductwork airtightness measurements in new French buildings: impacts of the type of ducts and ventilation systems*. in *39th AIVC Conference "Smart Ventilation for Buildings"*. 2018. Antibes Juans-Les-Pins, France.
83. Lipschutz, R., et al., *Infiltration and indoor air quality in energy efficient houses in Eugene, Oregon*. 1981, Lawrence Berkeley Laboratory: Berkeley, California, USA.
84. Vialle, P. *Air Tightness of Ventilation Ductwork Equipped with Joints*. in *27th AIVC and 4th Epic Conference "Technologies & sustainable policies for a radical decrease of the energy consumption in buildings"*. 2006. Lyon, France.
85. Relander, T.-O., T. Kvande, and J.V. Thue, *The influence of lightweight aggregate concrete element chimneys on the airtightness of wood-frame houses.* Energy and Buildings, 2010. **42**(5): p. 684-694.
86. Shaw, C. and W. Brown. *Effect of a gas furnace chimney on the air leakage characteristic of a two-storey detached house.* in *3rd AIVC Conference "Energy efficient domestic ventilation systems for achieving acceptable indoor air quality"*. 1982. London UK.
87. Skaar, E., *Air leakage at service penetrations in ceilings*. 1982, Institutt for Husbyggingsteknikk: Trondheim, Norway.
88. JCGM, *Evaluation of measurement data — Guide to the expression of uncertainty in measurement*, J.C.f.G.i. Metrology, Editor. 2008. p. 134.
89. Saarnio, P. *Airtightness, pressure differences and indoor climate in the experimental building, Kasarminkatu 24*. in *Workshop on indoor air quality and energy conservation*. 1983. Helsinki, Finland.

90. Fournier, M., S. Berthault, and F. Carrié. *In situ measurement of window air tightness : stakes, feasibility, and first results*. in *28th AIVC and 2nd Palenc Conference " Building Low Energy Cooling and Ventilation Technologies in the 21st Century"*. 2007. Crete, Greece.
91. Shapiro, A. and B. James. *Creating windows of energy saving opportunity*. in *Home Energy*. 1997. USA.
92. McGrath, P., *Prediction of air infiltration through building components; the assembly of a device to measure air infiltration through components with a suggested method of producing data which could be used to form the basis of a prediction model*, in *Inst. of Science and Technology*. 1982, University of Manchester: UK.
93. Lowinski, J., *Thermal performance of wood windows and doors.* ASHRAE Trans. ; (United States), 1979. **85**(1): p. 548-566.
94. Almeida, R.M.S.F., N.M.M. Ramos, and P.F. Pereira, *A contribution for the quantification of the influence of windows on the airtightness of Southern European buildings.* Energy and Buildings, 2017. **139**: p. 174-185.
95. Weidt, J., J. Weidt, and S. Selkowitz. *Field air leakage of newly installed residential windows*. in *ASHRAE/DOE Conference*. 1979. Florida, USA.
96. Larson, G., D. Nelson, and R. Kubasta, *Air infiltration through double-hung wood windows.* ASHVE Trans. ; (United States), 1930. **37**: p. 571-605.
97. Van Den Bossche, N. and A. Janssens, *Airtightness and watertightness of window frames: Comparison of performance and requirements.* Building and Environment, 2016. **110**: p. 129-139.
98. Carruthers, J. and C. Newman. *The repeatability and reproduceability of test results on windows and wall span elements and the expected results*. in *Paul Rousseau Symposium on the testing of wall elements and windows*. 1977. Vilvorde, Belgium.
99. Ward, I. and S. Sharples, *An investigation of the infiltration characteristics of windows and doors in a tall building using pressurisation techniques*. 1982, Department of Building Science, Faculty of Architectural Studies University of Sheffield: UK.
100. Persily, A. and R. Grot. *Pressurization testing of federal buildings*. in *Measured air leakage of buildings. A symposium on performance of building constructions*. 1984. Philadelphia, USA.
101. Relander, T.-O., J.T. Vincent, and A. Gustavsen. *Air tightness performance of different jointing methods for windows in wood-frame buildings*. in *8th Symposium on Building Physics in the Nordic Countries*. 2008. Copenhagen, Denmark.
102. Van Den Bossche, N., et al., *Airtightness of the window–wall interface in cavity brick walls.* Energy and Buildings, 2012. **45**: p. 32-42.
103. Zmeureanu, R., et al., *Measurements of Air Leakage through Revolving Doors of Institutional Building.* Journal of Architectural Engineering, 2001. **7**(4): p. 131-137.
104. Hallik, J., H. Gustavson, and T. Kalamees, *Air Leakage of Joints Filled with Polyurethane Foam.* Buildings, 2019. **9**(7): p. 172.
105. *EN 12114: Thermal Performance of Buildings–Air Permeability of Building Components and Building Elements-Laboratory Test Method*. 2000.
106. 283, A., *Standard Test Method for Determining Rate of Air Leakage Through Exterior Windows, Curtain Walls and Doors Under Specified Pressure Differences Across the Specimen.* 2004.
107. Ellis, P.D., *The Essential Guide to Effect Sizes: Statistical Power, Meta-Analysis, and the Interpretation of Research Results*. 2010, Cambridge: Cambridge University Press.

# Appendix C.

Prignon, M., Delmotte, C., Dawans, A., Altomonte S. and Van Moeseke, G. (2020). On the impact of regression techniques to airtightness measurement uncertainties. Energy and Buildings, **215**. https://doi.org/10.1016/j.enbuild.2020.109919.

Energy & Buildings 215 (2020) 109919

Contents lists available at ScienceDirect

Energy & Buildings

journal homepage: www.elsevier.com/locate/enbuild

# On the impact of regression technique to airtightness measurements uncertainties

Martin Prignon[a,*], Christophe Delmotte[b], Arnaud Dawans[c], Sergio Altomonte[d], Geoffrey van Moeseke[d]

[a] UCLouvain, Place du levant, 1, bte L5.05.02, B-1348 , Ottignies-Louvain-la-Neuve, Belgium
[b] BBRI, Belgium
[c] Entreprises Jacques Delens, Belgium
[d] UCLouvain, Belgium

ARTICLE INFO

*Article history:*
Received 20 November 2019
Revised 2 March 2020
Accepted 2 March 2020
Available online 3 March 2020

*Keywords:*
Uncertainty calculation
Airtightness measurements
Fan pressurization test
Air infiltration
Linear regression techniques
Weighted line of organic correlation
Iterative weighted least square
Ordinary least square

ABSTRACT

The Ordinary Least Square (OLS) method is often used in the estimation of buildings' airtightness. However, recent research demonstrated that this regression technique neglects a significant part of uncertainty. This paper investigates two alternative methods: Weighted Line of Organic Correlation (WLOC) and Iterative Weighted Least Square (IWLS). A series of 30 repeated tests were performed on a newly-constructed apartment in Brussels (Belgium). Real uncertainty and its estimation were compared for the three regression methods. In-situ observations showed that the statistical significance of differences between regression techniques depends on the considered pressure difference. Theoretical calculations showed that uncertainties estimated with IWLS and WLOC were higher than OLS. Lastly, comparing calculations and in-situ observations confirmed that IWLS and WLOC provide a better uncertainty estimation than OLS. Therefore, WLOC or IWLS should be preferred to OLS, especially in the presence of wind. WLOC is expected to be more robust than IWLS since it does not imply an iterative procedure. Along with ongoing work investigating other sources of errors, these findings contribute to a deeper understanding of uncertainty in fan pressurization tests.

© 2020 Elsevier B.V. All rights reserved.

## 1. Introduction

Excessive air infiltration in buildings can lead to several inconveniences, such as an increase of heating and cooling loads [1,2], a reduction of acoustic insulation [3], or a decrease of the hygrothermal performance of insulation materials [4]. The rate of air infiltration in a building is determined by its airtightness [5], whose direct measurement is an issue of major concern considering that, according to the literature, no predictive model can yet replace it [6,7].

Although the fan pressurization test (also called blower door test) has long been used by building professionals to measure airtightness [4], there is an important lack of knowledge when dealing with the uncertainty of the procedure. Over the last years, several European countries have imposed airtightness tests on new buildings and large retrofit interventions [8]. Therefore, reducing the uncertainty of these tests has become a key subject in this domain. In addition, it is essential that the reliability of airtightness measurements can be assessed. The uncertainty provides a direct information on the deviation of a result from the real value of the measured parameter. Without this information, results cannot be compared to each other or to reference values provided in regulations, specifications or standards [9]. Recently, various studies have been focusing on repeatability (i.e., successive measurements carried out under the same conditions) and reproducibility (i.e., successive measurements taken under changing conditions) of the test [10–14]. Research has also investigated several sources of uncertainty [15,16] among which wind is likely to be the most challenging, since it can cause different types of errors in both envelope pressure and air flow rate measurements.

As recent studies from the authors have demonstrated, wind speed and direction can have a strong impact on uncertainty in fan pressurization measurements, making the envelope pressure uncertainty non-negligible [17,18]. This implies that the most used regression technique, the Ordinary Least Square (OLS) method, might not be appropriate for fan pressurization measurements. The OLS method consists in minimizing the distance in the *y*-direction between the measurements and the fitted line. This method neglects the uncertainty in the *x*-direction, which is the pressure difference measurement in the fan pressurization test. In this con-

* Corresponding author.

https://doi.org/10.1016/j.enbuild.2020.109919
0378-7788/© 2020 Elsevier B.V. All rights reserved.

text, Sherman and Palmiter had already questioned the relevance of the Ordinary Least Square (OLS) regression method in 1995 [15]. In 2012, Okuyama and Onishi suggested the use of the Iterative Weighted Least Square (IWLS) regression method [19] and, in 2017, Delmotte suggested the use of the Weighted Line of Organic Correlation (WLOC) [18]. The IWLS method consists in minimizing the distance between the measurements and the fitted line in the *x*- and *y*- directions, while considering uncertainties on both axes in weighting these measurements. Since this minimization has no analytical solution, the IWLS method induces an iterative process for the determination of the weights and the slope of the fitting line. On the other hand, the WLOC method, which has an analytical solution, consists in minimizing the product of the distances between the *x*- and *y*- coordinates of the measurement points and the fitting line, when both variables are weighted. Since the inadequacy of OLS has been pointed out in the literature [15], the impact of a change of method requires detailed investigation.

Based on previous research [15–20], this paper aims to demonstrate that changing the regression technique in the fan pressurization test protocol allows taking into account the effect of wind in the uncertainty, influencing both the observed (measured) and calculated (estimated) uncertainty of the airtightness measurement. This is achieved by applying different regression techniques on the same dataset and comparing results both practically and theoretically. In this paper, the terms *observed* and *calculated* refer respectively to the practical and the theoretical estimations of uncertainty. Observed uncertainty is determined by repeating multiple times the same measurement and looking at the variation of the results. Calculated uncertainty is estimated by formulating hypotheses about the sources of error and then propagating them through the different steps of the procedure for the estimation of building airtightness. The observed uncertainty is, to this date, much more reliable than its calculated value and should, therefore, be considered as a better indicator of the real uncertainty. However, due to time constraints, it is hardly possible to determine this uncertainty *in-situ*, hence making the calculated uncertainty a more appropriate option. Since consideration of both is essential, observed and calculated uncertainties are discussed in this paper.

The paper is articulated in four parts: the first section illustrates the methodologies for theoretical calculation and *in-situ* observation of uncertainty, and the protocol for their determination; in the second part, the results obtained by applying both methods on a series of 30 tests in repeatability conditions are presented; the third section discusses the implications of the results in practice and research, and illustrates the limitations of the study; the paper is concluded by a summary of the findings and the further work that is needed in the field of uncertainties in airtightness measurements.

## 2. Methodology

Airtightness measurements using fan pressurization tests are increasingly required in specifications and regulations worldwide. A fan pressurization test consists in measuring the airflow induced by a pressure difference between two sides of the building envelope. A fan placed at one of the building openings (usually a door or a window) induces this pressure difference. This measurement procedure is regulated by the international standard ISO 9972:2015 [21]. A linear regression is then performed between multiple couples of pressure difference/airflow measurements to determine two characteristics of the building: its flow exponent ($n$, the slope of the regression line) and its leakage coefficient ($C$, related to the intercept of the regression line). The airflow at a given pressure difference (based on the requirement or specification) can be deduced from the regression line, as a result of the fan pressurisation test.

To be reliable and comprehensive, any measurement should be provided with an indication of its uncertainty in order to estimate the 'doubt' about its effective accuracy [9]. The uncertainty is generally expressed as the expected standard deviation that would be observed for a large number of repeated measurements. As previously illustrated, the uncertainty can be defined both practically (observed) and theoretically (calculated)

Each uncertainty definition method presents some advantages but also suffers from some drawbacks. While calculated uncertainty allows understanding how different sources of uncertainty affect the variable of interest, observed uncertainty works as a "black-box method" where the operator gets an uncertainty value without a fundamental characterization of the processes and phenomena behind it. However, observed uncertainty incorporates all sources of errors experienced during the testing period under the given conditions, while theoretical uncertainty requires assumptions to be made for each of them. One of the most relevant differences lies in the time needed for the uncertainty determination. Observed uncertainty requires multiple identical tests, which is time consuming and, therefore, hardly done in practice. Conversely, since calculated uncertainty only requires hypotheses made prior to the measurement, the calculation is performed simultaneously with the fan pressurization test, without requiring any additional time.

This paper studies both calculation and observation methods for uncertainty estimation and compares them for three regression techniques. On the one hand, analysing theoretical calculations allows understanding the impact of neglecting some sources of uncertainty on the measurement protocol. On the other, investigating observed uncertainty provides a reference value for the uncertainty, which is more reliable than a theoretical estimation due to the lack of knowledge on the sources of uncertainty. Lastly, comparing both methods allows quantifying and understanding the "gap" between a theoretical and a practical approach.

### 2.1. Observed uncertainties

In practice, a good estimate of uncertainty (i.e., $u_p(X)$) on a given variable is represented by the standard deviation (i.e., $s_p(X)$) of this variable measured repeatedly [9]. Therefore, observed uncertainty can be determined by repeating the same protocol for estimation of the variable and then computing the standard deviation (i.e., accounting for the amount of dispersion) of all these estimations. The sources of error considered in this estimate depend on the measurement conditions. For example, if estimations are made under various representative wind patterns, the error related to changes in wind conditions will be included in the determination of the observed uncertainty. Repeatability and reproducibility conditions refer to successive measurements carried out, respectively, under equal and changing circumstances. Perfect repeatability and reproducibility conditions are, in turn, the lower and upper limits of the observed uncertainty. In this study, the main experimental settings (i.e., operator and equipment) were kept constant between the tests. However, since wind conditions changed between measurements, these can be considered as near-repeatability conditions [10,11].

A series of 30 fan pressurization measurements was performed for this study. In the field of building airtightness measurements, no previous research has defined an appropriate sample size for robust statistical analysis. Therefore, the number of tests repeated during a measurement period is an arbitrary trade-off between the duration of the testing and the uncertainty on the standard deviation (i.e., the capability of the standard deviation to estimate the unknown true uncertainty) that is given by $(2[n-1])^{-0.5}$, where $n$ is the number of measurements performed. For 30 measurements, the uncertainty in $s_p(X)$ is 13.1% of the standard deviation calcu-

lated [9]. A short testing period (15 days) was chosen to avoid any impact of ageing and seasonal variations on airtightness, to limit the difference of outside temperature between tests, and to respect site constraints.

#### 2.1.1. Measurement protocol

Each test consisted in the measurement of 20 airflow-pressure difference couples between 10 and 100 Pa in both pressurization and depressurization. For both cases, these measurements were processed according to ISO 9972:2015 standard [21] to obtain $\ln(\Delta p_e)/\ln(q_e)$ couples. In practice, measurements made according to ISO 9972:2015 standard have five steps:

1. Measure $(\Delta p_m; q_m)$ couples;
2. Transform measured couples to envelope couples $(\Delta p_e; q_e)$, including inside-outside temperature difference and zero-flow pressure;
3. Compute $(\ln(\Delta p_e); \ln(q_e))$ couples;
4. Perform linear regression to obtain air flow exponent (n) and coefficient ($C_{env}$);
5. Compute the variable of interest (e.g., $Q_{50}$, $n_{50}$ or $Q_4$, depending on the case).

Where $\Delta p_m$ and $q_m$ are the measured pressure difference and air flow rate, $\Delta p_e$ and $q_e$ are the envelope pressure difference and airflow rate. $Q_{50}$ and $Q_4$ are respectively the airflow rate at 50 and 4 Pa, while $n_{50}$ is the air change rate per hour at 50 Pa.

In this work, for each test, step 4 was made three times: once for each linear regression (i.e., OLS, IWLS and WLOC methods), to derive three sets of regression parameters. Each set was therefore used to determine the air flow exponent ($n$) and air leakage coefficient ($C_L$) of the building (step 4) and, consequently, the relation between air flow rate through the envelope ($Q$) and the pressure difference ($\Delta p$) (step 5) either in depressurization or pressurization (Eq. (1)). Lastly, the air flow rate through the building envelope at a given pressure difference was computed as the average of pressurization and depressurization airflows at that pressure difference.

$$Q = C_L(\Delta p)^n \tag{1}$$

#### 2.1.2. Measured equipment and weather data

Pressure differences and air flow rates were recorded in October 2017 using a DG-700 pressure gauge (last calibrated four months before the tests) from The Energy Conservatory (TEC). According to the manufacturer, the accuracy in pressure measurement of the DG-700 is the greatest between $\pm$ 1% of the reading and $\pm$ 0.15 Pa, and it has a resolution of 0.1 Pa [23]. Regarding air flow rate measurements, the accuracy of the DG-700 in combination with a TEC BlowerDoor Model 4 is the greatest between $\pm$ 4% of the reading and $\pm$ 1.7 m³/h.

During the tests, a weather station (Ahlborn FMD 760) placed on the roof above the measurement site recorded the external air temperature, the wind speed and the wind direction every 10 s. The weather station provided 10-min averages for the external air temperature ($T_{ext}$), the mean wind speed ($\bar{v}_w$) and the mean wind direction. It also provided the maximum wind speed measured during these 10-min periods. A thermometer (Testo 417) was used to measure the internal air temperature ($T_{int}$) before each test with a maximum permissible error of $\pm$ 0.5 K and a resolution of 0.1 K. Table 1 shows, for each weather variable, the minimum, maximum, mean and standard deviation of all the values recorded by the weather station (10-min samples) and the thermometer (before each test) during the 15-day testing period. Wind direction was mostly from the west and southwest.

**Table 1**
Minimum, maximum, mean and standard deviation of weather data measured during the testing period.

| | Min | Max | Mean | Standard Deviation |
|---|---|---|---|---|
| $T_{ext}$ [ °C] | 8.8 | 24.3 | 14.2 | 2.77 |
| $T_{int}$ [ °C] | 20.5 | 22.0 | 21.3 | 0.57 |
| $\bar{v}_w$ [m/s] | 0 | 3.8 | 1.3 | 0.75 |
| $\max(v_w)$ [m/s] | 0.3 | 8.3 | 3.3 | 1.57 |

#### 2.1.3. Measurement site

The series of tests was performed on a newly built (2017) apartment within a period of 15 days in October 2017. The apartment was a masonry construction of 228 m³ with a floor area of 90 m² located on the second floor of a 3-storey building in Brussels (Belgium). Only two perimetral walls were exposed to the outside (Fig. 1). Over recent years, masonry apartments have represented a large share of new residential constructions in Brussels.

There were no airtightness requirements for the apartment itself, but the whole building (i.e., all the apartments pressurized simultaneously) had to reach a maximum air change rate of 0.6 $h^{-1}$ at 50 Pa. The preparation of the apartment during the tests was consistent with method 1 described in ISO 9972:2015 [21].

### 2.2. Theoretical calculation of uncertainty

In the current state of knowledge, observed uncertainties are much more reliable than calculated values. However, they are hardly determined in practice when performing a fan pressurization test since the procedure required can be demanding in terms of time and resources. On the contrary, calculated uncertainty – that is performed simultaneously with the fan pressurization test – can be more suitable for the estimation of uncertainty in the context of real practice.

Uncertainty can be computed theoretically by determining all possible sources of uncertainty and then propagating them from the step they occur to the last one (i.e., the determination of the variable of interest). These sources of uncertainty can be divided in three categories: precision, bias (systematic error), and modelization errors. Precision and bias errors are, respectively, random and fixed variations of the measured values around the true quantity that is unknown. Modelization errors come from assumptions behind the estimation method.

#### 2.2.1. Sources of error considered in calculations

Precision and bias errors derive mainly from equipment, for both pressure and airflow measurements. In fact, the value read during the measurement can be different from the “true quantity”, which is unknown, because of the accuracy and resolution of the instruments utilized. The equipment manufacturer often provides information about accuracy and resolution. These can be translated into uncertainty depending on the way errors are expressed. Specific guidelines can be used to deduce the uncertainty from the information provided [9]. Precision and bias errors occur also when measuring internal and external temperatures, or when estimating building volume or envelope area based on building plans. In addition to these inaccuracies, an important modelization error can be due to short-term variations in wind speed and direction. In practice, the pressure induced by weather conditions (i.e., zero-flow pressure) is measured before and after the fan pressurization test and is generally assumed constant during the test. However, previous studies by the authors have shown that this is a questionable assumption that comes along with an important uncertainty [17,18].

Although they are important in the context of airtightness estimation and deserve attention, this study did not focus on other

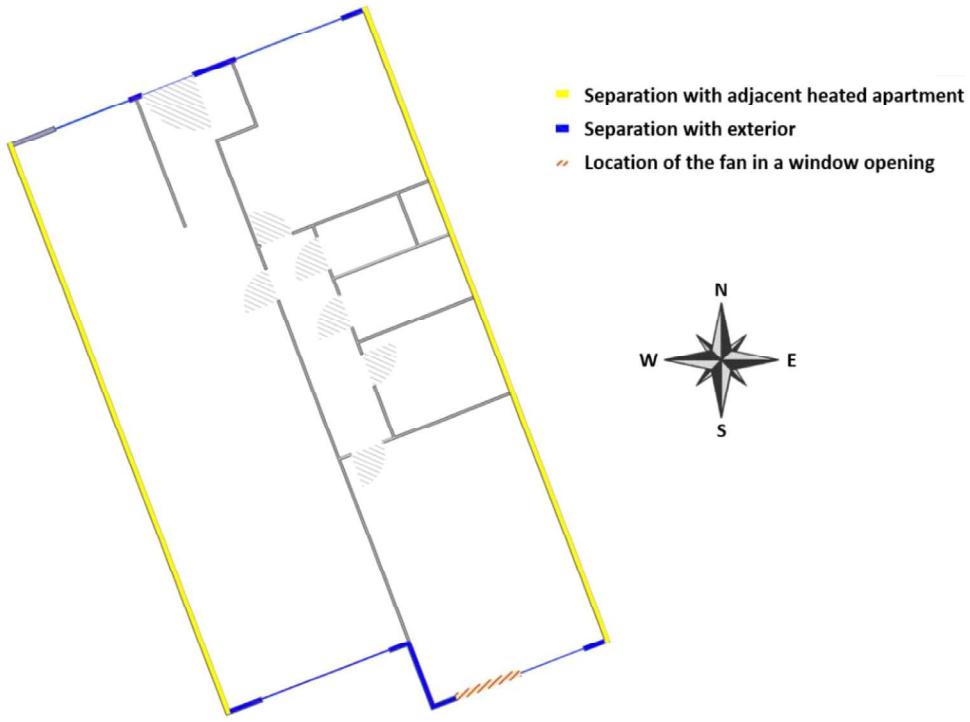



**Fig. 1.** Plan of the tested apartment, including separation type and fan location.

bias errors than those already accounted for in the accuracy provided by the manufacturer. In addition, only the modelization error due to zero-flow pressure approximation was considered. This is because these were the only bias and modelization errors identified in the repeatability conditions applied in this study. For example, the location of pressure taps could be considered as a source of error in the calculation. However, since the location is kept constant between tests, this error would not be observed in the repeatability test. Therefore, comparing calculated and observed uncertainty would only be relevant if both took into account the same sources of errors.

The source of errors considered in this study are quantified and illustrated in the third part of this paper (Section 3.2.1). These include: equipment accuracy for pressure and airflow measurements; equipment resolution for pressure measurement; equipment accuracy and resolution for temperature measurements; and, modelization error due to the zero-flow pressure hypothesis. Once sources of error are identified, one must propagate them from their occurrence to the variable of interest. In this study, the uncertainty calculation was performed for each of the 30 tests in both pressurization and depressurization, and it was then propagated to average air flow rate.

### 2.2.2. Uncertainty propagation

Error propagation occurs when one variable is obtained from others: when a response variable $y$ is obtained from explanatory variables ($x_i$, $x_j$, ...), the uncertainty in the response variable ($u(y)$) is deduced from uncertainties in explanatory variables ($u(x_i)$, $u(x_j)$, ...). This propagation is computed with Eq. (2), where $N$ is the number of explanatory variables, $f$ is the functions linking response and explanatory variables and $r(x_i, x_j)$'s are the correlation coefficients between each explanatory variable [9].

$$u(y) = \sqrt{\sum_{i=1}^{N}\left(\frac{\partial f}{\partial x_i}u(x_i)\right)^2 + 2\sum_{i=1}^{N-1}\sum_{j=i+1}^{N}\left(\frac{\partial f}{\partial x_i}\right)\left(\frac{\partial f}{\partial x_j}\right)u(x_i)u(x_j)r(x_i,x_j)} \quad (2)$$

The operator performing a fan pressurization test is interested in the uncertainty in the air flow rate and its derived quantities. In this context, each step of the protocol can be associated to various sources of error that propagate from step to step:

1. Measure ($\Delta p_m$; $q_m$) couples;
2. Transform measured couples to envelope couples ($\Delta p_e$; $q_e$), including inside-outside temperature difference and zero-flow pressure;
3. Compute ($\ln(\Delta p_e)$; $\ln(q_e)$) couples;
4. Perform linear regression to obtain air flow exponent (n) and coefficient ($C_{env}$);
5. Compute the variable of interest (e.g., $Q_{50}$, $n_{50}$ or $Q_4$, depending on the case).

Therefore, the uncertainty in measurements (i.e., pressure difference, air flow rate and temperature) must be propagated to the logarithm of the envelope pressure difference and airflow (i.e., $\ln(\Delta p_e)$ and $\ln(q_e)$), which are then used to perform the linear regression. Delmotte investigated in depth these multiple propagations and developed the relevant equations in previous research [20]. These equations are not discussed in this paper. However, in the study of Delmotte, only the uncertainty due to equipment accuracy and resolution was considered. That work was completed with another study by Delmotte where values for the uncertainty due to the zero-flow pressure hypothesis were suggested [18].

In this paper, the uncertainty due to the zero-flow pressure hypothesis was assumed uncorrelated with the uncertainty due to the accuracy and resolution of the equipment. This seems a reasonable hypothesis since the characteristics of the equipment are not expected to vary when testing conditions are within the oper-

ating range. Therefore, the total uncertainty in pressure measurement can be computed using Eq. (3):

$$u_p(\Delta p) = \sqrt{u_{p,m}^2(\Delta p) + u_{p,m}^2(\Delta p_{0,a}) + (\Delta p_{0,m})} \quad (3)$$

With, $u_p(\Delta p)$ the uncertainty in envelope pressure, $u_{p,\,m}(\Delta p)$ the uncertainty in pressure difference measurement due to the equipment, $u_{p,\,m}(\Delta p_{0,\,a})$ the uncertainty in pressure difference measurement due to short-term variations in wind-induced pressure, and $u_{p,\,m}(\Delta p_{0,\,m})$ the uncertainty in zero-flow pressure measurement due to the equipment.

Then, the uncertainty in air flow exponent ($n$) and air flow coefficient ($C_{env}$) must be computed. They depend on the uncertainties in $\ln(\Delta p_i)$ and $\ln(q_i)$, but also on the regression technique used. The choice of regression technique depends on its objective and on the uncertainty in the variables used to perform the regression [22]. Three different regression techniques are described in this section. The equations regarding regression parameters estimation and uncertainty calculation are provided in the Appendix.

In airtightness measurements, the most used method for linear regression is the Ordinary Least Square (OLS) method. OLS aims at minimizing the differences between the regression line and the $y$ coordinate of the points used to perform the regression (i.e., the vertical difference between regression line and measurements). This method is expected to provide a reliable calculation of parameter uncertainty when only one variable is subject to constant errors [22]. These assumptions (i.e., only one variable with errors and constant errors) are questioned by several authors [17–19]. The uncertainty in regression parameters with the OLS method can be computed on the basis of two approaches: based on calculated uncertainty in the $y$-variable; or, based on the distance between the regression line and the $y$ coordinate of the measurements (see Appendix for calculation details). The uncertainty in $y$-variable is calculated based on assumptions regarding sources of uncertainty in the air flow rate measurement (e.g., error in the equipment, see Section 2.2.1). The second approach is often used in practice since it is easy to compute and does not require assumptions from the operator. In this study, OLS-1 refers to a calculation based on sources of error and OLS-2 to a calculation based on the distance between the regression line and the $y$-coordinates of the measurements.

The constant uncertainty assumption can be removed by weighting the measurements that are subject to errors (i.e., $w_i x_i$ or $v_i y_i$ instead of $x_i$ or $y_i$). These weights depend on the uncertainty in each measurement. Therefore, one can use the Weighted Least Square (WLS) instead of the OLS method to consider non-constant uncertainties. This improved method is not discussed here since it still assumes that the uncertainty in the $x$ variable is negligible. However, the weighting of variables can be used with any method to remove the constant uncertainty constraint.

In 2013, Okuyama and Onishi suggested the use of the Iterative Weighted Least Square (IWLS) method in the context of building airtightness [19]. ISO/TS 28037:2010 developed the mathematics related to this method [24]. Unlike OLS and WLS, the IWLS method allows for non-constant uncertainty in both variables. This method consists in minimizing the sum of distances between the line and the $x$ and $y$ coordinates, when both variables are weighted based on their uncertainty [25]. Since the minimization of this sum has no analytical solution, an iterative approach must be used to solve the problem [26].

The Weighted Line of Organic Correlation (WLOC) method was suggested in 2017 [18]. Similar to IWLS, WLOC allows for non-constant uncertainties in both variables. The method consists in minimizing the product of the distances between the $x$ and $y$ coordinates and the line, when both variables are weighted. Although equations are more complex than IWLS, WLOC does not demand an iterative procedure. Therefore, it requires fewer computing resources and, contrary to the iterative process, it does not present any risk of non-convergence.

Each regression technique provides uncertainty in regression parameters (i.e., $u_{th}(n)$ and $u_{th}(c)$) and the correlation coefficient between both parameters (i.e., $r_{th}(n,\ c)$). These values are then combined with Eq. (4) [20] to obtain the uncertainty in air flow rate at a given pressure in pressurization or depressurization (i.e., $u_{th}(Q_{\Delta p\ \pm})$). In this equation, $T$ is the recorded temperature (external and internal temperature for depressurization and pressurization, respectively), $T_0$ is the reference temperature (i.e., 293.15 K) and $u_{th}(T)$ is the uncertainty in temperature measurement. In this equation, $c$ refers to the intercept of the regression line with the $y$ axis and is directly used in the calculations. However, the following section of this paper refers to the air flow coefficient $C_{env}$ (that is defined as $e^c$) instead of $c$. This is because $c$ is never mentioned in measurement protocols and is only useful when dealing with uncertainty calculations.

$$u_{th}(Q_{(\Delta p\pm)}) = \sqrt{\begin{aligned}&(e^c \Delta p^n (T_0/T)^{(1-n)} ln(\Delta pT/T_0) u_{th}(n))^2 \\ &+ (e^c \Delta p^n (T_0/T)^{(1-n)} u_{th}(c))^2 \\ &+ (e^c(a-1))/T \Delta p^n (T_0/T)^{(1-n)} u_{th}(T))^2 \\ &+ 2(e^c \Delta p^n (T_0/T)^{(1-n)})^2 ln(\Delta pT/T_0) u_{th}(n) u_{th}(c) r(n,c)\end{aligned}} \quad (4)$$

Lastly, since the total air flow rate at a given pressure is obtained by averaging airflow in pressurization and depressurization at that pressure, uncertainty in $Q_{\Delta p}$ is obtained with Eq. (5).

$$u_{th}\left(Q_{\Delta p}\right) = \sqrt{\frac{u_{th}^2\left(Q_{\Delta p\ -}\right)}{4} + \frac{u_{th}^2\left(Q_{\Delta p\ +}\right)}{4}} \quad (5)$$

## 3. Results

### 3.1. Observed uncertainty

#### 3.1.1. Air flow rate at 5, 50 and 100 Pa

Table 2 presents the mean values of air flow rate based on 30 tests, at pressure differences of 5, 50 and 100 Pa, in both pressurization and depressurization, and using the OLS, IWLS and WLOC methods.

Since the distribution of these data was not significantly different from normal (no $p_{val} \leq 0.05$ for the Shapiro-Wilk tests), and since the same set of data was used to compare different regression techniques, paired t-tests were used to evaluate the statistical significance of differences in means. The tests showed that, in depressurization, none of the differences were statistically significant. In pressurization, there was a statistically significant difference between OLS and WLOC at 5 Pa ($t = -2.38$, $p_{val} = 0.024$) and 50 Pa ($t = -7.59$, $p_{val} < 0.001$), and between OLS and IWLS at 50 Pa ($t = -3.59$, $p_{val} = 0.001$). In average, there was a statistically significant difference between OLS and IWLS at 50 Pa ($t = -2.82$, $p_{val} = 0.009$) and between OLS and WLOC at 50 Pa ($t = -3.62$, $p_{val} = 0.001$). However, none of these differences was found to have an effect size of substantive magnitude (Cohen's $d < 0.2$) according to Cohen's thresholds [27]. Coherent with previous research from the authors [15], Cohen's $d$ was used as an estimation of the magnitude (effect size) of the differences detected since the standard deviation of different groups were roughly the same ($p_{val}$ from F-tests are lower than 0.05 for all comparisons) [28]. The thresholds proposed by Cohen [29] were used to infer the practical relevance of effects as these benchmarks are appropriate to use in the absence of previous knowledge in the area [15].

**Table 2**
Air flow rate (in m³/h) at 5, 50 and 100 Pa in pressurization (Q+), depressurization (Q−) and average ($Q_m$) for OLS, IWLS and WLOC methods.

| | OLS (in m³/h) | | | IWLS (in m³/h) | | | WLOC (in m³/h) | | |
|---|---|---|---|---|---|---|---|---|---|
| | $Q+$ | $Q-$ | $Q_m$ | $Q+$ | $Q-$ | $Q_m$ | $Q+$ | $Q-$ | $Q_m$ |
| 5 Pa | 55.0 | 46.7 | 50.9 | 54.8 | 47.1 | 51.0 | 55.8 | 46.7 | 51.3 |
| 50 Pa | 280.0 | 225.7 | 252.8 | 280.5 | 225.6 | 253.1 | 280.3 | 225.6 | 252.9 |
| 100 Pa | 457.3 | 363.1 | 410.2 | 458.7 | 361.8 | 410.2 | 455.9 | 362.1 | 409.0 |

**Table 3**
Mean and standard deviation of the regression parameters for the 30 tests in both pressurization and depressurization, using three regression techniques.

| | OLS | | IWLS | | WLOC | |
|---|---|---|---|---|---|---|
| | Mean | Deviation | Mean | Deviation | Mean | Deviation |
| $n_+$ | 0.71 | 0.033 | 0.71 | 0.021 | 0.70 | 0.023 |
| $n_-$ | 0.69 | 0.039 | 0.68 | 0.016 | 0.68 | 0.017 |
| $C_{env,+}$ | 17.60 | 2.58 | 17.43 | 1.79 | 17.92 | 1.96 |
| $C_{env,-}$ | 15.48 | 2.40 | 15.65 | 1.02 | 15.56 | 1.14 |

### 3.1.2. Regression parameters

Table 3 presents the mean values and standard deviations of the regression parameters for different regression techniques in both pressurization and depressurization.

Paired t-tests showed that, in pressurization, the mean values of both $n$ and $C_{env}$ were significantly different between OLS and WLOC ($t = 2.48$, $p_{val} = 0.019$ for $n$ and $t = -2.56$, $p_{val} = 0.016$ for $C_{env}$). In depressurization, no statistically significant differences were detected in the comparisons. To estimate the effect size, Glass's $\Delta$ was used instead of Cohen's $d$ since this coefficient can be utilized when groups have different standard deviation but the same sample size [28]. None of the comparisons was found having an effect of substantive magnitude according to Cohen's benchmark ($d < 0.2$) [27]. Regarding the standard deviation, in depressurization, the difference between OLS and IWLS was found to be statistically significant for both $n$ and $C_{env}$ ($F = 6.04$, $p_{val} < 0.001$ and $F = 5.77$, $p_{val} < 0.001$). Significant differences in standard deviation were also detected between OLS and WLOC ($F = 5.05$, $p_{val} < 0.001$ and $F = 4.74$, $p_{val} < 0.001$). In pressurization, the difference between OLS and IWLS was found to be statistically significant for both $n$ and $C_{env}$ ($F = 2.33$, $p_{val} = 0.026$ and $F = 2.13$, $p_{val} = 0.046$), but not for the comparison between OLS and WLOC.

### 3.1.3. Standard deviation of air flow rate at a given pressure difference

Information on the standard deviation of regression parameters cannot be used to draw conclusions on the standard deviation of air flow rate because of the strong correlation between $n$ and $C_{env}$ [20]. To obtain these values, the standard deviation of the air flow rate at each pressure difference needs to be estimated (Fig. 2).

Fig. 2 shows that the standard deviation of the air flow rate around the centroid of the pressure measurement (in this case, around 50 Pa) is equivalent irrespective of the regression technique. In addition, the figure shows that using the OLS method leads to a higher standard deviation for air flow rates estimated away from the centroid pressure differences than using IWLS or WLOC.

Table 4 presents the standard deviation of air flow rates at 5, 50 and 100 Pa used to draw the figure. These values show that averaging pressurization and depressurization seems to reduce the standard deviation (i.e., standard deviation of $Q_m$ seems lower than standard deviation of $Q_+$ and $Q_-$ separately). This was expected since Eq. (2) shows that, when making the mean of two quantities with similar uncertainty, the uncertainty of the mean is lower than the uncertainty of individuals. Furthermore, looking at pressurization and depressurization separately shows that the uncertainty in IWLS and WLOC is lower than OLS when air flow rates are estimated away from the centroid pressure difference. However, results differ between modes. This is because standard deviations are expressed in%, and the air flow rates in pressurization and depressurization are different. Moreover, wind conditions cannot be kept identical between pressurization and depressurization tests.

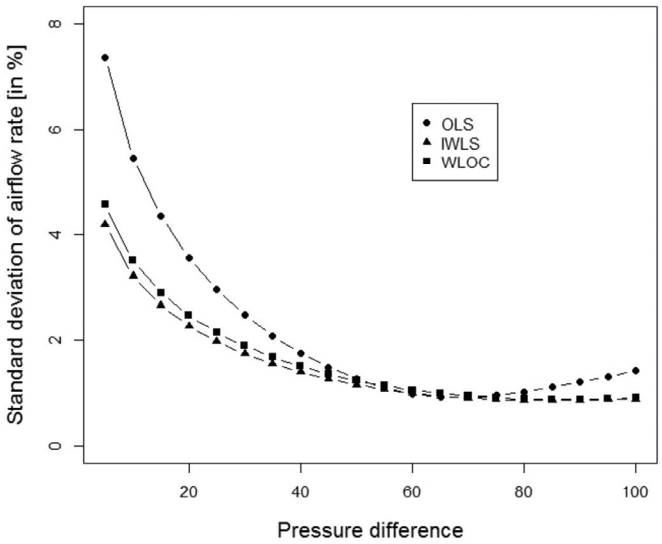



**Fig. 2.** Standard deviation of air flow rate (in%) at multiple pressure differences for the OLS, IWLS and WLOC methods.

## 3.2. Theoretical calculation of uncertainty

### 3.2.1. Uncertainties in envelope pressure difference ($ln(\Delta \mathbf{p_i})$) and in air flow rate through the building envelope ($ln(\mathbf{q_i})$)

Manufacturers often provide values for accuracy and resolution of their measurement equipment. These are usually expressed as maximum permissible error or 95% confidence interval. This study assumed that the information provided by the manufacturer (Section 2.1.2) corresponded to the maximum permissible error for both the manometer and the thermometer. In 2013, Delmotte proposed equations to determine the uncertainty in $x_i = \ln(\Delta p_i)$ and $y_i = \ln(q_i)$ based on the uncertainty in pressure difference, air flow rate, and temperature measurements [20]. Another study by Prignon et al. suggested that the uncertainty due to zero-flow pressure approximation is a constant value (the same for all the couples measured during a test) that depends on the standard deviation and the duration of the zero-flow pressure measurement (Table 5) [17]. These values were considered in the calculations performed in this study.

### 3.2.2. Error propagation

The equations presented in the Appendix were used on each test to compute the uncertainty in regression parameters and in air flow rate at a given pressure. Table 6 presents the mean values

**Table 4**
Standard deviation of air flow rate (in%) for depressurization, pressurization and average at 5, 50 and 100 Pa for OLS, IWLS and WLOC methods.

| | OLS | | | IWLS | | | WLOC | | |
|---|---|---|---|---|---|---|---|---|---|
| | $Q_+$ | $Q_-$ | $Q_m$ | $Q_+$ | $Q_-$ | $Q_m$ | $Q_+$ | $Q_-$ | $Q_m$ |
| 5 Pa | 9.40% | 9.39% | 7.37% | 6.72% | 4.14% | 4.18% | 7.19% | 4.60% | 4.56% |
| 50 Pa | 2.04% | 1.85% | 1.27% | 1.91% | 1.81% | 1.16% | 2.00% | 1.83% | 1.23% |
| 100 Pa | 1.29% | 2.95% | 1.42% | 1.16% | 2.08% | 0.89% | 1.16% | 2.08% | 0.90% |

**Table 5**
Uncertainty in zero-flow pressure approximation ($\boldsymbol{u}(\Delta \boldsymbol{p}_{0,a})$) as a function of the duration and the standard deviation ($\boldsymbol{\sigma}(\Delta \boldsymbol{p}_0)$) of zero-flow pressure measurements [17].

| | 30 s | 60 s | 90 s | 120 s |
|---|---|---|---|---|
| $\sigma(\Delta p_0) < 1$ | 0.45 Pa | 0.44 Pa | 0.43 Pa | 0.42 Pa |
| $1 < \sigma(\Delta p_0) < 2$ | 0.91 Pa | 0.81 Pa | 0.80 Pa | 0.80 Pa |
| $\sigma(\Delta p_0) > 2$ | 1.52 Pa | 1.46 Pa | 1.39 Pa | 1.39 Pa |

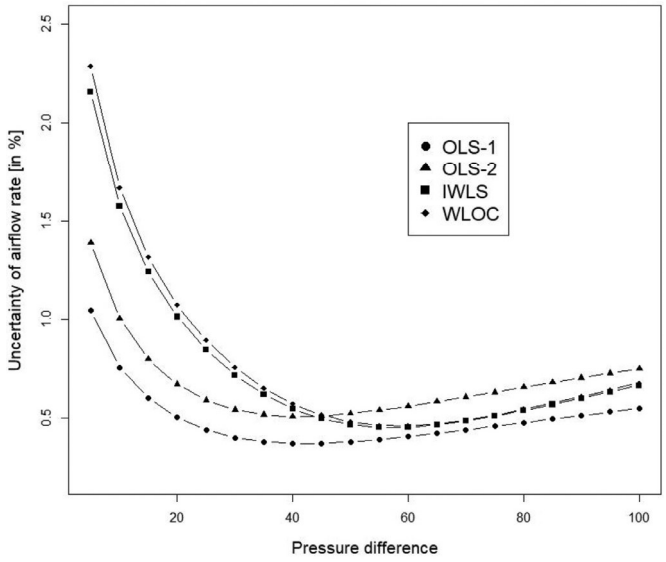



**Fig. 3.** Calculated uncertainty of air flow rate (in%) at multiple pressure differences for OLS-1, OLS-2, IWLS and WLOC methods.

of regression parameters and the mean of their calculated uncertainty for both pressurization and depressurization. These results show that the calculated uncertainties in regression parameters are similar between IWLS and WLOC, and are higher than the OLS-2 and OLS-1 methods.

Due to the high correlation between regression parameters [20], it is important to draw the conclusions based on the uncertainty of the air flow rate. Fig. 3 presents the mean calculated uncertainty in airflow rate at multiple pressure differences, for different regression techniques.

The figure shows that the IWLS and WLOC methods provide close results in terms of uncertainty calculation and are higher than the OLS-1 and OLS-2 methods. Paired t-tests show that all the comparisons (i.e., OLS-1 vs OLS-2, OLS-1 vs IWLS, OLS-1 vs. WLOC, OLS-2 vs. IWLS, OLS-2 vs. WLOC and IWLS vs WLOC) are highly statistically significant. However, when comparing IWLS and WLOC, all the computed Glass's $\Delta$ were below 0.2, meaning an effect of non-substantive magnitude according to Cohen's benchmarks. In addition, the graph presents a gap between the OLS-1 and OLS-2 lines, this highlighting an issue either in the suitability of the OLS method or in the assumptions about uncertainties in $\ln(q_e)$. This observation is confirmed by measuring the effect size since all Glass's $\Delta$ values are higher than 3.5 (large effect for values higher than 0.8 according to Cohen's benchmarks).

### *3.3. Comparison between in-situ observation and theoretical calculation of uncertainty*

#### *3.3.1. Comparison of regression parameters*

Figs. 4 and 5 show, for $n$ and $C_{env}$ respectively, the comparison between the calculated (solid lines) and observed (dotted lines) uncertainty in pressurization (grey zones) and depressurization (white zones) for each regression technique. Calculated uncertainties are mean averages of uncertainties calculated for 30 tests, while observed uncertainties are the standard deviation of the regression parameters obtained for repeated tests.

The comparison shows that the calculated uncertainties with the IWLS and WLOC methods fit better the observed uncertainty than when using the OLS method, whatever the mode (i.e., pressurization and depressurization) and the regression parameter. In addition, it shows that, even in the best case, there is still a gap between calculated and measured uncertainty, meaning that assumptions on uncertainty are not yet representing the reality.

#### *3.3.2. Comparison of air flow rate at multiple pressure differences*

Fig. 6 shows the uncertainty observed with OLS, IWLS and WLOC, and the uncertainties calculated with the OLS-1, OLS-2, IWLS and WLOC methods.

This comparison shows that, regardless of the regression technique utilized, the calculated uncertainty always underestimates the observed uncertainty, especially away from the centroid. In fact, the differences between calculated and observed uncertainties at 5, 50 and 100 Pa are 6.3%, 0.7% and 0.9% for OLS-1, and 6.0%,

**Table 6**
Value and calculated uncertainty of both regression parameters for the theoretical case in both pressurization and depressurization for the four cases (OLS-1, OLS-2, IWLS and WLOC).

| | OLS-1 | | OLS-2 | | IWLS | | WLOC | |
|---|---|---|---|---|---|---|---|---|
| | Val | Unc | Val | Unc | Val | Unc | Val | Unc |
| $n_+$ | 0.71 | 0.007 | 0.71 | 0.011 | 0.71 | 0.012 | 0.70 | 0.013 |
| $n_-$ | 0.69 | 0.006 | 0.69 | 0.010 | 0.68 | 0.012 | 0.68 | 0.013 |
| $C_{env,+}$ | 17.60 | 0.44 | 17.60 | 0.60 | 17.43 | 0.85 | 17.92 | 0.91 |
| $C_{env,-}$ | 15.48 | 0.37 | 15.48 | 0.55 | 15.65 | 0.79 | 15.56 | 0.84 |

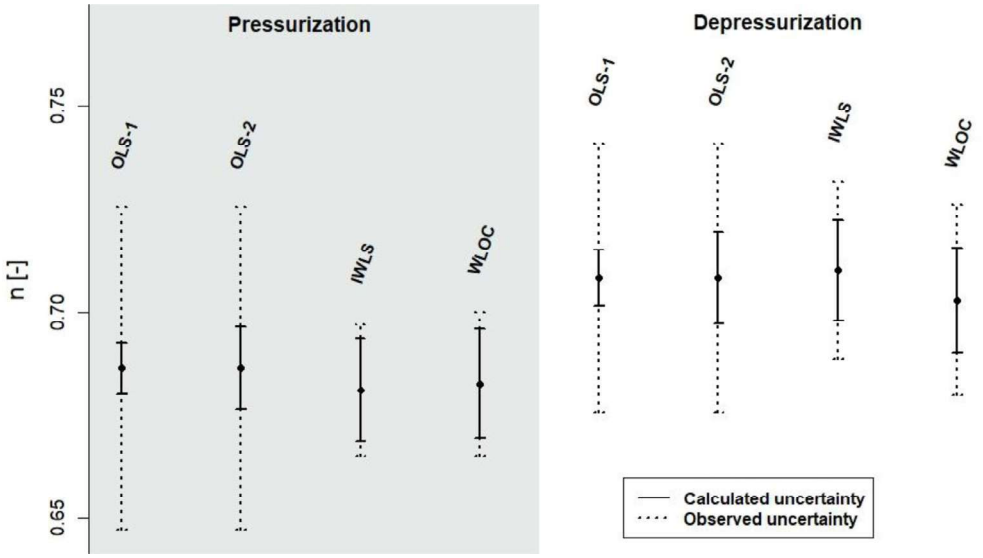



**Fig. 4.** Comparison between calculated (solid lines) and observed (dotted lines) uncertainty in pressurization and depressurization for $n$ values.

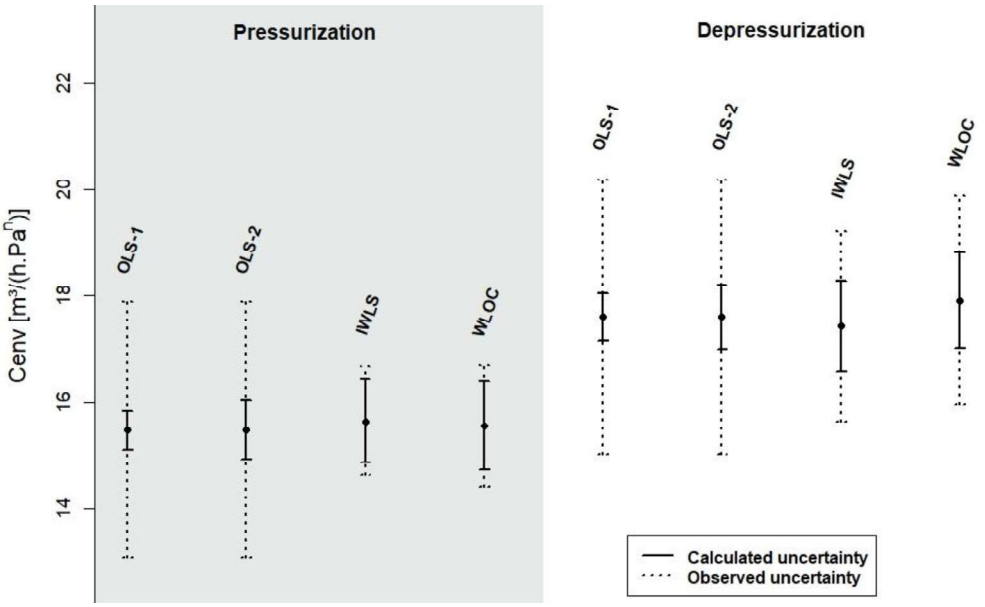



**Fig. 5.** Comparison between calculated (solid lines) and observed (dotted lines) uncertainty in pressurization and depressurization for $C_{env}$ values.

**Table 7**
Visualization of the results presented in Fig. 6 applied to a virtual case ($\boldsymbol{C} = 20$ and $\boldsymbol{n} = 0.67$).

| | at 5 Pa | at 50 Pa | at 100 Pa |
|---|---|---|---|
| Observed OLS | 59 ± 4.33 | 275 ± 3.49 | 438 ± 6.21 |
| Calculated OLS-1 | 59 ± 0.63 | 275 ± 1.57 | 438 ± 2.28 |
| Calculated OLS-2 | 59 ± 0.81 | 275 ± 1.84 | 438 ± 3.15 |
| Observed IWLS | 59 ± 2.46 | 275 ± 3.19 | 438 ± 3.89 |
| Calculated IWLS | 59 ± 1.28 | 275 ± 1.27 | 438 ± 3.02 |
| Observed WLOC | 59 ± 2.68 | 275 ± 3.38 | 438 ± 3.94 |
| Calculated WLOC | 59 ± 1.33 | 275 ± 1.46 | 438 ± 3.06 |

0.6% and 0.7% for OLS-2. These differences are lower when looking at IWLS and WLOC: at 5, 50 and 100 Pa these are, respectively, 2.0%, 0.7% and 0.2% for IWLS, and 2.3%, 0.7% and 0.2% for WLOC. Table 7 provides the example of a virtual case ($C = 20$ [m³/(h.Pa$^n$)], $n = 0.67$ [-]) in order to visualize the relevance of these results in the determination of airflow values.

The better fit between observed and calculated uncertainty using the IWLS and WLOC methods was expected since these methods allow to consider uncertainty in pressure difference, including the uncertainty due to the zero-flow pressure hypothesis that is known to have an important impact on the reliability of fan pressurization measurements.

Fig. 7 presents, for each test, the air flow rate at 5 (a, c and e) and 50 (b, d and f) Pa and their calculated expanded uncertainty for the OLS (a and b), IWLS (c and d) and WLOC (e and f) methods. These graphs allow to properly visualize the impact of changing the regression technique on the variability of the results and the estimation of their uncertainty. On the graphs: the crosses represent the airflows determined for each test; the error bars provide the calculated expanded uncertainty; and, the colored zones show the observed expanded uncertainty applied on the average value of the 30 estimated airflows. The expanded uncertainty is obtained by multiplying the uncertainty by a coverage factor ($k$). This defines a confidence interval $(y - k.u(y); y + k.u(y))$, which may be expected

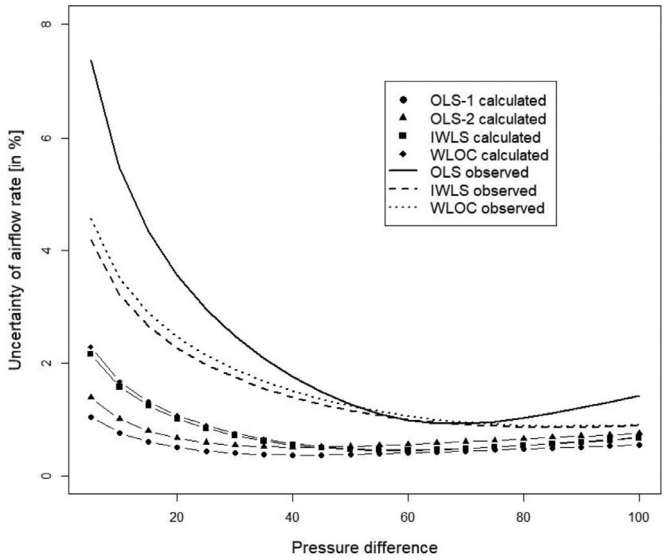



**Fig. 6.** Observed and calculated uncertainties in airflow rate as a function of pressure difference for different regression techniques.

to include large part (depending on the coverage factor) of the distribution of values that could be attributed to the measured quantity. The coverage factor used in Fig. 7 is 2, and it corresponds to a confidence interval of 95% [9]. If calculated and observed uncertainty are close, the size of the observed (i.e., colored zone) and calculated (i.e., error bars) expanded uncertainty should be of the same order of magnitude.

Fig. 7 confirms previous findings by illustrating that, at 50 Pa, the results of the three methods are equivalent and all underestimate the real uncertainty. For most tests, the 95% confidence interval calculated for each test is far from including 95% of the test results as it should for a robust estimation of the uncertainty. However, at 5 Pa there are strong differences between the OLS, IWLS and WLOC methods. In fact, real confidence intervals (colored zones) are much larger when using OLS with respect to the IWLS and WLOC methods. In addition, the 95% confidence intervals (error bars) calculated with IWLS and WLOC include much more test results than when computed with the OLS method. Consequently, the IWLS and WLOC methods provide a much better estimation of the uncertainty than OLS at low pressure difference. However, even with IWLS and WLOC calculations at 5 Pa, the calculated expanded uncertainty is still underestimating the observed 95% confidence interval.

## 4. Discussion

The limitations of the OLS regression technique in the context of airtightness measurements have long been recognized in the literature [15]. Research on other regression methods has intensified over the last years [10,19,20], assuming further relevance in light of recent studies that quantified the uncertainty in pressure difference due to the zero-flow pressure approximation [16,17]. Consistent with these scientific developments, this paper sought to quantify the impact of changing regression technique when including the uncertainty due to the zero-flow pressure hypothesis in the calculations.

The first part of the results (Section 3.1 – observed uncertainty) showed that changing the regression method has no effect on the mean average value of the air flow rate, whatever the pressure difference. However, it has an impact on the standard deviation of the air flow rate when the pressure difference is away from the centroid of the measurements. Also, the regression method has a statistically significant impact on the standard deviation of regression parameters. In fact, using the IWLS or WLOC methods rather than OLS leads to lower standard deviation in regression parameters and air flow rates at pressure differences away from the centroid of the measurements. This suggests that the OLS regression technique could still be used when looking at the airflow rate at 50 Pa, but only if the pressure sequence is chosen appropriately (i.e., having 50 Pa as the centroid of the measurements). In all other cases, other methods are likely to provide outcomes that are more robust. On these basis, the first part of the results presented in this paper can have some important implications in practice, especially in countries where airflow at low- or high-pressure difference is used in the regulations [30].

The second part of the results (Section 3.2 – calculated uncertainty) provided evidence that the uncertainty in $\ln(\Delta p_e)$ should not be neglected, especially on windy days where the uncertainty due to the zero-flow pressure hypothesis is important. This strengthens the view, shared by many authors, that the OLS method is not appropriate for determining the uncertainty in airtightness estimation [15,18–20]. Indeed, by neglecting the uncertainty in pressure difference, the OLS method disregards an important part of uncertainty due to variations in wind speed, which are known to have a relevant impact on uncertainty in airtightness estimation [15].

The third part of the results (Section 3.3 – uncertainty comparison) showed that, in terms of regression parameters and air flow rate, the IWLS and WLOC methods provide a more robust estimation of uncertainty than OLS-1 and OLS-2. However, although the uncertainty calculated with the IWLS and WLOC methods fits better the 'real' uncertainty, they are still underestimating its 'true' value.

On the basis of these findings, the authors suggest that the IWLS and WLOC methods should be preferred over the OLS method since they can offer more reliable results, except when looking at values of air flow rate around the centroid of pressure measurements. This can have an important impact in practice since most simulation software use the OLS-2 method to obtain values for regression parameters and for an estimation of their uncertainty from measurements. In addition, the WLOC method should be preferred over IWLS in order to avoid an iterative process, hence enabling a more robust computation procedure (i.e., no risk of non-convergence) and requiring fewer computing resources.

Before generalizing the results obtained in this research, some limitations should be acknowledged. First, the data analysed in this paper were obtained from only one apartment that cannot represent the entire building stock. Since uncertainty components vary from one building to another, a change of configuration could also alter the results of the analysis. Even if trends in the findings are expected to remain the same, their magnitude could be affected. Also, this study identified only part of the sources of error that could be encountered during a fan pressurization test. Other sources that can lead to uncertainty (e.g., the position of inside and outside pressure taps) were not considered in this study.

While this paper has discussed the impact of regression techniques on precision errors, it is important to notice that such techniques do not reduce bias error. Since it is not possible to calibrate on-site airtightness tests, bias is supposed to be limited by respecting the requirements of measurement standards (e.g. ISO 8872:2015 [21]). This issue is still open for more research. Also, since the flow exponent is not constant, and depends on the pressure difference [15,31], it can be expected that giving more weight to high pressure measurements (IWLS and WLOC regression techniques) may introduce bias error. This issue is linked to the very basic choice of the flow modelling and it was not investigated in this study.

Lastly, in this study authors have investigated two alternative regression methods (i.e., IWLS and WLOC) related to fan pressur-

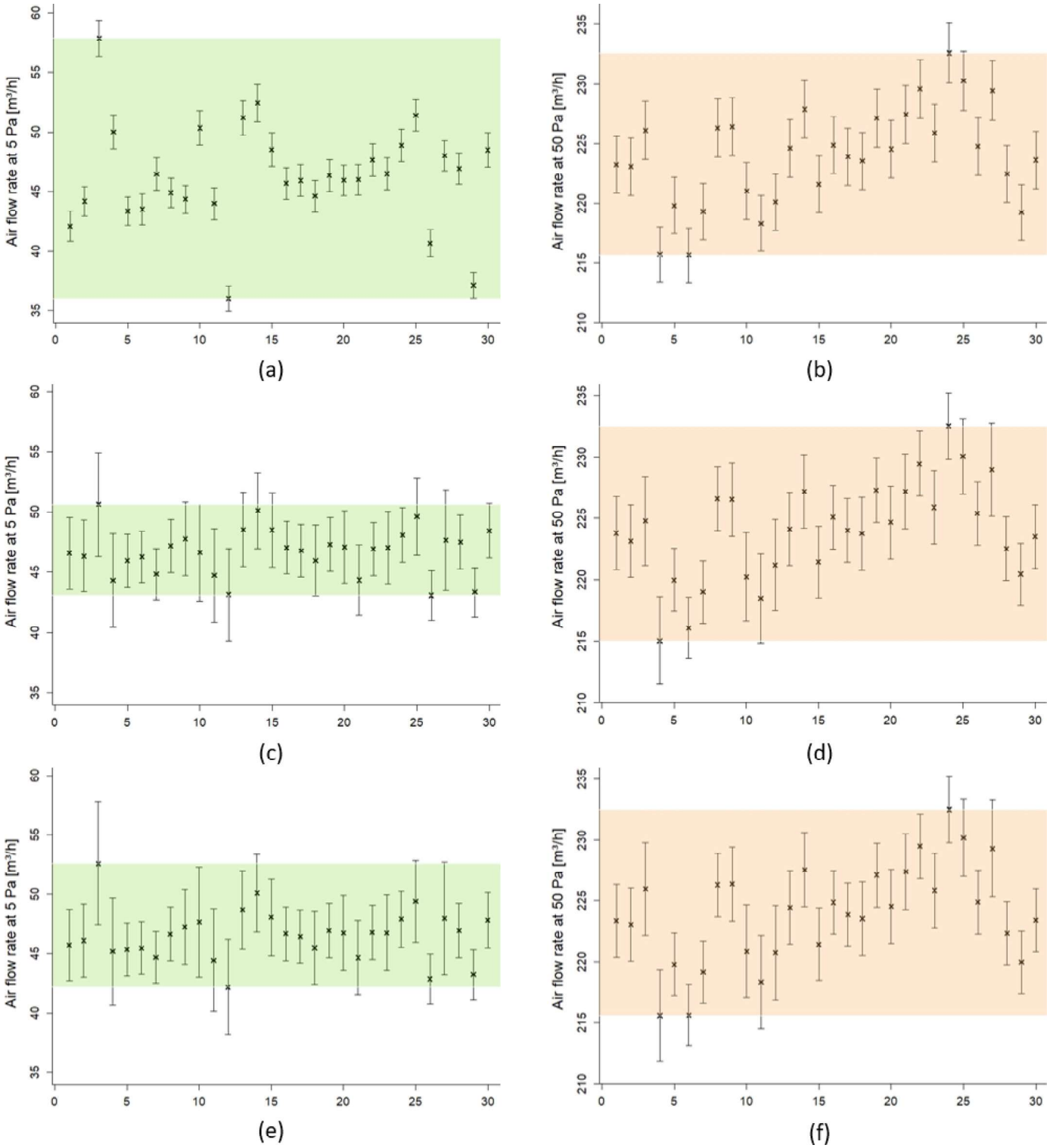



**Fig. 7.** Values, for each test, of the air flow rate at 5 (a, c and e) and 50 Pa (b, d and f) and calculated expanded uncertainty ($k = 2$) for OLS (a and b), IWLS (c and d) and WLOC (e and f) methods.

ization tests that have been already studied in the literature and that are consistent with the procedures required by current standards [21]. However, other methods could be explored to calculate and/or reduce the uncertainty resulting from fan pressurization measurements. among these are the Weighted Least Normal Square (WLNS) method, and the application of Bayesian statistics. The WLNS method consists in minimizing the normal distance (i.e., the perpendicular line) between the measurements and the regression line [22]. Conversely, the use of Bayesian statistics involves a change of approach in the determination of measurement uncertainties. Conventional *frequentist* inference uses methods such as maximum likelihood estimation (MLE) to produce parameter estimates and standard errors, and test the statistical significance of parameters (e.g., null-hypothesis testing) or set a confidence interval around an estimate [32]. Under this approach, model parameters are regarded as fixed quantities and their values are estimated

from random variables (i.e., data). Conversely, in *Bayesian* inference, the data are treated as fixed and the model parameters are considered as random. Bayesian methods consider each unknown parameter to have an associated *posterior probability distribution* that describes the uncertainty about population parameter values. The target of the analysis consists in estimating the posterior distribution of parameters as the normalized product of a *prior distribution*, reflecting previous knowledge, and the *likelihood* provided by the data. This allows assigning probabilities to parameters, making the inferential framework more intuitive [33]. The Bayesian approach is thus markedly different from classical statistics, where the population parameter has one (unknown) value. Bayesian statistics considers a probability distribution of possible values for each unknown parameter and the uncertainty is expressed by assigning to it a prior probability distribution of possible values that is independent from the data. Once data have been collected, the prior is combined with the likelihood to produce a posterior distribution that, typically, has smaller variance than the prior, since observing the data reduced the uncertainty on the possible population values [34]. In the context of fan pressurization measurements, for example, Bayesian statistics could be used to determine probability distributions, instead of single values, for flow exponent and leakage coefficients.

## 5. Conclusion

This study investigated how a change in regression technique can affect the estimation of building airtightness and its uncertainty. Analysis of the measured uncertainty, the calculated uncertainty, and their comparison led to the following main findings:

- The IWLS, WLOC and OLS methods provide the same mean average value for the air flow rate, whatever the pressure difference. The three methods result in the same standard deviation (i.e., observed uncertainty) for the air flow rate at pressure differences close to the centroid of the measurement (in this case, 50 Pa).
- Compared to OLS, the IWLS and WLOC methods reduce the standard deviation of $n$ in pressurization (from 0.033 to 0.021 for IWLS, and to 0.023 for WLOC) and in depressurization (from 0.039 to 0.016 for IWLS, and to 0.017 for WLOC). They also reduce the standard deviation of $C_{env}$ in both pressurization (from 0.143 to 0.098 for IWLS, and to 0.106 for WLOC) and depressurization (from 0.158 to 0.066 for IWLS, and to 0.072 for WLOC).
- The IWLS and WLOC methods lead to lower uncertainty than OLS for the air flow rate at a pressure away from the centroid of the measurements (4.18% and 4.56% instead of 7.37% at 5 Pa, and 0.89% and 0.90% instead of 1.42% at 100 Pa).
- Theoretical calculations using IWLS and WLOC methods provide a better estimate of the 'reference uncertainty' (i.e., the observed uncertainty) than using the OLS method. In this study, the differences between calculated and observed uncertainty of air flow rate estimated at 5, 50 and 100 Pa, were: 6.3%, 0.7% and 0.9% for OLS-1; 6.0%, 0.6% and 0.7% for OLS-2; 2.0%, 0.7% and 0.2% for IWLS; and 2.3%, 0.7% and 0.2% for WLOC.

Based on these findings, the authors suggest that IWLS or WLOC should be preferred over the most used OLS method. However, some constraints were identified in this study, highlighting relevant further work needed in the field of uncertainty in fan pressurization measurements. In fact, to generalize the findings, similar studies should be performed on buildings that experience different wind exposures and air flow rates of different magnitude. Then, other sources of errors (e.g., the position of inside and outside pressure taps) should also be investigated both in theory (calculations) and in practice (repeated tests) due to the gap that is still detected between observed and calculated uncertainty. This would allow to define a more complete and relevant model to deepen our fundamental understanding of uncertainty in fan pressurization tests. Further issues (i.e., bias in leakage exponent and in airflow at low pressure due to a change in regression technique) and methods for parameter estimation (i.e., WLNS, Bayesian statistics, etc.), not included in this study, could be relevant for future research.

## Declaration of Competing Interest

I wish to confirm that there are no known conflicts of interest associated with this publication and there has been no significant financial support for this work that could have influenced its outcome.

I confirm that the manuscript has been read and approved by all named authors and that there are no other persons who satisfied the criteria for authorship but are not listed. I further confirm that the order of authors listed in the manuscript has been approved by all of the authors.

I confirm that I have given due consideration to the protection of intellectual property associated with this work and that there are no impediments to publication, including the timing of publication, with respect to intellectual property. In so doing I confirm that I have followed the regulations of authors institutions concerning intellectual property.

I understand that I am (Corresponding Author) the sole contact for the Editorial process (including Editorial Manager and direct communications with the office). I am responsible for communicating with the other authors about progress, submissions of revisions and final approval of proofs. I confirm that I have provided a current, correct email address which is accessible by the Corresponding Author.

## CRediT authorship contribution statement

**Martin Prignon:** Conceptualization, Methodology, Software, Formal analysis, Investigation, Writing - original draft, Writing - review & editing, Visualization. **Christophe Delmotte:** Conceptualization, Software, Formal analysis. **Arnaud Dawans:** Methodology, Resources, Funding acquisition. **Sergio Altomonte:** Supervision, Formal analysis. **Geoffrey van Moeseke:** Resources, Funding acquisition, Project administration.

## Acknowledgment

This study was supported by an INNOVIRIS grant (2016-DOCT-09) awarded to the first author his PhD project at Architecture et Climat, UCLouvain. The tests were performed on a site from Entreprises Jacques Delens S.A.

## Appendix. Determination of Slope ($a$) and Intercept ($b$) for Different Regression Techniques

This Appendix provides the equations used to determine the regression parameters (i.e., slope $a$ and intercept $b$), the uncertainty of these parameters (i.e., $u(a)$, $u(b)$), and their correlation coefficient (i.e., $r(a, b)$) for the three methods studied in this paper. In the interest of simplification, $\Sigma x_i$ is used for $\sum_{i=1}^{N} x_i$. When relevant (i.e., for methods considering uncertainty in both variables), the calculations were developed assuming that uncertainties in both variables were uncorrelated. This hypothesis is acceptable since uncertainty in $\ln(q)$ is almost constant. Table 8 summarizes the symbols used in the equations of this Appendix and their definition.

**Table 8**
Symbols used in equations for OLS, IWLS and WLOC, and their definition.

| Symbol | Definition |
|---|---|
| $a$ and $b$ | Parameters of interest, respectively the slope and the intercept. |
| $u(a)$ and $u(b)$ | Uncertainties related to each parameter. |
| $r(a, b)$ | Correlation coefficient between both parameters. |
| $(x_i; y_i)$ | $x$ and $y$ coordinates for the $i_{th}$ measurement. For a fan pressurization test, these correspond to $\ln(\Delta p_i)$ and $\ln(q_i)$ respectively. |
| $N$ | Number of measurement used when performing the linear regression. |
| $s$ | Standard error of the regression. |
| $w(x_i)$ and $w(y_i)$ | Weights applied to the $x$ and $y$ values of the $i_{th}$ measurement. These depends on the source of errors considered. |
| $W_i$ | General weight applied on each measurement considering that both coordinates are subject to uncertainties. |
| $U_i$ and $V_i$ | Distance between the coordinate for the $i_{th}$ measurement and the average of all measurements, respectively for $x$- and $y$- coordinates. |
| $\beta$ | This parameter has no specific definition; York et al. used it to simplify equations [25]. |
| $v_i$ and $w_i$ | Weights applied to the $x$ and $y$ values of the $i_{th}$ measurement. These depends on the source of errors considered. |
| $\Delta x$ and $\Delta y$ | These parameters have no specific definitions; Delmotte used them to simplify equations [18]. |
| $u(a+b)$ | Uncertainty of the sum of parameters of interest. |

*A1. – Ordinary least square method*

The OLS method consists in finding the best straight line that minimizes the differences between the regression line and the $y$-coordinate of the points used to perform the regression (i.e., the vertical difference between regression line and measurements). In order to be valid, the OLS formulas require uncertainties on the x and y coordinates to be respectively negligible and constant. When performing the OLS method, the regression parameters are given by Eqs. (6) and (7).

$$a = \frac{N\sum x_i y_i - \sum x_i \sum y_i}{N\sum x_i^2 - \left(\sum x_i\right)^2} \tag{6}$$

$$b = \frac{\sum x_i^2 \sum y_i - \sum x_i \sum x_i y_i}{N\sum x_i^2 - \left(\sum x_i\right)^2} \tag{7}$$

With this method, uncertainty in regression parameters $a$ and $b$ is theoretically computed with Eqs. (8) and (9) respectively, where $N$ is the number of points used for the regression, $x_i$ is the $x$-axis value for each point (i.e. $\ln(\Delta p_i)$), and $s^2$ is the variance. It can be computed in two ways. Either it is equal to 1 over the square of the uncertainty in the $y$-axis (i.e., $1/u^2(\ln(q_i))$, or it is computed as the sum of the square of the distance between the regression line and the $y$ coordinate of the points. The correlation coefficient is given by Eq. (10).

$$u(a) = \sqrt{\frac{Ns^2}{N\sum x_i^2 - \left(\sum x_i\right)^2}} \tag{8}$$

$$u(b) = \sqrt{\frac{s^2\sum x_i^2}{N\sum x_i^2 - \left(\sum x_i\right)^2}} \tag{9}$$

$$r(a, b) = \frac{-\sum x_i}{\sqrt{N\ \sum x_i^2}} \tag{10}$$

*A2. – Iterative weighted least square method*

The IWLS method consists in finding the best straight line that minimizes the sum of the distances between the line and the $x$ and $y$ coordinates, when both variables are weighted based on their uncertainty. Since the minimization of this sum has no analytical solution, an iterative approach must be used to solve the problem. Equations in this section are taken from the work of York et al. (2004) that developed the unified equations for the iterative weighted least square regression method [25]. When performing the IWLS method, the weights are computed first with Eqs. (11) and (12).

$$w(x_i) = \frac{1}{u^2(x_i)} \tag{11}$$

$$w(y_i) = \frac{1}{u^2(y_i)} \tag{12}$$

Then a value for the slope ($a$) is assumed, and Eqs. (13)–(19) are repeated until the change in slope between two iterations corresponds to the desired accuracy.

$$W_i = \frac{w(x_i)w(y_i)}{w(x_i) + a^2 w(y_i)} \tag{13}$$

$$\bar{x} = \frac{\sum_{i=1}^{N} W_i x_i}{\sum_{i=1}^{N} W_i} \tag{14}$$

$$\bar{y} = \frac{\sum_{i=1}^{N} W_i y_i}{\sum_{i=1}^{N} W_i} \tag{15}$$

$$U_i = x_i - \bar{x} \tag{16}$$

$$V_i = y_i - \bar{y} \tag{17}$$

$$\beta_i = W_i\left[\frac{U_i}{w(y_i)} + \frac{aV_i}{w(x_i)}\right] \tag{18}$$

$$a = \frac{\sum_{i=1}^{N} W_i \beta_i V_i}{\sum_{i=1}^{N} W_i \beta_i U_i} \tag{19}$$

Lastly, once the desired accuracy is reached, the second regression parameter is estimated using Eq. (20).

$$b = \bar{y} - a\bar{x} \tag{20}$$

Using this method, uncertainties in regression parameters are computed after the last iteration with Eqs. (21) and (22), and the correlation coefficient is given by Eq. (23).

$$u(a) = \sqrt{\frac{1}{\sum W_i\left(\beta_i - \bar{\beta}\right)^2}} \tag{21}$$

$$u(b) = \sqrt{\frac{1}{\sum W_i} + \left(\bar{x} + \bar{\beta}\right)^2 u^2(a)} \tag{22}$$

$$r(a, b) = -\frac{\frac{\sum W_i x_i}{\sqrt{\sum W_i}}}{\sqrt{\sum W_i x_i^2}} \tag{23}$$

*A3. – Weighted line of organic correlation*

The WLOC method consists in finding the best straight line that minimizes the product of the distances between the $x$ and $y$ coordinates and the line, when both variables are weighted. Although equations are more complex than with IWLS, WLOC does not demand an iterative procedure. Equations in this section come from the work of Delmotte [18]. Similar to IWLS, the first steps in the Weighted Line of Organic Correlation (WLOC) method consists in computing weights for both variables with Eqs. (24) and (25).

$$v_i = \frac{1}{u(x_i)} \tag{24}$$

$$w_i = \frac{1}{u(y_i)} \tag{25}$$

Then, the weights are directly used to compute both regression parameters with Eqs. (26) and (27).

$$a = \frac{\sqrt{\sum v_i w_i \sum v_i w_i y_i^2 - \left(\sum v_i w_i y_i\right)^2}}{\sqrt{\sum v_i w_i \sum v_i w_i x_i^2 - \left(\sum v_i w_i x_i\right)^2}} \tag{26}$$

$$b = \frac{\sum v_i w_i y_i - a \sum v_i w_i x_i}{\sum v_i w_i} \tag{27}$$

Uncertainty in the slope is given by Eqs. (28)–(30).

$$u(a) = \sqrt{\sum \left(\frac{\partial a}{\partial x_i}\right) \frac{1}{v_i^2} + \left(\frac{\partial a}{\partial y_i}\right) \frac{1}{w_i^2}} \tag{28}$$

$$\frac{\partial a}{\partial x_i} = \sqrt{\frac{\Delta y}{\Delta x}} \, \frac{\left(\sum v_j w_j x_j\right) v_i w_i - \left(\sum v_j w_j\right) v_i w_i x_i}{\Delta x} \tag{29}$$

$$\frac{\partial a}{\partial y_i} = \sqrt{\frac{\Delta y}{\Delta x}} \, \frac{\left(\sum v_j w_j\right) v_i w_i y_i - \left(\sum v_j w_j y_j\right) v_i w_i}{\Delta y} \tag{30}$$

Uncertainty in the intercept is given by Eqs. (31)–(33).

$$u(b) = \sqrt{\sum \left(\frac{\partial b}{\partial x_i}\right) \frac{1}{v_i^2} + \left(\frac{\partial b}{\partial y_i}\right) \frac{1}{w_i^2}} \tag{31}$$

$$\frac{\partial b}{\partial x_i} = a \left( \frac{-v_i w_i}{\sum v_j w_j} - \frac{\left(\sum v_j w_j x_j\right)^2 v_i w_i}{\Delta x \sum v_j w_j} + \frac{\left(\sum v_j w_j x_j\right) v_i w_i x_i}{\Delta x} \right) \tag{32}$$

$$\frac{\partial b}{\partial y_i} = \frac{v_i w_i}{\sum v_j w_j} - \frac{\left(\sum v_j w_j x_j\right) v_i w_i y_i}{\sqrt{\Delta x}\sqrt{\Delta y}} + \frac{\left(\sum v_j w_j x_j\right)\left(\sum v_j w_j y_j\right) v_i w_i}{\sqrt{\Delta x}\sqrt{\Delta y} \sum v_j w_j} \tag{33}$$

In all these equations, $\Delta x$ and $\Delta y$ are given by Eqs. (34) and (35) respectively.

$$\Delta x = \sum v_i w_i \sum v_i w_i x_i^2 - \left(\sum v_i w_i x_i\right)^2 \tag{34}$$

$$\Delta y = \sum v_i w_i \sum v_i w_i y_i^2 - \left(\sum v_i w_i y_i\right)^2 \tag{35}$$

Lastly, the correlation coefficient is given by Eq. (36) where $u^2(a+b)$ is given by Eq. (37).

$$r(a,b) = \frac{u^2(a+b) - u^2(a) - u^2(b)}{2\, u(a)\, u(b)} \tag{36}$$

$$u^2(a+b) = \sum \left( \frac{\partial a}{\partial x_i} + \frac{\partial b}{\partial x_i} \right)^2 \frac{1}{v_i} + \left( \frac{\partial a}{\partial y_i} + \frac{\partial b}{\partial y_i} \right)^2 \frac{1}{w_i} \tag{37}$$

## References


[1] J. Jokisalo, J. Kurnitski, M. Korpi, T. Kalamees, J. Vinha, Building leakage, infiltration, and energy performance analyses for Finnish detached houses, Build. Environ. 44 (2) (2009) 377–387.
[2] T. Kalamees, Air tightness and air leakages of new lightweight single-family detached houses in Estonia, Build. Environ. 42 (6) (2007) 2369–2377.
[3] H.K. Park, H. Kim, Acoustic insulation performance of improved airtight windows, Constr. Build. Mater. 93 (2015) 542–550.
[4] X. Loncour, C. Mees, L'étanchéité à L'air Des Bâtiments, Centre Scientifique et Technique de la Construction (CSTC), 2015.
[5] M.H. Sherman, R. Chan, in: Building Airtightness: Research and Practice, 94720, Lawrence Berkeley National Laboratory, Berkeley CA, 2004, p. 46.
[6] R. Thor-Oskar, H. Sverre, T.J. Vincent, Airtightness estimation—A state of the art review and an en route upper limit evaluation principle to increase the chances that wood-frame houses with a vapour-and wind-barrier comply with the airtightness requirements, Energy Build. 54 (2012) 444–452.
[7] M. Prignon, G. Van Moeseke, Factors influencing airtightness and airtightness predictive models: a literature review, Energy Build. 146 (2017) 87–97.
[8] Jamieson, M., O. Brajterman, Y. Verstraeten, J. Arbon, J. Lonsdale, and M. Allington, Energy Performance of Buildings Directive (EPBD): Compliance Study: Final Report. 2015: Publications Office.
[9] JCGM, in: Evaluation of Measurement Data—Guide For the Expression of Uncertainty in Measurement, Joint Committee for Guides in Metrology, 2008, p. 134.
[10] C. Delmotte, J. Laverge, Interlaboratory tests for the determination of repeatability and reproducibility of buildings airtightness measurements, 32nd AIVC conference and 1st TightVent Conference: "Towards Optimal Airtightness Performance, 2011.
[11] J. Novak, Repeatability and reproductibility of blower door tests - four years' experience of round-robin tests in Czech Republic, 9th International Buildair Symposium, 2015.
[12] Persily, A., Repeatability and accuracy of pressurization testing, in *ASHRAE/DOE Conference Thermal Performance of the Exterior Envelopes of Buildings II*. 1982: Las Vegas, USA. p. 6–9.
[13] A.K. Kim, C.Y. Shaw, Seasonal variation in airtightness of two detached houses, in: Measured air Leakage of Buildings: A Symposium, ASTM International: Philadelphia, USA, 1986, pp. 16–32.
[14] W. Bracke, J. Laverge, N.V.D. Bossche, A. Janssens, Durability and measurement uncertainty of airtightness in extremely airtight dwellings, Int. J. Vent. 14 (4) (2016) 383–394.
[15] M. Sherman, L. Palmiter, Uncertainties in fan pressurization measurements, in: Airflow Performance of Building envelopes, components, and Systems, ASTM International, Philadelphia, USA, 1995, pp. 266–283.
[16] F.R. Carrié, V. Leprince, Uncertainties in building pressurisation tests due to steady wind, Energy Build. 116 (2016) 656–665.
[17] M. Prignon, A. Dawans, S. Altomonte, G. Van Moeseke, A method to quantify uncertainties in airtightness measurements: zero-flow and envelope pressure, Energy Build. 188 (2019) 12–24.
[18] C. Delmotte, Airtightness of buildings - Considerations regarding the zero-flow pressure and the weighted line of organic correlation, 38th AIVC Conference "Ventilating healthy low-energy buildings, 2017.
[19] H. Okuyama, Y. Onishi, Reconsideration of parameter estimation and reliability evaluation methods for building airtightness measurement using fan pressurization, Build. Environ. 47 (2012) 373–384.
[20] C. Delmotte, Airtightness of buildings-Calculation of combined standard uncertainty, 34th AIVC Conference "Energy conservation technologies for mitigation and adaptation in the built environment: the role of ventilation strategies and smart materials, 2013.
[21] ISO-9972, Performance Thermique Des Bâtiments - Détermination de La Perméabilité à L'air Des Bâtiments - Méthode de Pressurisation Par Ventilateur, Brussels, Belgium, 2015.
[22] D.R. Helsel, R.M. Hirsch, Statistical methods in water resources, in: Techniques of Water Resources Investigations, U.S. Geological Survey, 2002, p. 522.
[23] TEC, Operating Instruction for the DG-700 Pressure and Flow Gauge, The Energy Conservatory, 2012.
[24] ISO-28037, The Determination and Use of Straight-Line Calibration Functions, Switzerland, 2010.
[25] D. York, N.M. Evensen, M.L. Martınez, J.D.B. Delgado, Unified equations for the slope, intercept, and standard errors of the best straight line, Am. J. Phys. 72 (3) (2004) 367–375.
[26] C. Cantrell, Review of methods for linear least-squares fitting of data and application to atmospheric chemistry problems, Atmosph. Chem. Phys. 8 (17) (2008) 5477–5487.
[27] J. Cohen, A power primer, Psychol. Bull. 112 (1) (1992) 155.
[28] P. D Ellis, The Essential Guide to Effect sizes: Statistical power, meta-analysis, and the Interpretation of Research Results, 173, Cambridge University Press, Cambridge, 2010.
[29] C.J. Ferguson, An effect size primer: a guide for clinicians and researchers, Profess. Psychol. 40 (5) (2009) 532–538.

[30] D. Molle, P.-.M. Patry, RT 2012 Et RT Existant: Réglementation Thermique Et Efficacité énergétique, Eyrolles, 2015 Editions.
[31] M. Prignon, A. Dawans, G. van Moeseke, Uncertainties in airtightness measurements: regression methods and pressure sequences, 39th AIVC-7th TightVent & 5th venticool Conference Smart ventilation for buildings, 2018.
[32] G. Cumming, The new statistics: why and how, Psychol Sci 25 (1) (2014) 7–29.
[33] P. O'Neill, A tutorial introduction to bayesian inference for stochastic epidemic models using Markov chain Monte Carlo methods, Math. Biosci. 180 (2002) 103–114.
[34] J. Kruschke, Doing Bayesian data analysis: A tutorial With R and BUGS. Burlington, Academic Press/Elsevier, MA, 2011.

# Appendix D.

Prignon, M., Dawans, A. and Van Moeseke, G. (2018). Uncertainties in airtightness measurements: regression methods and pressure sequences. *In 39th AIVC – 7th TightVent & 5th Venticool Conference: Smart ventilation for buildings*. Antibes Juan-Les-Pins, France.

# Uncertainties in airtightness measurements: regression methods and pressure sequences

Martin Prignon*[1], Arnaud Dawans[2] and Geoffrey van Moeseke[1]

*1 Université catholique de Louvain*
*Place de l'université 1,*
*B-1348 Louvain-la-Neuve, Belgium*
** martin.prignon@uclouvain.be*

*2 Entreprises Jacques Delens S.A.,*
*Avenue du col-vert, 1,*
*1170 Brussels, Belgium*

## ABSTRACT

This paper presents the results of a series of 30 fan pressurization tests in reproducibility conditions performed within a period of 10 days in October 2017. The tested unit is a newly constructed unoccupied apartment in Brussels. These results make possible to compare different regression methods and evaluate the impact of pressure stations chosen for these regressions. The comparison of three different methods shows that the Weighted Line of Organic Correlation and the Iterative Weighted Least Square reduce the airflow rate standard deviation and give a better uncertainty calculation than Ordinary Least Square. Further work should focus on the generalization of these results in applying these methods to other sets of reproducibility tests. The comparison of different pressure sequences shows that the European standards are coherent in the imposed requirements and the given recommendations. In addition, when performing a regression method, one should avoid low-pressure stations as much as possible in order to reduce the airflow rate standard deviation at low- and high-pressure. Even if this work shows and confirms ways to improve the reliability of calculated combined standard uncertainties, there is still an important difference between these and the observed standard deviation. The investigation of such a difference should be a priority for further researchers focusing on airtightness uncertainties.

## KEYWORDS

Airtightness measurement, uncertainty calculation, regression methods, pressure sequence

## 1 INTRODUCTION

Although building professionals have used the fan pressurization method for years, the uncertainties related to airtightness measurements is still an important research topic. Recently, authors focus on the comparison between calculated uncertainty and standard deviation using new regression methods (Delmotte, 2017) and on the investigation of specific sources of uncertainties as such as wind (Carrié & Leprince, 2016). An important issue highlighted by researchers is the irrelevant use of Ordinary Least Square (OLS) regression method. Okuyama (Okuyama & Onishi, 2012) suggested the use of Iterative Weighted Least Square (IWLS) regression method in 2012, while Delmotte (Delmotte, 2017) suggested the use of the Weighted Line of Organic Correlation (WLOC) in 2017.

This paper deeply investigates the issue of regression methods by presenting the results of a reproducibility study. In addition, it uses the results of this study to evaluate the impact of pressure stations (i.e. the choice of pressure – airflow couples during a fan pressurization test) on the airflow rate.

## 2 METHODOLOGY

This paper presents the results of a series of 30 fan pressurization tests in reproducibility conditions performed within a period of 10 days in October 2017. Airtightness measurements

were carried out on a newly constructed (2017) unoccupied apartment in Brussels. The apartment is a masonry construction of 228 m³ with a floor area of 90 m² located on the second floor of a three-story building. There were no airtightness requirements for the apartment itself, but the whole building (i.e. all apartment pressurized simultaneously) had to reach an air change rate lower than 0.6 $h^{-1}$ at 50 Pa.

The operator recorded outside climatic data with a meteorological station placed on the roof above the apartment. Table 1 shows the minimum (min), maximum (max), average ($\mu$) and standard deviation ($\sigma$) of climatic data recorded during the series of tests. Mean wind speed is computed with 10-minutes averages.

Table 1: Minimum, maximum, average and standard deviation of main climatic data (temperatures and wind speed) recorded during the testing period.

| | **min** | **max** | $\boldsymbol{\mu}$ | $\boldsymbol{\sigma}$ |
|---|---|---|---|---|
| Outside temperature [°C] | 8.8 | 24.3 | 14.2 | 2.8 |
| Inside temperature [°C] | 20.5 | 22.0 | 21.3 | 0.6 |
| Mean wind speed [m/s] | 0.0 | 3.8 | 1.3 | 0.8 |
| Maximum wind speed [m/s] | 0.3 | 8.3 | 3.3 | 1.6 |

The same operator performed all the tests, with the same equipment and on the same apartment prepared according to method 1 of ISO 9972:2015 standards (ISO-9972, 2015). Since the climatic conditions varied within the 10-days period, this series of test is in reproducibility conditions instead of repeatability conditions (Novak, 2015). Indeed, repeatability conditions consider successive measurements carried out under the same conditions while reproducibility conditions refer to successive measurements performed under changed conditions of measurements (JCGM, 2008). However, it is important to differentiate the reproducibility conditions in this paper with the reproducibility conditions presented in airtightness literature. Indeed, in previous researches, reproducibility conditions refer to a change in operator performing the test while in this paper the same operator performs the whole series of 30 tests (Delmotte & Laverge, 2011; Novak, 2015).

## 2.1 Uncertainties in pressure and airflow measurements

When performing a linear regression method, the uncertainties of regression parameters (i.e. the slope $n$ and the intercept $c_e$) depend on the uncertainties of the response variable (i.e. $\ln(Q_e)$) and of the explanatory variable (i.e. $\ln(\Delta P_e)$).

Regarding airflow uncertainty ($u(\ln(Q_e))$), Delmotte developed equation to compute them based on the characteristics of the equipment (Delmotte, 2013). In the study presented in this paper, the maximum permissible error for the airflow measurement is the greatest between 4 % of the airflow measured and 1.7 m³/h. In addition, the maximum permissible error for the temperature measurement is 0.5 °C and the resolution of temperature measurement is 0.1 °C. Since this paper uses exactly the same equations to compute airflow rate uncertainties, they are not developed here.

Regarding envelope pressure uncertainty ($u(\ln(\Delta P_e))$), the equations used in this study are slightly different from Delmotte equations. First, this study considers the uncertainty given by the manufacturer for pressure measurement as a 95% confidence interval and not as a maximum permissible error. Therefore, equation 1 gives the uncertainty in pressure measurement ($u(\Delta p_m)$) for an equipment with a resolution of 0.1 Pa and a 95% confidence interval in the pressure measurement of the greatest between 1% of the reading and twice the resolution.

$$u(\Delta p_m) = \max\left(\sqrt{\left(\frac{0.01*\Delta p_m}{2}\right)^2 + \left(\frac{0.1}{\sqrt{12}}\right)^2}\,;\sqrt{\left(\frac{0.20}{2}\right)^2 + \left(\frac{0.1}{\sqrt{12}}\right)^2}\right) \quad (1)$$

Second, the uncertainty in zero-flow pressure has three terms (Equation 2). The two firsts are for the zero-flow pressure measured before and after the test ($u(\Delta P_{0,1})$ and $u(\Delta P_{0,2})$). Equation 1 allows computing the values of these terms since the same manometer measures the pressure during the test and the zero-flow pressure. The third term is the zero-flow pressure approximation ($u(\Delta P_{0,a})$). In a real fan pressurization test, the measurement of zero-flow pressure is not possible when the fan is working. Therefore, the operator measures the zero-flow pressure before and after the test. In calculations, the zero-flow pressure during the test is equal to the average of zero-flow pressure measured before and after the test. However, the real zero-flow pressure is constantly varying and the hypothesis of constant value is a source of uncertainty.

$$u(\Delta P_0) = \sqrt{\frac{u^2(\Delta P_{0,1})}{4} + \frac{u^2(\Delta P_{0,2})}{4} + u^2(\Delta P_{0,a})} \quad (2)$$

The evaluation of zero-flow pressure approximation uncertainty is difficult because it is not a type A evaluation of uncertainty. Type A evaluation method uses repeated measurement to compute uncertainty. In this case, the real zero-flow pressure is constantly varying and it is not possible to analyze its variation by performing a series of repeated measurements. One has then to evaluate the uncertainty by scientific judgement based on available information. This is the type B evaluation of uncertainty (JCGM, 2008).

The use of zero-flow pressure tests allows evaluating the uncertainty of zero-flow pressure approximation. A zero-flow pressure test is the measurement of zero-flow pressure every seconds during 14 minutes divided in three successive periods. The first and last periods (2 minutes each) are respectively the first and second approximation periods while the second period (i.e. the middle period of 10 minutes) is the “fictitious period”. The analyze of zero-flow pressure test consists in comparing the zero-flow pressure approximation with the zero-flow pressure measured during the fictitious period (i.e. the period where, in a real test, the zero-flow pressure is not measurable). The result of the zero-flow analysis for this apartment shows an uncertainty in zero-flow pressure approximation between 0.9 and 2.5 Pa, depending on the wind speed.

Then, uncertainties in pressure measurements and in zero-flow pressure are used to compute uncertainties in envelope pressure (Equation 3) and in explanatory variable (Equation 4).

$$u(\Delta P_e) = \sqrt{u^2(\Delta P_0) + u^2(\Delta p_m)} \quad (3)$$

$$u(\ln(\Delta P_e)) = \sqrt{\left(\frac{u(\Delta p_e)}{\Delta p_e}\right)^2} \quad (4)$$

Figure 2 shows, as an example, the uncertainties in explanatory and response variables as a function of the measured pressure for the first test of the series in depressurization.

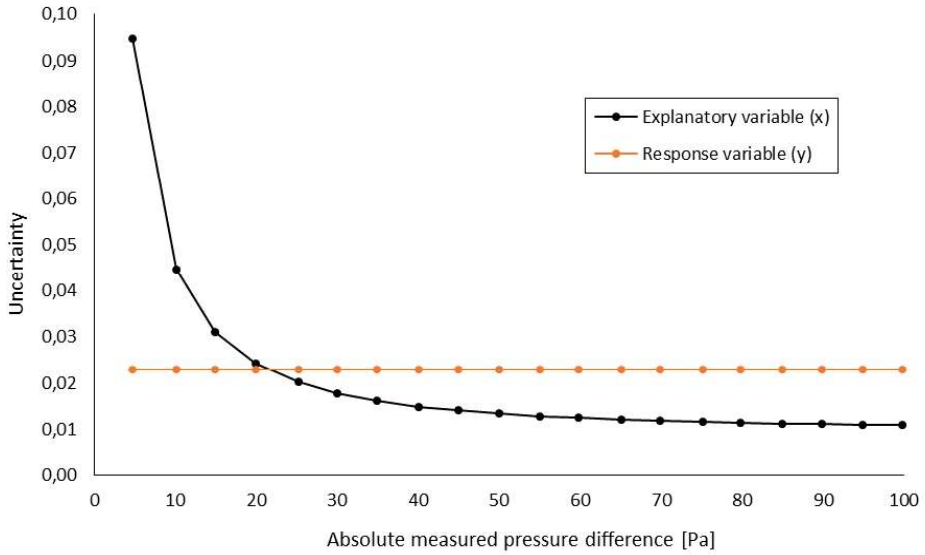



Figure 1: Combined standard uncertainty in explanatory ($x_i$) and response ($y_i$) variables as a function of the measure pressure difference for the first test of the series in depressurization case.

## 2.2 Regression methods

The uncertainty in regression parameters (i.e. the slope $n$ and the intercept $c_e$), and therefore in the building airtightness, depends on the uncertainties in explanatory and response variables, but also on the regression method. In practice, operators mainly use the Ordinary Least Square (OLS) regression method to determine the regression parameters. However, the OLS method is appropriate only when the uncertainties on the response variable are constant for all the points used for the regression and if the uncertainties on the explanatory variable are negligible (Delmotte, 2013). Helsel and Hirsch explained that for cases that do not meet these assumptions, the uncertainty on regression parameters computed with OLS were not reliable (Helsel & Hirsch, 2002). Since in the current case both variables have the same order of magnitude, Figure 1 shows that the uncertainty on the explanatory variable is non-negligible and OLS method is irrelevant. This paper investigates two alternative methods suggested in literature: the Iterative Weighted Least Square method (IWLS) and the Weighted Line of Organic Correlation method (WLOC) (Delmotte, 2017; Okuyama & Onishi, 2012).

*Iterative Weighted Least Square (IWLS)*

Multiple sets of equations exist to solve the iterative approach required to perform Iterative Weighted Least Square (IWLS) method. This section describes the unified equations developed by York (York, Evensen, Martınez, & Delgado, 2004). IWLS method consists in assuming a starting value for the slope and then re-compute this value based on uncertainties in variables.

This method has three main steps that repeats: (i) computation of weights (equations 5 to 7) (ii) computation of residuals (equations 8 to 11) and (iii) computation of the new slope (equations 12 and 13). The iteration process stops when the difference between two consecutive slopes (flow exponent) is lower than a chosen tolerance. In this study, the tolerance was set to $10^{-10}$. Once this the iteration stops, a fourth step (iv) gives the second regression parameter as a function of the slope and the means obtained from last iteration (Equation 14)

*Step (i)*

$$w(x_i) = \frac{1}{u^2(x_i)} \quad (5) \qquad w(y_i) = \frac{1}{u^2(y_i)} \quad (6)$$

$$W_i = \frac{w(x_i)w(y_i)}{w(x_i)+n^2 w(y_i)} \quad (7)$$

*Step (ii)*

$$\bar{x} = \frac{\sum_{i=1}^{N} W_i x_i}{\sum_{i=1}^{N} W_i} \quad (8) \qquad \bar{y} = \frac{\sum_{i=1}^{N} W_i y_i}{\sum_{i=1}^{N} W_i} \quad (9)$$

$$U_i = x_i - \bar{x} \quad (10) \qquad V_i = y_i - \bar{y} \quad (11)$$

*Step (iii)*

$$\beta_i = W_i \left[\frac{U_i}{w(y_i)} + \frac{mV_i}{w(x_i)}\right] \quad (12) \qquad n = \frac{\sum_{i=1}^{N} W_i \beta_i V_i}{\sum_{i=1}^{N} W_i \beta_i U_i} \quad (13)$$

*Step (iv)*

$$c_e = \bar{y} - n\bar{x} \quad (14)$$

Equations 12 and 13 give the uncertainties in both regression parameters. These equations are only valid if the uncertainties in explanatory and response variables are uncorrelated. This case meet this assumption since the uncertainty in explanatory variable is constant (Figure 1).

$$u(c_e) = \sqrt{\frac{1}{\sum_{i=1}^{N} W_i} + \left(\bar{x} + \bar{\beta}\right)^2 u^2(n)} \quad (15) \qquad u(n) = \sqrt{\frac{1}{\sum_{i=1}^{N} W_i (\beta_i - \bar{\beta})^2}} \quad (16)$$

*Weighted Line of Organic Correlation*

Another method for linear regression without iterative procedure is by minimizing the sum of the products of the horizontal and vertical distances between the observations and the fitting line. This method is the Line of Organic Correlation (Helsel & Hirsch, 2002), also called the geometric mean regression (GM) or the standardized major axis (MA) (Saqr & Khan, 2014). If uncertainties in both explanatory variables are constant, the regression parameters and their uncertainties are unbiased. However, this is not true in this case since the explanatory variable is not constant. To get rid of the "constant uncertainties in variables" constraint, it is possible to use a Weighted Line of Organic Correlation (WLOC) (Delmotte, 2017; Saqr & Khan, 2014). Delmotte recently developed in a conference paper the equations related to the WLOC method in the context of airtightness measurements (Delmotte, 2017).

*Methods comparison: standard deviation vs. computed uncertainties*

There are two ways to compute linear regression uncertainties. The first is by performing repeated measurements and by computing the standard deviation of the results. If the number of repeated measurement is enough, this is the "reference uncertainty" (i.e. the uncertainty considered as the true uncertainty). However, in practice, the operator performs only one test. In that case, the calculation of regression parameters depends on the regression method used (e.g. equations 15 and 16 for IWLS method) and on the uncertainties on variables (e.g. equations 1 to 4 for explanatory variable). These are the "calculated uncertainties". If all the sources of uncertainties in variables are considered and if the appropriate regression method is used, the "calculated uncertainties" should be equal to the "reference uncertainties" (i.e. standard deviation observed for repeated measurements).

This paper computes and compares for each regression method (1) the average and the standard deviation of the airflow rate for the 30 tests and (2) the ability to give a reliable calculation of uncertainties (i.e. the difference between "reference uncertainty" and "calculated uncertainty").

### 2.3 Sequence of pressure

ISO 9972:2015 standards (ISO-9972, 2015) give some requirements and recommendations regarding the pressure sequence in the fan pressurization test. Firstly, the lowest pressure station must be lower than the greatest between 10 Pa and five times the zero-flow pressure. Secondly, there must be minimum five pressure stations with constant steps between them. Thirdly, the distance between two stations must be lower or equal to 10 Pa. Fourthly, the highest-pressure station should be minimum 50 Pa (but standard recommends a higher value). Lastly, standard recommends taking the average between pressurization and depressurization as a result.

This paper focuses on four different pressure sequences consistent with European standards. Three numbers (*a:b:c*) define each pressure sequence: the lowest-pressure station (*a*), the highest-pressure station (*c*) and the step between two stations (*b*). The four sequences tested are *Sequence 1 – 5:5:100*, *Sequence 2 – 10:5:100*, *Sequence 3 – 10:10:100* and *Sequence 4 – 5:5:50*. These pressure sequences allows to investigate the impact of low-pressure stations (Sequence 2), the impact of reducing the number of pressure stations (Sequence 3) and the use of low-pressure stations only (Sequence 4).

## 3 RESULTS

The airflow rate at 50 Pa using OLS regression method on *10:10:100* sequence for the 30 tests are:

- Mean of 229 $m^3/h$ and standard deviation of 5.2 $m^3/h$ (2.3%) in depressurization,
- Mean of 277 $m^3/h$ and standard deviation of 4.4 $m^3/h$ (1.6%) in pressurization and
- Mean of 253 $m^3/h$ and standard deviation of 3.1 $m^3/h$ (1.1%) in average

Table 2 shows that the variation of results in this research is similar to the variations of previous reproducibility tests made in similar conditions.

Table 2: Results of multiple reproducibility tests previously performed in similar conditions (same operator, same equipment, same apartment and varying climatic conditions) available in literature.

| | **Number of tests** | **Average airflow rate at 50 Pa ($m^3/h$)** | **Standard deviation (%)** |
|---|---|---|---|
| (Persily, 1982) | 17 | 3860 | 1.1 % |
| (Kim & Shaw, 1986) | 7 | 1104 | 1.6 % |
| (Delmotte & Laverge, 2011) | 10 | 732 | 1.4 % |
| (Novak, 2015) | 92 | 1005 | 1.8 % |
| (Bracke, Laverge, Bossche, & Janssens, 2016) (1) | 58 | 234 | 1.4 % |
| (Bracke et al., 2016) (2) | 53 | 132 | 2.3 % |
| This paper | 30 | 253 | 1.2 % |

### 3.1 Change in regression method

Table 3 shows that the three different regression methods give similar values for the airflow rates at multiple pressure differences when averaging the results of the 30 tests.

Table 3: Average airflow rate for the 30 tests at low-pressure (10 Pa), mid-pressure (50 Pa) and high-pressure (100 Pa) differences

| | **Average airflow rate at 10 Pa ($m^3/h$)** | **Average airflow rate at 50 Pa ($m^3/h$)** | **Average airflow rate at 100 Pa ($m^3/h$)** |
|---|---|---|---|
| OLS | 82.70 | 252.62 | 409.15 |
| IWLS | 82.07 | 252.77 | 410.70 |
| WLOC | 82.76 | 252.80 | 409.17 |

On the contrary, the standard deviation of the airflow rates for the 30 tests depend on the regression method used. Figure 2 shows that at low- and high-pressure the airflow rates computed with WLOC and IWLS methods have lower standard deviation than with OLS method. At mid-pressure (i.e. around 50 Pa), none of the three methods seems to give lower standard deviation. These results are consistent with the observations made by Delmotte (Delmotte, 2017).

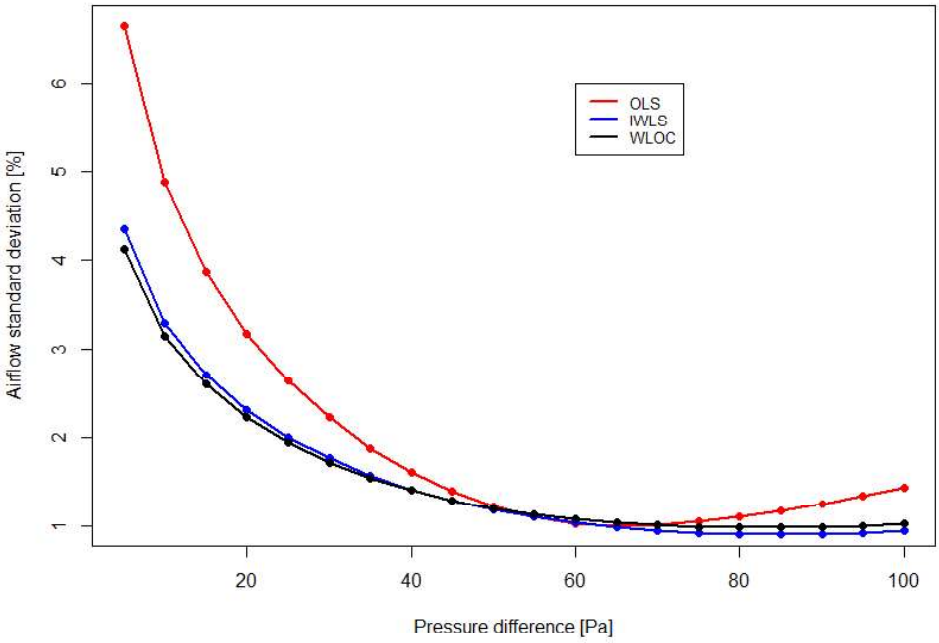



Figure 2: Standard deviation (in %) of the airflow rates computed for the 30 tests as a function of the pressure difference for the OLS, the IWLS and the WLOC regression methods.

In addition to its impact on standard deviation, the regression method also affects the calculated uncertainties. Figure 3 shows the average of 30 tests for both regression parameters (black dot), their calculated uncertainty (full blue line) and their standard deviation (dashed red line). These results firstly confirm the observation made on Figure 2: the use of IWLS and WLOC method instead of OLS method reduces the standard deviation of the regression parameters. Secondly, the uncertainties calculated using both IWLS and WLOC methods fit better the standard deviation (i.e. the "real uncertainties") than using OLS method. This means that using the equations in section 2.1 to compute uncertainties in variables, WLOC and IWLS methods are more reliable regarding the calculation of regression parameters uncertainties. However, there is still a difference between calculated uncertainties and standard deviation for WLOC and IWLS. Since this series of test meet the assumptions for WLOC and IWLS regression methods, the difference between real and calculated uncertainties implies that the method for computing variables uncertainty is still underestimating real uncertainties.

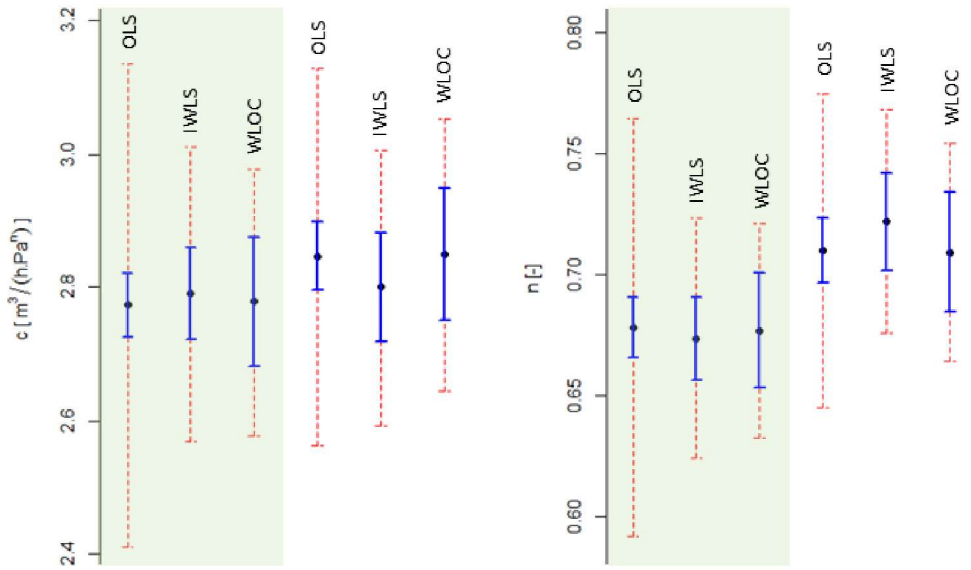



Figure 3: Average value (black dot), calculated uncertainty (full blue line) and standard deviation (dashed red line) of regression parameters in depressurization (green zones) and pressurization (white zones).

## 3.2 Change in sequence of pressure

Figure 4 shows the average of airflow rate values for the 30 tests at multiple pressure differences computed using OLS with four different pressure sequences. The three first sequences have all the same airflow averages but the fourth sequence (*5:5:50*, see section 2.3) shows a slightly higher average airflow rate at high-pressure.

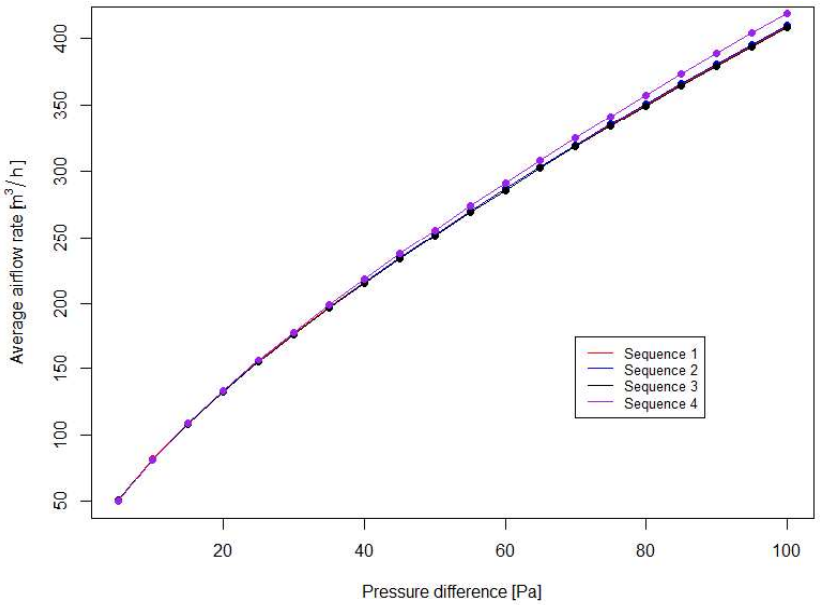



Figure 4: Average airflow rate for the 30 tests as a function of the pressure difference computed with OLS in four different pressure sequences

Figure 5 shows the impact of different pressure sequences on the standard deviation of airflow rate. Since the difference between WLOC and IWLS standard deviations is much lower than the difference with OLS (Figure 2), Figure 5 compares the four sequences using WLOC and OLS only. The Sequence 4 (*5:5:50*) has higher standard deviation at low and high pressure than

other. This is coherent with the recommendation of ISO 9972:2015 standard (ISO-9972, 2015) that suggests to perform the linear regression with a highest-pressure station higher than 50 Pa. Sequence 1 (*5:5:100*) has higher standard deviation at low- and high-pressure than Sequence 2 (*10:5:100*) and Sequence 3 (*10:10:100*). This indicates that the use of low-pressure station when performing the regression increases the variability of airflow rate at low-pressure. It seems logical since the uncertainty in explanatory variable is higher at low-pressure stations (Figure 1). Performing the regression using 19 points (*Sequence 2 – 10:5:100*) lead to lower standard deviation than using 10 points (*Sequence 3 – 10:10:100*). However, the results are close and the use of 10 points reduces the time of testing and therefore reduces the uncertainty related to zero-flow pressure approximation. In our point of view, the advantage of taking more points to perform the linear regression is not straightforward.

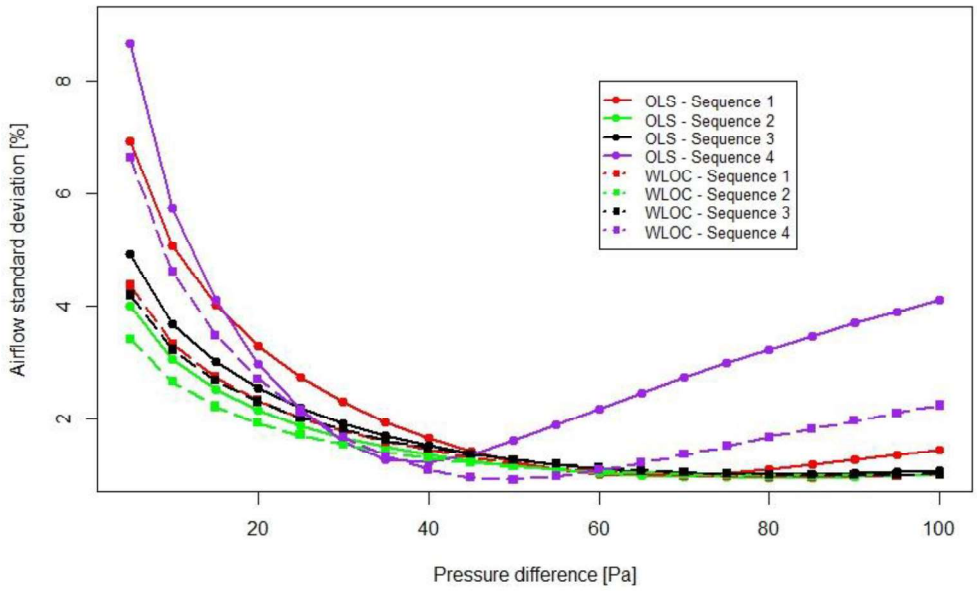



Figure 5: Airflow rate standard deviation (in %) for the 30 tests as a function of the pressure difference for four different pressure sequences computed using OLS (full lines) and WLOC (dashed lines).

Another interesting observation is that WLOC method reduces the airflow standard deviation, but it also reduces the impact of pressure sequences. Indeed, the range of possible standard deviations for different pressure sequences is lower when using WLOC than OLS. One could expect such a result since in WLOC, the stations with higher uncertainties (and therefore leading to an increase of standard deviation) have a lower weight in the determination of regression parameters. This highlights another advantage of WLOC method over OLS method.

## 4 CONCLUSIONS AND FURTHER WORK

This paper presents the results of a series of 30 tests in reproducibility conditions performed within a period of 10 days during October 2017. This series shows similar relative standard deviation than previous repeated measurements found in literature. Regarding the regression method applied on the 30 tests, IWLS and WLOC methods show similar averages and lower standard deviation than OLS for the airflow rate. In addition, the calculated uncertainties using IWLS and WLOC methods are closer to the real uncertainty (i.e. the standard deviation) than OLS. Regarding the sequence of pressure, results show that the recommendations of European standards were consistent, principally the need for a highest-pressure station higher than 50 Pa. Results also showed that the lowest-pressure station should be taken as high as possible (within the standard requirements) to reduce the airflow rate standard deviation.

The conclusions drawn from this series of tests lead to multiple possible further work. Firstly, these conclusions relate to the apartment tested. An important further work is the comparison of different regression methods on other series of tests in reproducibility condition to confirm and generalized the results found here. Secondly, further researches could also investigate other regression methods as grouping methods or instrumental variables (Gillard, 2010). Thirdly, even if the uncertainties computed with WLOC and IWLS methods seem better than with OLS, there are still differences between computed and real uncertainties. The quantification of uncertainties should be a priority in researches dealing with fan pressurization uncertainties.

## 5 ACKNOWLEDGEMENTS

Authors want to thank the company *Jacques Delens* for its mobilization in this work and the availability of their construction sites. This work is part of the "AirPath50" project funded by INNOVIRIS.

## 6 REFERENCES

Bracke, W., Laverge, J., Bossche, N. V. D., & Janssens, A. (2016). Durability and Measurement Uncertainty of Airtightness in Extremely Airtight Dwellings. *International Journal of Ventilation, 14*(4), 383-394.

Carrié, F. R., & Leprince, V. (2016). Uncertainties in building pressurisation tests due to steady wind. *Energy and buildings, 116*, 656-665.

Delmotte, C. (2013). *Airtightness of buildings-Calculation of combined standard uncertainty.* Paper presented at the 34th AIVC Conference "Energy conservation technologies for mitigation and adaptation in the built environment: the role of ventilation strategies and smart materials", Athens, Greece.

Delmotte, C. (2017). *Airtightness of Buildings - Considerations regarding the Zero-Flow Pressure and the Weighted Line of Organic Correlation.* Paper presented at the 38th AIVC Conference "Ventilating healthy low-energy buildings", Nottingham, UK.

Delmotte, C., & Laverge, J. (2011). *Interlaboratory tests for the determination of repeatability and reproducibility of buildings airtightness measurements.* Paper presented at the 32nd AIVC conference and 1st TightVent Conference: "Towards Optimal Airtightness Performance", Brussels, Belgium.

Gillard, J. W. (2010). An overview of linear structural models. *Revstat, 8*(1), 57-80.

Helsel, D. R., & Hirsch, R. M. (2002). Statistical Methods in Water Resources *Techniques of Water Resources Investigations* (Vol. Book 4, Chapter A3, pp. 522): U.S. Geological Survey.

ISO-9972. (2015). NBN EN ISO 9972:2015 - Performance thermique des bâtiments - Détermination de la perméabilité à l'air des bâtiments - Méthode de pressurisation par ventilateur (ISO 9972:2015) CEN, Brussels, Belgium.

JCGM. (2008). Evaluation of measurement data—guide for the expression of uncertainty in measurement. (pp. 134): Joint Committee for Guides in Metrology.

Kim, A. K., & Shaw, C. Y. (1986). Seasonal variation in airtightness of two detached houses *Measured Air Leakage of Buildings: A Symposium* (pp. 16-32). Philadelphia, USA: ASTM International.

Novak, J. (2015). *Repeatability and reproductibility of blower door tests - four years' experience of round-robin tests in Czech republic*. Paper presented at the 9th International Buildair Symposium, Germany.

Okuyama, H., & Onishi, Y. (2012). Reconsideration of parameter estimation and reliability evaluation methods for building airtightness measurement using fan pressurization. *Building and Environment, 47*, 373-384.

Persily, A. (1982). *Repeatability and accuracy of pressurization testing.* Paper presented at the ASHRAE/DOE Conference Thermal Performance of the Exterior Envelopes of Buildings II, Las Vegas, USA.

Saqr, A., & Khan, S. (2014). New weighted geometric mean method to estimate the slope of measurement error model. *Journal of Applied Statistical Science, 22*(3/4).

York, D., Evensen, N. M., Martınez, M. L., & Delgado, J. D. B. (2004). Unified equations for the slope, intercept, and standard errors of the best straight line. *American Journal of Physics, 72*(3), 367-375. doi:10.1119/1.1632486

# Appendix E.

Prignon, M., Dawans, A., Altomonte, S. and Van Moeseke, G. (2019). A method to quantify uncertainties in airtightness measurements: Zero-flow and envelope pressure. Energy and Buildings, **188–189**: 12–24. https://doi.org/10.1016/j.enbuild.2019.02.006.

Energy & Buildings 188–189 (2019) 12–24

Contents lists available at ScienceDirect

Energy & Buildings

journal homepage: www.elsevier.com/locate/enbuild

# A method to quantify uncertainties in airtightness measurements: Zero-flow and envelope pressure

Martin Prignon*, Arnaud Dawans, Sergio Altomonte, Geoffrey Van Moeseke

*Université catholique de Louvain, Louvain, Belgium*

ARTICLE INFO

*Article history:*
Received 1 October 2018
Revised 8 January 2019
Accepted 7 February 2019
Available online 8 February 2019

*Keywords:*
Airtightness measurement
Fan pressurization test
Uncertainties
Zero-flow pressure approximation
Multi-level modelling
Envelope pressure

ABSTRACT

In airtightness measurements using the fan pressurization method, the calculation of uncertainties does not take into account the zero-flow pressure approximation. It was recently suggested that neglecting the uncertainties related to zero-flow pressure approximation could be an unrealistic hypothesis. In this study, a method for quantifying this source of uncertainty is proposed, illustrated and discussed. The method is applied to a series of 31 zero-flow pressure tests performed on a newly-constructed apartment within a period of 15 days in Brussels, Belgium. For each test, 32 different zero-flow pressure approximations were compared. Since the data had a nested structure, multiple multi-level models were used for their analysis. The results show that, for the tested building, the zero-flow pressure approximation uncertainty is 0.45, 0.91 and 1.52 Pa respectively under low-, medium- and large-wind conditions. These uncertainties can be reduced to 0.42, 0.80 and 1.39 Pa when using longer zero-flow pressure measurement periods. As a comparison, uncertainty in pressure measurement at 50 Pa due to the equipment is 0.25 Pa. The uncertainty of zero-flow approximation makes the envelope pressure uncertainty non-negligible, therefore having an impact on the regression technique used to determine the building airtightness.

© 2019 Elsevier B.V. All rights reserved.

## 1. Introduction

The measurements of air tightness and infiltration in buildings is an issue of major concern. Kalamees [1] and Jokisalo et al. [2] showed that, in cold climates, air infiltration could be responsible for up to 30% of heating loads. Air infiltration has also been shown to have an impact on the efficiency of ventilation systems, on occupant comfort, and on acoustic insulation [3]. In 2014, Sadauskiene et al. observed that actual building energy use can significantly differ from the value calculated with regulation methods when airtightness is ignored [4]. In this context, however, there is a general consensus that no predictive model can currently replace airtightness measurements [5,6], this leaving a gap to fill in terms of the availability of reliable and easily implemented modelling methods.

Although fan pressurization tests (also called blower door tests) have been used for almost 50 years [3], there is an important lack of knowledge when dealing with the uncertainties related to these procedures. Several studies have analyzed total uncertainties in repeatability (i.e., successive measurements carried out under the same conditions) and reproducibility (i.e., successive measurements under changing conditions) testing [7–11]. Research has also focused on multiple sources of uncertainty [12–16] among which wind is likely the most challenging, since it can cause precision and bias errors in both envelope pressure and airflow measurements [14].

In envelope pressure measurements, the impact of wind – and more generally of weather conditions – is taken into account through the calculation of zero-flow pressure. The pressure difference measured during a fan pressurization test is the combination of the differential in pressure induced by the fan and that induced by climatic conditions (hence, the zero-flow pressure). One important step in the evaluation of envelope pressure difference is the separation of these two induced pressures. In practice, the measurement of zero-flow pressure is not possible during the fan pressurization test since this requires the fan to be stopped and sealed. The European standard EN ISO 9972:2015 [17] suggests to measure the zero-flow pressure before and after the test, and to assume that the zero-flow pressure during the test is the average of these measurements (Eq. (1)).

$$\Delta p_0 = \frac{\Delta p_{0,1m} + \Delta p_{0,2m}}{2} = \frac{1}{2}\left(\frac{\sum_{i=1}^{N} \Delta p_{0,1i}}{N} + \frac{\sum_{j=1}^{M} \Delta p_{0,2j}}{M}\right) \quad (1)$$

where: $\Delta p_0$ is the zero-flow pressure approximation; $\Delta p_{0,\,1m}$ and $\Delta p_{0,\,2m}$ are the averages of zero-flow pressure measurements

* Corresponding author.
*E-mail address:* martin.prignon@uclouvain.be (M. Prignon).

https://doi.org/10.1016/j.enbuild.2019.02.006
0378-7788/© 2019 Elsevier B.V. All rights reserved.

during a given measurement period, respectively before and after the fan pressurization test; $\Delta p_{0,1i}$ and $\Delta p_{0,2i}$ are the zero-flow pressures measured at each point during these periods; and, $N$ and $M$ are the number of measurements made within these periods. Standard EN ISO 9972:2015 requires that at least 10 measurements are made during a period of minimum 30 s [17].

This method leads to an important source of uncertainty because, in reality, the weather conditions, and therefore the zero-flow pressure, are not constant during the fan pressurization test. Uncertainties in zero-flow pressure have been studied by other authors [15], but Delmotte was the first to raise the issue of uncertainties due to zero-flow pressure approximation, although the sources of such uncertainties were not quantified [13].

In this paper, we propose and illustrate a new method for the quantification of uncertainties in zero-flow and envelope pressure, and we discuss the findings from its application to a series of 31 tests performed on a single apartment in Brussels, Belgium, within a period of 15 days in October 2017. The paper is structured as follows. In the Methodology section, we illustrate the tests performed, drive a comparison between different approximation techniques, and describe the statistical approach behind the newly-proposed quantification method. In the Results section, we provide the outcomes of the tests, the uncertainties quantified by the application of the new method, and the impact of the zero-flow pressure approximation uncertainties on envelope pressure uncertainties. In the Discussion section, we highlight the impact of our findings against the relevant literature and illustrate critically the limitations of this study. Finally, in the Conclusions, we summarize the outcomes of this work, describing the further research needed in the field of airtightness measurement uncertainties.

## 2. Methods

This section is divided in three parts. The first describes the weather data, the equipment used for the series of tests, and the apartment where measurements took place. The second offers a comparison between different zero-flow pressure approximation techniques and the indicator used for the evaluation. The last part focuses on the statistical analysis and on the justification of methodological choices.

### 2.1. Measurement method

#### 2.1.1. Zero-flow pressure test

A zero-flow pressure test consists in the measurement of zero-flow pressure every second during three successive periods. In this paper, the initial and last periods have been respectively labelled the first and second “approximation periods”, while the second period (i.e., the middle one) has been called the “fictitious period” (Fig. 1). The approximation periods correspond to the times when measurements are used to perform zero-flow pressure approximations. The fictitious period corresponds to the duration that a typical fan pressurization test would take in practice.

The paper by Delmotte [13] described for the first time a zero-flow pressure test. To remain consistent with his work, the present study adopted a fictitious period of 600 s. The duration of the fictitious period has a strong impact on the uncertainty. Indeed, a longer duration of the fictitious period might imply greater likelihood of weather variations of higher degree. 600 s correspond to the measurement of 10 couples with 30-s duration and 30-s delay between measurements. These three values (i.e., number of couples, measurement duration, and delay between measurements) could vary depending on the operator, equipment and weather conditions.

Approximation periods of 120 s were selected instead of the 30 s used in [13]. This is because Delmotte was interested in the uncertainties related to minimum standard requirements, while the present study focuses on the impact of approximation period duration on zero-flow pressure uncertainty.

**Table 1**
Minimum, maximum, mean ($M$) and standard deviation ($SD$) of weather-related data measured during the 15-day testing period.

| | Min | Max | $M$ | $SD$ |
|---|---|---|---|---|
| $T_{ext}$ [°C] | 8.8 | 24.3 | 14.2 | 2.77 |
| $T_{int}$ [°C] | 20.5 | 22.0 | 21.3 | 0.57 |
| $\bar{v}_w$ [m/s] | 0 | 3.8 | 1.3 | 0.75 |
| $\max(v_w)$ [m/s] | 0.3 | 8.3 | 3.3 | 1.57 |

#### 2.1.2. Measurement equipment and weather data

A DG-700 pressure gauge (last calibration in June 2017) from The Energy Conservatory (TEC) measured the pressure difference between inside and outside the apartment. According to the manufacturer, the standard uncertainty (i.e., the expected standard deviation for a large number of repeated measures) of the DG-700 is the greatest between $\pm 0.5\%$ of the reading and $\pm 0.1$ Pa, and it has a resolution of 0.1 Pa [18]. For the DG-700 pressure gauge, this uncertainty takes into account the uncertainty of the pressure reference used to calibrate the gauge, the uncertainty of the gauge itself (including hysteresis effect), the temperature effect on the sensor, and the drift of the sensor over time [19].

During the tests, a weather station (Ahlborn FMD 760) placed on the roof above the apartment measured the outside air temperature, the wind speed and the wind direction every 10 s. The weather station provided 10-min averages for the outside air temperature ($T_{ext}$), the mean wind speed ($\overline{v_w}$) and the mean wind direction. It also provided the maximum wind speed measured during these 10-min periods. A thermometer (Testo 417) was used to measure the inside air temperature ($T_{int}$) before each test with an accuracy of $\pm 0.5$°C and a resolution of 0.1 °C. Table 1 shows, for each weather variable, the minimum, maximum, mean ($M$) and standard deviation ($SD$) of all the values recorded by the weather station (10-min samples) and the thermometer (before each test) during the 15 days. Wind direction was mostly from west and southwest.

#### 2.1.3. Measured apartment

The 31 tests were performed on a newly constructed (2017) apartment within a period of 15 days in October 2017. A short testing period was chosen to avoid impacts of ageing and seasonal variations on airtightness. Since no previous research has defined an appropriate sample size for the statistical analysis of data, a large number of tests were repeated during this period. The apartment was a masonry construction of 228 m³ with a floor area of 90 m² located on the second floor of a 3-storey building in Brussels. Only two perimetral walls were exposed to the outside (Fig. 2). Over recent years, masonry apartments have represented a large share of new residential constructions in Brussels.

In the absence of a fan, if parts of the envelope are in underpressure others are in overpressure [13]. Pressure gauges placed at different locations undergo different zero-flow pressure. Therefore, the pressure gauge location is expected to have an influence on the uncertainty due to zero-flow pressure approximation. In this study, the pressure gauges were placed at the southeast façade because of the exposed surroundings of the building. Conversely, the northwest façade opens to an enclosed space surrounded by high buildings that could induce an undesirable wind effect.

There were no airtightness requirements for the apartment itself, but the whole building (i.e., all the apartments pressurized simultaneously) had to reach a maximum air change rate of

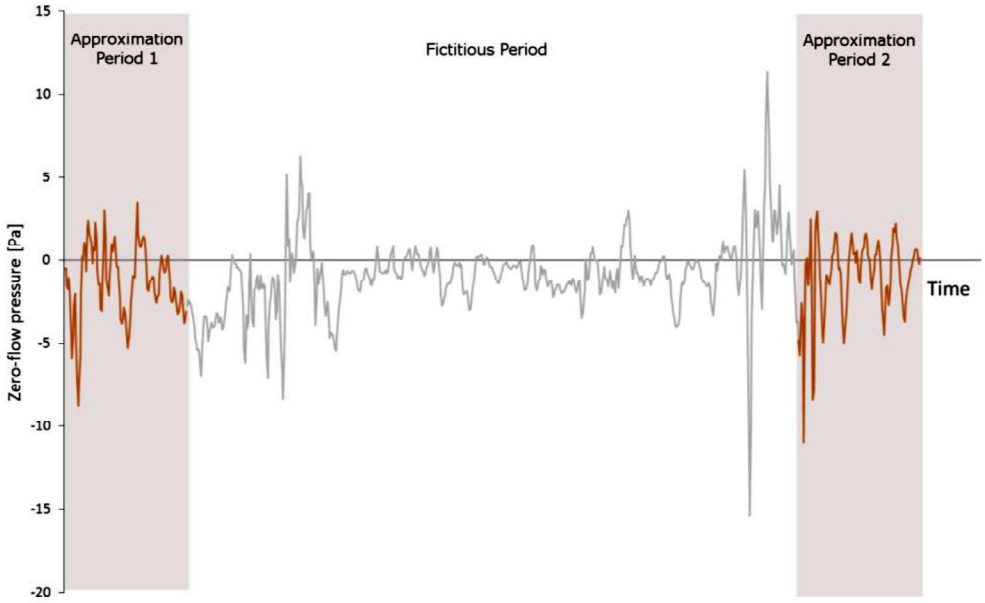



**Fig. 1.** Zero-flow pressure measured during a period of 840 s (one measurement every second), illustrating the three successive periods of a zero-flow pressure test.

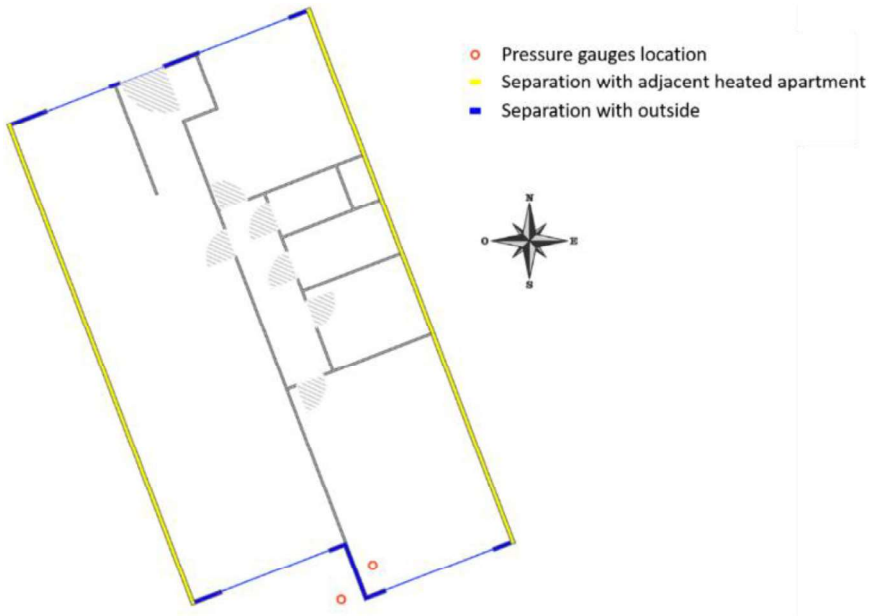



**Fig. 2.** Schematic plan of the tested apartment, including separation type (with adjacent heated apartment or with outside) and pressure gauges location.

0.6 $h^{-1}$ at 50 Pa. The preparation of the apartment during the tests was consistent with method 1 described in ISO 9972:2015 [17].

### 2.2. Approximations techniques

#### 2.2.1. Different approximations

The different approximation techniques compared in this study are obtained by varying three parameters: the duration of approximation periods, the time step between measurements, and the distribution of the approximation value over time. Except for the change in the distribution, whatever the values of the duration and the time step, the approximation always fits within the requirements of the European standard ISO 9972:2015 (i.e., at least 10 measurements made during a minimum of 30 s) [17].

The duration of the approximation periods takes four different values: 30, 60, 90 and 120 s. The time step between measurements is either 1 or 3 s. These values were selected to cover the minimum requirements (i.e., 30 s with a time step of 3 s). The longest period of 120 s was chosen to avoid greater approximation periods that might have had two drawbacks. First, it would have increased the testing period. Second, it would have inflated the probability to record a weather variation during the approximation period, hence not reflecting the conditions during the fictitious period.

For each combination of parameters and for each test, the same conditions (duration period and time step) are applied on approximation periods 1 and 2. The variation of the parameters taken for these two conditions affects the value of zero-flow pressure before and after the fictitious period, but not during it. The third param-

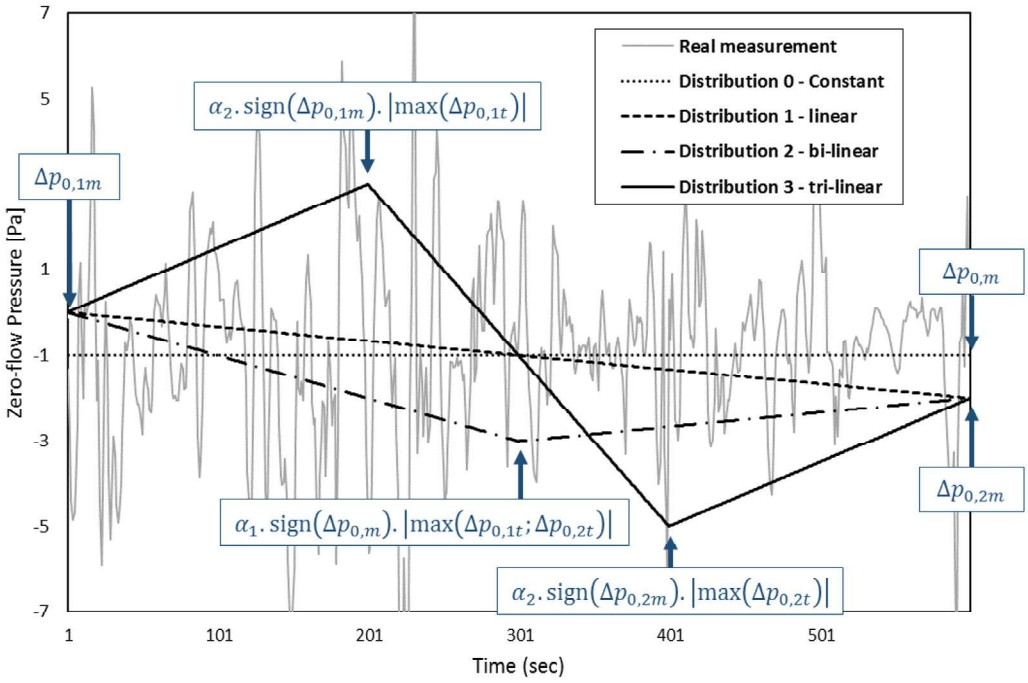



**Fig. 3.** Graphical representation of the four distributions (black) for a typical zero-flow pressure test compared to the real zero-flow pressure (light grey).

eter is the zero-flow pressure distribution, i.e. the variation of the approximation value during the fictitious period.

Fig. 3 graphically represents the four different distributions compared in this study.

The distribution 0 (constant distribution – dotted black line) is the distribution imposed by the standards. In distribution 0, the zero-flow pressure approximation is constant during the fictitious period and its value ($\Delta p_{0,\,m}$) is the mean of the zero-flow pressure measurements made before ($\Delta p_{01,\,m}$) and after ($\Delta p_{02,\,m}$) the fictitious period. In distribution 1 (linear distribution – dashed black line), the approximation value during the fictitious period goes from $\Delta p_{01,\,m}$ at time 0 to $\Delta p_{02,\,m}$ at time 600. Distribution 2 (bi-linear distribution – dashed and dotted black line) goes from $\Delta p_{01,\,m}$ at time 0 to a peak at time 300 and then to $\Delta p_{02,\,m}$ at time 600. The peak is defined as a percentage ($\alpha_1$ on the figure) of the maximum (if $\Delta p_{0,\,m}$ is positive) or the minimum (if it is negative) of the zero-flow pressure measurements made before and after the fictitious period. Distribution 3 (tri-linear distribution – solid line) starts from $\Delta p_{01,\,m}$ at time 0 and goes to $\Delta p_{02,\,m}$ at time 600, but it has two peaks at time 200 and time 400. These peaks are also percentages ($\alpha_2$) of maximum (or minimum, if negative values) of $\Delta p_{01,\,m}$ at time 200 and $\Delta p_{02,\,m}$ at time 400, respectively. Even if the two peaks are different, the same $\alpha_2$ is applied for both. The values of $\alpha_1$ and $\alpha_2$ were chosen to provide the best quality indicator (see Section 2.2.2) when averaging the 31 tests. No specific distribution relevant to all the zero-flow pressure tests was observed. Therefore, the linear distribution was chosen to take into account possible changes in steady wind pressure. Such change between the beginning and the end of the fictitious period is expected to be better approximated using a linear rather than a constant distribution. The choice of bi-linear and tri-linear distributions follows the same logic, yet considering that changes in steady wind pressure work in steps instead of progressive variations. However, it should be considered that these distributions were chosen to test the research hypotheses, while other distributions might be more suitable to verify other hypotheses.

In this study, each distribution (0, 1, 2 and 3) was applied to each time step (1 and 3), within each measurement period (30, 60, 90 and 120) and for each test (1 to 31), leading to a total of 992 approximations (32 for each test).

### 2.2.2. Quality indicator

In his study [13], Delmotte compared the average of zero-flow measurement during the fictitious period with the average of zero-flow approximation during the same period ($\Delta_{ijkl}$), according to Eq. (2):

$$\Delta_{ijkl} = \frac{\sum_{t=1}^{600} \Delta p_{0,it}}{600} - \frac{\sum_{t=1}^{600} \Delta \tilde{p}_{0,it\,jkl}}{600} \tag{2}$$

where, $\Delta p_{0,\,it}$ is the real zero-flow pressure measurement at time $i$ of test $t$, and $\Delta \tilde{p}_{0,it\,jkl}$ is the approximation of zero-flow pressure at time $i$ of test $t$ using the measurement period $j$. The parameter $k$ represents the time step and $l$ is the distribution.

The $\Delta_{ijkl}$ indicator gives information about the ability of an approximation technique to fit, in average, the real zero-flow pressure. However, no information is provided as to how the approximation fits locally the zero-flow pressure. For example, a linear approximation (distribution 1) with $\Delta p_{0,1m} = -1$ Pa and $\Delta p_{0,2m} = 1$ Pa would have the same $\Delta$ than a constant approximation (distribution 0) with $\Delta p_{0,m} = 0$, while the difference between approximation and real measurement at every point would be different.

Since this study focuses on the uncertainties of envelope pressure evaluation at each measurement, there is a strong interest in the ability of an approximation to fit the real zero-flow pressure at each measurement point. This was addressed by calculating the average of the differences between approximation and real measurement at every measurement point during the fictitious period ($\varepsilon_{ijkl}$). From this point, the "approximation quality" refers to this average, based on Eq. (3):

$$\varepsilon_{ijkl} = \frac{\sum_{t=1}^{600} \left| \Delta p_{0,it} - \Delta \tilde{p}_{0,it\,jkl} \right|}{600} \tag{3}$$

It should be noted that the square of the difference could be used instead of the absolute value if the evaluation aimed to penalize huge gaps between approximation and real measurement. However, this study was interested in $\varepsilon_{ijkl}$ values since it could be used for the quantification of uncertainties (see paragraph 3.3.2).

### 2.3. Statistical analysis

In this study, four different durations of approximation period are considered within each test, two time steps are tested within each duration, and four distributions are evaluated within each time step. This methodology leads to hierarchically structured data, hence requiring appropriate tools to perform a rigorous statistical analysis.

Traditional statistical tests (e.g., parametric tests such as a Student *t*-test or ANOVA) assume the data being independent from each other. This is not the case here since the results of different approximation techniques highly depend on the set of data used. When tests assuming independence are used to analyze dependent sets of data, there is a risk to inflate the occurrence of Type I errors. A Type I error occurs when a true null hypothesis is incorrectly rejected (i.e., an effect is statistically observed while in fact there isn't) [20]. This introduces biases in the estimation of parameters [20,21]. In addition, the use of tests dealing with dependent data, but ignoring their clustered structure, can cause an underestimation of standard errors [22]. Conversely, the statistical tool used for the analysis should consider the dependency of results and the nested structure of data. In this study, this was addressed by using multi-level modelling (MLM) [23].

#### 2.3.1. Multi-level modelling

Multi-level modelling is a method of analysis that deals with complex structures of data and recognizes their hierarchical structure by allowing for residuals at multiple levels in the hierarchy [22]. Indeed, MLM partitions the variance of the results into *between-level* (e.g., the variance of approximation quality between different tests) and *within-level* variance (e.g., the variance of approximation quality between different approximation techniques within the same test). This partition is made at each step of the hierarchy and is mathematically expressed in Eq. (4):

$$\varepsilon_{tjkl} = \gamma_0 + e_l + e_k + e_j + e_t \tag{4}$$

where $\gamma_0$ is the grand mean (i.e., the mean when considering all the results) and terms $e_l$, $e_k$, $e_j$ and $e_t$ are deviations from the grand mean specific to the type of distribution, the time step, the measurement period and the test, respectively.

Besides its ability to deal with nested data, MLM allows to decide whether a model parameter can be specified as a *fixed* or *random* effect. A fixed effect is a factor that does not change over time and that is applied equally on each unit at every level in the hierarchy, regardless of the level under which it is nested [20,25]. For example, the possible values of measurement periods remain the same (i.e., 30, 60, 90 and 120 s) whatever test is considered. On the contrary, random effects are expected to change within a level (i.e., from test to test) [25,26]. For example, weather conditions are likely to vary between different tests. One main difference between fixed and random effects is in the calculation of standard errors. In MLM, other sources of uncertainties can be added by the inclusion of further random effects into the model. As a result, fixed-effect models might underestimate the standard error and increases the Type I error rate [25,27]. When designing an experiment, it is good practice for the experimenter to decide in advance whether an effect is fixed (i.e., experimentally controlled) or random (i.e., occurs by chance).

#### 2.3.2. MLM comparison

The comparison of models with and without a given effect allows determining if this effect has an impact on the approximation quality. If a model with an effect has a significantly better fit than the same model without it, then it can be assumed that the effect has an impact on the approximation quality. Table 2 shows the four different models that have been compared in this study. Since the goodness-of-fit of each model depends on the effect chosen, the order of addition of the effects has an impact on the results. In this use of MLM, the logical order is not as obvious as in other domains (e.g., the hierarchy in educational research is straightforward: country, district, school, classroom, students). The order was chosen as follows: duration of the period, number of measurements and distribution of the value computed. However, it was checked that the conclusions (i.e., the effects having a statistical and practical significance) remained the same whatever the order.

**Table 2**
Different models compared in the analysis with fixed and random effects successively added.

| Model | Random effect | Fixed effects |
|---|---|---|
| Model 1 | Test ID | – |
| Model 2 | Test ID | Measurement period |
| Model 3 | Test ID | Measurement period and time step |
| Model 4 | Test ID | Measurement period, time step and distribution |

The simplest model, *model 1*, had only the test number (Test ID) as a random effect and no fixed effect. The other models (2, 3, and 4) were obtained by successively adding three fixed-effects: the measurement period, the time step, and the distribution. Hence: *model 2* had two effects (test ID and measurement period); *model 3* had three effects (test ID, measurement period and time step); *model 4* had four effects (test ID, measurement period, time step and distribution).

The measurement period, time step and distribution were experimentally controlled and were then considered as fixed effects. On the contrary, different tests (i.e., test ID) experienced variable weather conditions and were, therefore, considered as a random effect.

In the literature, researchers have mainly used the chi-square difference ($\chi^2_d$) test to compare the goodness-of-fit of MLM [28]. This test compares the Log Likelihood (LL) values of the restricted (i.e., less parameterized) and unrestricted (i.e., more parametrized) models based on Eq. (5):

$$\chi^2_d = -2LL_{restricted} - 2LL_{unrestricted} \tag{5}$$

Other authors have recommended the use of the Bayesian Information Criterion (BIC) instead of the chi-square difference [28,29]. This is because BIC adjusts the Log Likelihood value considering the number of parameters and the sample size. However, the interpretation of the BIC in model comparison is very subjective and the BIC should not be used in cases where the models differ only in fixed effects [29]. Therefore, in this study the $\chi^2_d$ test was used to test the statistical significance of the differences between the models.

Since the $\chi^2_d$ test is a null hypothesis significance testing (NHST), other than calculating the statistical significance (*p*-value) of the differences detected, it is important to also estimate the practical relevance of their magnitude (effect size). In fact, one of the main limitations of NHST is that *p*-values depend both on the size of the sample and on that of the influence under investigation [30]. In fact, a result may be found to be statistically significant either if the effect is strong or the sample is large [31]. The effect size is a standardized measure of the difference between models [24]. Due to the nature of the data, in this study the effect size was calculated using the pseudo square partial correlation ($r^2_p$, Eq. (6)), where $\sigma_i$ is the variability explained by model *i* [21,26].

$$r^2_p = 1 - \frac{\sigma_{unrestricted}}{\sigma_{restricted}} \tag{6}$$

When interpreting the size of an effect, authors often refer to the benchmarks proposed by Cohen [32,33]. As recommended in

the literature, these values are appropriate particularly in the absence of previous knowledge in the area [34]. Since this work is, to our knowledge, the first focusing on the quantification of uncertainties in zero-flow pressure approximation, the benchmarks by Cohen have been used [33], hence defining effect sizes as small, medium or large, respectively for $r_p^2 > 0.01$, $r_p^2 > 0.09$ and $r_p^2 > 0.25$ [32].

#### 2.3.3. Assessing the need for MLM

One way of testing the need for MLM is by comparing the variance of the approximation quality between different tests (i.e., the between-test variance) with the variance of the approximation quality between different approximations using the same set of data (i.e., the within-test variance). This is done by computing the intra-class correlation (ICC) according to Eq. (7):

$$ICC = \frac{\tau_{00}}{\tau_{00} + \sigma^2} \tag{7}$$

where, $\tau_{00}$ is the between-test variance and $\sigma^2$ is the residual variance (i.e., the within-test variance) [21,24,26].

The ICC can be defined as the amount of variation occurring between tests. A value of zero would indicate that all the variation occurs between different approximations and none of it occurs between different tests (when the same approximation is compared). In such cases, traditional statistical tools (e.g., ANOVA) can be used and MLM is not needed. A value of ICC higher than zero indicates an increase in the variation between tests, leading to postulate a violation of the assumption of independence, and therefore the need to use statistical analysis tools that are not strictly based on assuming independence in the collection of data [21,26].

In this paper, the variance of the approximation quality between tests was 0.672 while the residual variance was 0.098 ($ICC = 0.873$). According to Julian's benchmarks [36], ICC values greater than 0.45 correspond to large intra-class correlation. However, ICC values alone are not sufficient to assess the need for MLM. The design effect quantifies the violation of the assumption of independence on standard error estimates. It provides an estimate of the multiplier to apply on standard errors to take into account the bias resulting from a nested structure of the data [21]. The design effect can be calculated based on Eq. (8):

$$Design\ Effect = 1 + (n_c - 1)ICC \tag{8}$$

where, $n_c$ is the number of approximations per test (32, in our data).

The use of single-level modelling instead of MLM might not lead to misleading results when the design effect is smaller than 2 [21,37,38]. In this study, the computation of both ICC (0.873) and design effect (27.2) justified the need for MLM.

#### 2.3.4. Covariance structure and parameters estimation

One of the main advantages of MLM is the flexibility of the covariance matrix (i.e., the matrix that defines how the variances associated with each independent group are related to each other). In fact, multi-level modelling makes it is possible to specify direct assumptions regarding its structure [24]. Since the models used in our analysis featured only one random effect – and this was not a time-based study – an independent covariance matrix was used (that is, the variances of random effects are independent and have the same value) [20].

MLM can be fitted using two different methods for parameter estimation: the full information maximum likelihood (FIML) and the restricted maximum likelihood (REML) method. However, REML can only be used to compare models differing in random effects, and not in fixed effects [39,40]. Therefore, the use of FIML was preferred in this study.

## 3. Results

The results are presented in three sections. The first section illustrates the issue of zero-flow pressure approximation by comparing the real zero-flow pressure with the reference case (i.e., minimum standard requirements) for the 31 tests. The second section describes and analyses the results of the model comparison. The third section uses these results to quantify the uncertainty of both zero-flow pressure approximation and envelope pressure.

### 3.1. Zero-flow pressure in fictitious tests and reference case approximation

Table 3 gives the minimum, maximum, mean ($M$) and standard deviation ($SD$) of: the approximation quality for the reference case applied to the 31 tests; the mean; and, the standard deviation of zero-flow pressure ($\Delta p_{0,\,mi}$) measured during the fictitious periods for the 31 tests.

Comparing the mean average of zero-flow pressure and the approximation quality for the reference case illustrates the issue highlighted by Delmotte [13]. Indeed, the mean approximation quality (i.e., the mean difference between approximation and real zero-flow pressure measurement) using the reference case (1.26 Pa) is of considerable magnitude. As a comparison, the absolute value of the mean average zero-flow pressure measured during fictitious periods is 0.73 Pa. Clearly, these values are case-related and should not be generalized without further research. However, a large value of approximation quality can be expected whereas wind is known as one of the most important sources of uncertainty [14].

### 3.2. Comparison of approximation techniques

#### 3.2.1. Model comparison

Table 4 reports the results of the chi-square difference ($\chi_d^{2\ p}$) – with the interpretation of its statistical significance (NHST) – and the estimation of the pseudo-square partial correlation ($r_p^2$) in the comparison between models. The values of $\chi_d^{2\ p}$ and $r_p^2$ are computed considering both quality indicators, $\varepsilon$ and $\Delta$, as discussed in paragraph 2.2.2.

The comparison using $\varepsilon$ as quality indicator shows that the difference between models with and without the measurement period (model 1 vs 2) is statistically significant and practically relevant ($\chi_d^2 = 202.60$, $p < 0.01$ and $r_p^2 = 0.10$). The difference between models with and without the time step (model 2 vs 3) is not statistically significant and its magnitude is non-substantive ($\chi_d^2 = 0.84$, $p = 0.36$ and $r_p^2 < 0.01$), i.e. the influence detected

**Table 3**
Minimum, maximum, mean and standard deviation for (1) the approximation quality using reference case, (2) the average value and (3) the standard deviation of zero-flow pressure measurements.

| | Min [Pa] | Max [Pa] | M [Pa] | SD [Pa] |
|---|---|---|---|---|
| Approximation quality | 0.27 | 2.79 | 1.26 | 0.72 |
| Mean average of zero-flow pressure | −2.05 | 0.50 | −0.73 | 0.53 |
| Standard deviation of zero-flow pressure | 0.34 | 3.76 | 1.51 | 0.89 |

**Table 4**
Multi-Level Model comparison (statistical and practical significance) using $\varepsilon$ and $\Delta$ as quality indicators.

| Model Comparison | $\chi^{2\ p}_d(\varepsilon)$ | $r^2_p(\varepsilon)$ | $\chi^{2\ p}_d(\Delta)^{NHST}$ | $r^2_p(\Delta)$ |
|---|---|---|---|---|
| 1 vs 2 | 202.60** | 0.10 | 14.45** | <0.01 |
| 2 vs 3 | 0.844$^{N.S}$ | <0.01 | 0.614$^{N.S.}$ | <0.01 |
| 3 vs 4 | 4.835* | <0.01 | 4.295* | <0.01 |

$^{N.S.}$Not significant ($p > 0.05$),*Significant ($0.001 < p \leq 0.05$), **Highly significant ($p \leq 0.001$).
$r^2_p < 0.01$: effect with non-substantive magnitude, $r^2_p \geq 0.01$: small effect, $r^2_p \geq 0.09$: moderate effect, $r^2_p \geq 0.25$: large effect.

is not practically relevant. The difference between models with and without distribution (model 3 vs 4) is statistically significant and with an effect of non-substantive size ($\chi^2_d = 4.84$, $p = 0.03$ and $r^2_p < 0.01$). The use of the $\Delta$ quality indicator leads to the detection of differences between models whose magnitude is consistently not practically relevant ($r^2_p < 0.01$).

The random effect Test ID was useful to assess the need for MLM, although this parameter has no physical meaning. Since zero-flow pressure is induced by weather factors (wind pressure and temperature difference), which varied during the test period, the Test ID is expected to hide a random effect related to differences in conditions (leading to a strong variation of zero-flow pressure measurements). However, in this study, the focus is on zero-flow pressure and not on weather conditions. Therefore, the standard deviation of zero-flow pressure measurements during the fictitious period was used to replace the Test ID as a random effect. The 31 tests were divided in three deviation classes: class 1 for calm wind ($\sigma_1 \leq 1\,Pa$); class 2 for moderate wind ($1\,Pa < \sigma \leq 2\,Pa$); and, class 3 for strong wind ($\sigma > 2\,Pa$). In the absence of guidelines in the literature for this classification, the boundaries were chosen to have equal pressure steps (1 Pa) and adequate sample sizes in each class (respectively 416, 192 and 348 for classes 1, 2 and 3) between classes. Further work could more thoroughly investigate how the wind affects the standard deviation of zero-flow pressure measurements.

The model comparison allows determining how parameters affect the approximation quality. However, it gives no information about the quantification of their impact in terms of pressure difference. The next paragraph presents an in-depth analysis of the impact of deviation classes and measurement period on the zero-flow pressure approximation.

### 3.2.2. Pairwise comparisons

Fig. 4 shows the mean and 95% confidence interval of the approximation quality for 12 categories of approximations based on measurement period and grouped under the 3 standard deviation classes, hence providing a graphical overview of the results in terms of pressure difference.

Due to the samples sizes being unequal, preliminary tests were performed on the data to verify eventual violations of the assumptions of normality and homogeneity of variance. In fact, when both the sizes of samples and their variances differ, there is a risk of inflating the occurrence of Type I errors (i.e., the probability of falsely rejecting the null hypothesis) [20,41,42]. Since the data were not normally distributed (Kolmogorov–Smirnov test = 0.13, $p < 0.001$) [43], and the variances of the three deviation classes were significantly different (Levene's test = 40.74, $p < 0.001$), non-parametric Wilcoxon rank-sum tests were adopted to calculate the statistical significance of the differences detected [20]. In addition, considering that multiple tests were performed on the same data under the same hypothesis, Bonferroni corrections were applied to counterbalance the increase in familywise error rate caused by the significance level inflating across multiple pairwise comparisons. The familywise error is the probability of making at least one Type I error, and is calculated as $1 - (0.95)^n$, with $n$ being the number of comparisons performed [20]. The probability of making a Type

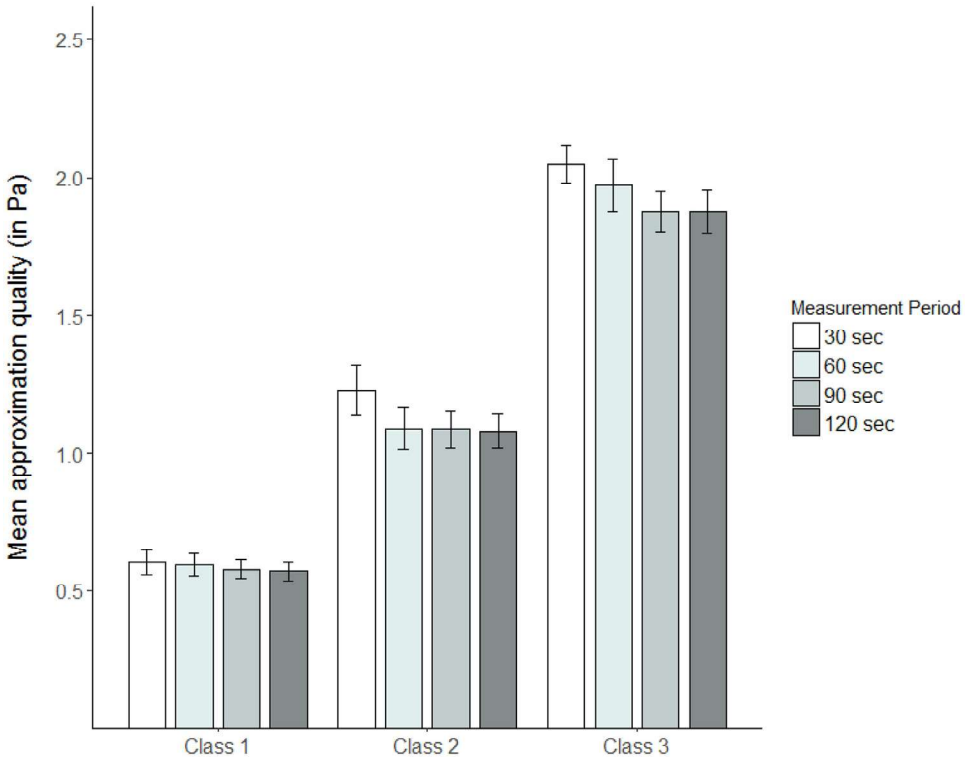



**Fig. 4.** Mean approximation quality of different approximations grouped in 12 categories.

**Table 5**
Between-classes and within-classes comparisons based on Wilcoxon parirwise comparisons with Bonferroni correction (effect sizes were estimated by Hedge's g coefficient).

| | $(N_1; N_2)$ | $(\varepsilon_1 - \varepsilon_2)^{NHST}$ | 95% $CI_L$ | 95% $CI_U$ | Effect size ($g$) |
|---|---|---|---|---|---|
| Between-class comparison | | | | | |
| Class 1 vs Class 2 | (416; 192) | −0.53** | −0.57 | −0.49 | −2.41 |
| Class 1 vs Class 3 | (416; 384) | −1.36** | −1.40 | −1.31 | −4.38 |
| Class 2 vs Class 3 | (192; 384) | −0.82** | −0.88 | −0.77 | −2.32 |
| Within-class comparison | | | | | |
| Class 1 ($N = 416$) | (104; 104) | | | | |
| 30 vs 60 | – | $0.01^{N.S}$ | 0.00 | 0.02 | 0.04 |
| 30 vs 90 | – | 0.03* | 0.01 | 0.04 | 0.12 |
| 30 vs 120 | – | 0.03* | 0.02 | 0.05 | 0.16 |
| 60 vs 90 | – | $0.02^{N.S}$ | 0.00 | 0.03 | 0.08 |
| 60 vs 120 | – | 0.02* | 0.01 | 0.04 | 0.12 |
| 90 vs 120 | – | $0.01^{N.S}$ | 0.00 | 0.02 | 0.05 |
| Class 2 ($N = 192$) | (48; 48) | | | | |
| 30 vs 60 | – | 0.14** | 0.11 | 0.16 | 0.50 |
| 30 vs 90 | – | 0.14** | 0.11 | 0.17 | 0.52 |
| 30 vs 120 | – | 0.15** | 0.12 | 0.18 | 0.56 |
| 60 vs 90 | – | $0.00^{N.S}$ | −0.01 | 0.02 | 0.01 |
| 60 vs 120 | – | $0.01^{N.S}$ | −0.01 | 0.03 | 0.04 |
| 90 vs 120 | – | $0.01^{N.S}$ | 0.00 | 0.01 | 0.03 |
| Class 3 ($N = 384$) | (96; 96) | | | | |
| 30 vs 60 | – | 0.08* | 0.03 | 0.12 | 0.19 |
| 30 vs 90 | – | 0.17** | 0.14 | 0.21 | 0.50 |
| 30 vs 120 | – | 0.17** | 0.13 | 0.21 | 0.48 |
| 60 vs 90 | – | 0.10** | 0.06 | 0.13 | 0.23 |
| 60 vs 120 | – | 0.10** | 0.06 | 0.13 | 0.22 |
| 90 vs 120 | – | $0.00^{N.S}$ | −0.01 | 0.01 | 0.00 |

$^{N.S.}$Not significant ($p > 0.016$), *Significant ($0.00033 < p \leq 0.016$), **Highly significant ($p \leq 0.00033$), for between-class comparison.
$^{N.S.}$Not significant ($p > 0.008$), *Significant ($0.00017 < p \leq 0.008$), **Highly significant ($p \leq 0.00017$), for within-class comparison.
$g < 0.2$: effect with non-substantive magnitude, $g \geq 0.2$: small effect, $g \geq 0.5$: moderate effect, $g \geq 0.8$: large effect sizes.

I error was respectively 26% and 14% for the within-class and the between-class comparisons. The Bonferroni correction ensures that the cumulative Type I error rate is kept below 0.05, although it is an adjustment method that is often considered as conservative and potentially vulnerable to Type II errors (i.e., the likelihood of failing to reject a false null hypothesis) [20].

Table 5 presents the results of the Wilcoxon tests with Bonferroni correction. For each comparison, the table provides the sample size of each group ($N_1$ and $N_2$), the difference between means and the interpretation of its statistical significance ($(\varepsilon_1 - \varepsilon_2)^{NHST}$), the lower and upper 95% confidence intervals for the mean difference (95% $CI_L$ and 95% $CI_U$), and the effect size estimated by the Hedge's g coefficient. This was preferred over other indicators of effect size (e.g., Cohen's d and Glass's $\Delta$) since the standard deviation of independent groups were not the same and sample sizes were different. In the calculation of Hedge's g, the standard deviation of each group is weighted with the sample size before pooling, according to Eq. (9) [30]:

$$g = \frac{\varepsilon_1 - \varepsilon_2}{\sigma^*_{pooled}} \tag{9}$$

where, $\sigma_{pooled}$ is the weighted pooled standard deviation and $\varepsilon_1$ and $\varepsilon_2$ are the mean approximation qualities for both groups. Cohen's benchmarks were used to infer small ($g \geq 0.2$), moderate ($g \geq 0.5$) and large ($g \geq 0.8$) effect sizes [32].

The results of the pairwise comparisons confirm the graphical observations from Fig. 4. The differences in means between deviation classes are statistically significant and practically relevant. The results of the comparisons between measurement periods, however, depend on the deviation class. Within class 1, the comparison 30 vs 90, 30 vs 120 and 60 vs 120 are statistically significant but all the differences detected have non-substantive magnitudes. Within class 2, all the comparisons featuring measurement periods of 30 s (i.e., 30 vs 60, 30 vs 90 and 30 vs 120) are highly statistically significant with differences of moderate magnitude. Within class 3, all the comparisons featuring periods of 30 s are statistically significant (30 vs 60) and highly significant (30 vs 90 and 30 vs 120) with practically relevant effect sizes (small for 30 vs 60; moderate for 30 vs 90 and 30 vs120). Within this class, the comparisons 60 vs 90 and 60 vs 120 are also highly statistically significant and have a practical effect of small magnitude.

#### 3.2.3. Standard deviation measurements

Since, in practice, the real zero-flow pressure cannot be measured during the fictitious period, its mean average and standard deviation cannot be computed. In order to check if the standard deviation of the measurements within approximation periods is a good indicator of the standard deviation within the fictitious period, a Spearman's rho correlation test was performed. This was preferred to the classical Pearson's r coefficient because the standard deviations were not normally distributed (Kolmogorov–Smirnov test = 0.17, $p < 0.001$) [30,35,44]. According to Cohen's benchmarks, the correlation between standard deviation measurements during the approximation and fictitious periods had a practical association effect of strong magnitude (Spearman's rho = 0.829, $p < 0.001$) [32].

### 3.3. Quantification of uncertainties in envelope pressure measurements

#### 3.3.1. Equation for standard uncertainty of envelope pressure

There are two types of uncertainty evaluation methods: Type A is when uncertainties can be evaluated by statistical analysis of a series of observations; Type B is when an estimate cannot be obtained from repeated measurements and the uncertainty must be evaluated by scientific judgement (e.g., previous measurements

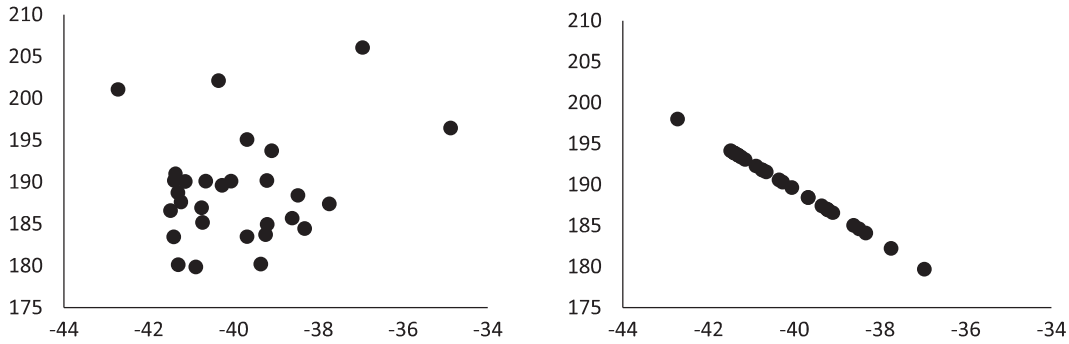



**Fig. 5.** 30 pressure-airflow couples measurements (one per second): when a −40 Pa target pressure is set during a typical fan pressurization test (left); if measurements were completely uncorrelated (right).

or manufacturer's specifications) [45]. In practice, the envelope pressure difference is obtained by averaging multiple measurements ($N$) of the same pressure difference. According to the literature [45], in case of Type A evaluation methods, the standard uncertainty is the square root of the experimental variance of the arithmetic mean (Eq. (10)) [12].

$$u_c(\Delta P_{env}) = \sqrt{\frac{s^2(\Delta P_{meas})}{N}} \tag{10}$$

where, $u_c(\Delta P_{env})$ is the standard uncertainty of the envelope pressure difference, $s^2(\Delta P_{meas})$ is the experimental standard deviation of the envelope pressure measurement, and $N$ is the number of repeated measurements.

When there are large wind fluctuations during a test, however, it might not always be appropriate to consider the envelope pressure measurement as a series of repeated independent measures. The left side of Fig. 5 shows this issue by plotting 30 pressure-airflow couples measured within an interval of 30 s during a typical fan pressurization test with a target pressure of −40 Pa. The right side of the figure shows the results if envelope pressure measurements were perfectly independent. Delmotte discussed this issue when dealing with standard uncertainty propagation [12,46].

When measurements are no longer independent, the type B evaluation method must be used. In such cases, the standard uncertainty is evaluated by scientific judgement based on the available information on the variability of the results [45]. In the development of the standard uncertainty calculation formula, Delmotte considered each measurement point separately, and therefore did not deal with propagation uncertainty when calculating the means [12]. Similarly, in this study the uncertainty on pressure envelope was considered at each measurement point and not on mean averages.

The envelope pressure is the difference between the pressure measured and the zero-flow pressure. Therefore, the standard uncertainty in envelope pressure difference can be computed with Eq. (11) [12,45]:

$$u_c(\Delta P_{env}) = \sqrt{u_c^2(\Delta P_u) + u_c^2(\Delta p_0)} \tag{11}$$

where, $u_c(\Delta P_u)$ is the uncertainty related to the pressure measured at gauge location and $u_c(\Delta p_0)$ is the uncertainty related to the zero-flow pressure estimation.

This equation is only valid if $\Delta P_u$ and $\Delta p_0$ are independent. In the calculation performed in this study, a constant distribution was considered for the zero-flow pressure approximation. Thus, $\Delta p_0$ is constant over the test while $\Delta P_u$ values are scattered Fig. 5; the assumption of independence is therefore satisfied. Since the hypotheses related to envelope pressure are considered acceptable (i.e., negligible uncertainty), the standard uncertainty of pressure measurement was deduced from the equipment described in paragraph 2.1.2 (i.e., the greatest between ±0.5% and ±0.1 Pa [18,19]).

*3.3.2. Standard uncertainty in zero-flow pressure*

The standard uncertainty in zero-flow pressure is composed of two parts: the zero-flow pressure measurement and its approximation. The uncertainty of zero-flow pressure measurement depends on the approximation technique and on the pressure gauge used. The standard uncertainty of the equipment used to measure zero-flow pressure in this study was assumed constant (±0.1 Pa) because the zero-flow pressure is always lower than 5 Pa (ISO 9972:2015 standard requirement [17]). Since the uncertainty of the measurement is constant, and it is independent of the approximation, Eq. (12) can be used to compute the standard uncertainty in zero-flow pressure:

$$u_c(\Delta p_0) = \sqrt{u_{c,m}^2(\Delta p_0) + u_{c,a}^2(\Delta p_0)} \tag{12}$$

where, $u_{c,\,m}(\Delta p_0)$ is the standard uncertainty related to the zero-flow pressure measurement, and $u_{c,\,a}(\Delta p_0)$ is the standard uncertainty related to the zero-flow pressure approximation.

The standard uncertainty related to zero-flow pressure measurement is the standard uncertainty of the equipment divided by two, since the zero-flow pressure is given by the average between pre- and post-test measurements and both have the same standard uncertainty [12].

The standard uncertainty in zero-flow pressure approximation cannot be evaluated by series of observations because the weather conditions cannot be kept constant between tests. Thus, it must be evaluated based on scientific judgement and available information on the variability of results. The indicator $\varepsilon$ is defined as the mean of $|\Delta p_{0,ti} - \Delta\tilde{p}_{0,ti}|$ and both $\Delta P_0$ (Shapiro-Wilk test: $W = 0.94$, $p = 0.08$; Komolgorov–Smirnov test: $D = 0.16$, $p = 0.37$) and $\varepsilon$ (Shapiro-Wilk test: $W = 0.94$, $p = 0.06$; Komolgorov–Smirnov test: $D = 0.16$, $p = 0.4$) follow distributions not significantly different from normal. Therefore, it can be assumed that $\Delta P_0 - \varepsilon/2$ and $\Delta P_0 + \varepsilon/2$ are respectively the lower and the upper limit of the interval containing 50% of the zero-flow pressure. Since the Z-scores of the normal distribution are respectively 0.675 and −0675 when considering 75% and 25% of the results, Eq. (13) can be used to find the standard deviation of the zero-flow pressure based on approximation quality.

$$\pm\ 0.675 = \frac{(\Delta p_{0,a} \pm \varepsilon/2) - \Delta p_0}{\sigma(\Delta p_0)} \tag{13}$$

It is assumed that the zero-flow pressure approximation ($\Delta P_{0,\,a}$) equals the average of the zero-flow pressure measurements made during the fictitious period ($\Delta P_0$). This hypothesis is acceptable since the difference between both is already considered in the term $\varepsilon$ of the equation. Therefore, the standard uncertainty of the approximation method ($u_{c,\,a}(\Delta p_0)$) is given by the standard deviation of the zero-flow pressure around its mean value ($= \varepsilon/1.35$) [45]. Table 6 provides $u_{c,\,a}(\Delta p_0)$ values obtained in this

**Table 6**
Values for the uncertainty due to zero-flow pressure approximation for the 12 groups of approximations considered in the in-depth analysis of this study [Pa].

| | 30 s | 60 s | 90 s | 120 s |
|---|---|---|---|---|
| Class 1 | 0.45 | 0.44 | 0.43 | 0.42 |
| Class 2 | 0.91 | 0.81 | 0.80 | 0.80 |
| Class 3 | 1.52 | 1.46 | 1.39 | 1.39 |

study for different deviation classes and measurement periods based on $\varepsilon$ averages.

The results presented in Table 6 confirm the observations made in the pairwise comparison (Fig. 4, Section 3.2.2). Indeed, increasing the approximation period to 60 s reduces the uncertainty within Class 2 and 3. Increasing the measurement period to 90 s reduces the uncertainty in Class 3.

*3.3.3. Standard uncertainty in envelope pressure*

Since only a constant distribution has been considered, Eq. (14) gives the total standard uncertainty of envelope pressure evaluation as a function of the measurement at the pressure gauge ($\Delta P_u$):

$$u_c(\Delta P_{env}) = \sqrt{\max(0.005 * \Delta P_u; 0.1)^2 + \frac{0.1^2}{2} + \left(\frac{\varepsilon}{1.35}\right)^2} \quad (14)$$

In the literature on uncertainties in airtightness evaluation, results are often given in terms of expended uncertainties [12,15]. The expanded uncertainty is applied when dealing with a Type B evaluation method and is the equivalent to the confidence interval in a Type A evaluation method. The expanded uncertainty is obtained by multiplying the standard uncertainty by a coverage factor ($k$). If the probability distribution is assumed normal, coverage factors of 2 and 3 correspond respectively to confidence intervals of $\approx$95% and $\approx$99% [45]. In this study, the envelope pressure was assumed normally distributed and a coverage factor of 2 was used to give an expanded uncertainty equivalent to a 95% confidence interval.

Fig. 6 represents the expanded uncertainty ($k = 2$) as a function of the pressure difference measured by pressure gauges ($\Delta P_u$) with (solid lines) and without (dashed lines) consideration of the zero-flow pressure approximation component in the envelope pressure uncertainty. The results are plotted for the three different deviation classes, considering for each class a measurement period of 30 s. The left part of the figure is the relative standard uncertainty (expressed in percentage of $\Delta P_u$), while the right part is the absolute standard uncertainty (in Pa).

These graphs show that the uncertainty due to zero-flow pressure approximation has a large impact on the envelope pressure uncertainty. Indeed, for a measurement at 50 Pa when using approximation periods of 30 s, the uncertainty due to zero-flow pressure approximation is 76%, 93% and 97% of the envelope pressure uncertainty for low-, medium- and high-wind conditions respectively.

Table 7 shows the differences in uncertainty calculations without the uncertainty due to zero-flow pressure approximation and with it for three different deviation classes.

The ISO 9972:2015 European standard allows the first measurement to be made at a pressure of three times the zero-flow pressure [17]. Although that multiplier is applied on the zero-flow pressure value and not on the deviation class, it is reasonable to expect that, for deviation class 3, a measurement at 10 Pa might be sometimes irrelevant.

The value presented in Table 7 and in Fig. 6 should be considered carefully in the calculations. Indeed, when performing a test, each airflow-pressure couple recorded is the average of multiple measurements. Furthermore, in practice the operator often tries to take a measurement when wind fluctuations are low. This reduces the impact of wind fluctuations and decreases this component of uncertainty. The values of uncertainties found might overestimate the uncertainty related to zero-flow pressure approximation encountered in practice.

## 4. Discussion

This study shows that the uncertainty due to zero-flow pressure approximation is substantial and can considerably increase the uncertainty in pressure measurements. Indeed, this uncertainty is 1.52 Pa for deviation class 3 when considering 30-s measurements for the approximation period, while at 50 Pa the uncertainty due to the equipment is 0.25 Pa. Fig. 7 represents the uncertainty in the $Y$ variable ($\ln(Q)$) and in the $X$ variable ($\ln(\Delta P)$), with (X1, dashed grey line) and without (X0, dotted grey line) consideration of the uncertainty due to zero-flow pressure approximation, as a function of the pressure measurement in a typical fan pressurization test performed on an apartment in Brussels.

This observation has an important impact on the protocol for building airtightness evaluation. A linear regression technique is generally used to determine building flow characteristics (i.e., flow exponent and leakage coefficient) from airflow-pressure couples, but the ISO 9972:2015 standard [17] gives no indication about the

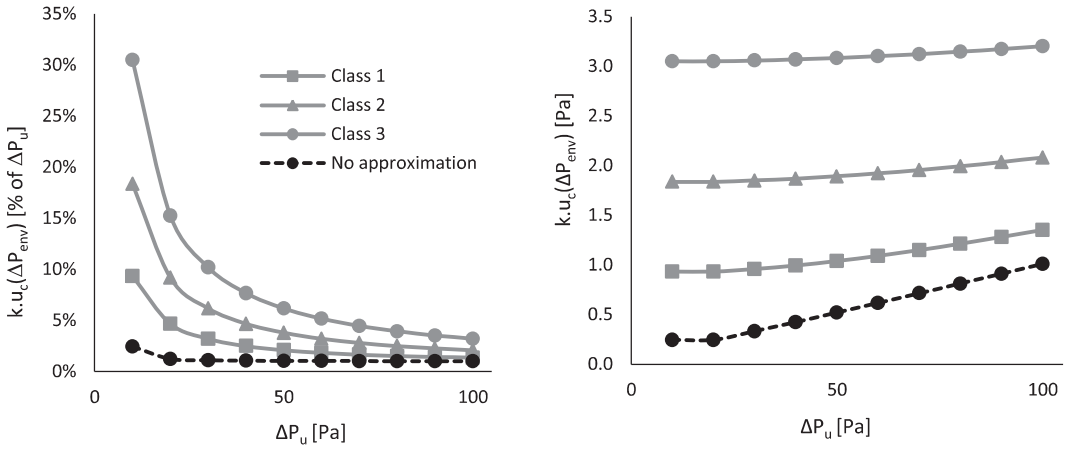



**Fig. 6.** Results of the calculations for relative (left, in % of $\Delta P_u$) and absolute (right, in Pa) expanded standard uncertainty of the envelope pressure evaluation with (solid lines) and without (dashed line) considration of the approximation uncertainty component.

**Table 7**
Results for the calculations of expanded standard uncertainty ($k=2$) of the envelope pressure in terms of % of $\Delta P_u$ and in terms of Pa. Results are given for low-, medium- and high-pressure.

| | Low pressure (10 Pa) | | Medium pressure (50 Pa) | | High pressure (100 Pa) | |
|---|---|---|---|---|---|---|
| | [Pa] | [%] | [Pa] | [%] | [Pa] | [%] |
| No approximation | 0.24 | 2.4 | 0.52 | 1.0 | 1.01 | 1.0 |
| Deviation class 1 | 0.93 | 9.3 | 1.04 | 2.1 | 1.35 | 1.4 |
| Deviation class 2 | 1.84 | 18.4 | 1.89 | 3.8 | 2.08 | 2.1 |
| Deviation class 3 | 3.05 | 30.5 | 3.08 | 6.2 | 3.20 | 3.2 |

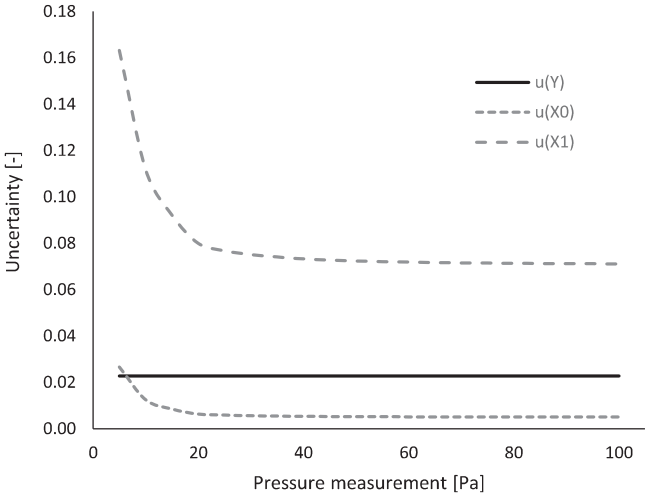



**Fig. 7.** Uncertainties in *Y* variable and *X* variable - with (X1) and without (X0) consideration of the zero-flow pressure approximation - as a function of the pressure measurement for a typical fan pressurization test.

choice of the method. The ordinary least square (OLS) method is often utilized in practice, but this method assumes that the uncertainties in the envelope pressure are negligible [47]. Various authors have already questioned the use of the OLS method, even without considering the uncertainty due to zero-flow pressure approximation [12,48]. The findings of this study strengthen, as illustrated by Fig. 7, their point of view in the debate and supports the development of other regression techniques, as for example the iterative weighted least square (IWLS) suggested by Okuyama and Onishi [48] or the weighted line of organic correlation (WLOC) proposed by Delmotte [13]. Recent research has also shown that using the OLS method leads to a poor estimation of uncertainties in building flow characteristics [13,49].

This study quantifies the impact of uncertainties in zero-flow pressure approximation on envelope pressure uncertainty. Its influence on the global uncertainty is more complex to quantify because the study of different regression techniques is also implied. It must be considered that this component has no impact on the uncertainty calculation using the OLS method since this assumes that the uncertainty in envelope pressure measurement is negligible. However, it has an impact on the calculation of uncertainties in regression parameters and on the estimation of the correlation between both coefficients when using other regression methods (e.g., WLOC or IWLS). In addition, its impact is expected to strongly vary depending on the variable of interest (e.g., airflow at 50 or 10 Pa) due to the weighting of the measurement induced by alternative regression methods. The study of the change in regression techniques and the uncertainty in zero-flow pressure approximation has an influence on the total uncertainty, and the airtightness estimation is an important work that should be conducted in further researches.

This study also finds that none of the three suggested distributions gives better results than the constant one (i.e., the distribution recommended in the ISO 9972:2015 standard [17]). This is not consistent with the bi-linear distribution suggested by Delmotte [13]. However, the results presented in the previous section do not imply that the constant distribution is the most appropriate. Indeed, this study has only tested constant $\alpha_i$ coefficients in the distribution while the standard deviation seems to have a strong impact on the approximation quality. It could be interesting in further research to test distributions with $\alpha_i$ coefficients depending on the zero-flow pressure variation (i.e., distributions depending on the test results) before claiming that uncertainties cannot be reduced by changing the zero-flow pressure distribution during the test.

Finally, this study shows that an increase of measurement period has a statistically significant and practically relevant positive impact on the approximation quality, especially on windy days. This is important because this modification is easy to implement in practice. When considering travel time, building preparation, equipment installation, and the measurement itself, a fan pressurization test can easily take half-a-day to complete. Therefore, the addition of 90 s to both approximation periods is negligible compared to the total duration of the test itself. Results showed that an increase of the approximation period from 30 to 60 s for class 2 and from 30 to 90 s for class 3 should be considered, respectively, for days with medium and high wind. Unfortunately, to our knowledge, no other author has yet studied the impact of this variable. One interesting further work would be the generalization of these observations on a large sample of zero-flow pressure tests performed on several different buildings.

In generalizing the findings of this study, some methodological limitations should be acknowledged. In fact, even if the results were obtained by rigorous statistical testing, the data on which they were based were specific to the sample analyzed. Other buildings could undergo other zero-flow pressure (e.g., due to a stack effect in high-rise buildings or different surroundings inducing other wind pressure). Since a correlation between the zero-flow pressure and its uncertainty can be expected, it is also reasonable to assume an influence of the building case on the zero-flow pressure approximation uncertainty. However, the method and the trends observed (e.g., the importance of the zero-flow pressure approximation uncertainty regarding the envelope pressure uncertainty or the reduction of uncertainty when taking higher approximation periods) should still be appropriate for other cases. In addition to the generalization of the results, applying this quantification method on a large sample of different buildings would also allow to analyze the impact of building-related parameters (e.g., dwelling type, volume or height, etc.) on uncertainty due to zero-flow pressure approximation. Another variable that could be tackled in further research is the location of the pressure gauge. As mentioned in Section 2.1.3, the location of the pressure gauge is expected to have an influence on the zero-flow pressure average and standard deviation and, therefore, on the uncertainty due to zero-flow pressure approximation.

## 5. Conclusion

This study provides 4 key-findings:

- Multi-level modelling can, and should, be used to estimate uncertainties due to zero-flow pressure approximation and to study the impact of different variables on it.
- The approximation period should be increased to 60 s on medium-wind days (to reduce the uncertainty by 11%), and to 90 s on high-wind days (to reduce the uncertainty by 9%).
- A change in the zero-flow pressure distribution or in the time step between measurements does not provide statistically or practically better results.
- Uncertainties in zero-flow pressure represents more than 75% of the envelope pressure uncertainties whatever the wind conditions, and therefore they have an impact on the choice of regression method used.

This study is an important step in the quantification of uncertainties in airtightness measurements, but further research in this field is needed, including: applying the proposed method on a large sample of data from different buildings; studying the impact of uncertainty due to zero-flow pressure on the airtightness estimation for different regression techniques (OLS, IWLS or WLOC); quantifying the other relevant uncertainty components of airtightness measurements uncertainties.

## Conflict of interest

I wish to confirm that there are no known conflicts of interest associated with this publication and there has been no significant financial support for this work that could have influenced its outcome.

I confirm that the manuscript has been read and approved by all named authors and that there are no other persons who satisfied the criteria for authorship but are not listed. I further confirm that the order of authors listed in the manuscript has been approved by all of the authors.

I confirm that I have given due consideration to the protection of intellectual property associated with this work and that there are no impediments to publication, including the timing of publication, with respect to intellectual property. In so doing I confirm that I have followed the regulations of authors institutions concerning intellectual property.

I understand that I am (Corresponding Author) the sole contact for the Editorial process (including Editorial Manager and direct communications with the office). I am responsible for communicating with the other authors about progress, submissions of revisions and final approval of proofs. I confirm that I have provided a current, correct email address which is accessible by the Corresponding Author.

## Acknowledgements

Authors gratefully acknowledge the support of Dr Michael Kent from the University of Nottingham in the statistical analysis of data. Authors also thank Christophe Delmotte from the Belgian Building Research Institute and Felipe Ossio from Pontificia Universidad Católica de Chile for helping with a proofreading of the paper. The tests were performed on a site from Jacques Delens Company and this work was supported by an INNOVIRIS grant (2016-DOCT-9) awarded to the first author for his PhD research at Architecture et Climat, Université catholique de Louvain.

## References

[1] T. Kalamees, Air tightness and air leakages of new lightweight single-family detached houses in Estonia, Build. Environ. 42 (6) (2007) 2369–2377.
[2] J. Jokisalo, et al., Building leakage, infiltration, and energy performance analyses for Finnish detached houses, Build. Environ. 44 (2) (2009) 377–387.
[3] X. Loncour, C. Mees, L'étanchéité à l'air des bâtiments, Centre Scientifique et Technique de la Construction (CSTC), 2015. Technical information note 255.
[4] J. Šadauskienė, et al., Impact of air tightness on the evaluation of building energy performance in Lithuania, Energies 7 (8) (2014) 4972–4987.
[5] R. Thor-Oskar, H. Sverre, T.J. Vincent, Airtightness estimation—a state of the art review and an en route upper limit evaluation principle to increase the chances that wood-frame houses with a vapour-and wind-barrier comply with the airtightness requirements, Energy Build. 54 (2012) 444–452.
[6] M. Prignon, G.V. Moeseke, Factors influencing airtightness and airtightness predictive models: a literature review, Energy Build. 146 (2017) 87–97.
[7] J. Novak, Repeatability and reproductibility of blower door tests - four years' experience of round-robin tests in Czech republic, 9th International Buildair Symposium, 2015.
[8] C. Delmotte, J. Laverge, Interlaboratory tests for the determination of repeatability and reproducibility of buildings airtightness measurements, 32nd AIVC Conference and 1st TightVent Conference: "Towards Optimal Airtightness Performance", 2011 Brussels, Belgium.
[9] A Persily, Repeatability and accuracy of pressurization testing, ASHRAE/DOE Conference Thermal Performance of the Exterior Envelopes of Buildings II, 1982 Las Vegas, USA.
[10] A.K. Kim, C.Y. Shaw, in: Seasonal Variation in Airtightness of Two Detached houses, in Measured Air Leakage of Buildings: A Symposium, ASTM International, Philadelphia, USA, 1986, pp. 16–32.
[11] W. Bracke, et al., Durability and measurement uncertainty of airtightness in extremely airtight dwellings, Int. J. Vent. 14 (4) (2016) 383–394.
[12] C. Delmotte, Airtightness of buildings-calculation of combined standard uncertainty, 34th AIVC Conference "Energy Conservation Technologies for Mitigation and Adaptation in the Built Environment: the Role of Ventilation Strategies and Smart Materials", 2013 Athens, Greece.
[13] C Delmotte, Airtightness of buildings - considerations regarding the zero-flow pressure and the weighted line of organic correlation, 38th AIVC Conference "Ventilating Healthy Low-Energy Buildings", 2017 Nottingham, UK.
[14] M. Sherman, L. Palmiter, Uncertainties in fan pressurization measurements, in: Airflow Performance of Building Envelopes, Components, and Systems, ASTM International, Philadelphia, USA, 1995, pp. 266–283.
[15] F.R. Carrié, V. Leprince, Uncertainties in building pressurisation tests due to steady wind, Energy Build. 116 (2016) 656–665.
[16] I. Walker, et al., Applying large datasets to developing a better understanding of air leakage measurement in homes, Int. J. Vent. 11 (4) (2013) 323–338.
[17] ISO-9972, NBN EN ISO 9972:2015 - Performance thermique des bâtiments - Détermination de la perméabilité à l'air des bâtiments - Méthode de pressurisation par ventilateur (ISO 9972:2015) CEN, Brussels, Belgium. 2015.
[18] TEC, Operating Instruction for the DG-700 Pressure and Flow Gauge, The Energy Conservatory, 2012.
[19] TEC, An Explication of the DG-1000 Accuracy Specifications, The Energy Conservatory, 2016.
[20] A. Field, J. Miles, Z. Field, in: Discovering Statistics Using R, SAGE Publications Ltd., London, 2012, p. 957.
[21] J.L. Peugh, A practical guide to multilevel modeling, J. School Psychol. 48 (1) (2010) 85–112.
[22] J. Rasbash, et al., A User's Guide to MLwiN, University of Bristol Centre for Multilevel Modelling, 2015.
[23] H. Goldstein, in: Multilevel Statistical Models, fourth ed., John Wiley & Sons Ltd, New York, 2010, pp. 1–14.
[24] M.G. Kent, et al., Temporal effects on glare response from daylight, Build. Environ. 113 (2017) 49–64.
[25] M.G. Kent, Temporal Effects in Glare Response, in Department of Architecture & Built Environment, University of Nottingham, United Kingdom, 2016.
[26] A.F. Hayes, A primer on multilevel modeling, Hum. Commun. Res. 32 (4) (2006) 385–410.
[27] S.N. Beretvas, D.A. Pastor, Using mixed-effects models in reliability generalization studies, Educ. Psychol. Meas. 63 (1) (2003) 75–95.
[28] T.A. Whittaker, C.F. Furlow, The comparison of model selection criteria when selecting among competing hierarchical linear models, J. Mod. Appl. Stat. Methods 8 (1) (2009) 173–193.
[29] H.J. Seltman, in: Experimental Design and Analysis, Carnegie Mellon University, Pittsburgh, 2012, p. 428. 2012.
[30] P. D Ellis, in: The Essential Guide to Effect Sizes: Statistical Power, Meta-Analysis, and the Interpretation of Research Results, Cambridge University Press, Cambridge, 2010, p. 173.
[31] S. Schiavon, S. Altomonte, Influence of factors unrelated to environmental quality on occupant satisfaction in LEED and non-LEED certified buildings, Build. Environ. 77 (2014) 148–159.
[32] J. Cohen, A power primer, Psychol. Bull. 112 (1) (1992) 155.
[33] J.A. Durlak, How to select, calculate, and interpret effect sizes, J. Pediatr. Psychol. 34 (9) (2009) 917–928.
[34] M.A. Volker, Reporting effect size estimates in school psychology research, Psychol. Schools 43 (6) (2006) 653–672.
[35] C.J. Ferguson, An effect size primer: a guide for clinicians and researchers, Prof. Psychol. 40 (5) (2009) 532–538.
[36] M.W. Julian, The consequences of ignoring multilevel data structures in nonhierarchical covariance modeling, Struct. Equ. Model. 8 (3) (2001) 325–352.
[37] C.J.M. Maas, J.J. Hox, Sufficient sample sizes for multilevel modeling, Methodology 1 (3) (2005) 86–92.

[38] B.O. Muthén, A. Satorra, Complex sample data in structural equation modeling, Sociol. Methodol. 25 (1995) 267–316.
[39] G.M. Verbeke, Linear mixed models for longitudinal data, in: Springer Series in Statistics, Springer-Verlag New York, 2000, p. 570.
[40] M.J. Gurka, Selecting the best linear mixed model under REML, Am. Stat. 60 (1) (2006) 19–26.
[41] J.C. De Winter, Using the Student's *t*-test with extremely small sample sizes, Pract. Assess. Res. Eval. 18 (10) (2013).
[42] D.W. Zimmerman, A note on preliminary tests of equality of variances, Br. J. Math. Stat. Psychol. 57 (1) (2004) 173–181.
[43] A. Field, G. Hole, How to Design and Report Experiments, Sage, 2002.
[44] J. Hauke, T. Kossowski, Comparison of values of Pearson's and Spearman's correlation coefficients on the same sets of data, Quaestiones Geographicae 30 (2) (2011) 87.
[45] JCGM, in: Evaluation of Measurement Data—Guide For the Expression of Uncertainty in Measurement, Joint Committee for Guides in Metrology, 2008, p. 134.
[46] C. Delmotte, in: Airtightness of Buildings - Calculation of Combined Standard Uncertainty, Belgian Building Research Institute - Laboratory Air Quality and Ventilation, Unpublished Report, 2013, p. 29.
[47] D.R. Helsel, R.M. Hirsch, in: Statistical Methods in Water Resources in Techniques of Water Resources Investigations, U.S. Geological Survey, 2002, p. 522.
[48] H. Okuyama, Y. Onishi, Reconsideration of parameter estimation and reliability evaluation methods for building airtightness measurement using fan pressurization, Build. Environ. 47 (2012) 373–384.
[49] M. Prignon, A. Dawans, G. van Moeseke, Uncertainties in airtightness measurements: regression methods and pressure sequences, 39th AIVC-7th TightVent & 5th Venticool Conference Smart Ventilation for Buildings, 2018.

# Appendix F.

Prignon, M., Dawans, A. and Van Moeseke, G. (2020). Quantification of uncertainty in zero-flow pressure approximation. International Journal of Ventilation. https://doi.org/10.1080/14733315.2020.1777020.

INTERNATIONAL JOURNAL OF VENTILATION
https://doi.org/10.1080/14733315.2020.1777020

Taylor & Francis
Taylor & Francis Group

Check for updates

# Quantification of uncertainty in zero-flow pressure approximation

Martin Prignon[a], Arnaud Dawans[b] and Geoffrey van Moeseke[a]

[a]UCLouvain, Place de l'Université, 1, Louvain-la-Neuve, Belgium; [b]Entreprises Jacques Delens, Watermael Boitsfort, Belgium

**ABSTRACT**

Multiple authors stated that, when performing fan pressurization test, Ordinary Least Square (OLS) method should not be used as a regression technique anymore. However, alternative methods require first to quantify components of uncertainty in pressure and air flow rate measurements. This work aims at quantifying the uncertainty in zero-flow pressure approximation, which is mainly due to short-term fluctuation of wind speed and direction. This has been done by statistically analysing the uncertainty indicator of 40 zero-flow pressure tests performed on 30 different units on eight different sites in Brussels. First, the analysis showed that this uncertainty could be reduced by increasing the period of measurement used to compute zero-flow pressure approximation. Second, it shows that the standard deviation of zero-flow pressure measurements was the variable with the most significant impact on the quality of the zero-flow pressure approximation. Third, it provides three different linear models to predict uncertainty as a function of different variables. This study experienced some limitations due to the available sample of tested units. These limitations lead to important further work: the validation of the model on another sample of buildings and its adaptation if needed. Further work should also focus on integrating these results on the uncertainty in envelope pressure measurements and on the uncertainty in airtightness estimation of the building.

**ARTICLE HISTORY**
Received 20 December 2020
Accepted 20 May 2020

**KEYWORDS**
Airtightness measurement; uncertainty; zero-flow pressure; fan pressurization test

## 1. Introduction

To be reliable, a measured quantity should always be given with its uncertainty. When performing a fan pressurization test, the uncertainty is often given as a function of the scattering of the data around the linear model obtained with an Ordinary Least Square (OLS) method. However, multiple authors stated that the uncertainty estimated with OLS was not reliable in the case of airtightness measurements because the method neglects uncertainty in pressure measurements (Prignon et al., 2018; Delmotte, 2017; Okuyama & Onishi, 2012). Therefore, other regression techniques should be used such as the Iterative Weighted Least Square (IWLS) (Okuyama & Onishi, 2012; ISO/TS-28037, 2010) or the Weighted Line of Organic Correlation (WLOC) (Delmotte, 2017). These methods require quantifying uncertainty in pressure and air flow rate measurements.

One of the main sources of uncertainty is the fluctuation of reading in the pressure measurements due to variation in weather conditions (Sherman & Palmiter, 1995). ISO 9972:2015 requires

CONTACT Martin Prignon martin.prignon@uclouvain.be UCLouvain, Architecture & Climat 1 Place du Levant L5.05.04 B-1348 Louvain-la-Neuve Belgium

© 2020 Informa UK Limited, trading as Taylor & Francis Group

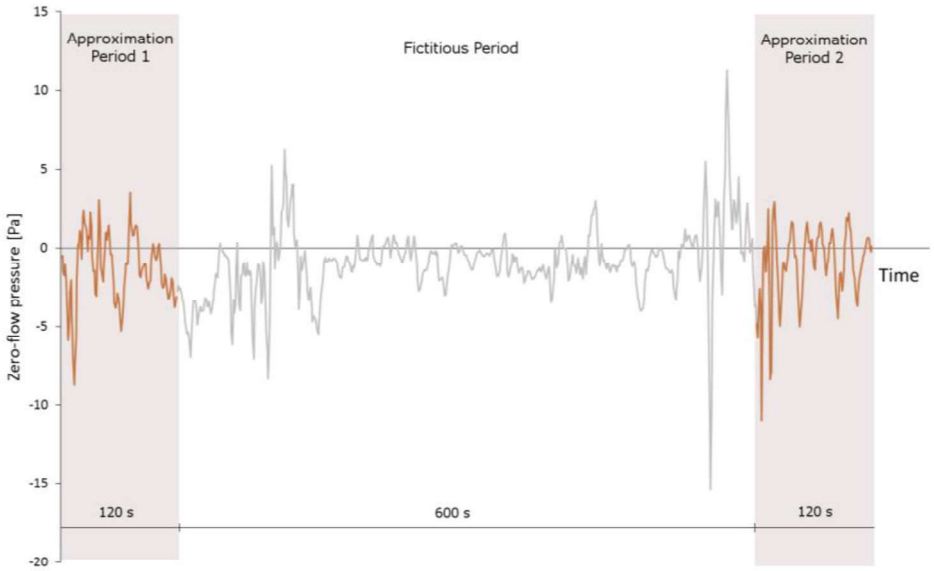



**Figure 1.** Illustration of the three successive periods of a zero-flow pressure test.

the measurement of inside and outside temperature, and of wind speed (in Beaufort scale), but none of them are used in the calculation to deal with fluctuations in weather conditions (ISO-9972 and NBN EN ISO 9972, 9972, 2015). In practice, pressure induced by weather conditions is handled in ISO 9972:2015 by measuring the zero-flow pressure (i.e., the pressure when there is no pressure induced by the fan). However, zero-flow pressure can be measured only when the fan is not working. Therefore, it has to be approximated during the test. This approximation goes along with an uncertainty: the uncertainty in zero-flow pressure approximation ($u(\Delta p_{0,a})$).

ISO 9972:2015 defines the zero-flow pressure during the test as the average of at least 10 zero-flow pressure measurements in 30 seconds before and after the fan pressurization test. Although ISO 9972:2015 does not impose requirements on maximum wind speed, it imposes requirements on zero-flow pressure. In fact, the operator has to measure the average of negative and positive values before ($\Delta p_{01,-}$ and $\Delta p_{01,+}$) and after ($\Delta p_{02,-}$ and $\Delta p_{02,+}$) the test. To be valid, none of these values should be higher than 5 Pa or lower than -5 Pa. In this study, all the tests are valid regarding these requirements.

In a previous work, we developed a method to quantify uncertainty due to zero-flow approximation based on a series of 30 tests performed on the same apartment (Prignon et al., 2019). Although the results of that work were useful, they could not be generalized since only one unit was tested. This study aims at finding a mathematical relation to predict uncertainty in zero-flow pressure approximation based on 40 zero-flow pressure tests performed on 30 different buildings.

## 2. Methodology

### *2.1. The zero-flow pressure test*

Delmotte used the zero-flow pressure test for the first time in 2017 (Delmotte, 2017). This test consists in measuring the zero-flow pressure every second during three successive periods: two approximation periods and one fictitious period (Figure 1). The two approximation periods correspond to the zero-flow pressure measurements used to compute the zero-flow pressure approximation in a traditional fan pressurization test. In his work, Delmotte considered periods of 30 seconds while in this work two periods of 120 seconds are considered. This is because this

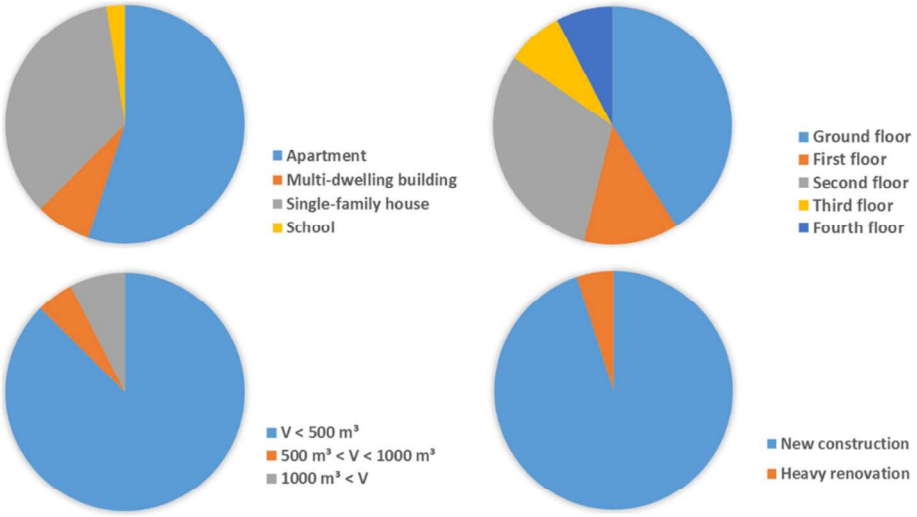



**Figure 2.** Repartition of the sample of units tested regarding four variables: type of units, storey of the measurement, volume of the unit and type of construction.

paper focuses also on how the duration of approximation periods affects the uncertainty. The fictitious period corresponds to the time a fan pressurization test would take in practice. In this research, a fictitious period of 600 seconds is considered, to remain consistent with the work of Delmotte.

The zero-flow pressure approximation is computed based on measurements made during the approximation periods according to ISO 9972:2015. Then, the zero-flow pressure approximation is compared to the zero-flow pressure measured every second during the fictitious period. The "uncertainty indicator" ($\varepsilon$) is the average of the difference between approximated and measured zero-flow pressure (Equation 1).

$$\varepsilon = \frac{\sum_{i=1}^{600} |\Delta p_{0,i} - \Delta\sim p_0|}{600} \tag{1}$$

Where $\Delta p_{0,i}$ is the zero-flow pressure measured every second ($i$) during the fictitious period and $\Delta\sim p_0$ is the zero-flow pressure approximation based on measurements made during approximation periods.

## 2.2. Tests description

In this research, 40 zero-flow pressure tests were performed on 30 different units (10 units experienced the same test twice, under different weather conditions), in eight different sites in Brussels (Belgium). The four pie charts in Figure 2 represent the repartition of four different variables among the 30 different units tested: the type of unit measured, the storey where the test was performed, the volume of the unit and the type of construction. It is important to point out that, there is only one non-residential unit (school). In addition, almost all tests (38) were performed on new constructions and only five units have a volume larger than 500 $m^3$. These limitations related to the sample are tackled in the conclusion section.

Multiple operators performed the measurements using different DG-700 manometers from TEC conservatory. According to the manufacturer, the maximum permissible error for these manometers is the maximum between 0.15 Pa and 1% of the reading, while it has a resolution of 0.1 Pa (TEC, 2012). All of these were calibrated for the last time at least one year before the test.

In this study, operators were asked to place pressure taps at the same place they would for a typical fan pressurization test.

### 2.3. Variables analysed

For each test, 7 different variables are investigated. $\Delta p_{0,a}$ (in Pa) is the value of the zero-flow pressure approximation computed according to ISO 9972:2015: it is the average of zero-flow pressure measured during first ($\Delta p_{0,1}$) and second ($\Delta p_{0,2}$) approximation periods. $\Delta$ (in Pa) is the difference between $\Delta p_{0,1}$ and $\Delta p_{0,2}$. $\sigma$ (in Pa) is the standard deviation of the zero-flow pressure measurements (both $\Delta p_{0,1}$ and $\Delta p_{0,2}$ combined). $w$ is the wind speed (in km/h) and is obtained from the closest weather station available. $V$ (in $m^3$) is the volume of the unit. $s$ is the storey where the measurement is taken. $\Delta T$ (in °C) is the difference between inside and outside temperature during the test. All these variables were tested for four different durations of approximation periods: 30 seconds, 60 seconds, 90 seconds and 120 seconds.

The wind speed is the only variable that was not directly available on site during the test. However, it was still considered in the variables because of its well-known impact on the pressure measurement uncertainty (Sherman & Palmiter, 1995; Carrié & Leprince, 2016). The distance between the closest weather station and the site varied between 300 and 1500 meter, and the data used is the average of one hour of wind speed measurement. These weather stations are often located on the roof of a building and, therefore, do not take into account the surroundings of the tested unit. However, this study is not interested in the physical impact of wind speed and wind pressure on uncertainty, but in a quantification of uncertainty based on data available during a fan pressurization test.

### 2.4. Statistical analysis

The statistical analysis aims at finding variables with the most significant impact on the uncertainty indicator ($\varepsilon$ – Equation 1) and at deducing a relation between the uncertainty indicator and these variables.

In the previous section, duration period was considered differently from other variables. This is because of the dependency implied by the experimental design: four duration periods are computed for each dataset while other variables only have one value for each dataset. Therefore, the impact of duration period cannot be deduced the same way as other variables. When data are nested (the duration of approximation periods are nested within the different tests), Multi-Level Modelling (MLM) should be used (Rasbash, 2015). The use of MLM in zero-flow pressure tests was deeply investigated in our previous work (Prignon et al., 2019). However, in this work the objective of MLM is to investigate if different models should be used for different approximation methods, and it can be answered simply by assessing the need for MLM.

MLM is needed when there is large intraclass correlation (ICC) ($> 0.45$) (Julian, 2001) and when the design effect is higher than 2 (Muthén & Satorra, 1995). ICC can be defined as the proportion of uncertainty indicator variation that occurs across tests (Peugh, 2010) and is computed using Equation (2). $\tau_{00}$ is the variation of uncertainty indicator between tests, and $\sigma 2$ is the average of uncertainty indicator variation for different periods within each test. The design effect quantifies how the dependence of data affects the estimate of standard error: it provides the multiplier to be applied to the standard error to take the nested structure of the data into account. It is computed using Equation (3) with $n_c$ the number of different periods measured by test (Peugh, 2010; Hayes, 2006).

$$ICC = \tau_{00}/(\tau_{00} + \sigma^2) \tag{2}$$

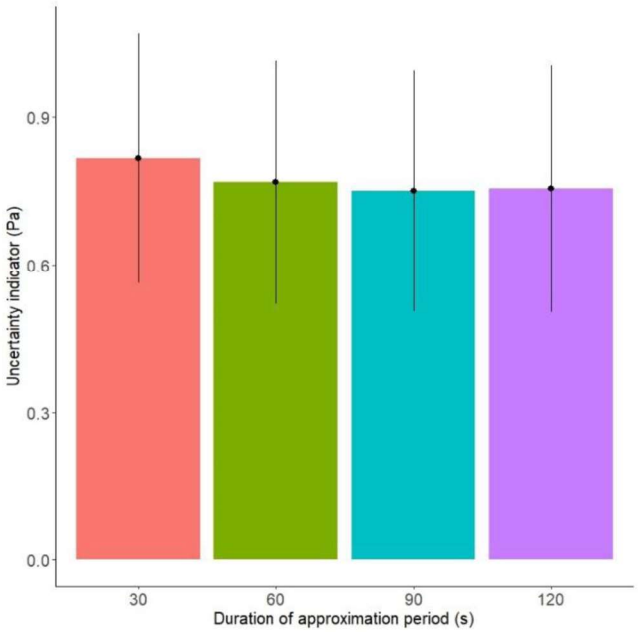



**Figure 3.** Bar graph of the 40 uncertainty indicators computed for the four different approximation periods.

$$Design\ \ Effect = 1 + (n_c - 1) * ICC \tag{3}$$

In this study, $\tau_{00}$ is 0.79, $\sigma 2$ is 0.07 and $n_c$ is 4. Therefore, *ICC* is 0.92 and Design effect is 3.76 and MLM is needed. This means that classic statistical tools cannot be used to study the impact of approximation period duration on the uncertainty indicator because of the nested structure of data.

The seven other variables are not nested in a hierarchical structure. Therefore, the statistical analysis can be made with classical statistical tool such as multiple regression. It aims at finding the linear combination of variables that matches as much as possible the uncertainty indicator (Field et al., 2012). A multiple regression provides a coefficient for each variable in the linear model, but it also provides information on the statistical significance of these variables (p-values) and the quality of the fitting of the model (multiple $R^2$). Multiple *R*2 can be interpreted as the *R*2 in a simple regression: it is the amount of variance in the outcome (i.e., the uncertainty indicator) explained by the model (Field et al., 2012).

## 3 Results

### *3.1. Duration of approximation periods*

Figure 3 shows the bar graph of the uncertainty indicator of the 40 tests for the four different duration of approximation periods. The period of 30 seconds is slightly worse than other periods, but all results remain in the same order of magnitude.

Table 1 presents the difference in means of uncertainty indicator for the four duration and the statistical significance of this difference. These were obtained using pairwise Wilcoxon rank-sum test with Bonferroni correction. Wilcoxon rank-sum test was used because datasets follow a distribution significantly different from normal (Shapiro-Wilk $= 0.82$, $p < 0.001$), and Bonferroni correction was used because multiple comparisons were performed on the same dataset.

**Table 1.** Results of the comparison using pairwise Wilcoxon rank-sum test with Bonferroni correction.

| vs | 30 | 60 | 90 |
|---|---|---|---|
| 60 | 0.04 * | | |
| 90 | 0.06 ** | 0.02 N.S. | |
| 120 | 0.05 * | 0.01 N.S. | −0.01 N.S. |

Results are highly significant (***), significant (**), slightly significant (*) or non-significant ($^{N.S.}$).

Results show that only the comparisons including 30 second periods are statistically significant (30vs90) or slightly significant (30vs60 and 30vs120). Other comparisons are statistically non-significant.

### 3.2. Multiple regression

The first multiple regression (Table 2) shows that two variables have no significant impact on the uncertainty indicator, whatever the duration: the difference of approximation in the first and in the second duration period ($\Delta$) and the temperature difference between inside and outside the unit during the test ($\Delta T$). Variables having the most significant impact are the standard deviation of the zero-flow pressure measurements ($\sigma$) and the wind speed ($w$). The statistical significance of some variables ($\Delta p_{0,a}$, $w$, $V$ and $s$) depends on the duration of the approximation periods.

Conclusions on the statistical significance of the volume and the storey should be drawn carefully. Regarding the storey ($s$), it is important to keep in mind that the zero-flow pressure was measured higher than the fourth floor only once. Similar study performed on high-rise buildings would probably give different results since wind speed magnitude and surroundings would be different. In addition, in high-rise buildings, stack effect has a huge impact on the zero-flow pressure. Regarding the volume ($V$), only five units have a volume larger than 500 $m^3$. Similar study performed on large-volume units could lead to different conclusions.

The second multiple regression (Table 3) confirms the first one: similar fitting is obtained when removing the two non-significant variables (multiple $R2$ between 0.73 and 0.74). The most significant variables are still $\sigma$ and $w$. The coefficients can be used to define a mathematical relation between the uncertainty indicator and these five variables. Equation (4) gives this relation in the case of 30-second approximation periods.

$$\varepsilon = -1.2 + 0.30 * \Delta p_{0,a} + 0.85 * \sigma + 0.07 * w + 1.3\ e^{-4} * V + 0.12 * s \tag{4}$$

In the third multiple regression (Table 4), the wind speed is removed from the variables since it is the only one that is not directly available during a fan pressurization test. The impact of the standard deviation is found highly significant, but other terms are almost all found not significant. $\Delta p_{0,a}$ is found slightly significant in the case of 30-second approximation periods only. The third multiple regression shows a larger decrease of the fitting quality (multiple $R2$ between 0.62 and 0.64). Equation (5) provides a mathematical relation between uncertainty indicator and multiple variables for approximation periods of 30 seconds.

$$\varepsilon = 0.04 + 0.27 * \Delta p_{0,a} + 1.1 * \sigma + 8.6\ e^{-5} * V + 0.04 * s \tag{5}$$

The last multiple regression shows that a simple linear model including only the standard deviation of the measurements as a predictor provides still good fitting (multiple $R^2$ between 0.55 and 0.61) (Table 5). The mathematical relation is highly simplified (Equation 6).

$$\varepsilon = 0.11 + 0.98 * \sigma \tag{6}$$

Although multiple $R2$ has a clear meaning (i.e., the amount of variance explained by the model), it can be sometimes difficult to visualize what it practically means. Figure 4 shows the predicted vs. the real uncertainty indicator for the three cases when considering approximation periods of 30 seconds. The predicted values are obtained when applying Equation (4)–(6), while

**Table 2.** Results of the multiple regression applied on all variables (7) for the four durations.

| Variables | Period 30 | | Period 60 | | Period 90 | | Period 120 | |
|---|---|---|---|---|---|---|---|---|
| Intercept | −1.2 e-00 | ** | −1.3 e-00 | ** | −1.2 e-00 | ** | −1.4 e-00 | ** |
| $\Delta P_{0,a}$ | 2.9 e-01 | ** | 1.3 e-01 | N.S. | 1.2 e-01 | N.S. | 1.0 e-01 | N.S. |
| $\Delta$ | −3.1 e-01 | N.S. | −3.1 e-01 | N.S. | −3.0 e-01 | N.S. | −3.1 e-01 | N.S. |
| $\sigma$ | 1.1 e-00 | *** | 9.5 e-01 | *** | 9.6 e-01 | *** | 8.8 e-01 | *** |
| $w$ | 7.4 e-02 | *** | 7.3 e-02 | ** | 6.0 e-02 | ** | 6.9 e-02 | ** |
| $V$ | 1.3 e-04 | ** | 1.4 e-04 | ** | 1.2 e-04 | * | 1.3 e-04 | * |
| $s$ | 8.6 e-02 | N.S. | 1.0 e-01 | N.S. | 1.0 e-01 | * | 1.3 e-01 | * |
| $\Delta T$ | 8.9 e-04 | N.S. | −3.7 e-03 | N.S. | −2.0 e-03 | N.S. | 5.9 e-03 | N.S. |
| Multiple $R^2$ | 0.77 | | 0.79 | | 0.76 | | 0.75 | |

***$p < 0.001$ is highly significant.
**$p < 0.01$ is significant.
*$p < 0.05$ is slightly significant and $p > 0.05$ ($^{N.S.}$) is not significant.

**Table 3.** Results of the multiple regression applied on main variables, including wind speed (5) for the four durations.

| Variables | Period 30 | | Period 60 | | Period 90 | | Period 120 | |
|---|---|---|---|---|---|---|---|---|
| Intercept | −1.2 e-00 | ** | −1.3 e-00 | ** | −1.2 e-01 | ** | −1.4 e-00 | *** |
| $\Delta p_{0,a}$ | 3.0 e-01 | ** | 1.3 e-01 | N.S. | 1.3 e-01 | N.S. | 1.2 e-01 | N.S. |
| $\sigma$ | 8.5 e-01 | *** | 7.8 e-01 | *** | 8.1 e-01 | *** | 7.7 e-01 | *** |
| $w$ | 7.4 e-02 | *** | 6.9 e-02 | ** | 6.2 e-02 | ** | 7.3 e-02 | *** |
| $V$ | 1.3 e-04 | ** | 1.4 e-04 | ** | 1.2 e-04 | * | 1.2 e-04 | * |
| $s$ | 1.2 e-01 | * | 1.2 e-01 | * | 1.3 e-01 | * | 1.5 e-01 | ** |
| Multiple $R^2$ | 0.74 | | 0.73 | | 0.74 | | 0.73 | |

p < 0.001 (***) is highly significant, p < 0.01 (**) is significant, p < 0.05 (*) is slightly significant and p > 0.05 ($^{N.S.}$) is not significant.

**Table 4.** Results of the multiple regression applied on main variables, without wind speed (4) for the four durations.

| Variables | Period 30 | | Period 60 | | Period 90 | | Period 120 | |
|---|---|---|---|---|---|---|---|---|
| Intercept | 3.8 e-02 | N.S. | −8.5 e-02 | N.S. | −1.7 e-02 | N.S. | −1.8 e-01 | N.S. |
| $\Delta p_{0,a}$ | 2.7 e-01 | * | 9.9 e-02 | N.S. | 9.9 e-02 | N.S. | 9.2 e-02 | N.S. |
| $\sigma$ | 1.1 e-00 | *** | 9.9 e-01 | *** | 1.0 e-00 | *** | 9.7 e-01 | *** |
| $V$ | 8.6 e-05 | N.S. | 1.0 e-04 | N.S. | 7.8 e-05 | N.S. | 6.9 e-05 | N.S. |
| $s$ | 4.3 e-02 | N.S | 5.3 e-02 | N.S. | 7.0 e-02 | N.S. | 7.7 e-02 | N.S. |
| Multiple $R^2$ | 0.64 | | 0.63 | | 0.66 | | 0.62 | |

$p < 0.001$ (***) is highly significant, $p < 0.01$ (**) is significant, $p < 0.05$ (*) is slightly significant and $p > 0.05$ ($^{N.S.}$) is not significant.

**Table 5.** Results of the multiple regression applied on standard of the measurement only for the four durations.

| Variables | Period 30 | | Period 60 | | Period 90 | | Period 120 | |
|---|---|---|---|---|---|---|---|---|
| Intercept | 1.1 e-01 | N.S. | 5.4 e-02 | N.S. | −3.1 e-02 | N.S. | −3.3 e-02 | N.S. |
| $\sigma$ | 9.8 e-01 | *** | 9.5 e-01 | *** | 9.6 e-01 | *** | 9.3 e-01 | *** |
| Multiple $R^2$ | 0.55 | | 0.57 | | 0.61 | | 0.57 | |

$p < 0.001$ (***) is highly significant, $p < 0.01$ (**) is significant, $p < 0.05$ (*) is slightly significant and $p > 0.05$ (N.S.) is not significant.

the real values are the data used to develop the models. The difference in multiple $R^2$ values is probably due to the tests with high value of uncertainty indicator. Indeed, the three points with high measured uncertainty indicator are better predict with the first model (Equation 4) than with the second (Equation 5) and the third (Equation 6) model.

## 4. Discussion

It was shown in a previous work that the zero-flow pressure measured during the fictitious period follows a normal distribution (Prignon et al., 2019). In normal distributions, each measurement has a Z-score that is its distance from the mean, expressed in standard deviation (Field et al., 2012). It is computed with Equation (7) where X is the measurement, and $\mu(\Delta p_0)$ and

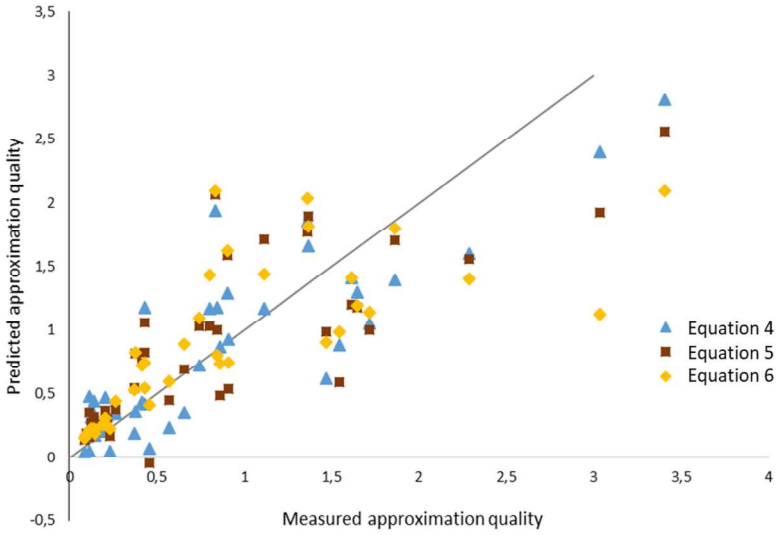



**Figure 4.** Representation of the predicted vs. measured uncertainty indicator for the three models.

$\sigma(\Delta p_0)$ are respectively the average and the standard deviation of the zero-flow pressure measurements during the fictitious period.

$$Z_{score} = \frac{X - \mu}{\sigma} \tag{7}$$

Since $\varepsilon$ is the average of the difference between approximated and real zero-flow pressure, it is reasonable to assume that $\Delta p_0 - \varepsilon/2$ and $\Delta p_0 + \varepsilon/2$ are the lower and the upper limit of the interval containing 50% of the zero-flow pressure measured during the fictitious period. For these limits Z-scores are respectively -0.675 and +0.675, and Equations (8) and (9) can be used to link uncertainty indicator and standard deviation.

$$0.675 = \frac{(\Delta p_{0,a} + \varepsilon/2) - \Delta p_0}{\sigma(\Delta p_0)} \tag{8}$$

$$-0.675 = \frac{(\Delta p_{0,a} - \varepsilon/2) - \Delta p_0}{\sigma(\Delta p_0)} \tag{9}$$

The zero-flow pressure approximation ($\Delta p_{0,a}$) is assumed to be equal to the average of the zero-flow pressure measurements made during the fictitious period ($\Delta p_0$). This hypothesis is only valid because short-term wind fluctuations are already taken into account in $\varepsilon$ and because long-term wind and temperature fluctuations are considered by taking the average of pre- and post-test zero-flow pressure measurements. In fact, without these wind and temperature fluctuations, zero-flow pressure is expected to remain constant during the 14 minutes.

Since fan pressurization measurement during fictitious period follows a normal distribution, the uncertainty in zero-flow pressure approximation ($u(\Delta p_{0,a})$) is given by the standard deviation of zero-flow pressure ($\sigma(\Delta p_0)$). Therefore, uncertainty in zero-flow approximation is given as a function of the uncertainty indicator only (Equation 10).

$$u(\Delta p_{0,a}) = \sigma(\Delta p_0) = \varepsilon/1.35 \tag{10}$$

In practice, each pressure difference – airflow couple is the average of multiple measurements. In addition, when performing a test, the operator often tires to record a measure when wind fluctuations are low. These actions reduce the impact of wind fluctuations and decrease the uncertainty due to zero-flow pressure approximation. Therefore Equation 9 should be considered as an upper limit.

## 5. Conclusion

This work is a step in the quantification of uncertainties in pressure measurements by quantifying uncertainty due to zero-flow pressure approximation ($u(\Delta p_{0,a})$). Main findings in this research are

- Uncertainty in pressure measurement is not negligible, and only regression methods that take into account uncertainty in pressure measurements should be used (e.g., Iterative Weighted Least Square (IWLS) or Weighted Line of Organic Correlation (WLOC) instead of Ordinary Least Square (OLS)).
- Zero-flow pressure should be measured during more than 30 seconds before and after the test to reduce uncertainty due to zero-flow pressure approximation.
- When performing IWLS or WLOC methods, $u(\Delta p_{0,a})$ should be computed using equation 9 combined with equation 4, 5 or 6 (depending on the data available).

Some limitations should be acknowledged before generalizing results. First, this research is limited by the dataset. As explained in the methodology section, the dataset contains only two renovations, five units with volume larger than 500 $m^3$, one non-residential building and one building with more than four stories. Second, the dataset was entirely used to create the model and none of them was used to validate the model.

Therefore, further work should focus on the validation of the suggested models and, if needed, on their adaptation for large-volume and high-rise units. Moreover, other components of uncertainty, their propagation and the correlation between different components should also be investigated.

## Acknowledgements

Authors want to thank the company *Jacques Delens* for its mobilization in this work and the availability of their construction sites. This work is part of the "AirPath50" project funded by INNOVIRIS.

## Disclosure statement

No potential conflict of interest was reported by the author(s).

## Notes on contributors

***Martin Prignon*** is a PhD student at Architecture et Climat, UCLouvain, Belgium. His works focuses on uncertainty calculations in the context of measurements of airtightness of buildings and building components.

***Arnaud Dawans*** is Head of Innovation and Sustainability at Jacques Delens S.A. (BESIX Group). Granted an Architectural and Civil Engineering Degree and a Master in Management from Solvay Brussels School, he actually manages to disrupt construction industry and help the company to be future proof.

***Geoffrey van Moeseke*** is professor of building physics at UCLouvain. He holds a master in architectural engineer and a PhD in applied sciences. His research activities focuses on buildings' energy efficiency.

## References

Carrié, F. R., & Leprince, V. (2016). Uncertainties in building pressurisation tests due to steady wind. *Energy and Buildings*, *116*, 656–665. https://doi.org/10.1016/j.enbuild.2016.01.029

Delmotte, C. (2017). Airtightness of buildings - considerations regarding the zero-flow pressure and the weighted line of organic correlation [Paper presentation]. 38th AIVC Conference ventilating healthy low-energy buildings, Nottingham, UK.

Field, A., Miles, J., & Field, Z. (2012). *Discovering statistics using R*. Sage Publications Ltd. 957.

Hayes, A. F. (2006). A primer on multilevel modeling. *Human Communication Research*, *32*(4), 385–410. https://doi.org/10.1111/j.1468-2958.2006.00281.x

ISO/TS-28037 (2010). *ISO TS 28037 The determination and use of straight-line calibration functions*.

ISO-9972, NBN EN ISO 9972 (2015). 2015 - Performance thermique des bâtiments - Détermination de la perméabilité à l'air des bâtiments - Méthode de pressurisation par ventilateur (ISO 9972:2015) CEN, Brussels, Belgium.

Julian, M. W. (2001). The consequences of ignoring multilevel data structures in nonhierarchical covariance modeling. *Structural Equation Modeling: A Multidisciplinary Journal*, *8*(3), 325–352. https://doi.org/10.1207/S15328007SEM0803_1

Muthén, B. O., & Satorra, A. (1995). Complex sample data in structural equation modeling. *Sociological Methodology*, *25*, 267–316. https://doi.org/10.2307/271070

Okuyama, H., & Onishi, Y. (2012). Reconsideration of parameter estimation and reliability evaluation methods for building airtightness measurement using fan pressurization. *Building and Environment*, *47*, 373–384. https://doi.org/10.1016/j.buildenv.2011.06.027

Peugh, J. L. (2010). A practical guide to multilevel modeling. *Journal of School Psychology*, *48*(1), 85–112. https://doi.org/10.1016/j.jsp.2009.09.002

Prignon, M., Dawans, A., & van Moeseke, G. (2018). Uncertainties in airtightness measurements: regression methods and pressure sequences [Paper presentation]. 39th AIVC-7th TightVent & 5th Venticool Conference Smart Ventilation for Buildings.

Prignon, M., Dawans, A., Altomonte, S., & Van Moeseke, G. (2019). A method to quantify uncertainties in airtightness measurements: zero-flow and envelope pressure. *Energy and Buildings*, *188/189*, 12–24. https://doi.org/10.1016/j.enbuild.2019.02.006

Rasbash, J. (2015). *A user's guide to MLwiN*. Centre for Multilevel Modelling.

Sherman, M., & Palmiter, L. (1995). *Uncertainties in fan pressurization measurements, in Airflow performance of building envelopes, components, and systems*. ASTM International. p. 266–283.

TEC (2012). *Operating instruction for the DG-700 pressure and flow gauge*. The Energy Conservatory.